

From the Institute of Anatomy
of the University of Lübeck
Director: Prof. Dr. med. Jürgen Westermann

"Dissecting the immunomodulatory roles of cell-derived nanoparticles (CDNPs) in infectious diseases"

Dissertation
for Fulfillment of
Requirements
for the Doctoral Degree
of the University of Lübeck

from the Department of Natural Sciences

Submitted by

Natalia Kunz
from Barnaul, Russia

Lübeck 2017

First referee: Dr. Kathrin Kalies

Second referee: Prof. Dr. Rudolf Manz

Date of oral examination: 20.04.2017

Approved for printing: 28.04.2017

Table of Contents

1. Abstract 1

Zusammenfassung 2

2. Introduction 4

2.1 The immune system 4

2.2 Self and non-self 4

2.2.1 Pattern recognition receptors (PRRs) 5

2.2.2 Natural antibodies and the complement system 7

2.2.3 The adaptive immune system 8

2.2.4 Recognition of xenogeneic non-self 9

2.3 Recognition of stressed and damaged self 9

2.3.1 Detection and discrimination of cell death 9

2.3.2 Damage-associated molecular patterns (DAMPs) 10

2.3.3 Resolution-associated molecular patterns (RAMPs) 11

2.4 Cell-cell communication under physiologic and stressed conditions 12

2.5 Cell-derived nanoparticles (CDNPs) 13

2.5.1 Infectious diseases models 15

2.5.1.1 *Leishmania major* infection 15

2.5.1.2 Sepsis 17

2.6 Aims of this thesis 19

3. Materials and Methods 20

3.1 Materials 20

3.1.1 Animals, pathogens and cells 20

3.1.2 Antibodies 20

3.1.3 Primer and probes 22

3.1.4 Culture media, master mixes and buffers 22

3.1.5 Reagents and kits 24

3.1.6 Technical equipment/instruments 26

3.1.7 Laboratory supplies 28

3.1.8 Software 29

3.2 Methods 30

3.2.1 CDNP preparation and characterization 30

3.2.1.1 CDNP preparation 30

3.2.1.1.1 Commercially available CDNPs (BK-RiV) 30

3.2.1.1.2 Isolation of CDNPs from murine MC3T3-E1 cell cultures 30

3.2.1.1.3 Isolation of CDNPs from the peritoneum of naïve and septic mice 31

3.2.1.1.4 Concentration of CDNPs 31

3.2.1.1.5 Pooling of individual CDNP preparations 31
3.2.1.1.6 Labeling of CDNPs 31
3.2.1.2 CDNP characterization 32
3.2.1.2.1 Nanoparticle Tracking Analysis (NTA) 32
3.2.1.2.2 Scanning electron microscopy (SEM) 33
3.2.1.2.3 SDS-PAGE 34
3.2.1.2.4 2D- gel electrophoresis and MALDI-TOF 34
3.2.1.2.5 Western Blot 38
3.2.2 Animal experiments 39
3.2.2.1 Leishmania major infection 39
3.2.2.1.1 Cultivation of *L. major* parasites 39
3.2.2.1.2 *L. major* infection 39
3.2.2.1.3 CDNP application 39
3.2.2.1.4 Determination of foot pad swelling 40
3.2.2.1.5 Tissue and organ harvesting 40
3.2.2.1.6 Determination of parasite loads 40
3.2.2.2 Polymicrobial sepsis induction by cecal ligation and puncture (CLP) 40
3.2.2.2.1 CLP 41
3.2.2.2.2 Survival studies 41
3.2.2.2.3 Determination of bacterial loads 41
3.2.3 Cell and microparticle isolation 41
3.2.3.1 Peritoneal lavage 41
3.2.3.2 Splenic cell isolation 42
3.2.3.3 Isolation and culture of BM-derived neutrophils 42
3.2.3.4 Microparticle generation and isolation 43
3.2.4 *In vitro* experiments 44
3.2.4.1 TLR stimulation 44
3.2.4.2 Cell incubation with CDNPs 45
3.2.4.3 Particle ingestion assays 45
3.2.4.3.1 CDNP ingestion by peritoneal cells 45
3.2.4.3.2 CDNP-MP co-incubation 45
3.2.4.3.3 MP ingestion 46
3.2.4.4 Bacterial killing assay 46
3.2.5 Gene expression analysis 46
3.2.5.1 Nucleic acid isolation 46
3.2.5.2 cDNA synthesis 47
3.2.5.3 Quantitative RT-PCR 47
3.2.6 Protein expression/secretion analysis 48
3.2.6.1 Determination of protein concentration by BCA 48
3.2.6.2 Flow Cytometry 48
3.2.6.2.1 Extracellular staining 49
3.2.6.2.2 Staining of intracellular cytokines 50
3.2.6.2.3 Staining of transcription factors 51
3.2.6.2.4 Staining and identification of NDMPs 51

3.2.6.3 ELISA 51
3.2.6.4 Cytometric bead array (CBA) 53
3.2.7 Determination of endotoxin contamination 54
3.2.8 Statistical analysis 55

4. Results 56
4.1 CDNPs have anti-inflammatory effects *in vitro*, independent of their xeneogeneic origin **56**
4.1.1 Xenogeneic CDNPs have anti-inflammatory effects on TLR-triggered macrophages *in vitro* 56
4.1.1.1 Xenogeneic CDNPs do not alter IFNβ and TNFα expression of resting peritoneal macrophages *in vitro* 56
4.1.1.2 Xenogeneic CDNPs modulate IFNβ and TNFα expression of TLR-stimulated peritoneal macrophages in vitro 57
4.1.1.2.1 Xenogeneic CDNPs have no effect on LPS- or Poly(I:C)-stimulated macrophages 58
4.1.1.2.2 Xenogeneic CDNPs reduce TNFα expression in response to resiquimod 4 hours after incubation 59
4.1.1.2.3 Xenogeneic CDNPs reduce zymosan-induced IFNβ expression 4 hours and TNFα expression 24 hours after incubation 60
4.1.2 Allogeneic CDNPs demonstrate the same anti-inflammatory effects on TLR-triggered macrophages as xenogeneic CDNPs 62
4.1.2.1 Murine Fibroblasts stressed by nutrient deprivation produce CDNPs 62
4.1.2.2 Both allogeneic and xenogeneic CDNPs induce the same anti-inflammatory phenotype in activated macrophages 65
4.1.2.2.1 Both allogeneic and xenogeneic CDNPs reduce zymosan-induced TNFα expression 65
4.1.2.2.2 Allogeneic and xenogeneic CDNPs also reduce the expression of zymosan-induced IL-1β 66
4.1.2.2.3 Allogeneic and xenogeneic CDNPs increase the expression of zymosan-induced IL-10 68
4.1.2.2.4 Allogeneic CDNPs induce an anti-inflammatory phenotype in Pam_3CSK_4-stimulated macrophages 70
4.2 Only CDNPs derived from stressed cells show anti-inflammatory effects *in vitro* and annexin A5 might be the mediator **71**
4.2.1 CDNPs are also produced by unstressed cells 71
4.2.2 The immunomodulatory effect of CDNP *in vitro* is dependent on their origin from stressed cells 72
4.2.2.1 Only CDNPs derived from stressed cells reduce zymosan-induced TNFα secretion 73
4.2.2.2 Both s- and usCDNPs are ingested by APCs and induce antigen-presentation 73
4.2.2.2.1 Both s- and usCDNP are ingested by APCs 74

4.2.2.2.2 Ingestion of both s- and usCDNPs slightly increases the activation of peritoneal macrophages 75
4.2.2.2.3 Only sCDNPs reduce $CD4^+$ T cell activation in response to LPS stimulation 76
4.2.3 Identification of annexin A5 as a possible mediator for the anti-inflammatory effects of sCDNPs 77
4.3 CDNPs are beneficial in sepsis and slightly modulate *L. major* infection 82
4.3.1 CDNPs induce an anti-inflammatory milieu at the infection site, drive DC activation and increase Treg frequencies in the draining lymph node of *L. major*-infected mice 82
4.3.1.1 CDNPs increase MHCII surface expression on DCs in the draining lymph node of *L. major*-infected mice 82
4.3.1.2 CDNPs shift the ratio of naïve vs. effector memory $CD4^+$ T cells in the draining lymph node of *L. major*-infected mice to the effector side 84
4.3.1.3 CDNPs shift the milieu in the draining lymph node and at the site of infection towards Th2 86
4.3.1.4 CDNPs increase the frequency of $Foxp3^+$ T cells in the draining lymph node and elevate IL-10 levels at the infection site 87
4.3.1.5 CDNP treatment has no effect on the clinical outcome of *L. major* infection 89
4.3.2 CDNPs have protective effects in CLP-induced sepsis 91
4.3.2.1 CDNPs increase the survival of septic mice 92
4.3.2.2 CDNPs are ingested by effector cells at the infection site 4 hours after CLP 92
4.3.2.3 CDNPs ingestion induces cell activation at the infection site 4 hours after CLP 95
4.3.2.4 CDNP treatment reduces IL-6 and IL-10 levels at the site of infection 24 hours after CLP 96
4.3.2.5 CDNP treatment increases NDMP levels at the site of infection 24 hours after CLP 98
4.3.2.6 CDNPs reduce peritoneal bacterial loads 24 hours post CLP 100
4.3.2.7 Identification of possible mechanisms mediating the enhanced immune response in CDNP-treated mice 100
4.3.2.7.1 CDNPs directly impact IL-6 expression and secretion *in vitro* 100
4.3.2.7.2 CDNPs impede the production and function of immuno-suppressing NDMPs *in vitro* 102
4.3.2.7.3 CDNPs directly reduce bacterial growth *in vitro* 104
4.4 Endogenous CDNPs accumulate at the infection site in sepsis 106
4.4.1 Endogenous CDNPs accumulate at the infection site in sepsis 106
4.4.2 Endogenous CDNPs contain annexin A5 109

5. Discussion 110
5.1 Xenogeneic CDNPs do not induce xenogeneic rejection *in vitro* 110
5.1.1 Xenogeneic and allogeneic CDNPs reduce the expression of pro-

inflammatory cytokines after TLR-stimulation 111
5.1.2 Possible protective roles for anti-inflammatory CDNPs in viral infections 113
5.2 The anti-inflammatory effects of CDNPs *in vitro* and *in vivo* are dependent on their origin from stressed cells 114
5.2.1 The induction of anti-inflammatory T cell phenotypes *in vitro* and *in vivo* requires sCDNPs 114
5.2.2 CDNPs display the anti-inflammatory properties of RAMPs 115
5.2.3 Stressed-induced enrichement of annexin A5 might be the mediator of the anti-inflammatory effect of CDNPs 115
5.3 CDNPs have different effects in distinct infection models 118
5.3.1 CDNPs shift the T cell polarization towards anti-inflammatory and regulatory T cell subsets but have no impact on the clinical outcome of *L. major* infection 118
5.3.1.1 CDNPs induce DC maturation 118
5.3.1.2 CDNPS decrease the ratio of naïve vs. effector (memory) $CD4^+$ T cells 119
5.3.1.3 CDNPs shift the micromilieu at the infection site to the anti-inflammatory side 120
5.3.2 CDNPs are beneficial in sepsis 122
5.3.3 CDNPs enhance the activation of effector cells at the infection site of sepsis 122
5.3.4 CDNPs reduce bacterial loads at the infection site of sepsis 124
5.3.5 The impact of CDNP on survival in sepsis 126
5.3.6 Hypothetic model of immune-enhancement in sepsis due to the initial anti-inflammatory effect of CDNPs 126
5.4 CDNPs are endogenously produced *in vivo* 127
5.4.1 Possible mechanisms of CDNP release and uptake 128
5.5 Implication for the potential use of CDNPs as therapeutics 129

6. References 131

7. Appendix 151
7.1 Supplemental data 152
7.2 Abbrevations 155
7.3 List of Figures 161
7.4 List of Tables 163
7.5 Curriculum Vitae 164
7.6 Contributions to Conferences 165
7.7 Publications 166
7.8 Acknowledgements 167
7.9 Declaration 169

1. Abstract

Infectious diseases remain one of the major health problems worldwide. Cell-derived nanoparticles (CDNPs), which were described as endogenous mediators of intercellular communication under conditions of cellular stress, have emerged as new modulators of infections. The immunomodulatory capacities of CDNPs led to their industrial production and therapeutic use on a case-by-case basis in doctor's practices. Although, most of these treatments were described to be beneficial, the lack of understanding of their basic mechanisms of action and their origin from xenogeneic and stressed cells raised safety concerns and thus prevent their test in clinical studies. The present study demonstrates for the first time that xenogeneic CDNPs do not elicit pro-inflammatory responses in resting and activated macrophages *in vitro*. Surprisingly, they reduce the expression of zymosan-induced pro-inflammatory cytokines while increasing the expression of anti-inflammatory IL-10 instead. Moreover, *in vitro* and *in vivo* experiments confirmed that their origin from stressed cells is essential for their anti-inflammatory effects: only CDNPs derived from stressed cells reduce TNFα secretion by zymosan-stimulated macrophages and reduce $CD4^+$ T cell activation *in vitro*, while increasing dendritic cell activation and polarization towards anti-inflammatory Th2 and regulatory T cell subsets in *Leishmania major*- (*L. major-)* infected mice *in vivo*. Annexin A5 isoforms are considerably enriched in CDNPs derived from stressed versus unstressed cells, suggesting that this might be the active component of CDNPs. However, despite their clear immunomodulatory effects in *L. major* infection, CDNP treatment did not affect the clinical outcome of this disease. Thus, the effects of CDNPs were tested in the setting of polymicrobial sepsis. CDNP-treated mice demonstrated improved survival rates and an approximately 2-log lower bacterial load compared to control mice 24 hours after sepsis induction. In order to investigate the potential cellular mechanisms underlying the better infection control of CDNP-treated mice, CFSE-labeled CDNPs were injected into the peritoneum of septic mice. CDNPs were preferentially ingested by F4/80 macrophages, but were also taken up by inflammatory monocytes and neutrophils. Cells which ingested CDNPs exhibited increased activation as compared to those not ingesting. Furthermore anti-inflammatory IL-10 levels at the infection site were reduced by CDNPs. Finally, the accumulation of CDNPs at the infection site, were severe cellular stress occurs, was confirmed. Altogether our results indicate that CDNPs are an endogenous stress-induced mechanism to resolve inflammation. Importantly, CDNPs have therapeutic potential in infections with detrimental excessive inflammation such as sepsis.

Zusammenfassung

Die Bekämpfung von Infektionskrankheiten stellt eine der größten globalen Herausforderungen unserer Zeit dar. Zelluläre Nanopartikel (Cell-derived nanoparticles, CDNPs), beschrieben als endogene Mediatoren der interzellulären Kommunikation im Kontext von zellulärem Stress, wurden als neue Modulatoren von Infektionen identifiziert. Die immunomodulatorischen Eigenschaften solcher CDNPs führten zu ihrer industriellen Produktion und ihrem therapeutischen Einsatz auf Einzelfallbasis unter medizinischer Aufsicht. Obwohl solche Behandlungen ausnahmslos als vorteilhaft beschrieben wurden, verursacht das fehlende Wissen um ihre prinzipiellen Wirkmechanismus sowie ihr Ursprung aus xenogenen und gestressten Zellen Bedenken bezüglich ihrer immunologischen Verträglichkeit, was ihren Einsatz in klinischen Studien bislang verhinderte. Die vorliegende Arbeit demonstriert nun erstmals dass xenogene CDNPs keine immunogene Wirkung in naïven oder stimulierten Makrophagen *in vitro* besitzen. Überaschenderweise reduzieren sie stattdessen sogar die Zymosan-induzierte Expression pro-inflammatorischer Cytokine und erhöhen die Expression von anti-inflammatorischem IL-10. Weitere *in vitro* und *in vivo* Experimente bestätigten, dass der Ursprung aus gestressten Zellen sogar notwendig für diesen anti-inflammatorischen Effekt ist: Nur aus gestressten Zellen isolierte CDNPs reduzierten die TNFα-Sekretion von Zymosan-stimulierten Makrophagen und verringerten die Aktivierung von $CD4^+$ T Zellen *in vitro*, während sie die Aktivierung von Dendritischen Zellen erhöhten und die Polarisation von T Zellen in Richtung von anti-inflammatorischen sowie regulatorischen Subtypen in *Leishmania major*- (*L. major-)*infizierten Mäusen verschoben. Annexin A5 Isoformen sind in CDNPs aus gestressten Zellen im Vergleich zu solchen aus ungestressten Zellen angereichert, und stellen somit vermutlich die aktive Komponente der CDNPs dar. Jedoch haben CDNPs trotz ihres klaren immunomodulatorischen Effekts in der *L. major*-Infektion keinen Einfluss auf die Stärke der Krankheitsausprägung. Daher wurde der klinische Effekt von CDNPs in einem Mausmodell der Sepsis getestet. Mäuse, die mit CDNPs behandelt wurden zeigten höhere Überlebensraten und eine um ca. 2 Logstufen reduzierte Bakterienlast 24 Stunden nach Sepsisinduktion. CDNPs wurden hauptsächlich von F4/80 Makrophagen aufgenommen, fanden sich aber auch innerhalb von inflammatorischen Monozyten und Neutrophilen. Zellen, die CDNPs aufgenommen haben zeigten erhöhte Zellaktivierung als solche, die keine CDNPs aufgenommen haben. Darüber hinaus verringerten CDNPs die Sekretion von anti-inflammatorischem IL-10 an der Infektionsstelle. Schließlich wurde die Ansammlung von endogen produzierten CDNPs in der zellfreien Peritonealflüssigkeit gezeigt. Insgesamt implizieren die hier dargestellten Ergebnisse, dass

CDNPs einen endogenen, stress-induzierten Mechanismus zur Auflösung von Entzündungen darstellen. Ein therapeutischer Einsatz von CDNPs erscheint auf Basis dieser Ergebnisse besonders dort angebracht, wo Infektionen mit überschießenden, schädlichen Entzündungsreaktionen einhergehen, wie etwa in der Sepsis.

2. Introduction

2.1 The immune system

The immune system comprise a network of cells, tissues and organs which form the body's defense against foreign pathogens, toxins as well as its own abnormal cells. The first step in host defense is executed by the unspecific innate immune response. This response is mediated by innate cells such as macrophages and neutrophils which phagocytose and eliminate pathogens. In addition, humoral components such as the complement system participate in the innate host defense. The next layer of immune protection is formed by the adaptive, specific immune response. Antigen-presenting cells (APCs), such as dendritic cells (DCs) take up, process and present foreign antigens in the context of MHC molecules. When such an antigen-presenting DC encounters a lymphocyte with a specific receptor for this distinct antigen, the lymphocyte gets activated by the interaction of its receptor with the antigen-MHC complex and further co-stimulatory molecules upregulated on the surface of the DC. Activated B cells undergo somatic hypermutation to further select for antigen-specificity and then mature to antibody-producing plasma cells. Activated $CD8^+$ and $CD4^+$ T cells undergo clonal expansion and either directly lyse intracellular parasites ($CD8^+$ T cells) or polarize to effector T cells ($CD4^+$ T cells). The best characterized Th cell subsets are Th1 cells producing IFNγ and activating macrophages to kill intracellular parasites and Th2 cells which secrete IL-4 and induce a response against extracellular helminth infections.

2.2 Self and non-self recognition

To properly defend the body from invading pathogens, it is essential for the immune system to effectively discriminate between harmless self-antigens and potentially dangerous invading non-self parasites. Not only would the misinterpretation of non-self as harmless lead to uncontrolled infection and disease, self-reactivity likewise would induce harmful autoinflammation and -immunity. Hence, self/non-self discrimination is one of the very core tasks of the immune system. While the innate immune response detects non-self mainly by pattern recognition receptors (PRRs), adaptive immunity relies on the selection of non-self-reactive lymphocytes during maturation and the activity of suppressive T regulatory (Treg) cells.

2.2.1 Pattern recognition receptors (PRRs)

Innate immune cells have developed a large repertoire of germ-line encoded pattern recognition receptors (PRRs) to detect and identify diverse pathogens such as bacteria, parasites, viruses and helminths. PRRs recognize structurally conserved pathogen-associated molecular patterns (PAMPs), with different PRRs being specialized in the detection of distinct microbe-specific PAMPs, thereby allowing a tailored immune response. PRRs are mainly expressed on immune cells, including monocytes/macrophages, DCs, B cells and specific T cells subsets. However, they are also found on cells involved in barrier functions such as epithelial cells and fibroblasts [1].

Four main classes of PRRs have been described so far: Toll-like receptors (TLRs), Nucleotide-binding oligomerization domain (NOD)-like receptors, Retinoic-acid-inducible protein I (RIG-I)-like receptors and C-type lectin receptors (CLRs).

The best-characterized group of PRRs are TLRs, a family of type I integral membrane glycoproteins expressed on the surface membrane of cells and their endosomal compartments. The extracellular TLR domain is characterized by leucine-rich-repeat (LRR) motifs recognizing PAMPs, while its cytoplasmic signaling domain contains a Toll/IL-1 receptor (TIR) homology domain [2]. Triggering of TLRs induces dimerization of TLRs and their cytoplasmatic domains, initiating the recruitment of adaptor molecules with a TIR domain, namely MyD88 and/or TRIF, to its cytoplasmatic portion and resulting in a downstream cascade of activated signal molecules. Ultimately, TLR signaling leads to the activation of transcription factors regulating the expression of genes involved in the antimicrobial host defense. The main target genes are cytokines, with MyD88-dependant signaling primarily inducing the expression of pro-inflammatory cytokines such as TFNα and MyD88-independent signaling inducing the expression of antiviral IFNβ (Fig. 2-1). Further targets are genes for the expression of adhesion molecules, costimulatory molecules, growth factors and enzymes that generate inflammatory mediators such inducible nitric oxide synthase (iNOS).

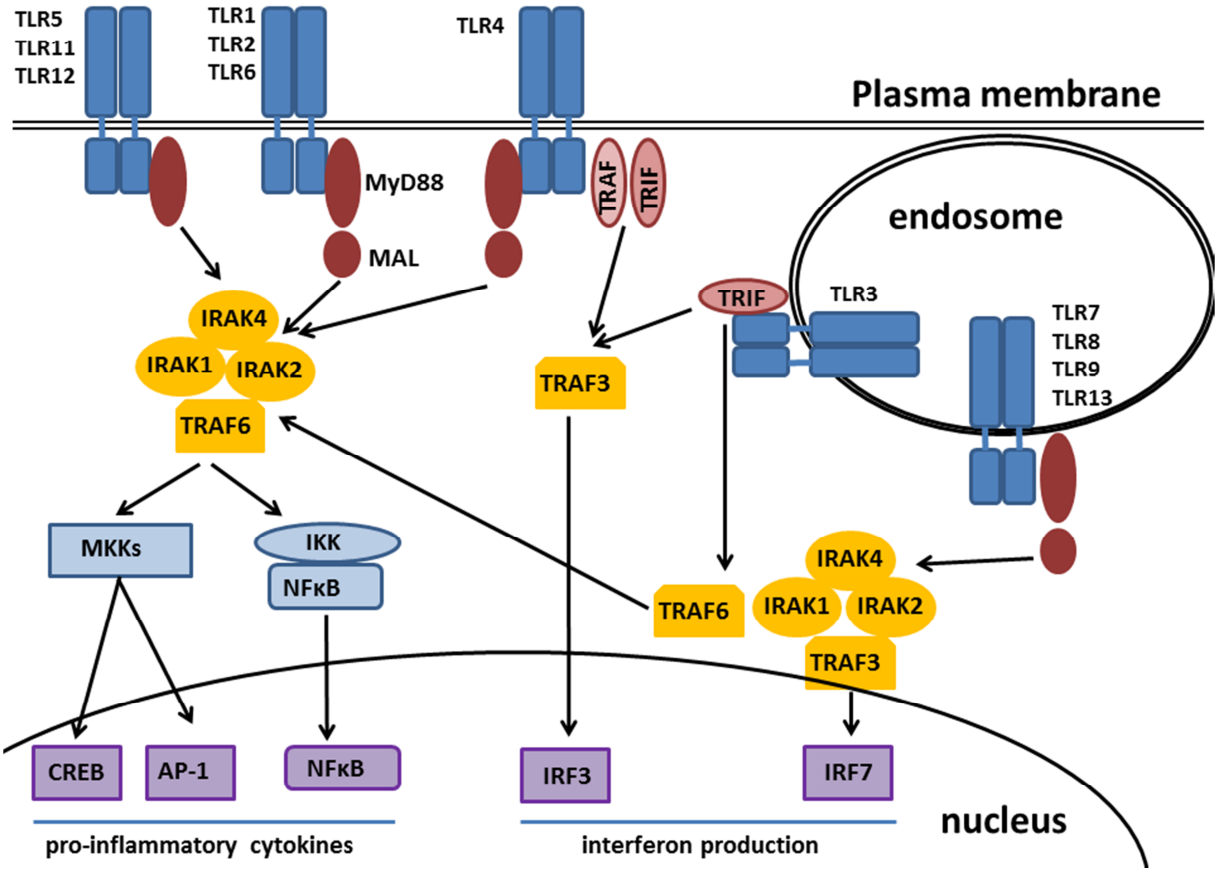


Fig. 2-1: MyD88-dependent and MyD88-independent signaling pathways of TLRs (modified from [3]). TLR triggering leads to the recruitment of TIR domain containing proteins to the cytoplasmic portion of TLRs. These are either MyD88 or TRIF. All extracellular TLRs use a MyD88-dependant signaling pathway to activate the transcription factors CREB, AP-1 and/or NFκB resulting in the transcription of pro-inflammatory cytokines such as TNFα. TLR4 triggering additionally activates the TRIF-dependent, MyD88-independent signaling pathway thereby activating the transcription factor IRF3 and thus inducing the transcription of IFNβ. Regarding the endosomal TLRs, TLR3 triggering activates MyD88-independent expression of IFNβ, while all other endosomal TLRs induce MyD88-dependant IRF7 activation ultimately leading to the transcription of IFNα.

AP-1: activator protein 1, CREB: cyclic adenosine monophosphate-responsive element-binding protein, IKK: inhibitor of NF-κB kinase, IRAK: interleukin-1 receptor-associated kinase, IRF: interferon-regulatory factor, Mal: MyD88-adaptor like protein (also called Tirap), MKK: mitogen-activated protein kinase kinase, NF-κB : nuclear factor-κB, TRAF: TNF receptor-associated factor, TRAM: TRIF-related adapter molecule, TRIF: TIR-domain-containing adapter-inducing interferon-β.

The 12 murine TLRs can be classified according to their ligand specificity, the adaptor proteins they recruit, as well as their expression patterns and cellular localization. Owing to the key importance of TLRs in the discrimination of self vs. non-self, a short description of all TLR members will follow below:

TLR1, TLR2, TLR6: TLR2 forms functional heterodimers with TLR1 and TLR6 recognizing bacterial and mycobacterial lipopeptides and lipoproteins [4]. In addition, this TLR is able to recognize lipophosphoglycans (LPGs) from protozoa such as *Leishmania major* (*L. major*) [5,6]. Triggering by bacterial and viral glycoproteins has also been reported [7]. **TLR4** in conjunction with MD2, CD14 and LPS-binding protein, is triggered by the lipid A component of lipopolysaccharide (LPS), a cell wall component of gram-negative bacteria [4]. **TLR3** is triggered by viral double-stranded (ds) RNA, while the structurally conserved **TLR7** and **TLR8** sense single-stranded (ss) RNA of viral origin [7,8]. Interestingly, neither of these TLRs is triggered by host RNA, although ssRNA is abundantly present in the cell. This is mainly attributed to the localization of these TLRs inside endosomes, where only foreign RNAs can be found [8]. **TLR9** is triggered by DNA of bacterial and viral origin, which is rich in unmethylated CpG motifs. In contrast, vertebrate DNA contains significantly less of these motifs protecting it from recognition [7,8]. Similar to TLR3, 7, and 8, TLR9 is mainly expressed in endosomes, further preventing the recognition of endogenous DNA [8]. **TLR5** detects the protein flagellin, the principal component of bacterial flagella [7,8] and **TLR11, TLR12 and TLR13** have been reported to recognize profilin from *Toxoplasma gondii* and the CGGAAAGACC motif of bacterial ribosomal RNA [9].

2.2.2 Natural antibodies and the complement system

Additional innate immune mechanisms to discriminate self from non-self are natural antibodies and the complement system. Natural antibodies of the subclasses IgM, IgG3 and IgA are constitutively secreted by innate immune cells with B1 cells being the major producers [10]. B1 cells comprise a distinct B-cell subset that almost exclusively resides in the peritoneal cavity, but is also found in the spleen and bone marrow (BM). Since natural antibodies are germline encoded and do not undergo somatic hypermutation their repertoire does not possess antigen specificity. Instead, the natural antibody repertoire recognizes a wide range of microbial patterns such as bacterial toxins, but also non-protein antigens like phosphatidylcholine and carbohydrate determinants. Natural antibodies fulfill their anti-microbial functions by neutralization and triggering of Fc receptors such as Fcα/γ/μR on B cells and DCs and thus induce pathogen clearance [11,12]. In addition, natural antibodies

activate the complement system, a network of around 50 different molecules ranging from factors circulating in the blood and tissue fluids to membrane-bound receptors and its regulators [13]. Complement activation initiates an activation cascade which ultimately leads to phagocytotic bacterial clearance and/or bacterial lysis.

2.2.3 The adaptive immune system

Downstream events of PRR and complement activation all induce cytokine secretion, thereby activating T cells and instructing T cell polarization. Consequently, the innate self/non-self discrimination already has a high impact on the adaptive immune response. In addition, T and B cells use very own, unique self/non-self discrimination strategies.

Since the adaptive immune system recognizes proteins, and pathogenic proteins are not structurally different from self-proteins; adaptive immune cells have to learn to differentiate self from non-self proteins during their maturation [14]. This process is called central tolerance. For both, B- and T cells this is achieved via negative selection in the thymus and BM respectively. T- and B- cells gain an extensively diverse receptor repertoire during their development. By chance, a great amount of these randomly generated receptors will recognize self-antigens. Thus, in order to avoid autoreactivity, pre-T- and -B cells undergo a tight negative selection processes [15,16]. To this end, thymic epithelial cells present self-antigens to T cells in the context of MHCI and MHCII, while B cells encounter self-antigens in the BM [17,18]. Cells that demonstrate high affinities to self-antigens are subjected to cell death or anergy. In case of T cells, self-reactivity can also induce the polarization to tolerogenic Tregs [18].

Since central tolerance cannot eliminate all self-reactive lymphocytes, there is an additional layer of peripheral tolerance preventing autoreactivity. First, recognition of the peptide-MHC-T cell receptor (TCR) complex is not sufficient to induce T cell activation. Only the additional signal from costimulatory molecules expressed on APCs will induce activation and proliferation [16]. Such costimulatory molecules in turn are often induced after activation of PRRs or other pathogen recognition pathways discussed above, while self-antigens fail to activate them. Moreover, the concentration of the TCR ligand, i.e. the antigen dose, is playing a crucial role in the induction of peripheral tolerance [14]. Similar to central tolerance, peripheral tolerance is then established by deletion of self-reactive T cells, anergy or polarization to Tregs [16].

2.2.4 Recognition of xenogeneic non-self

The previous chapters described how the host immune system discriminates between self- and pathogen-derived antigens. However, the immune system is also able to recognize non-self molecules from other species, i.e. xenogeneic molecules. In principle, all of the mechanisms described above are also able to recognize xenogeneic material. However, the main mechanisms responsible for the detection of xenogeneic antigens are PRRs such as TLRs [19], as well as natural antibodies [20]. Human natural antibodies, for example, were shown to be highly reactive against Galα1,3Galβ1,4GlcNAc residues present on porcine tissue [21,22]. Opsonization of xenogeneic material with natural antibodies activates the complement system [23,24]. The consequences of these pathways is xenograft rejection including complement-mediated recruitment of inflammatory cells such as neutrophils and monocytes [25], tissue destruction and heammorhage due to the loss of endothelial integrity. Finally, the xenograft itself, but also surrounding tissues might be damaged, destroyed and subjected to necrosis [25]. Hence, the transplantation of xenogeneic material bears great risks of severe and possibly life threatening immune reactions.

2.3 Recognition of stressed and damaged self

For a long time, self and non-self discrimination was regarded as the key concept in immunology. However, not only external antigens can pose a dangerous threat to the body, but also its own cells and molecules, e.g. if they are abnormal or damaged. Thus, in 1994 Matzinger introduced the danger concept [26] which stated that the principal function of the immune system is to combat danger in general, independent of its self- non-self origin. Consequently, next to detecting foreign antigens, the immune system also reacts to cell damage and -death caused by stress or infection [26–28].

2.3.1 Detection and discrimination of cell death

Since cell death occurs ubiquitously in the human body with an estimated one million physiological deaths in the course of tissue turnover per second, the immune system needs a precise machinery to discriminate healthy and dangerous kinds of cell death [29]. Apoptosis is often described as a physiological, programmed cell death. This process is highly controlled, as it does not occur spontaneously, but is induced by a set of tightly regulated caspases, nucleases and proteases. Apoptosis is characterized by cell shrinking, membrane blebbing, cytosolic and nuclear condensation and segmentation of DNA. Finally, the cell falls apart by

formation of apoptotic bodies. Accordingly, apoptotic cells and bodies retain their membrane integrity throughout the whole process [30,31]. In contrast, necrosis is described as a more unordered form of cell death induced by cell damage or infection. The consequence is cell swelling, rapture and lysis [31].

In fact, the immune system can discriminate physiological (apoptosis) from pathogenic (necrotic) cell death using two basic mechanisms. First, apoptotic cells expose phosphatidylserine (PS) on their surface, which is recognized by APCs. Ingestion of such cells leads to the suppression of APC maturation, thereby rendering the APC tolerogenic and even induces the secretion of anti-inflammatory cytokines upon stimulation [32–34]. Secondly, natural IgM antibodies with a strong preference for apoptotic cells/bodies have been shown to promote silent phagocytic clearance [12]. Indeed, it was shown that only necrotic cells co-injected with non-immunogenic antigens induced APC maturation and elicited antigen-specific T cell responses, while apoptotic cells did not provoke immune cell activation [34]. However more recent studies challenged this too simplified view by demonstrating that i) necrosis itself is highly controlled and different forms of necrosis exist inducing different immune responses including anti-inflammatory ones [35], ii) lysed/necrotic lymphocytes do not always induce cell activation, [36], and iii) apoptotic cells are also able to elicit immune responses [37,38].

2.3.2 Damage-associated molecular patterns (DAMPs)

Hence, it has been proposed that many subtypes of cell-death such as immunogenic and non-immunogenic apoptosis exists and each of them is defined by subtle differences in the release of danger-associated components which might be decisive for the induction of inflammation [29,39]. Such components were termed damage-associated molecular patterns (DAMPs) and defined as intracellular molecules, which are thus normally hidden from the immune system. However, when the cell becomes stressed, injured or damaged it actively or passively (via cell death) releases DAMPs into the extracellular space, therefore allowing their detection by and subsequent activation of the immune system. Likewise, extracellular matrix molecules are normally sequestrated inside the matrix and only become immunogenic when released upon tissue injury [40,41]. Just like PAMPs, DAMPs are able to activate PRRs such as TLRs. Consequently, DAMPs induce the expression of pro-inflammatory cytokines and drive APC maturation thereby inducing the expression of costimulatory molecules needed to initiate T cell activation [42].

The first identified DAMPs were heat shock proteins (HSPs), among them HSP60 [43], HSP70 [44] and HSP72 [45]. Further intracellular DAMPs include S100 proteins [46], high mobility group box protein 1 (HMGB1) [47], uric acid [48] and ATP [49]. Self-RNA (mRNA and ssRNA) was identified as a DAMP as well [50,51]. Extracellular matrix molecules acting as DAMPs include biglycan, tenascin-C, versican, oligosaccharides of hyaluronic acid and heparin sulfate [27]. Initially, all of these DAMPs were shown to activate TLRs, however newer studies suggest, that at least some of these original results, in particular those concerning HSPs, were actually due to endotoxin contaminations frequently present in recombinant proteins expressed by *Escherichia coli* [27]. Unexpectedly, some molecules formerly classified as DAMPs, even showed anti-inflammatory and resolving properties when highly purified and endotoxin-free proteins were used [52,53]. Accordingly, such molecules were re-named as resolution-associated molecular patterns (RAMPs) [53].

Other molecules were indeed shown to be pro-inflammatory, however not in their original intracellular form, but after chemical modifications. Good examples are HMGB1 which only acts immunogenic when it is reduced [54] and uric acid which elicits immune response as a microcrystal [55].

2.3.3 Resolution-associated molecular patterns (RAMPs)

RAMPs were defined as endogenous molecules released upon cellular stress and damage. However, in contrast to DAMPs they do not induce inflammation, but resolve it via antagonizing pro-inflammatory mediators and deactivating immune cells, while expanding regulatory cells [53]. As such, they are mediating immunological homeostasis similar to other regulatory mediators such as lipoxins and resolvins [56]. Likely, damaged cells can release both DAMPs and RAMPs simultaneously, in order to prevent an exacerbating immune response leading to chronic inflammation, which has been implicated to evolve upon uncontrolled or prolonged DAMP release [27]. This idea is in line with the concept of a coordinated resolving program initiated at the very beginning of each inflammatory response [57].

The following proteins have been re-classified as RAMPs so far: HSP10, HSP27, BiP and crystallins [53]. The homeostatic function of HSPs in particular has been studied extensively and it was suggested to be part of the physiological cell communication system [58]. Figure 2-2 integrates the concepts of PAMPs, DAMPs and RAMPs.

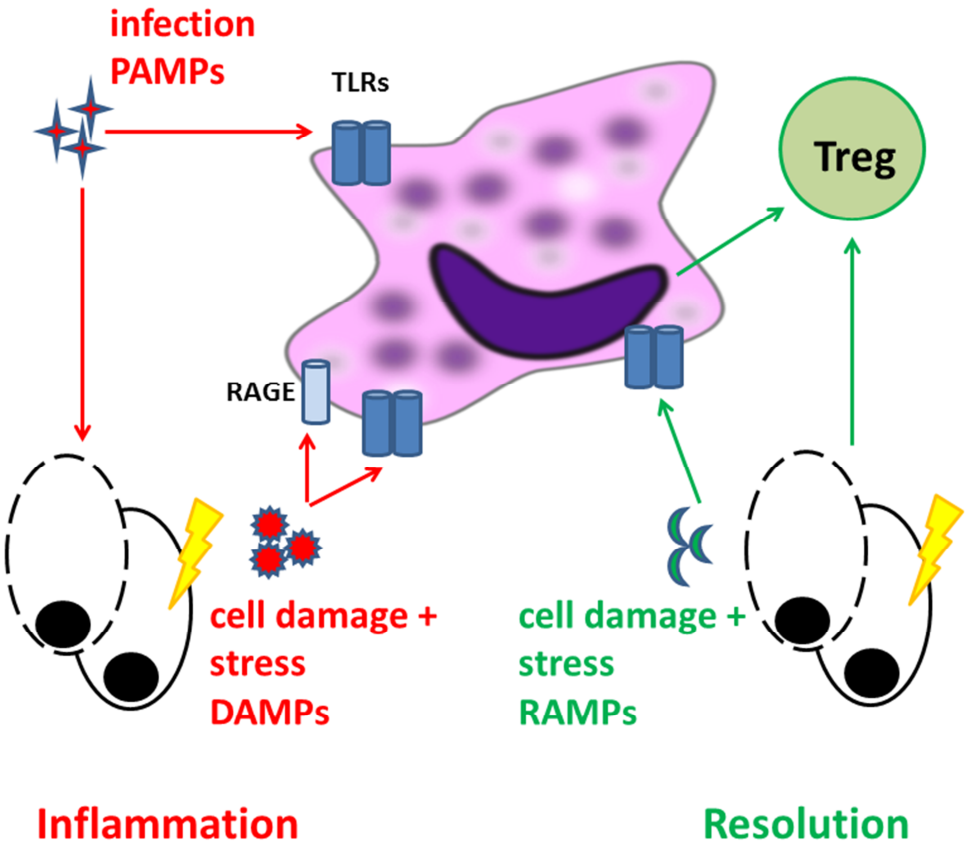


Fig. 2-2: Integrative concept of PAMPs, DAMPs and RAMPs (modified from [53]). Pathogens possess evolutionary conserved PAMPs which are recognized by PRRs such as TLRs thereby inducing inflammation. In addition, pathogens induce pathological cellular stress or damage, leading to the release of pro-inflammatory endogenous DAMPs. Similar to PAMPs, DAMPs trigger TLRs, but also the DAMP-specific receptor RAGE. Both result in the initiation of a pro-inflammatory response. RAMPs may be induced together with DAMPs to resolve the inflammatory response. Alternatively, RAMPs are released by physiological (mild) stress and cell damage to prevent inflammation and maintain tolerance.
RAGE: Receptor for advanced glycation end products.

2.4 Cell-cell communication under physiologic and stressed conditions

Even under physiological conditions, cells are consistently communicating with each other. This is mainly done by use of soluble molecules such as cytokines or hormones released into the extracellular space and “received” by surrounding cells via specific receptors on the cell surface. Furthermore, cells can release mediators enclosed in exosomes, microparticles (MPs) and apoptotic bodies. All of them are membrane surrounded vesicles carrying different cargos, which differ in their size and formation mechanisms. Exosomes are released via

exocytosis and measure 40-100nm in size. MPs bud directly from the cell surface and are bigger then exosomes (200-900nm). Apoptotic bodies likewise blebb from the cell membrane but represent the biggest particles measuring 1-4µm [59]. Additional forms of cell-cell communication include a direct transfer via cellular synapses (trogocytosis) [60] and nanotubes [61]. Small molecules can also be exchanged between adjacent cells by gap junctions [62].

Under physiologic conditions, cell-cell communication serves to synchronize and coordinate basic cellular processes such as gene expression and metabolic activities. Similarly, in the case of cellular stress it could prime the cells for an efficient use of their resources and suppress a propagation of the initial insults thereby preventing cell exhaustion [58].

HSPs and other RAMPs might constitute an additional cell communication method which is solely used under conditions of cellular stress [58]. The expression of such stress proteins is upregulated under conditions of cellular stress such as acute inflammation, hypoxia, hypoglycemia and heat, all of which induce protein denaturation [58,63]. Accumulation of misfolded and denaturated proteins inside the endoplasmatic reticulum (ER) initiates the coordinated, conserved unfold protein response (UPR). The main function of the UPR is to clear this accumulation, by helping misfolded proteins to re-fold correctly. Inside the cell, HSPs act as chaperons providing a protected microenvironment for proteins to fold/re-fold and thus allowing for optimal protein function despite suboptimal conditions [64]. To this purpose, the expression of stress proteins is selectively upregulated, while the expression of all other proteins is stopped. Interestingly, HSPs do not only exert intracellular functions, but can also be secreted into the extracellular space via a non-classical secretion pathway. Hence, extracellular HSPs were classified as mediators of cellular stress which act as survival signals for surrounding cells. This stress response was named stress observation system (SOS) [58]. Indeed, it was shown that HSP release is beneficial for the recovery from stress [63,65].

Cell-derived nanoparticles, which contain HSPs, might also be part of a stress response system.

2.5 Cell-derived nanoparticles (CDNPs)

First reports describing the presence of cell-derived nanoparticles, then called "*Biokomplex-Reaktionsmuster in Vertebratenzellen*" (BK-RiV, biocomplex reaction pattern in vertebrate cells), emerged in 1986. Using an electron microscope (EM), they were characterized as spherical entities with a diameter of 50±15 nm, which localized intra-, as well as extracellularly. Intracellularly, groups of several CDNPs were sometimes found inside a lipid

membrane. CDNPs contain small traces of RNA and DNA, but are mainly composed of intracellular proteins. The most abundant components are HSPs and annexins [66,67]. Typical components of CDNPs are listed in Tab.1.

Tab. 1: Typical composition of CDNPs [66,67]

proteins		nucleic acids
14-3-3ε	Myosin (light chain)	ribosomal RNA
14-3-3ζ	natural killer enhancing factor	mRNA
Actin	Nm23	RNA
Aldolase	Nucleolin	DNA
α-actinin	PDI	
Annexin I	Proteasom C6	
Annexin I isoform (H156Y)	Proteasom I	
Annexin V	Proteasom δ	
Calreticulin	Ribosomale protein L7	
Enolase	S100A2	
ER-60	S100A4	
Ezrin	Vimentin	
Galectin-3	Hevein-homologue with the partial sequence	
gCAP39	XQXGRQAGG- KLXPDN	
Glutathion-S Transferase	Stratherin-homologue with the partial sequence	
Heat shock protein 27	FGYGYGPYQPVPEQP	
Heat shock protein 70		
Histon 2A		
Histon 2B		

CDNPs were detected *in vitro* and *ex vivo* in stressed cultures of primary cells and cell lines which were infected with different viruses. Hence their production was attributed to cellular stress such as nutrient deprivation, hypoxia and infection-induced inflammation. Since CDNPs were only present in samples showing low or intermediate virus replication, but were absent in samples with massive virus loads, the authors speculated that CDNPs represent an endogenous resistance mechanism protecting the host cell from infection [68]. Further experiments in the context of virus-induced mouth-and-foot disease confirmed that treatment with xenogeneic CDNPs derived from stressed cell cultures proves beneficial, reducing the phenotypical symptoms and increasing survival rates of infected guinea pigs [69]. Based on the positive *in vivo* results, commercial CDNP production under GMP conditions in an endotoxin-free environment was established by Varicula Life Science AG using a porcine cell line stressed by nutrient deprivation. Commercially available CDNPs were used for s.c. and i.m. injections in humans carrying infectious diseases such as hepatitis C and HIV on a single

case basis and under constant medical supervision as an adjuvants therapy. However, despite numerous positively responding patients and no reported side effects, no clinical trials needed for an approval of CDNP therapy on a bigger scale were conducted yet [67]. The main reason is the lack of profound research on CDNPs and their mode of action.

2.5.1 Infectious diseases models

Infectious diseases are defined as disorders of "a body, system or organ structure resulting from the presence and activity of a microbial agent" [70]. Classically, these agents are classified as intracellular, such as viruses or intracellular parasites or extracellular such as bacteria [71]. Previous findings suggest that CDNPs have protective effects in viral infections in mice and humans [69,72]. Whether this effect is restricted to viral infections is not known. Therefore, this study focused on the immunomodulatory effects of CDNPs in intracellular infections of *L. major* and polybacterial sepsis. Since *L. major* represents an intracellular parasite, it is likely that the immunomodulatory effects in this model are similar to the ones observed in viral infections. In contrast, polymicrobial sepsis is induced by extracellular bacteria and no data regarding the impact of CDNPs in such models exists so far.

2.5.1.1 *Leishmania major* infection

The protozoan *Leishmania* spp. is an intracellular parasite within the family of *Trypanosomatidae* [73]. *Leishmania* are transmitted by female sandflies which inoculates metacyclic promastigotes into the skin of a mammalian host while feeding on blood [74]. This infective form of *Leishmania* is characterized by its motile, flagellated and elongated appearance. Once inside the host, promastigotes are rapidly phagocytosed by APCs such as neutrophils and macrophages and replicate inside their phagolysosome. Moreover, they transform to their intracellular amastigote appearance by losing their flagellum and assuming a condensed, oval form [73].

Leishmania cause leishmaniasis, a neglected infectious diseases prevalent in 88 countries worldwide with an incidence of over 2 million annually [75]. The clinic manifestation of leishmaniasis is mainly dependent on the *Leishmania* species and the genetic background of the host ranging from localized and self-healing skin lesions (cutaneous leishmaniasis) to potentially fatal dissemination to inner organs (visceral leishmaniasis). Cutaneous leishmaniasis mainly caused by the species *L. major* is the most prevalent clinical manifestation [76].

Infection of mice with *L. major* is an established immunological model to study intracellular infections and T cell differentiation [77]. Since *L. major* is an intracellular parasite, its elimination relies on the formation of a Th1 response. Various studies demonstrate that CpG-rich *Leishmania* DNA triggers TLR 9 [78,79] and LPG expressed on the surface of the parasite triggers TLR2 [80,81] thereby driving Th1-inducing IL-12 production. Th1 cells then produce large amounts of IFNγ and migrate to the infection site, where they in turn activate macrophages to produce reactive nitrogen species killing the intracellular parasite [82]. Indeed, most laboratory mouse strains infected with *L. major* including C57BL/6 mice, react similar to human hosts and develop initial symptoms like swelling and ulceration of the skin at the infection site, which eventually heal (Fig. 2-3). However, the healing of *L. major*-induced leishmaniasis is not sterile: a small reservoir of surviving parasites is controlled by IL-10-releasing $CD4^+$ $CD25^+$ Tregs warranting a lifelong immunization [83].

In contrast, genetic susceptible mouse strains like BALB/c "wrongly" induce Th2 polarization, an immune response generally assigned to combat extracellular infections via IL-4 release, induction of antibody production and activation of granulozytes and mast cells [82]. Such Th2-polarizing mouse strains fail to control infection leading to systemic inflammation (Fig. 2-3) [84].

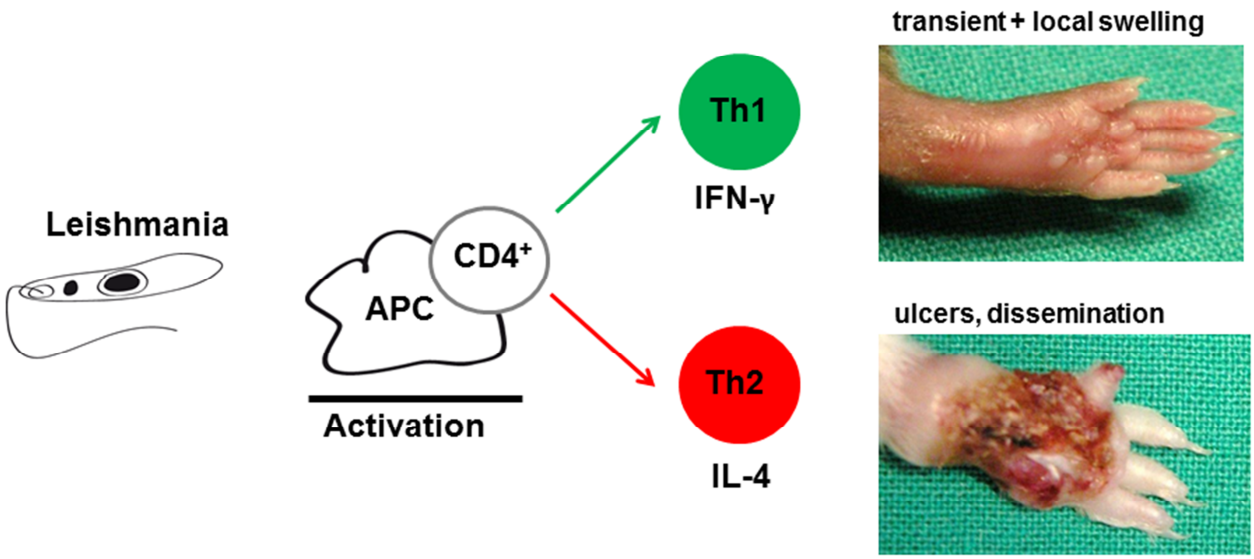


Fig. 2-3: T cell polarization and its consequences in *Leishmania* infection. When *Leishmania* are injected into the foot pad skin, they infect APCs which then present *Leishmania* antigens to T cells. Depending on the genetic background, T cells polarize rather to Th1 cells which are crucial for healing or Th2 cells which are ineffective in fighting the disease, leading to permanent foot pad swelling, ulceration of the skin and dissemination of the parasite to visceral organs.

2.5.1.2 Sepsis

Sepsis is a severe medical condition characterized by a dysregulated, systemic host response to infection, leading to multiple organ failure and death [85]. Sepsis proceeds in two distinct, but overlapping phases: an initial pro-inflammatory “cytokine-storm” and the subsequent immunosuppressed state (Fig. 2-4). During the first phase, monocytes, macrophages, and neutrophils are recruited to the infection site and excessively secrete pro-inflammatory mediators such as IL-1β, TNFα and IL-6, chemokines and reactive oxygen species (ROS). Importantly, this release is not limited to the infection site, but becomes systemic [86], resulting in vascular leakage and organ damage. In this phase, bacterial antigens are ingested and cleared by ROS releasing macrophages. Additionally, APCs which have ingested bacterial antigens activate adaptive lymphocytes via antigen presentation in the context MHC II [87,88].

However, while most patients survive the early hyper-inflammation, the immunosuppressed phase is regarded as the major cause of death among septic patients [87,89]. It is believed that this compensatory anti-inflammatory response syndrome (CARS) is caused by excessive apoptosis of immune cells over-activated and thus exhausted in the hyperinflammatory phase [87,90,91]. PS-expressing apoptotic cells are ingested by macrophages in a tolerogenic manner, leading to the release of anti-inflammatory IL-10 and TGFβ [92]. In addition, neutrophils release PS-expressing microparticles (neutrophil-derived microparticles, NDMPs) having the same anti-inflammatory effect as apoptotic cells [93–95]. Consequently, cell functions are heavily impaired under this state [87,96] as reflected by reduced surface expression of activation markers, limited phagocytosis and bacterial clearance, as well as diminished antigen presentation. Paralyzed effector cells are unable to eradicate the primary infection, rendering the immune system highly susceptible to secondary infections [88].

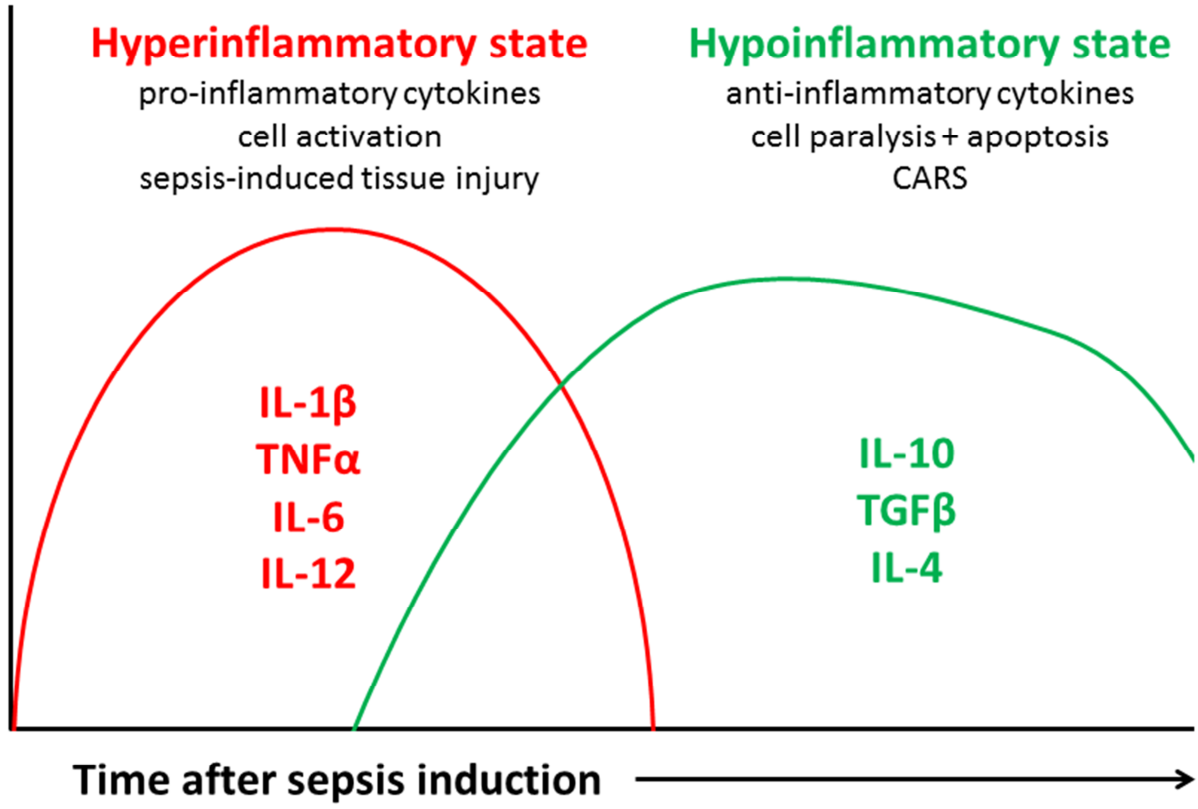


Fig. 2-4: The two phases of sepsis (modified from [97])**.** Sepsis first induces a hyperinflammatory state, followed by the immunosuppressed CARS.

2.6 Aims of this thesis

Infectious diseases remain one of the major health problems worldwide. CDNPs, which were described as endogenous mediators of intercellular communication under conditions of cellular stress, emerged as new modulators of infectious diseases [69]. These immunomodulatory capacities of CDNPs led to their industrial production and therapeutic use on a single scale basis in doctoral practices. Although, most of these treatments were described to be beneficial [67], the lack of understanding of their basic mechanisms of action and their origin from xenogeneic and stressed cells prevented their use on a broader scale or their test in clinical studies. In particular, the xenogeneic origin of commercially available CDNPs raises concerns of a potentially dangerous rejection reaction. Moreover, their origin from stressed cells might classify CDNPs as immunogenic and thus potentially dangerous DAMPs. However, CDNPs have also been proposed to have anti-inflammatory and resolving properties, which would make them beneficial RAMPs instead [66]. This notion is supported by the presence of HSPs, implicating that they might act as particulate mediators of cell survival similar to HSPs alone [58]. Yet, all evidence for the presence of CDNPs was only found *in vitro* and *ex vivo*, while their *in vivo* production never was assessed. Therefore, it is unknown whether CDNPs indeed are released *in vivo*. Hence, it remains controversial whether CDNPs act as DAMPs, RAMPs or are part of the cell-cell communication as part of SOS. Finally it is not known, whether the beneficial effect of CDNPs is limited to viral infections, intracellular pathogens or also protects against extracellular bacteria. Therefore, the present study focuses on elucidating following questions:

i) Do xenogeneic CDNPs evoke immunogenicity?
ii) What is the basis of the immunomodulatory effect of CDNPs? Is this effect induced by stress? What is the active component of CDNPs?
iii) Is the beneficial effect of CDNPs limited to viral infections or does it also holds true in a model of intracellular *L. major* infection and extracellular infections such as sepsis?
iv) Are CDNPs endogenous mediators of cell-cell communication?

3. Materials and Methods

3.1 Materials

3.1.1 Animals, pathogens and cells

C57BL/6J	Charles River Laboratories GmbH, Sulzfeld, Germany
C57BL/6J	Charles River Laboratories, Wilmington, MA, USA
C57BL/6J	ENVIGO, Indianapolis, IN, USA
Murine fibroblast-like cell line MC3T3-E1	Deutsche Sammlung von Mikroorganismen und Zellkulturen, Braunschweig, Germany
Pseudomonas aeruginosa (PA01)	Prof. Charles C. Caldwell, Department of Surgery, University of Cincinnati, USA
Leishmania major (MHOM/IL/81/FE/BNI)	Prof. Dr. Tamás Laskay, Department of Infectious Diseases and Microbiology, University of Lübeck, Germany

3.1.2 Antibodies

Antibody	Clone	Dilution	Manufacturer
Akaline Phosphatase-conjugated Mouse anti-FITC Antibody	Polyclonal	1:5000	Jackson Immuno Research, West Grove, PA, USA
AlexaFluor 647 anti-mouse CD8	5H10	1:300	Caltag Medsystems Ltd., Buckingham, UK
Alexa Fluor 647 Rat anti-mouse F4/80	CI:A3-1	1:100	AbD Serotec, Kidlington, UK
AlexaFluor 647 anti-mouse IFNγ	XMG1.2	1:100	BD Biosciences, San Jose, CA, USA
Annexin V Antibody	Polyclonal	1 :200 to 1 :1000	GeneTex, Irvine, CA, USA
APC anti-mouse CD11c	N418	1:100	eBioscience, San Diego, CA, USA
APC anti-mouse F4/80	BM8	1:50	eBioscience, San Diego, CA, USA
APC anti-mouse/rat Foxp3	FJK-16s	1:100	eBioscience, San Diego, CA, USA
APC-Cy7 Rat anti-Mouse CD11b	M1/70	1:100	BD Biosciences, San Jose, CA, USA
APC-Cy7 anti-mouse Ly-6C	AL-21	1:100	BD Biosciences, San Jose, CA, USA

Antibody	Clone	Dilution	Manufacturer
FITC anti-mouse/human CD11b	M1/70	1:100	Biolegend, San Diego, CA, USA
FITC anti-mouse CD25	PC61	1:100	Biolegend, San Diego, CA, USA
FITC anti-mouse CD4	GK 1.5	1:2,500	eBioscience, San Diego, CA, USA
FITC anti-mouse CD44	IM7	1:400	BD Biosciences, San Jose, CA, USA
FITC-conjugated goat anti rabbit IgG antibody	polyclonal	1:200	Jackson Immuno Research, West Grove, PA, USA
Infrared dye-conjugated anti–rabbit IgG IRDye800	polyclonal	1:10,000	Rockland Immunochemicals, Pottstown, PA, USA
PE Hamster anti-mouse CD11c	HL3	1 :100	BD Biosciences, San Jose, CA, USA
PE anti-mouse CD62L	Me 14	1 :300	eBioscience, San Diego, CA, USA
PE anti-mouse CD69	H1.2F3	1 :100	eBioscience, San Diego, CA, USA
PE anti-mouse F4/80	BM8	1:100	Biolegend, San Diego, CA, USA
PE anti-mouse IL-10	JES5-16E3	1 :100	eBioscience, San Diego, CA, USA
PE anti-mouse IL-4	11B11	1 :100	Biolegend, San Diego, CA, USA
PE anti-mouse Ly-6G	1A8	1 :100	BD Biosciences, San Jose, CA, USA
PE anti-mouse MHC calss II (I-A/I-E)	M5/114.15.2	1 :100	eBioscience, San Diego, CA, USA
PE Mouse anti-mouse I-Ab	AF6-120.1	1 :100	BD Biosciences, San Jose, CA, USA
PerCP-Cy5.5 anti-mouse B220	RA3-6B2	1 :100	eBioscience, San Diego, CA, USA
PerCP-eFluor 710 anti-mouse CD4	RM 4-5	1 :300	eBioscience, San Diego, CA, USA
PerCP-Cy5.5 Rat anti-mouse Ly-6G	1A8	1 :100	BD Biosciences, San Jose, CA, USA
Purified Rat anti-mouse CD16/CD32 (Fc-Block)	2.4G2	1 :1000	BD Biosciences, San Jose, CA, USA

3.1.3 Primer and probes

Name	Sequenz in 5´→3´	Accession-Nr.
BDNF forward	CCTGGATGCCGCAAACATGTC	NM_007540.4
BDNF reverse	CTGCCGCTGTGACCCACTC	
BDNF probe	TCACACACGCTCAGCTCCCCACGG	
IFN-β forward	GGAGCAGCTGAATGGAAAGATC	
IFN-β reverse	CTCTTGGATGGCAAAGGCAG	
IFN-β probe	CTGCATCTTCTCCGTCATCTCCATAGGGATC	
IFN-γ forward	GCAAGGCGAAAAAGGATGC	NM_008337.3
IFN-γ reverse	GACCACTCGGATGAGCTCATTG	
IFN-γ probe	TGCCAAGTTTGAGGTCAACAACCCACAG	
IL-1β forward	CTTCCAGGATGAGGACATGAG	NM_008361.4
IL-1β reverse	CACACCAGCAGGTTATCATC	
IL-1β probe	CATCTTTGAAGAAGAGCCCATCCTCTGTGAC	
IL-4 forward	GAGACTCTTTCGGGCTTTTCG	NM_021283.2
IL-4 reverse	AGGCTTTCCAGGAAGTCTTTCAG	
IL-4 probe	CCTGGATTCATCGATAAGCTGCACCATG	
IL-6 forward	CTCCCAACAGACCTGTCTATAC	NM_031168.2
IL-6 reverse	GTGCATCATCGTTGTTCATAC	
IL-6 probe	TGCCATTGCACAACTCTTTTCTCATTTCCACG	
IL-10 forward	TCCCTGGGTGAGAAGCTGAAG	NM_010548.2
IL-10 reverse	CACCTGCTCCACTGCCTTG	
IL-10 probe	CTGAGGCGCTGTCATCGATTTCTCCC	
Kinetoplast forward	CCTATTCACTTACACCAA	EU370908.1
Kinetoplaste reverse	GGGTAGCGTGGGCATTCT	
MLN51 forward	CCAAGCCAGCCTTCATTCTTG	NM_138660.2
MLN51 reverse	TAACGCTTAGCTCGACCACTCTG	
POLA forward	TGTCGCTTGCAGACCAGATG	AF009147
POLA reverse	GCATCGCAGGTGTGAGCAC	
POLA probe	CAGCAACAACTTCGAGCCTGGCACC	
TNFα forward	CCCTCACACTCAGATCATCTTCTC	NM_013693
TNFα reverse	TGG CTC AGC CAC TCC AG	
TNFα probe	CTGTAGCCCACGTCGTAGCAAACCAC	

3.1.4 Culture media, master mixes and buffers

0.9% sodium chloride injection, USP	Hospira, Lake Forest, IL, USA
2D gelelectrophoresis equilibration buffer I	50 mM Tris-HCl, 6 M urea, 30% (v/v) glycerol, 2% SDS 2% (w/v) DTT

2D gelelectrophoresis equilibration buffer II	50 mM Tris-HCl, 6 M urea, 30% (v/v) glycerol, 2% SDS 2.5% (w/v) iodoacetamid
3% Thioglycalate	Sigma-Aldrich, St. Louis, MO, USA
Annexin V Binding Buffer (10x)	BD Pharmingen Inc., San Diego, CA, USA
CDNP culture medium	MEM, 2 mM L- Glutamin, 1 mM Sodium Pyruvat, 100 U/ml Penicillin, 100 U/ml Streptomycin, 10 % (v/v) FCS 1.95µl 2-Mercaptoetnanol
Coomassie Blue destaining solution	10 % (v/v) Acetic Acid, 40 % (v/v) Methanol in A. dest
Coomassie Blue staining solution	0.2 % (w/v) Coomassie Brilliant Blue, 10 % (v/v) Acetic Acid, 40 % (v/v) Methanol in A. dest
Digestion buffer I	25 mM ammoniumbicarbonate
Digestion buffer II	25 mM ammoniumbicarbonate, 50% acetonitrile (v/v)
DNase Reaction Buffer (10x)	Sigma Aldrich Chemie GmbH, München, Germany
Erythrocyte Lysis Buffer	8.26 g NH4Cl 1 g NaHCO3 0.037 g EDTA 1 L Aqua dest.
FACS Buffer	500 ml PBS 0.5% BSA
First Strand Buffer	Invitrogen GmbH, Karlsruhe, Germany
HBSS	Gibco, Carlsbad, CA, USA
Laemmli Buffer	Bio-Rad, Hercules, CA, USA
Master-Mix for cDNA-Synthesis	4 µl 5 x First Strand Buffer, 2 µl 0,1 M DTT, 1 µl 10 mM dNTP, 1 µl Random-Primer (250 ng/µl), 0,5 µl Reverse Transkriptase
Master-Mix for quantitative real-time PCR (SybrGreen)	0,2 µl 0,1 mM Primer forward, 0,2 µl 0,1 mM Primer reverse, 1,6 µl Aqua dest., 10 µl 2x SybrGreenMM, qPCR Mastermix
Master-Mix for quantitative real-time PCR (TaqMan)	0,18 µl 0,1 mM Primer forward, 0,18 µl 0,1 mM Primer reverse, 0,04 µl TaqMan probe, 1,6 µl A.dest., 10 µl 2x TaqMM, qPCR Mastermix

MEM Non-essential amino acid solution	Sigma Aldrich Chemie GmbH, München, Germany
Minimal Essential Medium (MEM)	Sigma Aldrich Chemie GmbH, München, Germany
NuPage MES Running Buffer (20x)	Thermo Fischer Scientific, Carlsbad, CA, USA
NuPage Transfer Buffer (20x)	Thermo Fischer Scientific, Carlsbad, CA, USA
PBS	2,5 mM KCl, 1,5 mM KH_2PO_4, 140 mM NaCl, 6,5 mM Na_2HPO_4 in A. bidest, pH 7,25
PBS, sterile	Sigma-Aldrich Chemie GmbH, Taufkirchen, Germany
RPMI-1640, without L-Glutamine	Corning Inc., New York, NY, USA
RPMI-1640, without L-Glutamine	Lonza Inc., Allendale, NJ, USA
RPMI-1640, without L-Glutamine	Sigma-Aldrich Chemie GmbH, Taufkirchen, Germany
RPMI-1640 complete	RPMI 1640, 2 mM L- Glutamin, 100 U/ml Penicillin, 100 U/ml Streptomycin, 10 % (v/v) FCS 1.95µl 2-Mercaptoetnanol
SEM fixation solution (according to Monti-Graziadei)	2% glutaraldehyde, 0.6% paraformaldehyde 0.1M cacodylate buffer, pH 7.2
Sybr©Green qPCR Mastermix (2x)	Life Technologies, Carlsbad, CA, USA
TaqMM, qPCR Mastermix for probe analysis (2x)	Life Technologies, Carlsbad, CA, USA
Trypan Blue staining solution	0,1% (w/v) Trypan Blue, 1% (v/v) Methanol, 15% (v/v) Ethanol In DEPC-H_2O
Trypsin solution	3.5 ng/µl trypsin
Tween-PBS	1000 ml PBS 1ml 0.1% Tween 20

3.1.5 Reagents and kits

2-Mercaptoethanol	Sigma Aldrich Chemie GmbH, München; Germany
Acetic Acid	C. Roth GmbH & Co. KG, Karlsruhe, Germany
Amplification Grade DnaseI	Sigma Aldrich Chemie GmbH, München; Germany
BCA Protein Assay Kit	Pierce, Waltham, MA, USA

BK-RiV (official trade name of therapeutic CDNPs)	Varicula Life Science AG, Teterow; Germany
Bovine Serum Albumin	Sigma Aldrich Chemie GmbH, München; Germany
Bovine Serum Albumin Fraction V	Fisher Scientific, Carlsbad, CA, USA
Brefeldin A	eBioscience, San Diego, CA, USA
Chloroforme	C. Roth GmbH & Co. KG, Karlsruhe, Germany
Coomassie Brilliant Blue	Sigma Aldrich Chemie GmbH, München; Germany
CFSE	Biolegend, San Diego, CA, USA
Cy3, Cy5	NH Dyeagnostics, Halle, Germany
DEPC-H_2O	0,1 % DEPC (v/v) in Aqua dest
DMSO	Sigma Aldrich Chemie GmbH, München; Germany
DNAse I	Sigma Aldrich Chemie GmbH, München; Germany
dNTP-Mix 10 mM	Fisher Scientific, Carlsbad, CA, USA
DTT, 0,1M	Invitrogen GmbH, Karlsruhe, Germany
ECF substrate	GE Healthcare, Little Chalfont, United Kingdom
Ethanol 75%, 99,8 %	C. C. Roth GmbH & Co. KG, Karlsruhe, Germany
Fetal Calf Serum (FCS)	Sigma Aldrich Chemie GmbH, München; Germany
Fixation/Permeabilization Kit	BD Biosciences, San Jose, CA, USA
Foxp3 Fix/Perm Buffer Set	Biolegend, San Diego, CA, USA
Gene JET Genomic DNA Purification Kit	Thermo Fisher Scientific, Waltham, MA, USA
Histopaque 1077	Sigma-Aldrich, St. Louis, MO, USA
Histopaque 1119	Sigma-Aldrich, St. Louis, MO, USA
innuPREP RNA Mini Kit	Analytik Jena, Jena, Germany
Ionomycin	Merck Millipore, Billerica, MA, USA
LAL Chromogenic Endotoxin Quantitation Kit	Pierce, Waltham, MA, USA
LEGENDplex Mouse Th1 panel	Biolegend, San Diego, CA, USA
L-Glutamine	Sigma Aldrich Chemie GmbH, München; Germany
LPS	Sigma Aldrich Chemie GmbH, München, Germany
LPS	Curtesy of Norbert Reiling, Microbial Interface Biology, Research Center Borstel, Leibniz-Center for Medicine and Bioscience, Borstel, Germany [98]
Methanol	C. C. Roth GmbH & Co. KG, Karlsruhe, Germany
Mouse IL-6 ELISA Ready-SET-Go	eBioscience, San Diego, CA, USA
Mouse TNF alpha ELISA Ready-SET-Go	eBioscience, San Diego, CA, USA

Sodium Pyruvat	Sigma Aldrich Chemie GmbH, München; Germany
Pam_3CSK_4	EMC microcollections GmbH, Tübingen, Germany
Paraformaldehyde	Merck KGaA, Darmstadt, Germany
Primer und TaqMan-probes	biomers.net GmbH, Ulm, Germany
Random-Primer 250 ng/µl	Promega GmbH, Mannheim, Germany
RevertAid H Minus Reverse Transcriptase	Life Technologies, Carlsbad, CA, USA
Sulfuric acid 2 M	50 ml sulfuric acid 98%, 200 ml Aqua dest
Sulfuric acid 98%	Merck KGaA, Darmstadt, Germany
Stop Solution	Sigma Aldrich Chemie GmbH, München, Germany
SuperScript TM II RT	Invitrogen GmbH, Karlsruhe, Germany
Thioglycolate	Sigma, St. Louis, MO, USA
Tween20	Serva GmbH, Heidelberg, Germany
Triton-X 100 detergent	Bio-Rad, Hercules, CA, USA
Trypsin (sequencing grade)	Promega, Madison, WI, USA
PageRuler Prestained Protein Ladder	Thermo Fisher Scientific, Waltham, MA, USA
Penicillin/Streptomycin	Sigma Aldrich Chemie GmbH, München; Germany
PMA	Sigma Aldrich Chemie GmbH, München; Germany
Poly (I:C)	Enzo Life Sciences, Exeter, UK
PrecisionPlus Protein DualColor Standard	Bio-Rad, Hercules, CA, USA
PVFD membrane	Thermo Fisher Scientific, Waltham, MA, USA
Resiquimod	Enzo Life Sciences, Exeter, UK
Trypan Blue	Waldeck GmbH & Co., Münster, Germany
Zymosan A	Sigma-Aldrich Chemie GmbH, Taufkirchen, Germany

3.1.6 Technical equipment/instruments

AcT 10 Hematology Analyzer	Beckman Coulter, Brea, CA, USA
Accuri Flow Cytometer	BD Biosciences, Heidelberg, Germany
Attune acoustic focusing cytometer	Life Technologies, Grand Island, NY, USA
Avanti J-20 XPI Centrifuge	Beckman Coulter, Brea, CA, USA
ELx405 Microplate Washer	BioTek Instruments, Winooski, USA
Ettan Spot Picker	GE Healthcare, Little Chalfont, United Kingdom
EVO HD 15-LS	Zeiss, Oberkochen, Germany
IKA MS2 Minishaker Vortex	IKA works INC, Wilmington, USA
Caliper Oditest 0-10 mm	Kroeplin GmbH, Schlüchtern, Germany

Centrifuge 5417 R	Eppendorf AG, Hamburg, Germany
FluorChem 8900	Fisher Scientific, Carlsbad, CA , USA
Galaxy Mini Centrifuge	VWR International GmbH, Darmstadt, Germany
Gel Electrophoresis Apparatus Criterion Cell	Bio-Rad, Hercules, CA, USA
Gel iX Imager	Intas Science Imaging, Göttingen, Germany
µQuant Microplate Spectrophotometer	BioTek Instruments, Winooski, USA
Megafuge 1.0 R /2.0 R Heraeus	Kendro Laboratory Products GmbH, Hanau, Germany
MiniSpin Plus Centrifuge	Eppendorf AG, Hamburg, Germany
NanoDrop 2000	Thermo Fisher Scientific, Waltham, MA, USA
Nanosight NS300	Malvern Instruments, Malvern, UK
Neubauer improved counting chamber	Glaswarenfabrik Karl Hecht GmbH, Sondheim, Germany
Odyssey Infrared Imaging System	Li-Cor Biosciences, Lincoln, NE, USA
Pipettes	Eppendorf AG, Hamburg, Germany
Pipetman Pipette	Gilson International B.V., Limburg, Germany
Protean IEF cell	Bio-Rad, Hercules, CA, USA
Real-Time PCR ABI PRISM 7000	Applied Biosystems, Darmstadt, Germany
Real-Time PCR ABI PRISM 7900 HT	Applied Biosystems, Darmstadt, Germany
Safety clean bench 51424/3	MDH Limited, Hampshire, UK
Semi-Dry Blotting System IMM-1A	The W.E.P. company, US
Semi-Dry Blotting System Owl HEP-1 Panther	Thermo Fisher Scientific, Waltham, MA, USA
StepOne Plus Real time PCR	Applied Biosystems, Darmstadt, Germany
Thermomixer comfort	Eppendorf AG, Hamburg, Germany
Thermomixer compact	Eppendorf AG, Hamburg, Germany
Ultraflex-TOF/TOF mass spectrometer	Bruker Daltoniks, Bremen, Germany
Vacuum Centrifuge Concentrator 5301	Eppendorf AG, Hamburg, Germany
Vortexer VF2	Janke & Kunkel, IKA GmbH, Staufen im Breisgau, Germany
Water Bath	Köttermann GmbH, Uetze/Hänigsen, Germany
ZOOM Dual Power Supply	Invitrogen by Life Technologies, Grand Island, NY, USA

3.1.7 Laboratory supplies

10 cm Petri Dishes	Sarstedt AG & Co., Nümbrecht, Germany
17 cm IPG strips pH 4-7	Bio-Rad, Hercules, CA, USA
23- and 26-gauge Needles	B. Braun Melsung AG, Melsung, Germany
40 µm cell strainer	Greiner Bio One, Kremsmünster, Austria
48 Well Tissue Culture Plates	Greiner Bio One, Kremsmünster, Austria
96 Well Multiply Fast PCR Plates for Suspension Cultures	Sarstedt AG & Co., Nümbrecht, Germany
96 Well Multiply PCR Plates	Sarstedt AG & Co., Nümbrecht, Germany
96 Well Tissue Culture Plates for adherent cells	Sarstedt AG & Co., Nümbrecht, Germany
96 Well Plates, polypropylene, v- bottom	Greiner Bio One, Kremsmünster, Austria
Acetate Foil for Microplates	Sarstedt AG & Co., Nümbrecht, Germany
AnchorChip target	Bruker Daltoniks, Bremen, Germany
Aurelia Quest gloves	Supermax Healthcare Inc., Aurora, USA
Cell culture flasks (25, 75, 175 cm^2)	Sigma Aldrich Chemie GmbH, München; Germany
FACS Tubes 5 ml	BD Pharmingen Inc., San Diego, CA, USA
Flow Cytometer Calibration and Size Reference Beads	Thermo Fisher Scientific, Waltham, MA, USA
Glass slides and cover tips	Gerhard Menzel GmbH, Braunschweig, Germany
MicroFine Insuline syringes, 1ml	BD Biosciences, Heidelberg, Germany
Nunc-Immuno™ 96 Micro Well Plates	Thermo Fisher Scientific, Waltham, USA
NuPage Novex 4-12% Bis-Tris-Gel 1.0 mm x 12 well	Life Technologies, Carlsbad, CA, USA
NuPage Novex 10% Bis-Tris-Gel 1.0 mm x 12 well	Life Technologies, Carlsbad, CA, USA
Omnifix 1 ml Syringes	B. Braun Melsung AG, Melsung, Germany
PCR Optical Adhesive Cover	Life Technologies, Carlsbad, CA, USA
Pipette tips 20-300µl	Eppendorf AG, Hamburg, Germany
Pipette tips 10µl, 200 µl, 1000 µl	Nerbe plus, Winsen (Luhe), Germany
Pipette tips 10µl, 200 µl, 1000 µl	Sarstedt AG & Co., Nümbrecht, Germany
Reaction tubes 1,5 ml	Sarstedt AG & Co., Nümbrecht, Germany
Reaction Tubes 15 and 50 ml	Nerbe plus, Winsen (Luhe), Germany
Roller Bottles 4970 ml	Greiner Bio One, Kremsmünster, Austria
Safe Lock Tubes 1,5 ml	Eppendorf AG, Hamburg, Germany
Scalpel blades	Dimeda Instrumente GmbH, Tuttlingen, Germany
Thermanox coverslips	Thermo Fisher Scientific, Waltham, USA
Tryptic soy agar plates	Fisher Scientific, Waltham, MA, USA
Vivaspin 2 concentrators (MWCO 3000)	Sartorius AG, Göttingen, Germany

3.1.8 Software

7000 Sequence Detection System 1.2.3	Applied Biosystems, Darmstadt, Germany
7900 HT Sequence Detection System 2.2.2	Applied Biosystems, Darmstadt, Germany
Adobe Illustrator CS3	Adobe Systems Inc., San Jose, CA, USA
Adobe Photoshop CS3	Adobe Systems Inc., San Jose, CA, USA
Compass 1.3	Bruker Daltoniks, Bremen, Germany
ELISA analysis app	http://www.elisaanalysis.com/app
FlowJo 10	Tree Star, Ashland, OR, USA
GraphPad Prism 5	GraphPad Software Inc., La Jolla, USA
GraphPad Prism 6	GraphPad Software Inc., La Jolla, USA
Grubb‘s outlier test	http://www.graphpad.com/quickcalcs/Grubbs1.cfm
KCjunior 1.41.8	BioTek Instruments GmbH, Bad Friedrichshall, Germany
Mendeley Desktop 1.16.1	Mendeley Ltd., London, UK
Microsoft Excel 2010	Microsoft Deutschland GmbH, Unterschleißheim, Germany
Microsoft PowerPoint 2010	Microsoft Deutschland GmbH, Unterschleißheim, Germany
Microsoft Word 2010	Microsoft Deutschland GmbH, Unterschleißheim, Germany
NTA 2.3	Malvern Instruments, Malvern, UK
NTA 3.1	Malvern Instruments, Malvern, UK
SameSpots 4.0	Nonlinear Dynamics, Newcastle on Tyne, UK

3.2 Methods

3.2.1 CDNP preparation and characterization

3.2.1.1 CDNP preparation

In the course of the present study, CDNPs were obtained from three different sources: i) commercially available porcine CDNPs, ii) CDNPs isolated from murine fibroblast-like cell cultures and, iii) CDNPs isolated from the peritoneum of naïve and septic mice.

3.2.1.1.1 Commercially available CDNPs (BK-RiV)

CDNPs are distributed under the registered trade name BK-RiV (*Biokomplex-Reaktionsmuster in Vertebratenzellen*) by Varicula Life Science AG, Teterow, Germany. Varicula Life Science uses the embryonic porcine cell line EFN-R, which is stressed by nutrient deprivation [66]. CDNPs are extracted by disruption of the plasma membrane, differential centrifugation and chloroform treatment.

3.2.1.1.2 Isolation of CDNPs from murine MC3T3-E1 cell cultures

The CDNP isolation protocol used by Varicula Life Science AG [66], was adapted to obtain CDNPs from a murine cell line: The embryonic fibroblast cell line MC3T3-E1 was initially cultured in 25cm^2 cell culture flasks, then scaled up to 75 and 175cm^2 flasks and finally transferred into roller bottles after reaching confluency. Cells were then stressed by culture in serum-deprived media. After 2 days, stressed cells were immediately frozen at -20°C to avoid necrosis. The frozen cells were pelleted 20 min at 4,000g and resuspended in 10x PBS. The cells were sonicated 2 x 3 min at max. power to disrupt their plasma membranes and release intracellular CDNPs. CDNP isolation was then carried out by differential centrifugation: Cell debris, nuclei and apoptotic bodies were pelleted 20 min at 4,000g and the supernatant was further subjected to a 150 min centrifugation at 50,000g. The pellet containing CDNPs, microparticles (MPs) and exosomes was resuspended in 10x PBS and tilted with 5% chloroform for 30 sec to disperse lipid layers surrounding MPs and exosomes. Finally, remnants were pelleted for 15 min at 9,000g. The supernatant was deemed containing CDNPs. A schematic overview of the isolation process can be found on page 64 in Fig. 4-1-5.
CDNPs were also isolated from unstressed cells (usCDNPs), following the same protocol, except that cultivation in serum-deprived media was replaced by cultivation in complete media.

3.2.1.1.3 Isolation of CDNPs from the peritoneum of naïve and septic mice

The protocol described under 3.2.1.1.2 was further adapted to obtain mouse-derived CDNPs: Peritoneal fluid of naïve mice or mice subjected to CLP was collected via standard peritoneal lavage technique (see 3.2.3.1). Cell-free supernatant was obtained after centrifugation at 450g for 10 minutes followed by a second centrifugation at 25,000g for 30 minutes. The pellet, composed of apoptotic bodies and MPs, was discarded and the supernatant was incubated with 1% Triton-X for 10 minutes to remove exosomes [99]. Samples were then centrifuged at 100,000g for 60 min to pellet CDNPs and suspended in HBSS.

3.2.1.1.4 Concentration of CDNPs

In order to obtain the maximal effect of CDNPs for the *in vitro* experiments in chapters 4.1 and 4.2, single lots of commercially available and cell culture-derived CDNPs were concentrated. Vivaspins with a molecular weight cut-off (MWCO) of 3,000kDa were used for this purpose. CDNP solutions were applied on Vivaspin columns and centrifuged 30 min at 4,000g at RT. The eluate was discarded and CDNP concentrates were recovered after inverting the column and centrifuging it again at 4,000g for 7 min. Protein concentrations of concentrated CDNP solutions were measured by BCA assay (see 3.2.6.1) and adjusted to 1 mg/ml with PBS.

3.2.1.1.5 Pooling of individual CDNP preparations

To account for different protein concentrations among individual CDNP preparations, CDNPs used in chapter 4.3 were pooled. Therefore, a total amount of 1mg from 6 individual preparations of sCDNPs or usCDNPs, respectively, were mixed and adjusted to a concentration of 100 µg/ml.

3.2.1.1.6 Labeling of CDNPs

In order to determine the ingestion of CDNPs *in vitro* and *in vivo*, CDNPs were labeled with carboxyfluorescein succinimidyl ester (CFSE) according to the manufacturer's instructions. Briefly, CFSE was diluted to 1,25mM in DMSO and added to 125µl CDNP solution (100 µg/ml) or PBS control, mixed and incubated 20 min at 37°C on a rocker. An equal volume of RPMI with 10% FCS was added and incubated 10 min at 37°C on a rocker to capture unbound CFSE.

3.2.1.2 CDNP characterization

Particularity and size of CDNPs was assessed by Nanoparticle Tracking Analysis (NTA) and scanning electron microscopy (SEM). The protein content was analyzed by 1- and 2D gel electrophoresis, MALDI-TOF and Western Blot.

3.2.1.2.1 Nanoparticle Tracking Analysis (NTA)

NTA is a new, innovative method for detection and sizing of 30 to 1,000nm small particles. It is based on tracking the Brownian motion of particles in real time. Therefore, a laser beam is directed at the sample chamber which is continuously supplied with a particle suspension. When the laser beam meets a particle, the light is scattered and can be captured by a charge-coupled device (CCD) camera with 20x magnification. The NTA software subsequently identifies single particles on the captured film sequence and tracks their individual Brownian motion. The Stokes Einstein equation is then used to relate the particle diffusion coefficient mirroring its speed (area/time) to its diameter:

$$Dt = \frac{TK_B}{3\pi\eta d}$$

With Dt: particle diffusion coefficient; T: temperature; K_B: Bolzman constant; η:viscosity; d: hydrodynamic diameter.

This workflow allows for an accurate sizing of mono- and polydisperesed nanoparticles [100]. Moreover, NTA can also be used for multi-parameter analyses by labeling the particles of interest with fluorochrome-conjugated antibodies and using additional lasers for their excitation.

Concretely, NTA measurements were performed using a NanoSight NS300. CDNP suspensions were diluted with RPMI from Lonza containing low amounts of particles, and filled into a sterile syringe fitted with a 0.22µm filter. The syringe was connected to a pump which injected the sample into the sample chamber at a flow rate of 30. Camera focus and camera level were adjusted manually to allow the best particle visualization. Light scattering and Brownian motion of particles were recorded with the NTA 2.3 or 3.1 software. 4 sequences of 60 sec each were captured per sample. Detection thresholds providing the optimal discrimination between particles and background were set manually.

3.2.1.2.2 Scanning electron microscopy (SEM)

SEM analyses the surfaces of organic and non-organic specimens using a focused beam of accelerated electrons. The SEM process begins with an electron gun generating and accelerating a beam of electrons by heating of a tungsten cathode. A set of electromagnetic lenses focusses this beam onto the sample which is placed inside a vacuum chamber. This is necessary to prevent interactions of electrons with molecules in the air. Instead, incident electrons strike the sample with high speed, thereby ejecting secondary electrons from its surface. To increase such interactions, biological SEM samples are typically sputter-coated with a thin layer of a conductive noble metal such as platin or gold [101]. The focused electron beam is hitting the sample on a very distinct spot. To image the whole sample, the beam therefore is moved in a raster over the sample. Each beam-sample interaction spot is processed into a pixel on the monitor with the darkness (or grayscale value) of the pixel mirroring the signal intensity (the numbers of secondary electrons detected). Hence, the magnification M of the SEM is defined as the ratio of the length of the monitor ($L_{monitor}$) and the length of the sample (L_{sample}) [102]:

$$M = L_{monitor}/L_{sample.}$$

Thus, a reduction of the length of the scanned area on the sample surface results in increased magnification. The final results of SEM are high resolution, black-and white, three-dimensional images of the sample topography. Since SEM is not restricted by the limits of optical lenses, magnifications much higher than those of conventional light microscopes (up to 10nm) can be achieved [103].

Sample preparations for SEM include sputtering and dehydration. The sputter process is based on the ionization of argon gas inside an electric field. The positively charged argon ions are attracted to the negatively charged noble metals; they collide and etch atoms from the metal. The negatively charged metal ions are attracted to the anode, where the sample is placed. This way, the metal ions settle on the surface of the sample as a thin layer [101]. Besides sputter-coating, the samples also need to be dehydrated in order to prevent the vaporization of water inside the vacuum sample chamber [104].

SEM sample preparation and analysis was carried out by the work group of Matthias Klinger, Institute for Anatomy, Luebeck. Briefly, SEM samples were settled on thermanox coverslips and fixed with Monti-Graziadei solution for 2h at 22°C. Samples were then dehydrated in a rising alcohol series ranging from 30, to 40, 50, 60, 70, 80, 90 and finally 100% ethanol for 15 min at a time. Dehydrated samples were placed on aluminum stabs and sputtered with gold or platin. Analysis was performed using an EVO HD 15-LS machine.

3.2.1.2.3 SDS-PAGE

Sodium dodecyl sulphate-polyacrylamide gel electrophoresis (SDS-PAGE) separates proteins in an applied electric field according to their molecular weight. Since the tertiary structure of proteins as well as their net charge would also affect protein migration, both properties need to be neutralized prior to separation. Therefore, samples are heated and dissolved in sample buffer SDS, which on the one hand denaturates i.e. linearizes, the proteins and on the other hand encases them with a negative charge. Since approximately 1.4g SDS binds 1g protein, all proteins have the same charge to mass ratio and their migration in an applied electrical field is based on their molecular weight only. SDS-treated samples are then loaded on polyacrylamide gels and voltage is applied. The negatively loaded proteins migrate to the positive anode, with the migration distance of a protein being negatively proportional to the log of its molecular weight. The exact weight can be estimated based on a protein ladder: a mixture of proteins of known seizes simultaneously run with the samples. The gel itself is divided into two layers, a stacking gel which is concentrating the samples at a collective starting line and a running gel, which has a higher acrylamide content slowing the migration of larger particles, thereby allowing a better separation of proteins.

In the present thesis, SDS-PAGE as described by Laemmli was used to elucidate the protein content of CDNPs [105]. Briefly, 15µl of sample were mixed with 5µl 4× Laemmli buffer containing 500mM DTT and heated at 95°C for 5 min. Samples were then loaded on a 4-12% Bis-Tris polyacrylamide gel. The gel was run in running buffer at 45mA and 500V, until the running front reached the end of the gel. Gels were fixed by incubation in 15% acetic acid for 15 min and equilibrated by incubation in a 30% methanol, 10% acetic acid solution for 15 min. Protein bands were then stained with the non-specific protein dye coomassie brilliant blue by a 30-60 min incubation in coomassie brilliant blue staining solution followed by overnight incubation with coomassie brilliant blue destaining solution.

3.2.1.2.4 2D-gel electrophoresis and MALDI-TOF

Protein expression patterns of CDNPs derived from stressed (sCDNPs) and unstressed cells (usCDNPs) were compared by fluorescence-based multiplex two-dimensional (2D)-difference gel electrophoresis (2D DIGE) and proteins enriched in sCDNPs were identified by MALDI-TOF (matrix-assisted laser desorption/ionization – time of flight). 2D DIGE, MALDI-TOF and analysis were conducted by Prof. Dr. Timo Gemoll, Section for Translational Oncology and Biobanking, Universitätsklinikum Lübeck, Germany.

2D DIGE

2D DIGE combines traditional SDS-PAGE (3.2.1.2.3) with isoelectric focusing (IEF), a method to separate proteins based on their isoelectric point, i.e., the pH at which a protein carries an electrical net charge of zero. Both separations are run orthogonally, leading to much higher protein separations than single separation techniques. Protein profiles, obtained this way allow qualitatively and quantitatively comparisons between different samples [106]. Since IEF requires unaltered native protein charges, IEF is usually run as the first dimension, while SDS treatment masking individual protein charges needed for SDS-PAGE is performed in a second step (second dimension).

Labeling: In order to discriminate proteins from different samples, each sample is labeled with a distinct dye. The dye concentration added is limited to ensure that each labeled protein carries only one label and is later visualized as a single spot on the gel [107]. **IEF:** Isoelectric focusing is performed in an immobilized pH gradient (IPG) on a gel strip. The pH immobilization on IPG strips is achieved by acrylamide derivatives with defined pK values (so-called immobilines), which are interspersed into the polyacrylamide matrix. When an electrical field is applied to the IPG strip, negatively charged proteins will migrate towards higher pH and become deproteinated until they accumulate at a pH where they carry no charge. **Equilibration:** Since SDS-PAGE requires proteins to be denaturated and negatively charged (see 3.2.1.2.3), focused samples are equilibrated in buffer containing DTT, iodacetamide and SDS. **SDS-PAGE:** Finally, the IPG strip is placed on the edge of a conventional SDS gel in a 90 degree angle from the first separation and run as an SDS-PAGE.

2D-DIGE was carried out as described before [108,109]. Briefly, s- and usCDNPs were labeled with Cy3 and Cy5, respectively. 50µg of each sample and 50µg internal standard were diluted in 450µl rehydration buffer and loaded on a rehydration/equilibration tray. 24cm long IPG strips with a pH ranging from 4 to 7 were placed on the sample. Samples were loaded on the IPG strips via active rehydration at 50V overnight. IEF was performed at 20°C, 40-50,000Vhr, and a max. current of 50µA per IPG strip. Focused IPG strips were equilibrated in SDS-containing buffer in a two-step process. First, IPG strips were equilibrated in 6 ml buffer I containing sulfhydril group-reducing DTT for 15 min. In the second step, IPG strips were equilibrated for additional 15 min in 6 ml buffer II containing iodoacetamid alkalyting these groups to prevent reoxidization. Equilibrated IPG strips were applied on SDS gels and then run at constant 1000V and 13°C for 4.5 hours.

The gels were then scanned with a 16-bit grayscale flatbed scanner for detection of significantly expressed spots. SameSpots software was used to quantify the expression of individual proteins based on their spot size and the expression patterns between s- and usCDNP samples were subsequently compared. This analysis revealed a common set of 52 proteins enriched in sCDNPs, which were automatically excised using a spot picker, digested in-gel and identified by MALDI-TOF.

In-gel digestion: Since whole proteins are too big to be unambiguously identified by mass spectroscopy, samples are usually fragmented by proteolytic enzymes before analysis. This leads to a set of characteristic peptide fragments which can be identified using a software such as Mascot which compares the derived peptide fragments with a data base containing digested peptides from known proteins. This technique is called protein fingerprinting.
Excised gel pieces were destained and washed for 10 min in digestion buffer I, followed by a 10 min wash in digestion buffer II. Subsequently, acetonitrile was added to dehydrate the gel pieces. The dry gel pieces were rehydrated with 10µL of a 4°C trypsin solution in digestion buffer I and proteins were digested at 37°C for 4 h. Peptides were then extracted for 30 min with 10µL 0.1% trifluoroacetic acid.

MALDI-TOF: Matrix-assisted laser desorption/ionization – time of flight (MALDI-TOF) is a very sensitive method to determine the molecular masses of molecules thereby allowing their characterization and identification. The starting point for this process is MALDI: The peptide sample is mixed with a large excess of a UV-absorbing matrix compound to allow co-crystallization and applied on a plate. A pulsed laser with 337nm wavelength is then used to irradiate the matrix-sample-mixture. The matrix absorbs the laser light and converts it to heat energy, leading to vaporization of the matrix together with the imbedded peptides. Furthermore, the matrix is also able to serve as a proton donor or acceptor, respectively, producing singly or multiply charged ions of the peptides [110]. Thus, the desorption/ionization process leaves a mixture of peptides consisting the initial neutral molecule [M], molecules with one or more added proton(s) $[M+nH]^+$, molecules with one or more removed proton(s) $[M-nH]^-$, as well as molecules with added other ions from the matrix, such as sodium ions $[M+Na]^+$. The next step consists of the identification of these charged peptides by time of flight analysis (TOF). TOF is based on the acceleration of these differently charged peptide mixture towards a detector. During the acceleration, all peptides

are subjected to the same accelerating energy, however as they all have different molecular masses and charges, their arrival at the detector differs based on their mass-to-charge ratio:

$$t = \sqrt{m/z}$$

with t:time of flight, m:mass, z: charge [111].

Thus, TOF identifies single peptides based on their time of flight. The peptide masses can then be calculated using the above formula. The analysis software produces a peak list containing the molecular weights of all fragments detected. The peak list for a protein digested by an enzyme is characteristic and the protein can therefore be identified by a comparison of the peak list with a database containing known protein sequences (usually SwissProt).

Practically, protein spots extracted from gels were directly transferred to a MALDI AnchorChip target containing hydrophilic anchors to localize the samples at a distinct position. The samples were then analyzed in a time-of-flight Ultraflex-TOF/TOF mass spectrometer. Acquired mass spectra were calibrated and annotated as described before [108].

This way, 19 of the 52 proteins enriched in sCDNPs were considered significantly upregulated ($p \leq 0.05$). Fold-change (FC) of these proteins was calculated as

$$\mathbf{2}^{(\boldsymbol{mean\ sCDNPs - mean\ usCDNPs})}$$

Annexin A5 was identified as the protein showing the highest enrichment in s- vs. usCDNPs (14.96-fold). This finding was further validated via Western Blot (3.2.1.2.5.).

Principal component analysis (PCA): PCA is a statistical method to reduce the dimensionality of big multivariable datasets to the most important information leading to a better interpretability of the data [112]. Basically, the information is reduced to uncorrelated variables which demonstrate the highest variation, while variables which are correlated and therefore redundant are neglected. However, it does not use the variables *per se*, but further summarizes them by linear combinations of different variables to principle components (PCs) [113]. The first PC having the highest variation is then transformed to the x-axis, while the second PC with the second largest variation is plotted on the y-axis. [114]. The plotted values of PC1 and PC2 make it possible to visually determine similarities and differences between samples. Similar samples cluster together, while unrelated samples do not [113].

PCA using expression data of all identified proteins was used to demonstrate that proteins from s- and usCDNPs were able to group. The statistical software package R version 2.10.1 was used for all statistical analyses with R packages nlme version 3.1-96 (mixed effect model) and FactoMineR version 1.14 (PCA).

3.2.1.2.5 Western Blot

Annexin A5 content in CDNPs was evaluated by Western Blot. Different Western Blot protocols were used in Lübeck (analysis of cell culture-derived CDNPs, protocol I) and Cincinnati (analysis of CLP-derived CDNPs, protocol II).

Protocol I

30µl cell culture-derived CDNPs were mixed with 6µl 6× Laemmli buffer and denaturated at 95°C for 5 min. Samples were then run on a 4-12% Bis-Tris polyacrylamide gel in MES buffer and antioxidant solution containing DTT in the upper buffer chamber. After transferring the protein to a PVDF membrane for 50 min at 300mA, the membrane was blocked with 3% BSA-solution for 60 min. The primary anti-annexin A5 antibody was applied in a 1:1000 dilution in 5% milk and incubated overnight at 4°C. The membrane was then washed with Tween-PBS and incubated with the second infrared dye-conjugated anti rabbit IgG antibody in a 1:10,000 dilution in Tween-PBS for 60 minutes at room temperature. After a washing step, protein bands were visualized using an Odyssey Infrared Imaging System.

Protocol II

15µl mouse-derived CDNPs were mixed with 5µl 4× Laemmli buffer and denaturated at 60°C for 20 min. Samples were then run on a 10% Bis-Tris polyacrylamide gel in MES buffer. After transferring the protein to a PVDF membrane for 60 min at 75mA, the membrane was blocked with 3% BSA-solution for 60 min. The primary anti-annexin A5 antibody was applied in a 1:300 dilution in 3% BSA and incubated overnight at 4°C. The membrane was then washed with Tween-PBS and incubated with the second FITC-conjugated goat anti rabbit IgG antibody in a 1:200 dilution in 3% BSA for 90 minutes. After a washing step, the membrane was incubated for 60 min with the tertiary akaline phosphatase-conjugated mouse anti-FITC antibody, diluted 1:5,000 in 3% BSA. Finally, the membrane was washed again and developed using 1 ml ECF substrate. Protein bands were visualized using a CCD-based gel image device.

3.2.2 Animal experiments

Animals in all experiments were randomly assigned to a treatment group and animals from different treatment groups were housed together in one cage.

3.2.2.1 *Leishmania major* infection

All *Leishmania* experiments were performed in Lübeck. Female C57BL/6J mice aged 6 weeks were purchased from Charles River Laboratories GmbH (Sulzfeld) und acclimatized in the central animal facility of the University of Lübeck for 2 weeks. Mice were housed in specific pathogen-free (SFP) conditions and fed standard laboratory mouse chow and water *ad libitum*. All experiments were performed in accordance with the German Animal Protection Law and were approved by the Ethics Board of the Ministry of Environment (Ministerium für Energiewende, Landwirtschaft, Umwelt und ländliche Räume des Landes Schleswig-Holstein, Kiel, # V242-7224.122-1(33-4/14)).

3.2.2.1.1 Cultivation of *L. major* parasites

L. major (strain MHOM/IL/81/FE/BNI) were provided by courtesy of Prof. T. Laskay from the Department of Infectious Diseases and Microbiology, University of Lübeck. Promastigote *L. major* were cultured at his institute in biphasic Novy-Nicolle-McNeal-RPMI medium at 27°C and 5% CO_2. When the parasites reached the stationary phase, they were harvested by centrifugation at 3,500 rpm for 10 min. After two additional washing steps with RPMI, *L. major* promastigotes were counted with a *Neubauer improved* counting chamber and adjusted to $40x10^6$ parasites/ml in RPMI.

3.2.2.1.2 *L. major* infection

C57BL/6 mice aged 8 weeks were infected with $2x10^6$ viable *L. major* promastigotes in 50µl RPMI 1640 medium, by s.c. injection into the left hint foot pad.

3.2.2.1.3 CDNP application

CDNP application was based on therapeutic administration of CDNPs. 50µl s- or usCDNPs (~100µg/ml) were injected s.c., alternately into the left and right hint leg of infected mice. The first CDNP application was carried out 1 hour post infection, followed by injections each Monday, Wednesday and Friday.

3.2.2.1.4 Determination of foot pad swelling

Foot pad swelling of *L. major*-infected mice was used as an indicator for the severity of infection-induced inflammation. Once a week, the thickness of both hind foot pads was measured with a caliper. Foot pad swelling was then defined as the thickness difference of infected and uninfected foot pads.

3.2.2.1.5 Tissue and organ harvesting

Mice were sacrificed after 4 weeks of infection, at the plateau of foot pad swelling [115]. Foot pad skins were removed with a scalpel right under the bone. The popliteal lymph node, which is the main draining lymph node for the foot pad, was dissected, weighted and carefully intersected into two pieces, both of which were weighted again. Foot pad skins and one piece of the lymph node were immediately frozen in liquid nitrogen and stored at -80°C until they were subjected to cryosection. The second part of the lymph node was used for cell count determination and FACS-analysis (see 3.2.6.2). Cell counts of the whole lymph node were calculated based on the weight of the analyzed lymph node piece in proportion to the weight of the whole lymph node.

3.2.2.1.6 Determination of parasite loads

Parasite loads in the foot pad skin mirror how the host copes with *L. major* infection. The better the infection is controlled, the lower the parasite burden in the skin. Expression of *Leishmania* DNA polymerase alpha catalytic polypeptide (POLA) and *Leishmania* kinetoplasts were used as surrogate markers for *L. major* presence [116,117]. Foot pad skins were processed to 12µm cryosections and 10 cryosections were lysed to isolate DNA using the Gene JET Genomic DNA Purification Kit according to the manufacturer's instructions. Purified DNA was subjected to PCR as described under 3.2.5.3. In contrast to mRNA, parasite DNA levels were normalized to the murine single copy gene BDNF.

3.2.2.2 Polymicrobial sepsis induction by cecal ligation and puncture (CLP)

All sepsis experiments were performed in Cincinnati. Male C57BL/6J mice from ENVIGO or Charles River Laboratories (Wilmington, MA) aged 7-8 weeks were utilized for these experiments. The mice were housed in standard environmental conditions and fed with standard laboratory mouse chow and water *ad libitum*. All experiments were approved by the

Institutional Animal Care and Use Committee of the University of Cincinnati (IACUC # 08-09-19-01).

3.2.2.2.1 CLP

CLP was used to induce polymicrobial sepsis as described previously [118]. Briefly, mice were anesthetized with isoflurane and a small mid-abdominal incision was made. The cecum was exteriorized and the latter third of the cecum was ligated with a 4-0 silk suture without obstructing bowel continuity. The cecum was then punctured with a 23-guage needle and gently squeezed to extrude a small amount of stool. After re-placing the cecum in the abdomen, PBS or CDNPs were injected into the peritoneum. If not stated otherwise, 5µg CDNPs were applied per mouse. The abdominal incision was then closed in two-layers with 4-0 silk suture. Finally, animals were resuscitated with 1 mL of 0.9% sterile saline and allowed to recover on a heating blanket for one hour.

The CLPs procedure was conducted by Brent T. Xia and Lisa England, Department of Surgery, University of Cincinnati.

3.2.2.2.2 Survival studies

CLP was performed as described above, however a 18-gauge needle was used. Survival was followed for 96 hours.

3.2.2.2.3 Determination of bacterial loads

Peritoneal lavages were aseptically collected in sterile 0.9% saline, and serially diluted 1:10 to 1:10,000 in PBS. Samples were plated on tryptic soy agar plates and incubated at 37°C for 24 hours. Colony-forming units (CFUs) were counted in all non-confluent grown plates.

3.2.3 Cell and microparticle isolation

To determine the *in vitro* effects of CDNPs, CDNPs were incubated with different cell types or cell-derived MPs, respectively. The following paragraphs describe the cell isolation techniques used to obtain these cells/MPs.

3.2.3.1 Peritoneal lavage

The peritoneal cavity is the space enclosed by the peritoneum, a serous membrane. It harbors important organs such as the stomach, liver, gallbladder, spleen and intestines and is filled

with peritoneal fluid. Peritoneal fluid from naïve mice also contains immune cells, including ~35% macrophages, ~50% innate B1 cells, ~10% adaptive B2 cells, as well as ~5% T cells. Peritoneal lavages are used to harvest these cells. They were performed as described before [119]. Briefly, naïve C57BL/6 mice were euthanized in a CO_2 chamber. The outer skin was cut open and pulled back to expose the whole peritoneum. 5-8 ml ice cold PBS were carefully injected with a 27-gauge needle without puncturing the organs. In order to dis-attach peritoneal macrophages from the peritoneum, the peritoneum was gently massaged. The needle was then re-injected and the peritoneal fluid aspirated. Finally, the peritoneal wall was cut open and washed 4-5 times by applying 1 ml ice cold PBS on the inner skin of the peritoneum followed by aspiration. Harvested cells were pelleted 10 min at 450g, counted and adjusted to $1x10^6$ cells/ml in complete RMPI medium.

3.2.3.2 Splenic cell isolation

The spleen belongs to secondary lymphatic tissues, where antigens from the blood system are recognized and adaptive B and T cells are activated. Moreover, the spleen removes old, while holding a big reservoir of fresh red blood cells. Thus, red blood cells have to be lysed in order to obtain the immune cells localized in the spleen.

Naïve C57BL/6 mice were euthanized in a CO_2 chamber, the peritoneal cavity was cut open and the spleen was dissected. Spleens were kept in ice cold PBS until used. A single cell solution was obtained by grinding the spleen between two frozen specimen slides above a petri dish filled with complete RPMI medium. Isolated cells were peletted 10 min at 450g and resuspended in 2-3 ml erythrocyte lysis buffer. After 2-3 min of incubation, 10 ml RPMI medium was added and cell were peletted again 10 min at 450g. Finally, cells were adjusted to $2x10^6$ cells/ml in complete RMPI medium.

3.2.3.3 Isolation and culture of BM-derived neutrophils

The BM constitutes a reservoir for neutrophils where they differentiate from stem cells. As such, around 10% of all BM cells are neutrophils, which are continuously released into the blood under basal conditions and mobilized in high amounts during inflammation [120].

BM-derived neutrophils were isolated as described previously [121]. Briefly, naïve C57BL/6 mice were euthanized in a CO_2 chamber. The outer skin was cut open and pulled back to expose the abdomen and extremities. The legs were dislocated from the hip and stored in RPMI media until further processed. Tibea and femur were separated by bending and the knee joint was removed. The bones were extricated from muscles and the epiphyses were removed

with scissors. A 25-gauge needle was inserted into one open bone end and BM was flushed out by injecting RPMI medium. BM from 3-4 mice was pooled and clumps were disassociated by vigorous pipetting followed by filtering through a 40µm cell strainer. BM cells were pelleted 10 min at 450g, resuspended in 3 ml erythrocyte lysis buffer and incubated for 3 min at RT. Erythrocyte lysis buffer was then diluted with 30ml HBSS and cells were centrifuged 10 min at 450g. The pellet resuspended in 1 ml HBSS, was carefully placed on top of a tube containing 3ml histopaque 1077 layered over 3ml histopaque 1911. This gradient was centrifuged 30 min at 1,000g on a centrifuge with swing-out bucket rotor without brakes. Neutrophils, mononuclear cells such as lymphocytes and erythrocytes have different densities and thus are separated during centrifugation. Erythrocytes are aggregated by polysucrose and thus possess the highest density leading to their sedimentation at the bottom. Polynuclear granulocytes accumulate at the interface between both histopaques, whereas the low density mononuclear cells are found in the upper layer. The clearly visible neutrophil band at the interphase of both histopaques was collected and washed with 10ml HBSS at 450g for 10 min. The pellet was resuspended in complete RPMI medium and adjusted to $1x10^6$ cells/ml. Purity of isolated neutrophils (~80%) was confirmed via flow cytometry. Neutrophils were identified as $Ly6G^+CB220^-Ter\text{-}119^-$. The main cell contaminants were $B220^+$ B cells. However, further purification was not conducted as it harbors a risk of non-specific neutrophil activation [122]. $1x10^6$ cells/ml cells were cultured in 500ml complete RPMI medium on a 48 well plate at 37°C.

3.2.3.4 Microparticle generation and isolation

Neutrophil-derived microparticles (NDMPs) were obtained either from BM-derived neutrophils cultured for 24h or from peritoneal fluid of mice (naïve or post CLP) collected via standard peritoneal lavage technique (see 3.2.3.1). For experiments deiscribed under 3.2.4.3.2 and -3, mice were injected intraperitoneally with 1 ml 3% thioglycolate 24 hours prior to harvesting, to increase the amount of generated MPs [123]. In all cases, cell-free supernatant was obtained after centrifugation at 450g for 10 minutes followed by a second centrifugation at 10,000g for 10 min. The pellet, composed of apoptotic bodies was discarded and the supernatant was centrifuged at 25,000g for 30 minutes to pellet MPs. MPs were suspended in HBSS. NDMPs were enumerated via NTA after staining with for the neutrophil specific marker $Ly6G^+$ [124] with PE-conjugated antibodies and detected using the PE-detecting channel.

3.2.4 *In vitro* experiments

3.2.4.1 TLR stimulation

Naïve C57BL/6 mice were euthanized in a CO_2 chamber and peritoneal lavages were collected. Peritoneal cells were centrifuged at 450g for 10 min and pellets were adjusted to $1x10^6$ cells/ml in RPMI medium containing 1% FCS. 100µl were incubated at 37°C on 96 well plates for 2 hours in order to allow macrophages to adhere. Non-adherent cells were aspirated and new complete RPMI supplemented with 50µg/ml concentrated CDNPs and one of the following TLR ligands was added: zymosan, LPS, Poly(I:C), resiquimod or Pam_3CSK_4. Tab. 2 summarizes the concentrations and TLRs triggered by these ligands. All TLR ligands were titrated to obtain the maximal stimulatory dose in preliminary experiments. Following 24h incubation at 37°C, supernatant was aspired and adherent cells dissolved in 400µl of guanidinium-isothiocyanate-containing lysis buffer from the innuPrep RNA Mini Kit for isolation of total RNA.

Tab. 2: TLR ligands used to stimulate peritoneal macrophages.

TLR	ligand	conc.	description	mimics	reference
TLR2/TLR6 (also triggers dectin 1)	zymosan	100ng/ml	Preparation of cell wall from *S. cerevisiae*	lipoproteins and β-gulacane	[125,126]
TLR2/TLR1	Pam_3CSK_4	1 ng/ml	tripalmitoylated lipopeptide	acylated amino terminus of bacterial lipoproteins	[125,127]
TLR3	Poly(I:C)	100µg/ml	ds of an poly(I) polymer annealed to a poly(C) polymer	dsRNA	[128]
TLR4	LPS (sigma) LPS (Borstel)	20 ng/ml 1 ng/ml	bacteria-derived LPS		[129]
TLR7/8	resiquimod	4 µg/ml	imidazoquinoline amine analog of guanosine	ssRNA	[130]

3.2.4.2 Cell incubation with CDNPs

The following protocol was used for all *in vitro* experiments of chapter 4.2: Naïve C57BL/6 mice were euthanized in a CO_2 chamber in order to harvest peritoneal lavages and spleens. Peritoneal cells were centrifuged at 450g for 10 min and pellets were adjusted to $1x10^6$ cells/ml in complete RPMI medium. 500µl were incubated on 48 well plates for 2 hours at 37°C in order to allow macrophages to adhere. Similarly, splenic cells were isolated as described under 3.2.3.2 and adjusted to $1x10^6$ cells/ml in complete RPMI medium. 5 µg/ml pooled CDNPs and 1 ng/ml LPS (Borstel), where indicated, were added. LPS (Borstel) was titrated to obtain the maximal stimulatory dose in preliminary experiments. Following 2 or 24h of incubation at 37°C, supernatant was aspired and cells subjected to cytometric analysis.

3.2.4.3 Particle ingestion assays

The following assays were used to determine whether i) CDNPs are ingested by peritoneal cells and ii) whether incubation with CDNPs alters the ingestion of NDMPs by peritoneal cells.

3.2.4.3.1 CDNP ingestion by peritoneal cells

Naïve C57BL/6 mice were euthanized in a CO_2 chamber and peritoneal lavages were collected. Peritoneal cells were centrifuged at 450g for 10 min and pellets were adjusted to $1x10^6$ cells/ml in RPMI medium containing 1% FCS. 500µl were incubated on 48 well plates for 2 hours at 37°C in order to allow macrophages to adhere. 5 µg/ml CFSE-labeled CDNPs and 1 ng/ml LPS (Borstel), where indicated, were added. Simultaneously, an aliquot was incubated at 4°C to inhibit internalization. Ingestion was stopped after 2 hours by a brief incubation on ice; supernatant was then aspired and cells subjected to cytometric analysis. To determine internalized protein, the median fluorescence intensity (MFI) of $CFSE^+$ cells incubated at 4°C was subtracted from the MFI of $CFSE^+$ cells incubated at 37°C.

3.2.4.3.2 CDNP-MP co-incubation

NDMPs were isolated from peritoneal lavages of thioglycolate (TGA) -elicited mice and incubated with CFSE-labeled CDNPs for 30min at 37°C in the presence of Ca^{2+}-containing annexin V binding buffer. NDMPs were then labeled with PE-conjugated anti-Ly6G antibodies and CDNP-NDMP binding was identified as $CSFE^+Ly\text{-}6G^+$ particles by flow cytometry.

3.2.4.3.3 MP ingestion

NDMPs were isolated from peritoneal lavages of TGA-elicited mice and stained with CFSE (see 3.2.1.1.6) before the final centrifugation step. Since NDMPs were pelleted in this step, there was no need to quench excess CFSE and no BSA was added. CFSE-labeled NDMPs were pre-incubated with CDNPs for 30min at 37°C in the presence of Ca^{2+}-containing annexin V binding buffer and then incubated with peritoneal macrophages for 2 additional hours. NDMP-ingesting macrophages were identified by CFSE positivity after surface fluorescence quenching with trypan blue [131].

3.2.4.4 Bacterial killing assay

To determine the direct effect of CDNPs on bacteria growth and survival, bacterial growth assays were performed as describe [132]. Briefly, the *Pseudomonas aeroginosa* (*P. aeruginosa*) strain PA01 was grown for 14 hours on tryptic soy agar plates, then harvested and diluted to a density of 3 x 10^3 CFU/ml in PBS. Indicated amounts of CDNPs were added to the bacteria and incubated for 2h at 37°C under shaking at 125 rpm. Incubations with buffer alone served as controls. 100µl aliquots of the bacterial suspensions were then plated on LB agar plates and incubated overnight at 37°C followed by the counting of CFUs.

3.2.5 Gene expression analysis

Cytokine expression was determined in peritoneal cells incubated with CDNPs as well as in the foot pad skins of *L. major* infected mice.

3.2.5.1 Nucleic acid isolation

The innuPrep RNA Mini Kit was used for isolation of total RNA according to the manufacturer's instructions. 10 cryosections of *L. major* infected tissues were dissolved in 700µl lysis buffer and vortexed for 1 min. In order to homogenize the tissue, the solution was aspired with a 1 ml syringe at least 10 times. Cell pellets from cultured cells were directly dissolved in 400µl lysis buffer. 700µl or 400µl 70%Ethanol were added, respectively, and the solution applied on spin filter columns in receiver tubes. Nucleic acids were allowed to bind to the column at 12,000 rpm for 2 min. The eluate was discarded and the column washed with 500µl high salt (HS) wash buffer for 1 min at 12,000 rpm. The eluate was discarded and a secondary wash was conducted with 700µl low salt (LS) wash buffer at 12,000 rpm for 2 min.

Next, the spin filter column was placed in a new receiver tube and dried for 2 min at 12,000 rpm. Nucleic acid was released from the column by adding 20µl RNAse-free H_2O, incubating for 1 min, then eluted for 1 min at 8,000g. Maximal nucleic acid recovery was achieved by re-placing the eluate on the column and re-eluation for 1 min at 8,000g.
Samples derived from cryosections were subjected to an additional 20 min evaporation step at 60°C in a vacuum centrifuge in order to further concentrate the sample. Finally, all samples were resuspended in 8µl RNAse-free H_2O.

3.2.5.2 cDNA synthesis

8µl nucleic acids as isolated under 3.2.5.1 were incubated for 15 min at RT with 1µl 10x DNase buffer and 1µl DNase I. DNA degradation was stopped by addition of 1.5µl stop solution and incubation at 85°C for 5 min. 2µl RNA-free H_20 and 1µl random primer mix was added and allowed to anneal for 5 min at 65°C. Finally, 5.5µl of a master mix containing reverse transcriptase, dNTPs and 5x buffer was added and incubated for 10 min at RT, followed by a 60 min incubation at 47°C allowing for the transcription of RNA to cDNA. RT activity was stopped by incubation at 70°C for 10 min.

3.2.5.3 Quantitative RT-PCR

1.25µl cDNA was mixed with 6.75 *A. dest* and added to each well of a 96 well plate. 4µl PCR master mix was added and the plate was centrifuged for 30 sec at the highest speed in order to concentrate the sample in the well. Quantitative RT-PCR was performed on an ABI machine using the specifications given in Tab. 3.

Tab. 3: Specifications used for quantitative RT-PCR

	temperature	duration	repeats
polymerase activation	95°C	10 min	1x
denaturation	95°C	45 s	50x
hybridization + elongation	60°C	1 min	50x

PCR results were analyzed using 7000 Sequence Detection System 1.2.3- and 7900 HT Sequence Detection System 2.2.2 software. The relative mRNA concentration was calculated based on the cycle of threshold (C_T) denominating the amplification cycle in which fluorescence exceeds the background level. The relative gene expression was calculated by setting the expression of the gene of interest in relation to the expression of a stably expressed

housekeeping gene MLN51 (metastatic lympnnode 51) [13] based on the following formula [133]:

$$2^{-\Delta C_T} = 2^{C_T^{(housekeeping\ gene)} - C_T^{(gene\ of\ interest)}}$$

Where indicated, the expression was further normalized by dividing the values of treated samples by the values obtained for controls [133] :

$$2^{-\Delta\Delta C_T} = 2^{-\Delta C_T^{(treated)}} / 2^{-\Delta C_T^{(control)}}$$

3.2.6 Protein expression/secretion analysis

3.2.6.1 Determination of protein concentration by BCA

The protein concentration of CDNPs was determined using the bicinchoninic acid (BCA) assay. This standard assay uses the biuret reaction, whereby peptides with at least three amino acid residues reduce Cu^{2+} to Cu^{+} ions. In a second step, two BCA molecules form a purple colored chelate with each Cu^{+} ion. Since the Cu^{2+} reduction is proportional to the protein concentration and the amount of Cu^{+} in turn determines the amount of chelate and therefore the intensity of the purple color, protein levels can be quantified using a photometric analysis [134].

Here, a BCA assay kit was used according to the manufacturer's instructions. Briefly, the provided BSA standard was diluted to obtain a concentration range between 0 and 1,500 µg/ml. Reagent A was mixed with reagent B in a ratio of 50:1 and 200µl of this mixture were incubated 30 min at 37°C with 10µl standards or sample, respectively. The optical density (OD) of each sample was measured on a nanodrop photometer using the BCA program.

3.2.6.2 Flow Cytometry

Flow cytometry or fluorescence-activated cell sorting (FACS) is a laser light based high-throughput method to quantify multiple cell parameters such as size, complexity (granularity) and fluorescence. Therefore, a single cell suspension is incubated with fluorochrome-conjugated antibodies directed at the antigens of interest. A flow cytometer aspirates the

sample and uses a sheath fluid to create a laminar flow which focuses and separates the cells, so that each single cell passes the flow cell individually. Here, each cell passes beams from different lasers depending on the configuration of the cytometer; most cytometers are employed with at least an argon laser (488nm) and a HeNe laser (633nm). The laser light is scattered, with the cell size being proportional to the forward scatter (FSC) and the granularity of a cell correlating with the side scatter (SSC). These parameters allow the identification of distinct cell types, dead cells and debris. Furthermore, the laser light excites the fluorochromes conjugated to the antigen-specific antibodies to a higher energy state. Excited fluorochromes return to their resting state, whereby they emit light energy which is focused by dichroic mirrors and band pass filters that isolate particular wavelength bands (fluorescence channels). Photomultiplier tubes (PMTs) then convert the light into electrical signals that are amplified and digitalized [135]. A computer can then visualize the signal intensity of each single cell as a distinct event within a histogram or a two-dimensional dot-plot. Subpopulations of cells show different expression levels of specific marker molecules and thus different fluorochrome intensities. These subpopulations can be separated by drawing a "gate" around them (gating). The MFI then measures the expression level and the percentage of cells within a specific gate determines the frequency of cells expressing this marker. The use of multiple fluorochromes with different emission wavelengths allows the measurement of several antigens at once, allowing for a precise phenotyping of cells. However, emission is usually not limited to one exact wavelength, but shows at least a Gaussian distribution which can be quite broad. Moreover, some flourophores show an additional small peak at additional wavelengths. Therefore, the use of multiple fluorophores is always associated with spillover in neighboring channels. Compensation is used to correct this spillover by a subtraction of the over spilling signals. To this end, aliquots of the sample are stained with one single fluorochrome (single stains) and over spilling signals are corrected until no signal is detectable in the nonspecific channels [136].

3.2.6.2.1 Extracellular staining

Cell suspensions were adjusted to 0.5 -2x10^6 cells/ml and centrifuged for 5 min at 450g. The cell pellet was resuspended in 100µl staining solution containing an Fcγ Block to prevent unspecific binding of antibodies to Fcγ Rs and the antibodies to identify the cells and markers of interest (for fluorochromes and concentrations see 3.1.2). This mixture was incubated 15 min at 4°C. For washing, 200µl FACS buffer was added and the cells were centrifuged for 5 min at 450g. Cells were resuspended in 100µl FACS buffer and centrifuged for 5 min at 450g,

then resuspended in FACS buffer and subjected to flow cytometry. Cells were analyzed on an Accuri C6 flow cytometer or an Attune acoustic focusing cytometer, respectively. The flow rate was set to 1,000 events/min and compensation was set manually according to the manufacturer's instructions. Gates were set based on fluorescence minus one (FMO) controls, which included all fluorochromes except the one needed for setting the gate and thus allowed the determination of the threshold [137]. Data was analyzed and visualized with FlowJo X software or the cytometer based analysis programs, respectively.

Since peritoneal macrophages derived from naïve and septic mice showed high non-specific staining, the staining protocol for these cells was changed as follows: After the initial centrifugation of cells, pellets were resuspended in 50µl Fcγ Block solution containing Fcγ Block (diluted 1:50) and rat serum (diluted 1:20) and incubated 10 min at RT. Subsequently, 50µl of 2x concentrated staining solution was added and incubated 20 min at 4°C.

3.2.6.2.2 Staining of intracellular cytokines

The staining of intracellular antigens requires an additional step to permeabilize the cell membrane in order to allow antibodies to enter the inside of a cell. Moreover, the cytokine concentration inside a cell is normally very low, since cytokines are not stored but rapidly secreted. Thus, to measure the potential of a cell to secrete certain cytokines, cells are usually restimulated with the unspecific mitogens phorbol-12-myristat-13-acetat (PMA) and ionomycin. PMA activates protein kinase C (PKC) which in turn increases intracellular Ca^{2+} levels, while ionomycin is an ionophore likewise increasing Ca^{2+} influx. In addition, a secretion inhibitor such as Brefeldin A is used to retain the cytokines inside the cell.

To determine the cytokine expression of T cells, single cell suspensions from draining lymph nodes of *L. major*-infected mice were adjusted to $1x10^6$ cells/ml in complete RPMI medium and 1ml was applied per well on a 48 well plate. 5nM PMA and 1 µg/ml ionomycin were added per well and the plate was incubated for 1 hour at 37°C. 5 µg/ml Brefeldin A was added per well and the plate was further incubated for 4 hours at 37°C. Restimulated cells were then harvested and subjected to extracellular staining as described above. However, after the incubation with the staining solution, cells were washed by adding 1ml PBS and centrifuged for 5 min at 450g. The pelleted cells were resuspended in 200µl Fix/Perm solution and incubated 20 min at 4°C. 1ml PermWash was added after incubation and the cells were centrifuged for 10 min at 300g. The cell pellet was resuspended in 100µl intracellular staining solution containing an Fcγ Block to prevent unspecific binding of the antibodies to Fcγ receptors and the antibodies to identify intracellular cytokines (for fluorochromes and

concentrations see 3.1.2) in PermWash. This mixture was incubated 30 min at 4°C. For washing, 1ml PermWash was added and the cells were centrifuged for 10 min at 300g. Cells were resuspended in 100µl PermWash and again centrifuged for 10 min at 300g, then resuspended in 4% paraformaldehyde and subjected to flow cytometry as described above.

3.2.6.2.3 Staining of transcription factors

To detect the transcription factor Foxp3, an optimized permeabilization buffer was used in order to permeabilize not only the plasma membrane, but also the nucleus. Foxp3 staining was either conducted on unstimulated cells or on restimulated cells, when cytokine production was determined simultaneously. Thus, the same protocol as for intracellular cytokine staining, with or without restimulation was used. However, following changes were applied: After extracellular staining and washing with PBS, cells were permeabilized in 1ml Foxp3 Fix/Perm buffer instead of regular Fix/Perm solution. Cells were incubated 20 min at RT and 1ml PermWash was added, followed by centrifugation for 10 min at 300g. The cell pellet was resuspended in 1ml Foxp3 Perm buffer and again centrifugation for 10 min at 300g. 1ml Foxp3 Perm buffer was added to the cell pellet and incubated for 15 min at RT. Then the intracellular staining protocol was followed with the difference that Foxp3 Perm buffer was used instead of regular Perm/Wash.

3.2.6.2.4 Staining and identification of NDMPs

Flow cytometry is not only used to characterize cells, but can also detect any other particles, including nuclei, microorganisms, chromosomes and latex beads. However, since such small particles have similar FSC and SSC characteristics as dead cells and debris and since such debris itself possesses a significant degree of autofluorescence, appropriate size controls have to be used.

For the detection of NDMPs, MPs were first incubated with PE-conjugated anti-Ly-6G antibodies for 20 min at RT and then analyzed on the flow cytometer without further washing steps. Appropriate size gates were set by using 0.3, 1.1 and 3.0µm latex beads as calibrators. NDMPs were found in a gate ranging between 0.3 and 1.1 µm as previously described [138].

3.2.6.3 ELISA

The enzyme-linked immunosorbent assay (ELISA) uses antigen-specific antibodies to detect the antigen of interest. Therefore, an ELISA plate is coated with the antigen-specific capture

antibody capturing such antigen. The plate with the capture antibody is first incubated with a BSA- solution to mask all non-specific binding epitopes. Subsequently, the antigen suspension is applied and incubated, while unbound antigens are flushed out in the following washing step. Next, an antigen-specific antibody binding at an additional epitope of the antigen of interest is applied. The secondary antibody is directed against the Fc part of the first one and mediates the high sensitivity of the ELISA via its conjugation to horseradish peroxidase (HRP): One molecule of HRP turn over a large amount of added substrate, thereby amplifying the signal. Since the blue intermediate of this enzymatic reaction is unstable, sulfuric acid is added to catalyze the turnover to a yellow end product. The intensity of the color is proportional to the antigen level, thereby allowing the determination of the antigen concentration via a photometric measurement at 450nm.

Practically, the Mouse IL-6 ELISA Ready-SET-Go kit was used to determine the IL-6 concentration in the supernatant of peritoneal macrophages according to the manufacturer's instructions. Briefly, a 96 well ELISA plate was coated with 100µl capture antibody per well and incubated at 4°C overnight. The plate was then flicked and washed 3 times with 300µl wash buffer. Unspecific epitopes were blocked with 200µl blocking solution and incubated for 1 hour at RT. Plates were then flicked and washed 1 time with 300µl wash buffer. Lyophilized IL-6 standard was reconstituted in *A. dest*, incubated for 15 min at RT and serially diluted with ELISA diluent until an 8 point standard curve ranging from 10,000 to 0 pg/ml was obtained. 100µl standard and samples, respectively, were applied on the plate and incubated for 2 hours at RT under constant shaking. After 4 washes with 300µl washing buffer each, 100µl of the detection antibody conjugated with biotin was applied per well and incubated for 1 hour at RT under constant shaking. Following 4 washes with 300µl washing buffer each, 100µl biotin-binding avidin conjugated with HRP were applied per well and incubated 30 min at RT under constant shaking. Finally, the plate was flicked and washed 5 times with 300µl washing buffer. 100µl of the HRP substrate TMB were added per well and incubated at RT until the color of the highest standard turned deep blue. The reaction was then stopped by adding 50µl of 2M sulfonic acid per well. The plate was measured photometrically at 450nm. The standard curve was fitted with a five-parameter logistic regression algorithm and the samples were set in relation to this curve using the ELISA analysis software under http://www.elisaanalysis.com/app.

3.2.6.4 Cytometric bead array (CBA)

TNFα, IL-6 and IL-10 levels in the supernatant of peritoneal macrophages and in the peritoneal fluid from septic mice were determined using a cytometric bead array (CBA). This assay uses a similar principle as a conventional ELISA, however, the capture antibodies are not coated on a plate, but attached to latex beads. The advantage of this technique is that different beads conjugated to different capture antibodies can be used, so that multiple antigens can be detected simultaneously. The beads are later identified by their different size as well as the different levels of fluorophore I which they are conjugated to. When the antigen mix is added, distinct antigens bind to the bead capturing their specific antibody. After pelleting antigen-bound beads, unbound antigen is aspired and a detection antibody conjugated with biotin is added. In the final step, biotin-binding streptavidin conjugated to fluorophore II is added. Thus, the intensity of fluorophore II is proportional to the antigen bound on the beads. Antigen levels are finally analyzed via FACS: First, the antigen is identified based on bead size and intensity of fluorophore I, then the antigen concentration is determined by measuring fluorophore II intensity of each distinct bead population.

In this case, the LEGENDplex Mouse Th1 panel (5 plex) was used to detect cytokine concentrations according to the manufacturere's instructions. Briefly, the TNFα-, IL-6- and IL-10 detection beads conjugated to different levels of APC were vortexed for 1 min, then pooled and diluted based on the manufacturer's instruction. 25µl of beads were then applied on a 96 well plate with v-shaped wells. Lyophilized standard was reconstituted in assay buffer, incubated for 10 min at RT and serially diluted with assay buffer until an 8 point standard curve ranging from 10,000 to 0 pg/ml was obtained. 25µl standard and samples, respectively, 25µl assay buffer and 25µl biotin-conjugated detection antibodies were applied on the plate and incubated for 2 hours at RT under constant shaking. Without washing the plate, 25µl biotin-binding streptavidin conjugated with PE were applied per well and incubated for 30 more min at RT under constant shaking. In order to remove unbound antigen and antibodies, the beads were pelleted for 5 min at 1,000g and supernatant was aspired with a pipette. 200µl wash buffer were added, the plate was shaken for 1 min and the centrifugation step was repeated. The pelleted beads were resuspended in 200µl wash buffer and bead size, as well as APC intensity was measured to differentiate TNFα-, IL-6- and IL-10 beads, followed by the measurement of PE intensity in order to determine the cytokine concentrations. The MFI of PE obtained for each cytokine population was set in relation to the standard curve, which was fitted with a five-parameter logistic regression algorithm using the ELISA analysis software under http://www.elisaanalysis.com/app.

3.2.7 Determination of endotoxin contamination

Endotoxin is a synonym for LPS, emphasizing its toxic impact. Hence, endotoxins are part of the LPS complex in gram-negative bacteria, which is released during their lysis, but also during cell division [139]. Since endotoxin activates TLR4 and induces inflammation, endotoxin contaminations have to be excluded when elucidating the immunomodulatory effects of CDNPs. Therefore, endotoxin contamination of pooled CDNP preparations was determined using the chromogenic Limulus Amebocyte Lysate (LAL) assay. LAL is an aqueous blood cell extract derived from horseshoe crabs. Amebocytes, the "white blood cells" of this animal, detect endotoxins and initiate a defense reaction by inducing an enzyme cascade. The cascade finally results in a gel comprised of coagulated proteins [139]. Kits for chromogenic endotoxin detection contain a synthetic substrate for a proenzyme activated in this cascade. The product of the detection reaction is of yellow color and thus the amount of endotoxin which is proportional to enzyme activity can be determined photometrically [140]. An endotoxin standard for absolute endotoxin quantification is also included. Endotoxin is quantified in endotoxin units (EUs), with 1EU equaling approximately 100pg LPS, an amount generated by 10^5 bacteria [141].

The chromogenic LAL assay was performed according to the manufacturer's instructions. Briefly, the endotoxin standard was diluted with endotoxin-free water and vortexed for 15 min. The standard was subsequently serially diluted with endotoxin-free water until a 6 point standard curve ranging from 1 to 0 EU/ml was obtained. Samples were diluted 1:2 in endotoxin-free water and 30µl of sample or standard, respectively, were pipetted per well on a pre-warmed 96 well ELISA plate. 30µl LAL diluted in endotoxin-free water were added per well. Finally, 60µl reconstituted LAL substrate was added per well and incubated for 6 min at 37°C in an incubator. The enzymatic reaction was stopped by adding 30µl 25% acetic acid and the plate was measured at 405nm on a photometer. The linear standard curve was used to determine endotoxin concentration.

Before comparing the immunomodulatory effects of us- and sCDNPs, endotoxin levels in both preparations were determined. Endotoxin is a known contaminant present in media, sera, glass- and plastic ware. Even small concentrations of endotoxins of 0.05 EU/ml can lead to activation of immune cells [142]. Since no consistent threshold for non-immunogenic endotoxin levels exists, the definition of BioLegend was applied: endotoxin levels < 0.1 EU/µg were considered low and levels < 0.01 EU/µg were considered ultra-low with already low levels being non-immunogenic in functional *in vitro* and *in vivo* assays [143]. The pooled sCDNP preparation contained 0.0195 EU/µg, while pooled usCDNPs contained 0.0155

EU/µg (Fig. 3-1). Hence, the endotoxin contaminations of both preparations were considered negligible.

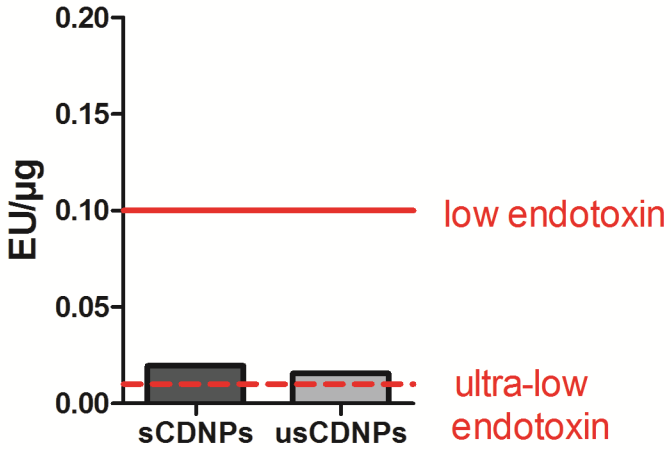


Fig. 3-1: CDNP preparations derived from stressed and unstressed cells contain very low endotoxin levels. s- and usCDNP mixtures containing equal protein amounts from 4-6 individual preparations were adjusted to 100µg/ml. Endotoxin content was measured by LAL chromogenic endotoxin quantification assay. Red lines depict thresholds for low (solid) and ultra-low (dashed) endotoxin contents as defined by manufacturers such as BioLegend [143].

3.2.8 Statistical analysis

Data was analyzed using Prism 5.0 and Prism 6.0, and presented as mean±SEM. Data was first subjected to a visual inspection as recommended by Tukey and Wierdsma [144,145]. If the data contained one single outlier, the Grubbs test under http://www.graphpad.com/quickcalcs/Grubbs1.cfm was used to determine whether this outlier was significant and the data point was removed from analysis when significance was reached [146,147]. In contrast, skewed datasets with heavy tails were transformed by normalization or log-transformation, to allow the use of more powerful parametric tests. In the rare cases, where data couldn't be transformed to an approximately normal distribution [148], nonparametric tests were used.

For comparison of two independent groups, Student's t-test (normal distribution) or Mann-Whitney U-test was used, dependent samples were analyzed with Student's t-test (normal distribution) for paired samples or Wilcoxon Signed Rank test. Three or more groups were compared using standard or repeated-measurements ANOVA with Bonferroni post-hoc tests. A p value of ≤ 0.05 was considered statistically significant.

4. Results

4.1 CDNPs have anti-inflammatory effects *in vitro*, independent of their xenogeneic origin

Therapeutic CDNPs, as well as CDNPs used for previous experiments in mouse models were derived from porcine cells. Therefore, the effects observed using such xenogeneic CDNPs might be mediated by a xenogeneic rejection reaction. To test whether this holds true, the production of CDNPs from a murine cell line with C57BL/6 background was established. Since the immunomodulatory effects of CDNPs are not well characterized, initial experiments screened for the effects of xenogeneic CDNPs on peritoneal macrophages stimulated with TLR ligands *in vitro*. Based on the results of this screening, an *in vitro* assay was established in order to compare the effects of xenogeneic (porcine) and allogeneic (murine cells) CDNPs. CDNPs were concentrated to 1 mg/ml and used in a concentration of 50 µg/ml in order to obtain the maximal immunomodulatory effect.

4.1.1 Xenogeneic CDNPs have anti-inflammatory effects on TLR-triggered macrophages *in vitro*

To test whether xenogeneic CDNPs evoke rejection, the immunogenicity of commercially available porcine CDNPs to murine cells was tested. To this end, resting and TLR-stimulated peritoneal macrophages were incubated with CDNPs and gene expression of pro-inflammatory cytokines was analyzed as readout.

4.1.1.1 Xenogeneic CDNPs do not alter IFNβ and TNFα expression of resting peritoneal macrophages *in vitro*

Xenogeneic CDNPs were incubated 4 or 24 hours with resting peritoneal macrophages to test whether they activate unstimulated macrophages. The gene expression of the pro-inflammatory cytokines IFNβ and TNFα were used as readout of cell activation. Both cytokines are critical for the generation of an effective defense against infection. IFNβ is expressed in a MyD88-independent manner after TLR triggering by nucleic acids [149], which are present in CDNPs [66]. TNFα in contrast, is expressed following the activation of a MyD88-dependent signal pathway [3]. Surprisingly, xenogeneic CDNPs did not alter IFNβ- or TNFα expression in unstimulated macrophages (Fig. 4-1-1).

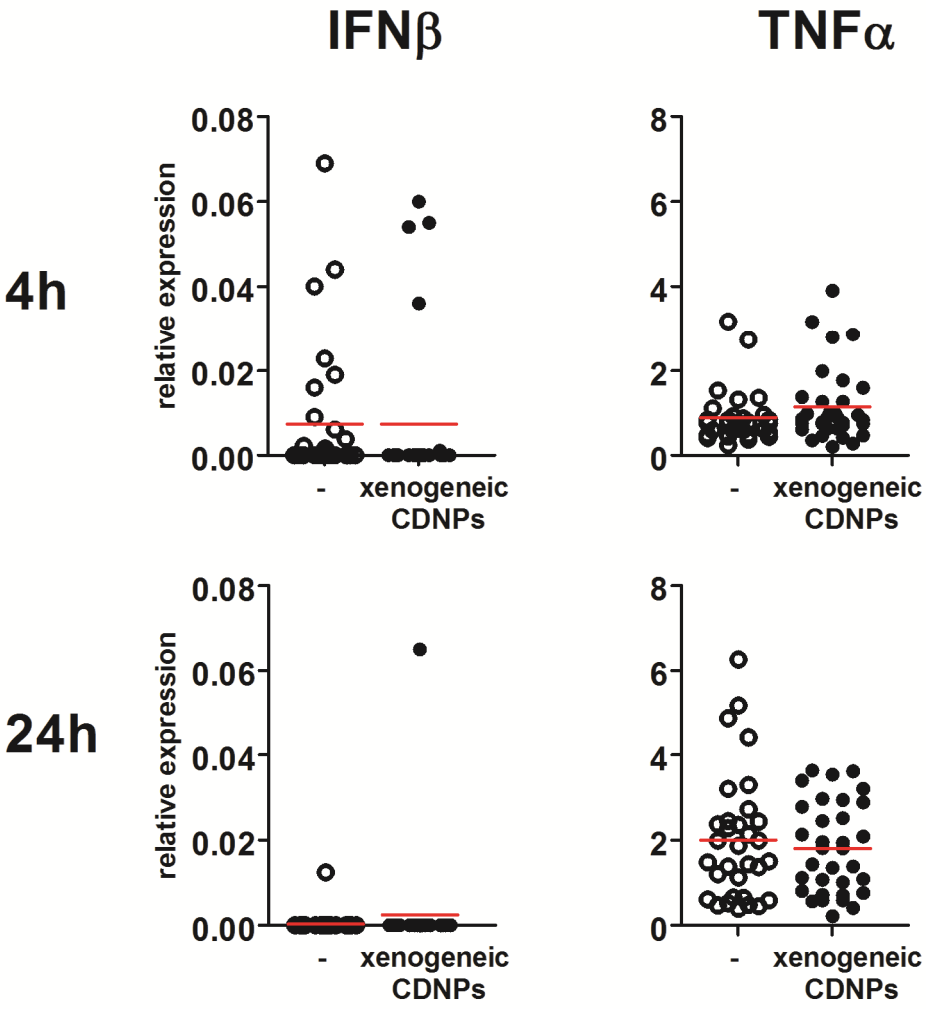


Fig. 4-1-1: Incubation with xenogeneic CDNPs has no effect on unstimulated peritoneal macrophages. Peritoneal lavages from naïve C56BL/6 mice were harvested and $1x10^5$ cells were pre-incubated 2 hours in media containing 1% serum to let macrophages adhere. Supernatants were then replaced with media containing 5% serum and the resulting culture enriched in macrophages was incubated with 50µg /ml xenogeneic CDNPs. 4 or 24 hours later cells were lysed and mRNA levels of IFNβ and TNFα were determined using quantitative RT- PCR. mRNA expression levels were adjusted to the housekeeping gene MLN51. n=21-33 cell preparations from individual mice.

4.1.1.2 Xenogeneic CDNPs modulate IFNβ and TNFα expression of TLR-stimulated peritoneal macrophages *in vitro*

Since xenogeneic CDNPs had no effect on unstimulated macrophages, stimulation experiments with four prototypic TLR ligands were carried out to determine whether they augment the cytokine response of cells primed by TLR-induced inflammation.

4.1.1.2.1 Xenogeneic CDNPs have no effect on LPS- or Poly(I:C)-stimulated macrophages

Peritoneal macrophages were stimulated with LPS triggering TLR4 or, Poly(I:C) triggering TLR3, respectively, and incubated with xenogeneic CDNPs. mRNA levels of IFNβ and TNFα were assessed 4 and 24h later. However, incubation with xenogeneic CDNPs had no effect on TLR4- and TLR3-induced IFNβ and TNFα expression (Fig. 4-1-2).

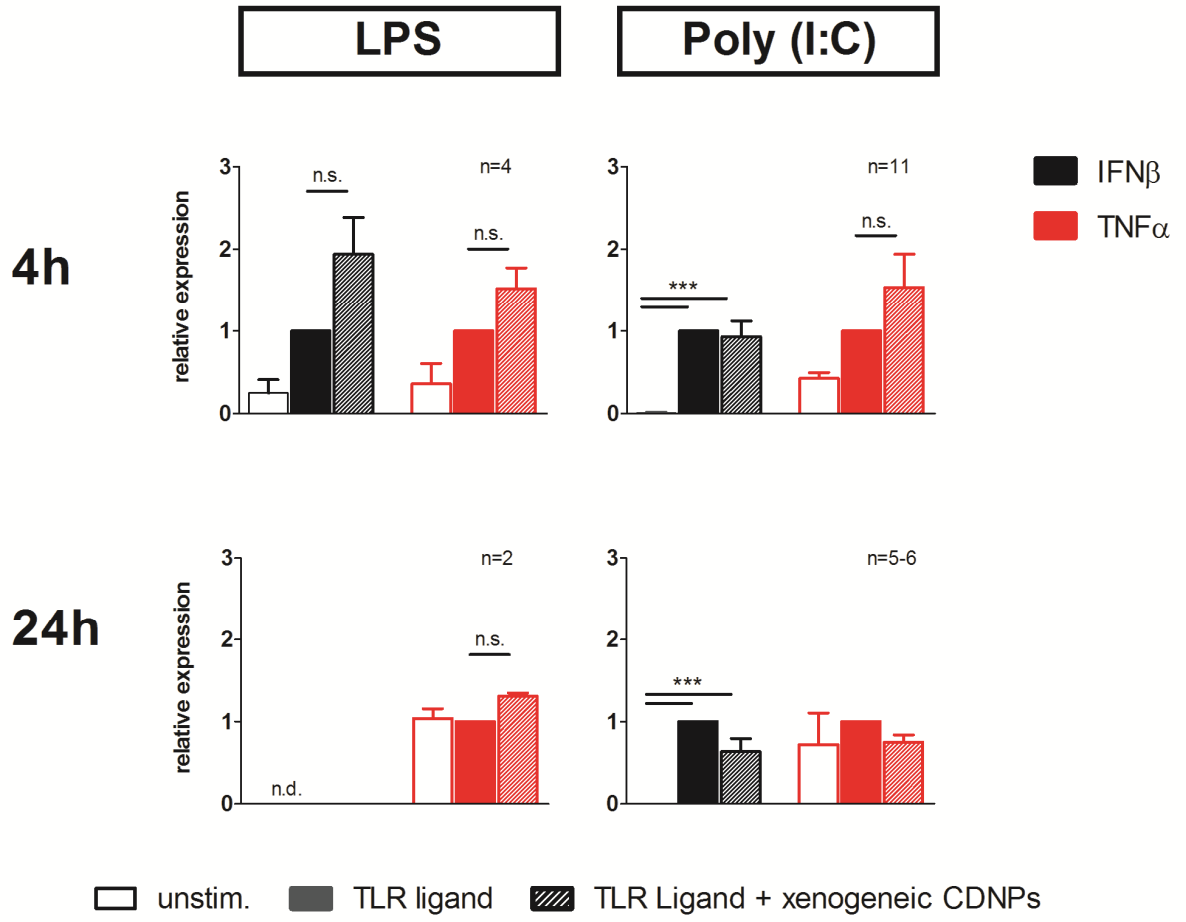


Fig. 4-1-2: Xenogeneic CDNPs do not alter cytokine expression of LPS- or Poly(I:C)-triggered macrophages. Peritoneal lavages from naïve C56BL/6 mice were harvested and $1x10^5$ cells were pre-incubated 2 hours in media containing 1% serum to let macrophages adhere. Supernatants were then replaced with media containing 5% serum and the resulting culture enriched in macrophages was incubated with 50 µg /ml xenogeneic CDNPs and 20 ng/ml LPS or 100 µg/ml Poly(I:C), respectively. 4 or 24 hours later cells were lysed and mRNA levels of IFNβ and TNFα were determined using quantitative RT-PCR. mRNA expression levels were adjusted to the housekeeping gene MLN51 and then normalized to the cytokine expression of stimulated cells. n=2-11 cell preparations from individual mice. Data are expressed as means ± SEM. Significance was determined using repeated measurements ANOVA with Bonferroni post-hoc test. ***$p<0.001$.

4.1.1.2.2 Xenogeneic CDNPs reduce TNFα expression in response to resiquimod 4 hours after incubation

By contrast, incubation of peritoneal macrophages stimulated with TLR7/8 triggering resiquimod with xenogeneic CDNPs significantly affected the expression of pro-inflammatory cytokine mRNA. Interestingly, contrary to the expectation, mRNA levels were not increased, but downregulated by 22% 4 hours after incubation (Fig. 4-1-3). However, this difference disappeared after 24 hours of incubation. Resiquimod-induced IFNβ expression, in contrast, was not affected by xenogeneic CDNPs.

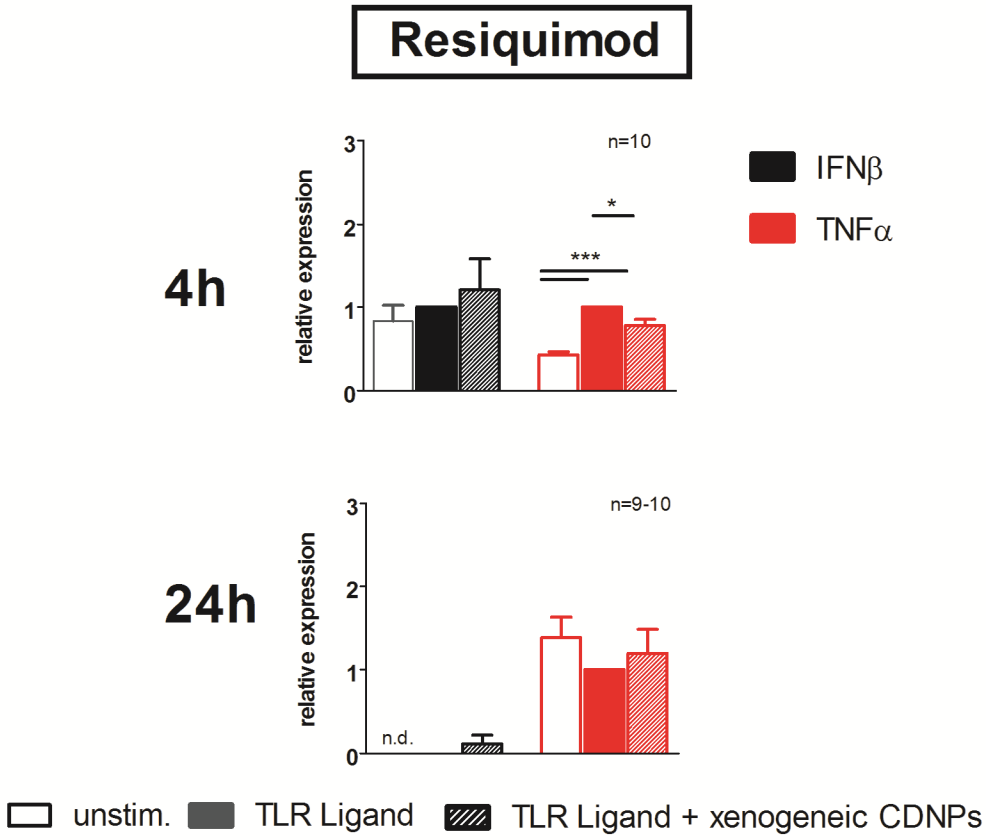


Fig. 4-1-3: Xenogeneic CDNPs decrease TLR7/8-triggered TNFα expression 4 hours after incubation. Peritoneal lavages from naïve C56BL/6 mice were harvested and $1x10^5$ cells were pre-incubated 2 hours in media containing 1% serum to let macrophages adhere. Supernatants were then replaced with media containing 5% serum and the resulting culture enriched in macrophages was incubated with 50µg /ml xenogeneic CDNPs and 4 µg/ml resiquimod. 4 or 24 hours later cells were lysed and mRNA levels of IFNβ and TNFα were determined using quantitative RT-PCR. mRNA expression levels were adjusted to the housekeeping gene MLN51 and then normalized to the cytokine expression of stimulated cells. n=9-10 cell preparations from individual mice. Data are expressed as means ± SEM. Significance was determined using repeated measurements ANOVA with Bonferroni post-hoc test. *p<0.05, ***p<0.001.

4.1.1.2.3 Xenogeneic CDNPs reduce zymosan-induced IFNβ expression 4 hours and TNFα expression 24 hours after incubation

Surprisingly, also zymosan-induced IFNβ and TNFα expression was downregulated in response to incubation with xenogeneic CDNPs. IFNβ was reduced 4-fold 4 hours after incubation; however the reduced IFNβ levels were still 3-fold increased in comparison to unstimulated cells (Fig 4-1-4). Intriguingly, incubation with xenogeneic CDNPs diminished

zymosan-induced TNFα expression 4-fold, almost reaching the expression levels of unstimulated cells (Fig. 4-1-4). Thus, xenogeneic CDNPs reverse zymosan-triggered TNFα expression 24 hours after stimulation.

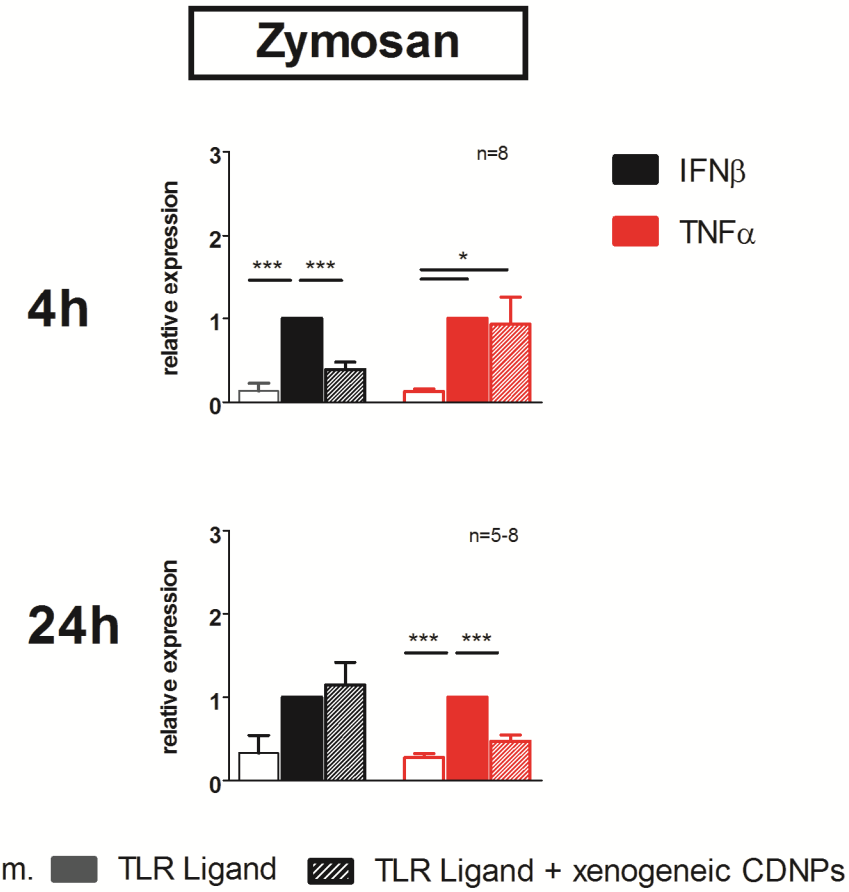


Fig. 4-1-4: Xenogeneic CDNPs decrease TLR2-triggered IFNβ and TNFα expression 4 and 24 hours after incubation, respectively. Peritoneal lavages from naïve C56BL/6 mice were harvested and $1x10^5$ cells were pre-incubated 2 hours in media containing 1% serum to let macrophages adhere. Supernatants were then replaced with media containing 5% serum and the resulting culture enriched in macrophages was incubated with 50µg /ml xenogeneic CDNPs and 100 ng/ml zymosan. 4 or 24 hours later cells were lysed and mRNA levels of IFNβ and TNFα were determined using quantitative RT-PCR. mRNA expression levels were adjusted to the housekeeping gene MLN51 and then normalized to the cytokine expression of stimulated cells. n=5-8 cell preparations from individual mice. Data are expressed as means ± SEM. Significance was determined using repeated measurements ANOVA with Bonferroni post-hoc test. *p<0.05, ***p<0.001

4.1.2 Allogeneic CDNPs demonstrate the same anti-inflammatory effects on TLR-triggered macrophages as xenogeneic CDNPs

To test whether the reduction of zymosan-induced TNFα mRNA levels 24h post incubation was due to their xenogeneic origin, the production of allogeneic CDNPs from a murine cell line with C57BL/6 background was established and the effects of xenegeneic and allogeneic CDNPs were compared *in vitro*.

4.1.2.1 Murine fibroblasts stressed by nutrient deprivation produce CDNPs

The embryonic fibroblast-like cell line MC3T3-E3 was chosen to establish the production of murine CDNPs. This choice was based on the following criteria: i) the cell line should be of embryonic origin since embryonic cells were shown to produce the highest amounts of CDNPs compared to adult tissues [68] ii) therapeutically applied xenogeneic CDNPs are also derived from an embryonic cell line [66], and iii) the cell line should originate from C57BL/6 mice allowing for its application in C57BL/6 mice without evoking xenogeneic rejection.

To induce CDNP production, MC3T3-E3 cells were grown to confluency and stressed for two days by cultivation in serum-free media. Stressed cells were sonicated to disrupt their plasma membranes and release CDNPs. Resulting cell debris, nuclei and apoptotic bodies (<1 µm) were pelleted at 4,000g and discarded. Supernatants containing smaller particles (MPs, CDNPs and exosomes) were pelleted at 50,000g. Chloroform treatment was used to disrupt lipid membranes surrounding MPs and exosomes. Remnants and debris of this treatment were pelleted at 9,000g, while the supernatant containing CDNPs was analyzed further. A schematic overview of the isolation process is given in Fig. 4-1-5.

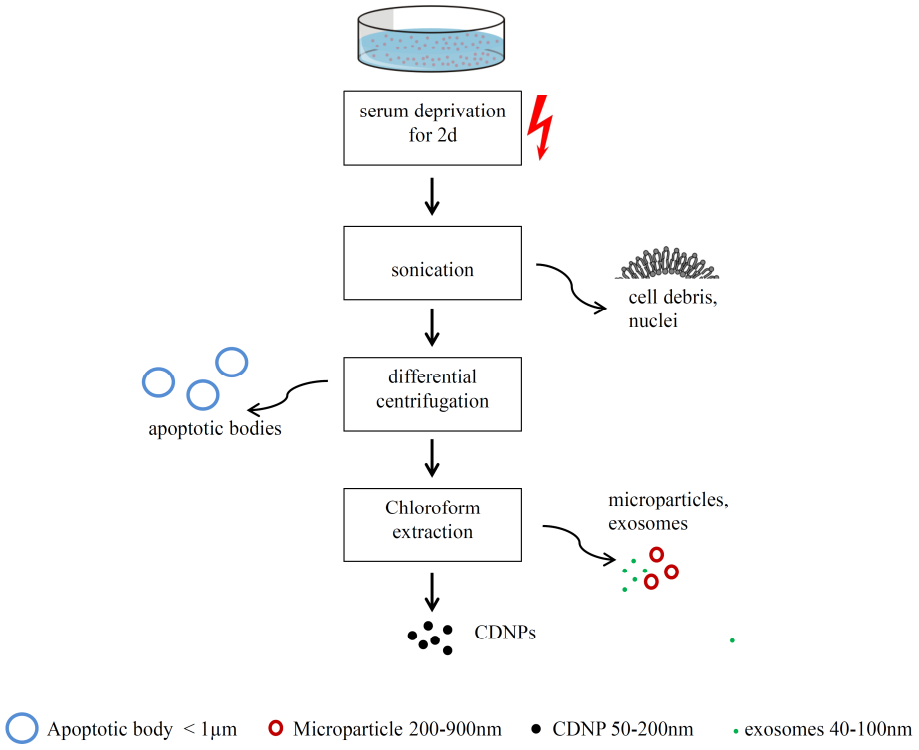


Fig. 4-1-5: Production of murine CDNPs: Murine fibroblast-like cells were stressed by serum deprivation and purified from cell debris, nuclei, apoptotic bodies, MPs and exosomes via differential centrifugation and chloroform extraction.

CDNPs are characterized by their particularity, size and composition [66,68]. Therefore, NTA, SEM and SDS gel electrophoresis were used to confirm CDNP presence in the isolates from stressed cells. To determine particularity, CDNP isolates were analyzed with NTA and SEM. Both methods clearly confirm the presence of particles (Fig. 4-1-6 A and B). CDNPs were described to measure between 50 and 200nm, depending on the method used. While NTA characterizes CDNPs as around 200nm [99], CDNPs exhibit diameters of approximately 50nm under SEM [68,99]. This difference is likely due to the dehydrating and thus shrinking treatment the samples undergo for EM preparation [150]. Comparison of CDNPs from xenogeneic and murine cells using NTA reveals similar size ranges of 50 to 350nm and similar means of 184 or 195nm, respectively, among xenogeneic and murine CDNPs (Fig. 4-1-6 B). Similarly, individual CDNPs from both xenogeneic and murine origin appear as spherical structures with diameters of approximately 60nm under the SEM (Fig. 4-1-6 A left panels), while CDNP aggregates reach much larger sizes (Fig. 4-1-6 A, right panels). The protein content of CDNPs from xenogeneic and murine CDNPs is not identical, but similar as

judged by the protein pattern after SDS gel electrophoresis (Fig. 4-1-6 C). In particular, murine CDNPs seem to be enriched in certain proteins as compared to xenogeneic CDNPs (c.f. bands at ~40-45 and at ~100kDa). Thus, NTA, SED and SDS gel electrophoresis together show that CDNPs are present in isolates from stressed murine cells. Moreover, Fig. 4-1-6 C confirms that individual CDNP preparations from murine cells show highly reproducible protein patterns (lines 1 to 5), while the amount of proteins in each preparation varies slightly (c.f. line 1 and 3).

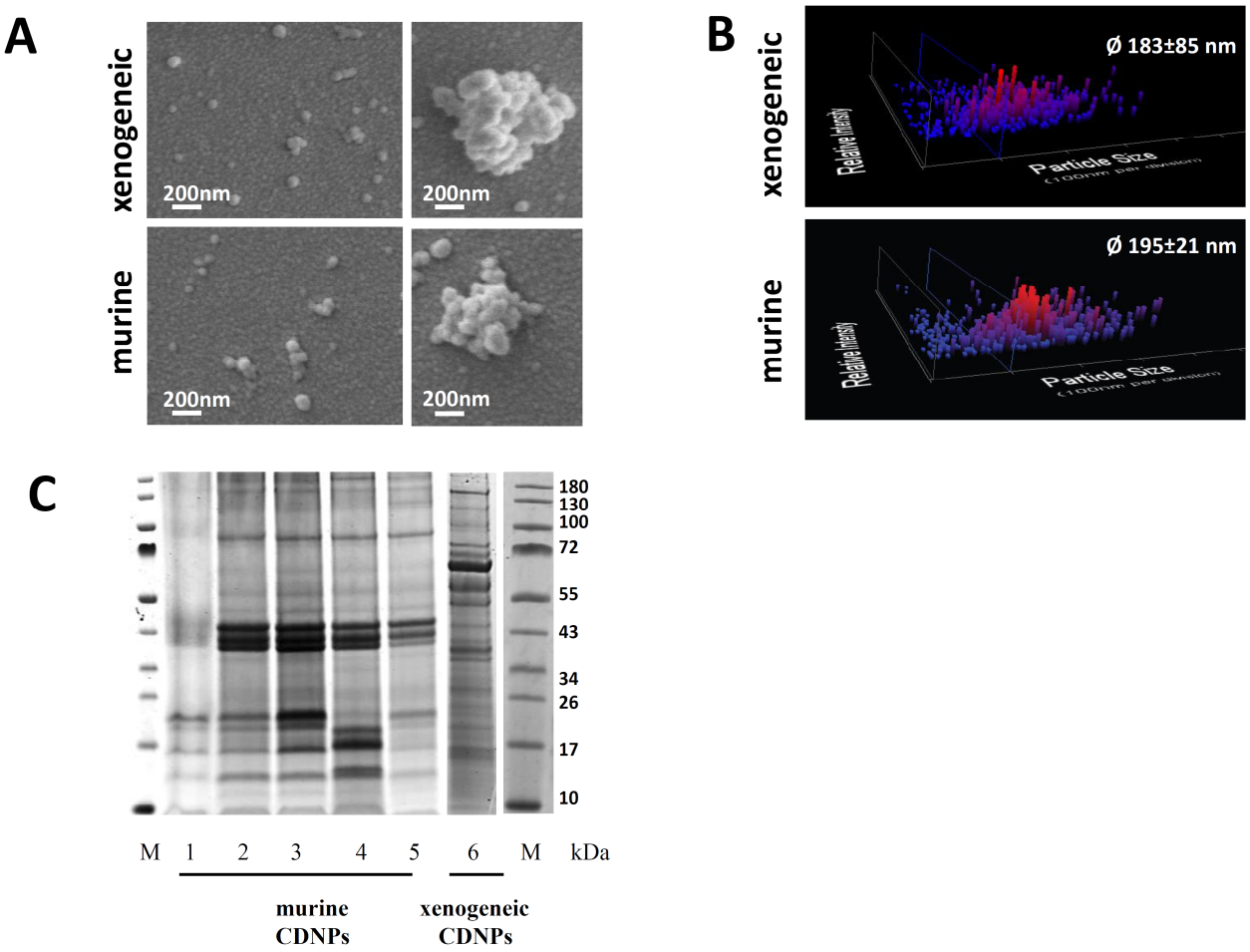


Fig. 4-1-6: Murine CDNPs display similar particularity, size and composition as xenogeneic CDNPs. A) Representative SEM images of xenogeneic and murine CDNPs. CDNPs are present as individual particles (left panel) or aggregated clusters (right panel). B) Representative images of size distributions from xenogeneic and murine CDNPs as assessed by NTA . The x axis represents particle size; divisors represent 100nm each. C) SDS gel electrophoresis was performed on isolates from murine (lanes 1-5) and xenogeneic (line 6) cells. Protein patterns were detected after coomassie blue staining.

4.1.2.2 Both allogeneic and xenogeneic CDNPs induce the same anti-inflammatory phenotype in activated macrophages

Having established that xenogeneic CDNPs significantly alter zymosan-stimulated cytokine expression after 24 hours of incubation (Fig.4-1-4), the subsequent set of experiments was performed to determine whether murine CDNPs show the same effects.

4.1.2.2.1 Both allogeneic and xenogeneic CDNPs reduce zymosan-induced TNFα expression

Peritoneal macrophages treated with xenogeneic or allogeneic CDNPs were stimulated with zymosan for 24h and gene expression of TNFα was assessed via quantitative RT-PCR. Zymosan-stimulated macrophages treated with murine CDNPs showed similar downregulation of TNFα mRNA levels as xenogeneic CDNPs (36% and 51%, respectively; Fig. 4-1-7).

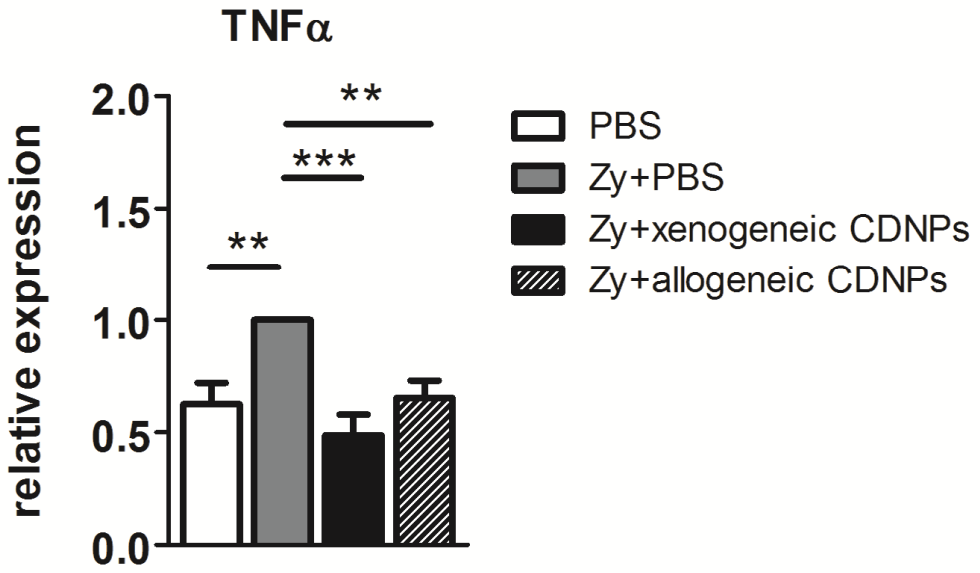


Fig. 4-1-7: Similar to xenogeneic CDNPs, allogeneic CDNPs decrease the TNFα expression of zymosan-stimulated macrophages 24 hours after incubation. Peritoneal lavages from naïve C56BL/6 mice were harvested and $1x10^5$ cells were pre-incubated 2 hours in media containing 1% serum to let macrophages adhere. Supernatants were then replaced with media containing 5% serum and the resulting culture enriched in macrophages was stimulated with 100 ng/ml zymosan (zy) and incubated with 50µg xenogeneic or allogeneic CDNPs per ml. 24 hours later cells were lysed and cytokine mRNA levels were determined using quantitative RT- PCR. mRNA expression levels were adjusted to the housekeeping gene MLN51 and normalized to expression levels of stimulated cells. n=5 cell preparations from individual mice. Data are expressed as means ± SEM. Significance was determined using repeated measurements ANOVA with Bonferroni post-hoc test. **p<0.01, ***p<0.001.

4.1.2.2.2 Allogeneic and xenogeneic CDNPs also reduce the expression of zymosan-induced IL-1β

To test, whether the CDNP-mediated reduction of pro-inflammatory cytokines is restricted to TNFα, mRNA levels of further MyD88-dependent cytokines were assessed after treatment of zymosan-stimulated macrophages with CDNPs: Together with TNFα, IL-1β and IL-6 comprise the most important cytokines in the acute phase response, the first, rapid and systemic response to invading pathogens [151,152]. Similar to TNFα, IL-1β expression was reduced by approximately 45% with both xenogeneic and allogeneic CDNPs (Fig. 4-1-8). IL-6 expression, in contrast, was differentially altered by xenogeneic and allogeneic CDNPs (Fig. 4-1-8). While xenogeneic CDNPs increased zymosan-induced IL-6 expression by 45%, murine CDNPs reduced IL-6 mRNA levels by 30%. Although, both alterations were not

significant compared to untreated macrophages, this finding suggests that allogeneic CDNPs have even stronger counter-inflammatory effects than xenogeneic CDNPs.

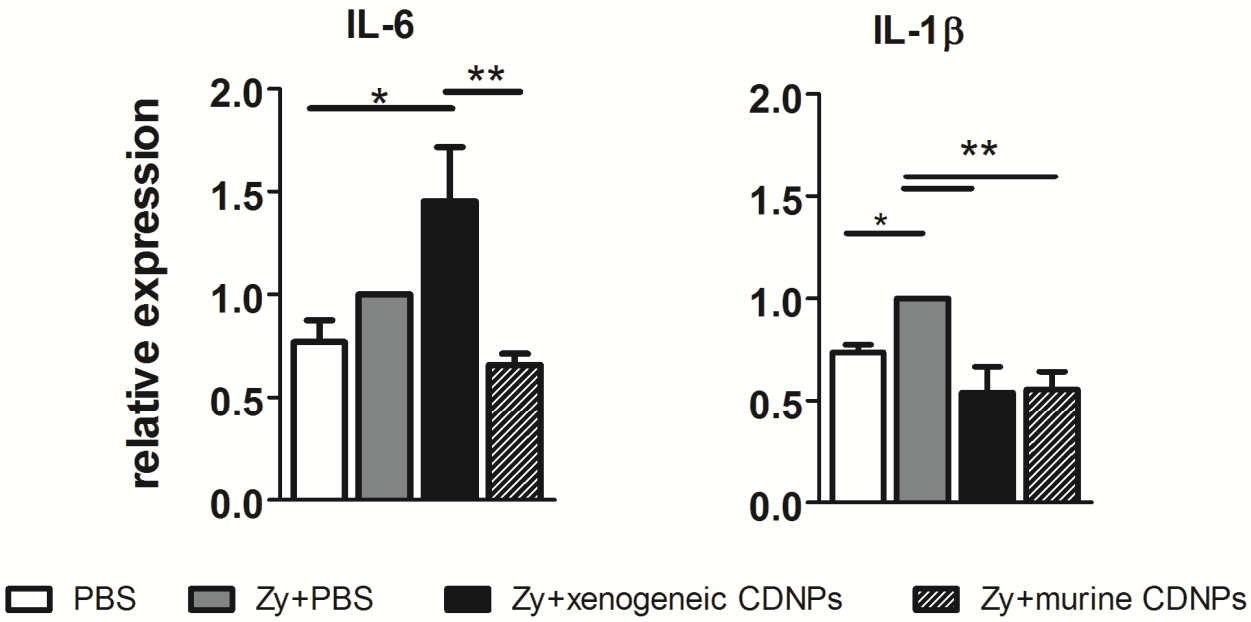


Fig. 4-1-8: Xenogeneic and allogeneic CDNPs both reduce IL-1β expression of zymosan-stimulated macrophages, while IL-6 expression is reduced by allogeneic CDNPs only. Peritoneal lavages from naïve C56BL/6 mice were harvested and $1x10^5$ cells were pre-incubated 2 hours in media containing 1% serum to let macrophages adhere. Supernatants were then replaced with media containing 5% serum and the resulting culture enriched in macrophages was stimulated with 100 ng/ml zymosan and incubated with 50µg xenogeneic or murine CDNPs per ml. 24 hours later cells were lysed and cytokine mRNA levels were determined using quantitative RT-PCR. mRNA expression levels were adjusted to the housekeeping gene MLN51 and normalized to expression levels of stimulated cells. n=5 cell preparations from individual mice. Data are expressed as means ± SEM. Significance was determined using repeated measurements ANOVA with Bonferroni post-hoc test. *$p<0.05$,**$p<0.01$.

4.1.2.2.3 Allogeneic and xenogeneic CDNPs increase the expression of zymosan-induced IL-10

Since the CDNP-mediated reduction of pro-inflammatory cytokines points towards an anti-inflammatory effect of CDNPs, the direct effect of xenogeneic and allogeneic CDNPs on the expression of the anti-inflammatory cytokine IL-10 was assessed. Strikingly, IL-10 expression was significantly increased 6- to 8-fold with xenogeneic and allogeneic CDNPs alike (Fig. 4-1-9). Thus, both xenogeneic and allogeneic CDNPs clearly possess anti-inflammatory properties.

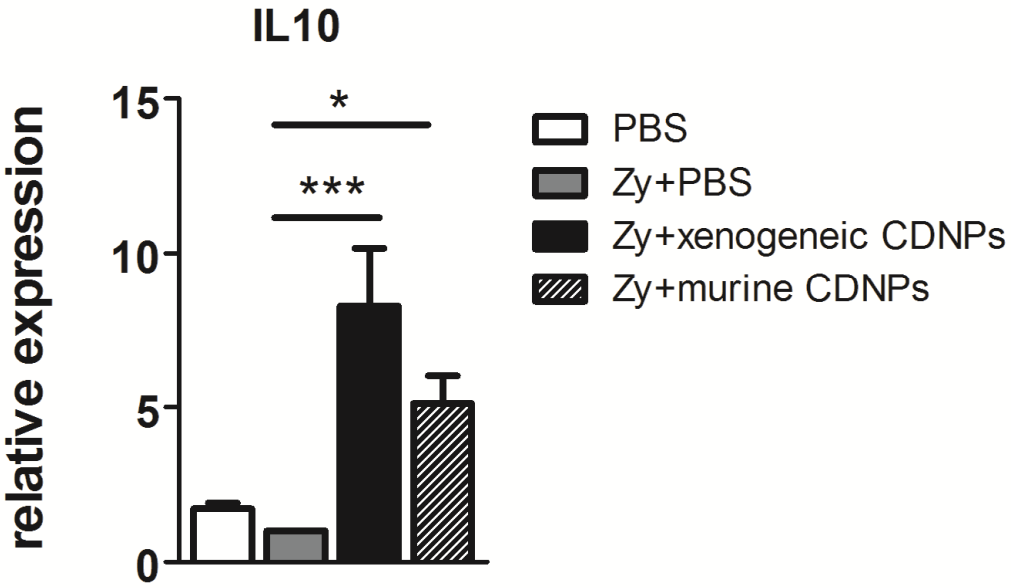


Fig. 4-1-9: Xenogeneic and allogeneic CDNPs increase zymosan-induced IL-10 expression. Peritoneal lavages from naïve C56BL/6 mice were harvested and $1x10^5$ cells were pre-incubated 2 hours in media containing 1% serum to let macrophages adhere. Supernatants were then replaced with media containing 5% serum and the resulting culture enriched in macrophages was stimulated with 100 ng/ml zymosan and incubated with 50µg xenogeneic or murine CDNPs per ml. 24 hours later cells were lysed and cytokine mRNA levels were determined using quantitative RT-PCR. mRNA expression levels were adjusted to the housekeeping gene MLN51 and normalized to expression levels of stimulated cells. n=5 cell preparations from individual mice. Data are expressed as means ± SEM. Significance was determined using repeated measurements ANOVA with Bonferroni post-hoc test. *$p<0.05$, ***$p<0.001$.

4.1.2.2.4 Allogeneic CDNPs induce an anti-inflammatory phenotype in Pam_3CSK_4-stimulated macrophages

Zymosan needs to be phagocytosed in order to activate TLR-2/TLR-6 inside the phagosome [125,153]. Since CDNPs and zymosan were added simultaneously, the uptake of CDNPs might have inhibited the ingestion of zymosan and therefore impair zymosan-induced cytokine expression. Such a mechanism would not explain increased IL-10 mRNA after CDNP-treatment, but it would account for reduced expression of pro-inflammatory cytokines. To test whether impaired zymosan-phagocytosis could be the reason for reduced expression of TNFα, IL-6 and IL-1β after treatment with CDNPs, peritoneal macrophages were stimulated with the synthetic triacylated lipoprotein Pam_3CSK_4, which is sensed by TLR-2/TLR-1 on the cell-surface [154]. To account for different expression kinetics after Pam_3CSK_4-stimulation, mRNA levels were assessed 4 and 24 hours after stimulation/treatment with allogeneic CDNPs. Since Pam_3CSK_4 did not induce a TNFα mRNA upregulation in the concentrations used, CDNPs had no effect on TNFα in this assay (Fig. 4-1-10). However, CDNP treatment reduced Pam_3CSK-induced IL-6 mRNA by 40% after 24 hours of stimulation and IL-1β mRNA by 20% and 40% after 4 and 24 hour of stimulation, respectively (Fig. 4-1-10), indicating that CDNPs indeed reduce the expression of pro-inflammatory cytokines upon TLR-2 triggering.

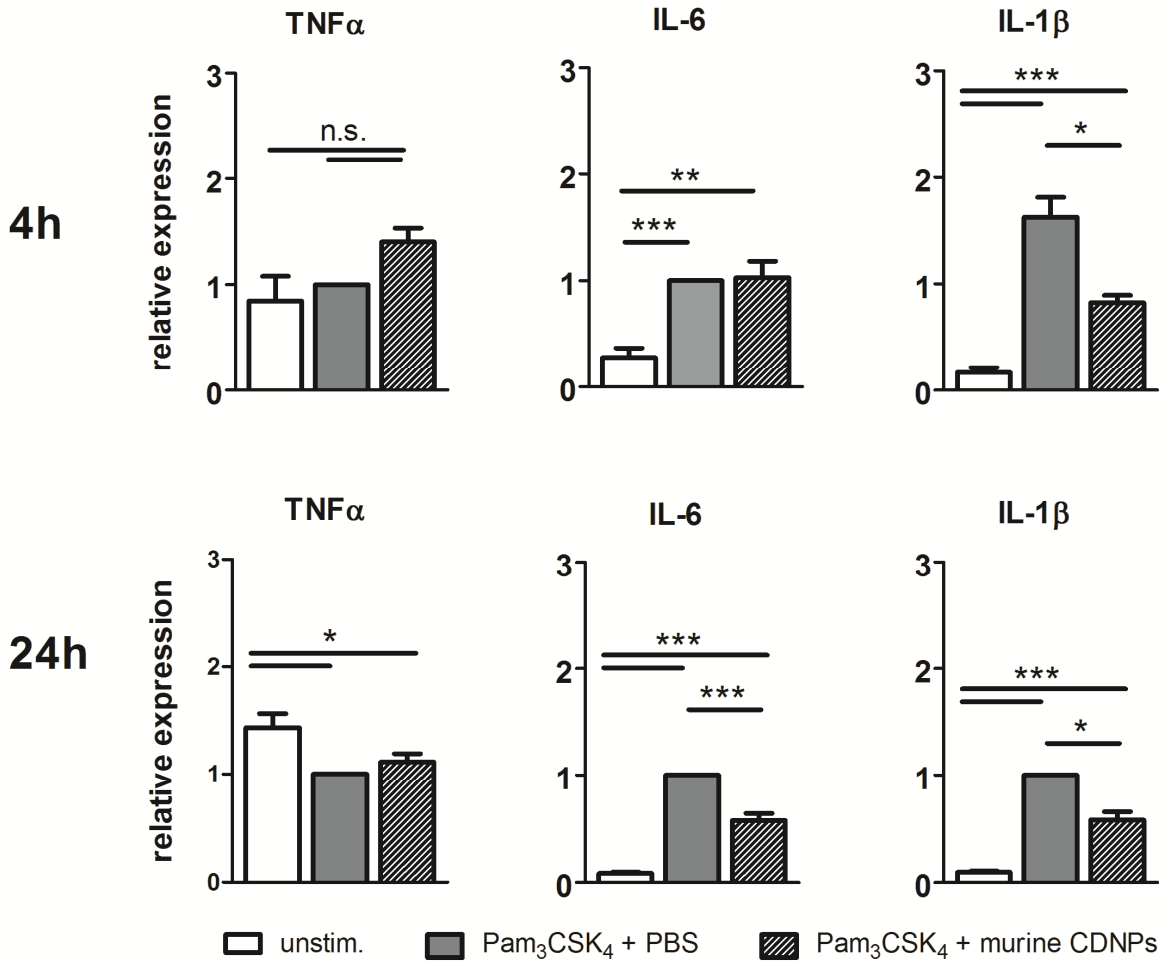


Fig. 4-1-10: Allogeneic CDNPs also alter the cytokine expression of peritoneal macrophages after stimulation with Pam_3CSK_4. Peritoneal lavages from naïve C56BL/6 mice were harvested and $1x10^5$ cells were pre-incubated 2 hours in media containing 1% serum to let macrophages adhere. Supernatants were then replaced with media containing 5% serum and the resulting culture enriched in macrophages was stimulated with 500 ng/ml Pam_3CSK_4 and incubated with 50 µg/ml allogeneic CDNPs. 4 or 24 hours later cells were lysed and cytokine mRNA levels were determined using quantitative RT-PCR. mRNA expression levels were adjusted to the housekeeping gene MLN51 and normalized to expression levels of stimulated cells. n=5 cell preparations from individual mice. Data are expressed as means ± SEM. Significance was determined using repeated measurements ANOVA with Bonferroni post-hoc test. *p<0.05,**p<0.01, ***p<0.001.

4.2 Only CDNPs derived from stressed cells show anti-inflammatory effects *in vitro* and annexin A5 might be the mediator

It was speculated that CDNPs are produced as a specific response to stress such as hypoxia, nutrient deprivation or infection [66,68]. According to the company producing CDNPs, however, CDNPs can also be derived from unstressed cells, albeit in very low concentrations [155]. Thus, to evaluate whether stress during CDNPs formation is altering their functional properties, CDNPs from unstressed cells (usCDNPs) were produced and their immunomodulatory effects were compared to CDNPs derived from stressed cells (sCDNPs). Moreover, the composition of s- and usCDNPs was compared in order to identify the possible mediator for the functional divergence of s- and usCDNPs.

4.2.1 CDNPs are also produced by unstressed cells

To test whether unstressed, healthy murine cells also produce CDNPs, fibroblast-like cells were cultured as described under 3.2.1.1.2, but without stressing the cells by culture in serum-free media. Preparations from both stressed and unstressed cells were subjected to the same isolation process. To account for slight differences in protein composition and concentration of individual preparations, 5 to 6 independently isolated preparations of s- and usCDNPs, respectively, were pooled. Similar as in chapter 4.1.2.1, SEM, NTA and SDS gel electrophoresis were used to identify CDNPs. The results revealed that unstressed cells indeed produce CDNPs. The size (approximately 60nm) and spherical appearance of single and aggregated usCDNPs is similar to sCDNPs under SEM (Fig. 4-2-1 A). The mean size and distribution of us- and sCDNPs is also comparable when determined by NTA (Fig. 4-2-1 B). In contrast, the protein pattern of usCDNPs after SDS gel electrophoresis differed significantly from the pattern obtained from sCDNPs, indicationg an altered protein composition after exposure to stress (Fig. 4-2-1 C). In particular, usCDNPs lack the three bands between 35 and 40 kDa, observed in sCDNPs.

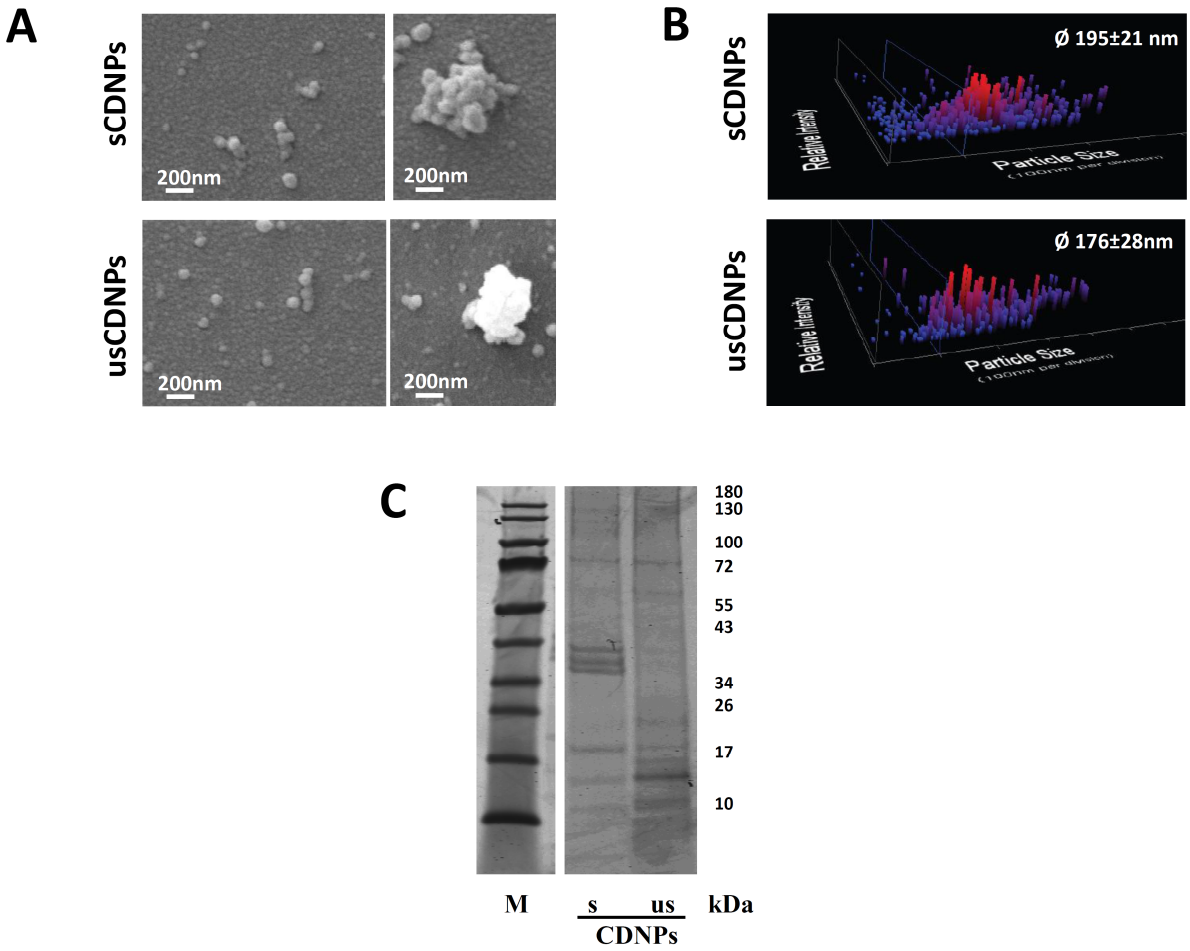


Fig. 4-2-1: Unstressed cells also produce CDNPs: A) Representative SEM images. B) Representative images of size distributions as assessed by NTA . The x axis represents particle size; divisors represent 100nm each. C) SDS gel electrophoresis. Protein patterns were detected after coomassie blue staining.

4.2.2 The immunomodulatory effect of CDNP *in vitro* is dependent on their origin from stressed cells

After establishing the production of CDNPs from unstressed cells, the effects of sCDNPs and usCDNPs were compared *in vitro*. To this end, the assay established in chapter 4.1 as well as further analyses were used.

4.2.2.1 Only CDNPs derived from stressed cells reduce zymosan-induced TNFα secretion

To test, whether the origin from stressed cells is necessary for their anti-inflammatory function, the effect of CDNPs on zymosan-induced TNFα protein levels were assessed. Indeed, sCDNPs reduced zymosan-induced TNFα secretion by 25% (Fig. 4-2-2). By contrast, usCDNPs had no detectable effect on zymosan-induced TNFα secretion.

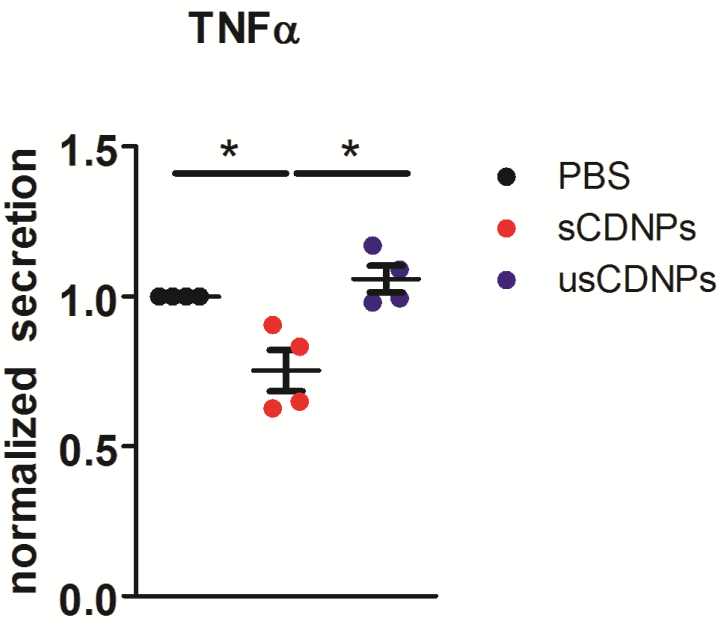


Fig. 4-2-2: Only sCDNPs reduce zymosan-induced TNFα secretion. Peritoneal lavages from naïve C56BL/6 mice were harvested. 1x10^5 cells were pre-incubated 2 hours in media containing 1% serum to let macrophages adhere. Supernatants were then replaced with media containing 5% serum and the resulting culture enriched in macrophages was incubated with 100ng/ml zymosan and 50µg s- or usCDNPs per ml for 24 hours at 37°C. TNFα- protein levels in the supernatants were determined by CBA and normalized to the TNFα levels of zymosan-stimulated cells incubated with PBS. n=4 cell preparations pooled from several mice. Data are expressed as means ± SEM. Significance was determined using repeated measurements ANOVA with Bonferroni post-hoc test. *p<0.05.

4.2.2.2 Both s- and usCDNPs are ingested by APCs and induce antigen-presentation

To investigate, whether the anti-inflammatory effect selectively induced by sCDNPs is the result of different uptake and processing of CDNPs, the ingestion of CDNPs by peritoneal macrophages and its consequences on MHCII surface expression as a surrogate marker for antigen-presentation were assessed.

4.2.2.2.1 Both s- and usCDNP are ingested by APCs

To evaluate whether s- and usCDNPs are equally well ingested, s- and usCDNPs were labeled with CFSE and incubated for 2 hours at 37°C with resting or LPS-activated peritoneal cells *in vitro*. To differentiate between ingestion and surface binding, one cell aliquot was incubated at 4°C to inhibit active uptake. After incubation, peritoneal cells were stained for $F4/80^+$ macrophages ($F4/80^+CD11b^+$, Fig. 4-2-3 A) and analyzed for CFSE expression. The CSFE MFI of cell incubated at 4°C (cell surface bound CDNPs) was subsequently subtracted from the CFSE MFI of cells incubated at 37°C to obtain ingested CFSE (i.e. CDNP) levels (Fig. 4-2-3 B).

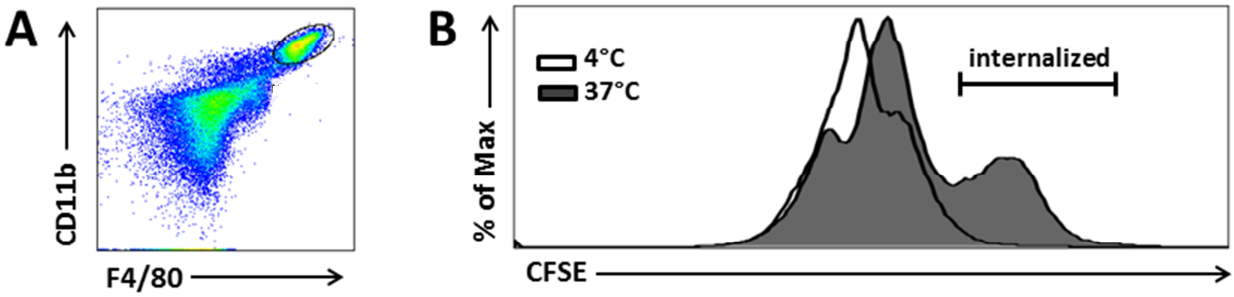


Fig. 4-2-3: Gating strategies for the identification of peritoneal macrophages and CDNP ingestion. Peritoneal lavages from naïve C56BL/6 mice were harvested and $5x10^5$ cells were pre-incubated 2 hours to let macrophages adhere. 10 µg/ml CFSE-labeled s- or usCDNPs were added and 1 ng/ml LPS was used for stimulation where indicated. Cells were harvested following 2 hours of incubation at 37°C, stained for B220, CD11b and F4/80 surface expression and analyzed by flow cytometry. A) Macrophages were considered $F4/80^+CD11b^+$. B) Internalization of CDNPs was determined by incubating one aliquot of cells at 4°C to prevent active uptake and one aliquote at 37°C. CFSE MFIs of cells incubated at 4°c were subtracted from those incubated at 37° to obtain true ingestion values. Representative data for sCDNP ingestion by macrophages is shown.

Peritoneal $F4/80^+$ macrophages ingested both s- and usCDNPs in considerable amounts, irrespective of cell stimulation (Fig. 4-2-4). Of note, unstimulated macrophages ingested 40% more usCDNPs than sCDNPs, however the ingestion levels of s- and usCDNPs equalized after LPS-stimulation.

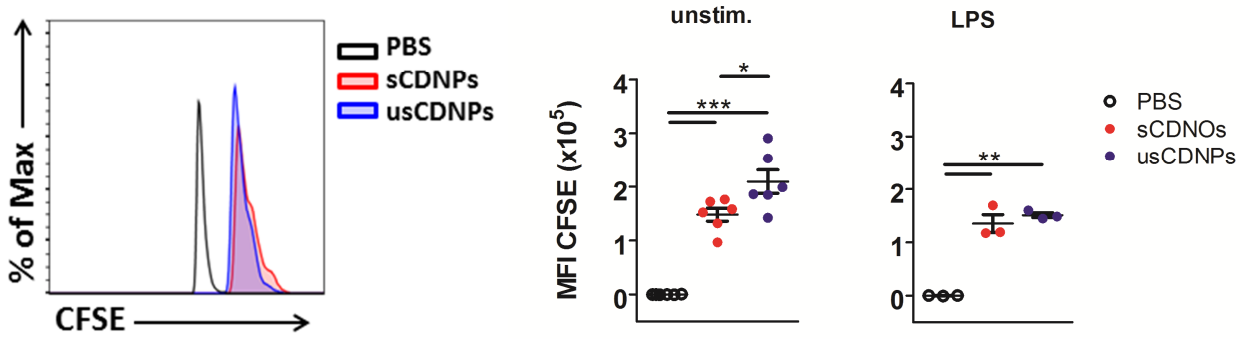


Fig. 4-2-4: Peritoneal macrophages ingest both s- and usCDNPs. Peritoneal lavages from naïve C56BL/6 mice were harvested and $5x10^5$ cells were pre-incubated 2 hours to let macrophages adhere. 10 µg/ml CFSE-labeled s- or usCDNPs were added and 1 ng/ml LPS was used for stimulation where indicated. Cells were harvested following 2 hours of incubation at 37°C, stained for B220, CD11b and F4/80 surface expression and analyzed by flow cytometry. Representative histograms and quantifications for CFSE fluorescence after subtraction of MFI levels at 4°C for PBS, s- and usCDNPs are shown. n=3-6 cell preparations from individual mice. Data are expressed as means ± SEM. Significance was determined using repeated measurements ANOVA with Bonferroni post-hoc test. *p<0.05, **p<0.01, ***p<0.001.

4.2.2.2.2 Ingestion of both s- and usCDNPs slightly increases the activation of peritoneal macrophages

To test, whether both s- and usCDNPs increase APC activation after ingestion, surface expression of MHCII was determined via flow cytometry. 24 hour after incubation, unstimulated macrophages treated with both s- and usCDNPs clearly, but non-significantly upregulated their MHCII surface expression 1.4- (sCDNPs) to 1.6-fold (usCDNPs, Fig. 4-2-5). LPS-stimulated macrophages similarly upregulated their MHCII expression 1.2- (sCDNPs) to 1.4-fold (usCDNPs), although only the latter reached significant levels. Thus, s- and usCDNP both slightly activate peritoneal macrophages.

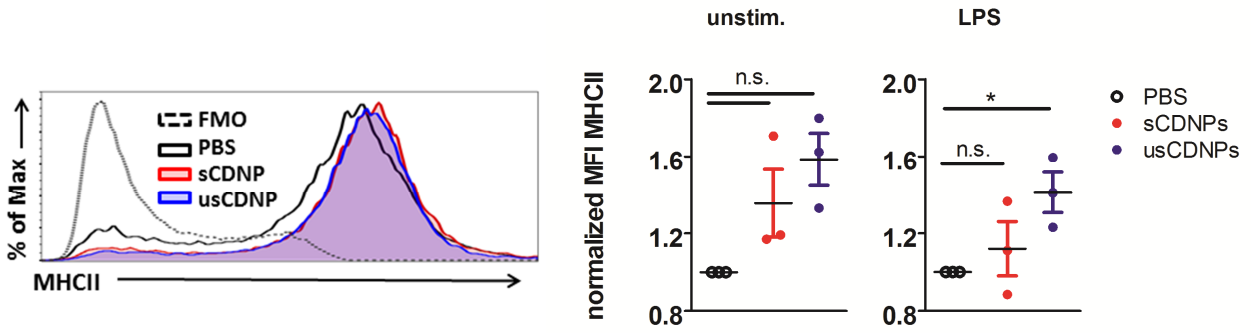


Fig. 4-2-5: Both s- and usCDNPs slightly increase MHCII surface expression on macrophages. Peritoneal lavages from naïve C56BL/6 mice were harvested and $5x10^5$ cells were pre-incubated 2 hours to let macrophages adhere. 10 µg/ml s- or usCDNPs were added and incubated for 24 hours at 37°C. 1 ng/ml LPS was used for stimulation where indicated. Cells were harvested following 2 hours of incubation at 37°C, stained for B220, CD11b, F4/80 and MHCII surface expression and analyzed by flow cytometry. Representative histograms and quantifications of MHCII expression on $F4/80^+CD11b^+$ macrophages are shown. MHCII surface expression was normalized to expression levels on PBS-treated cells from each mouse. n=3 cell preparations from individual mice. Data are expressed as means ± SEM. Significance was determined using repeated measurements ANOVA with Bonferroni post-hoc test. *p<0.05.

4.2.2.2.3 Only sCDNPs reduce $CD4^+$ T cell activation in response to LPS stimulation

Since both s- and usCDNPs similarly increase MHCII expression, which is indicative for their presentation as antigens, the effect of CDNP treatment on the activation status of T cells was determined following a 24 hour incubation of unstimulated or LPS-stimulated splenic cells with s- and usCDNPs, respectively. This way, APCs were able to ingest CDNPs and present them in the context of MHCII to affect T cell activation. Activation of adaptive immune cells was quantified using the early activation marker CD69, a member of the C-type lectin domain family involved in lymphocyte migration and cytokine secretion [156–158]. Uunstimulated $CD4^+$ T cells incubated with either s- or usCDNPs did not show altered CD69 surface expression (Fig. 4-2-6). However, when sCDNPs were incubated with LPS-stimulated $CD4^+$ T cells, CD69 expression was decreased by 20%, while usCDNPs had no effect on LPS-induced CD69 surface expression (Fig. 4-2-6).

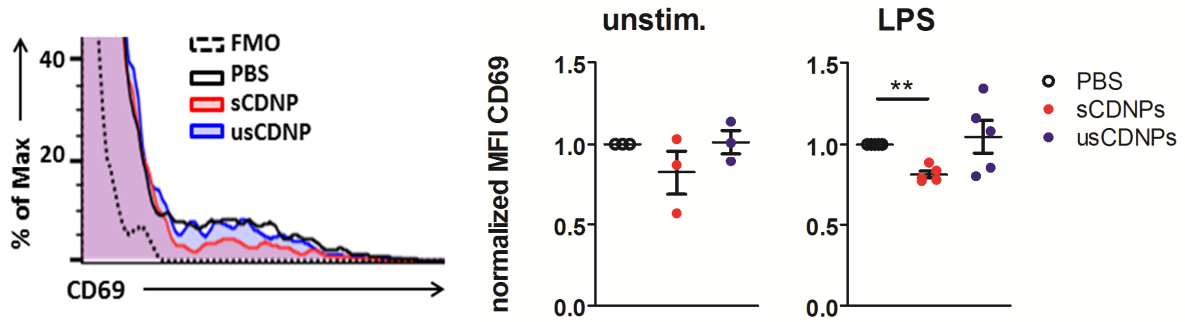


Fig. 4-2-6: Only sCDNPs reduce LPS-induced CD4$^+$ T cell activation. Spleens from naïve C56BL/6 mice were harvested and red blood cells lysed. 1x10^6 cells were incubated with 10 µg/ml s- and usCDNPs for 24 hours. 1 ng/ml LPS was used for stimulation where indicated. Cells were harvested and stained for CD4, CD8, B220 expression. CD4$^+$ T cells were gated as B220$^-$CD4$^+$. CD69 surface expression of unstimulated and LPS-stimulated CD4$^+$ cells was quantified and normalized to expression levels of PBS-treated cells. Representative FACS plot of LPS-stimulated cells is shown. n=3-5 cell preparations from individual mice. Data are expressed as means ± SEM. Significance was determined using repeated measurements ANOVA with Bonferroni post-hoc test. **p<0.01.

4.2.3 Identification of annexin A5 as a possible mediator for the anti-inflammatory effects of sCDNPs

Based on the different protein expression patterns of s- and usCDNPs (Fig. 4-2-1 C), it is reasonable to speculate that the different protein composition induced by stress is responsible for the anti-inflammatory effect of s- in contrast to usCDNPs. To identify the proteins enriched by stress, 2DIGE separating proteins by their molecular weight and isoelectric points, was performed. Overlays of Cy3-labeled s- and Cy5-labeled usCDNPs revealed that only few proteins were co-expressed by s- and usCDNPs (depicted as yellow spots in Fig. 4-2-7) Instead, sCDNPs were enriched in certain proteins (red spots in Fig. 4-2-7), while clearly lacking other proteins present in usCDNPs (green spots, Fig. 4-2-7).

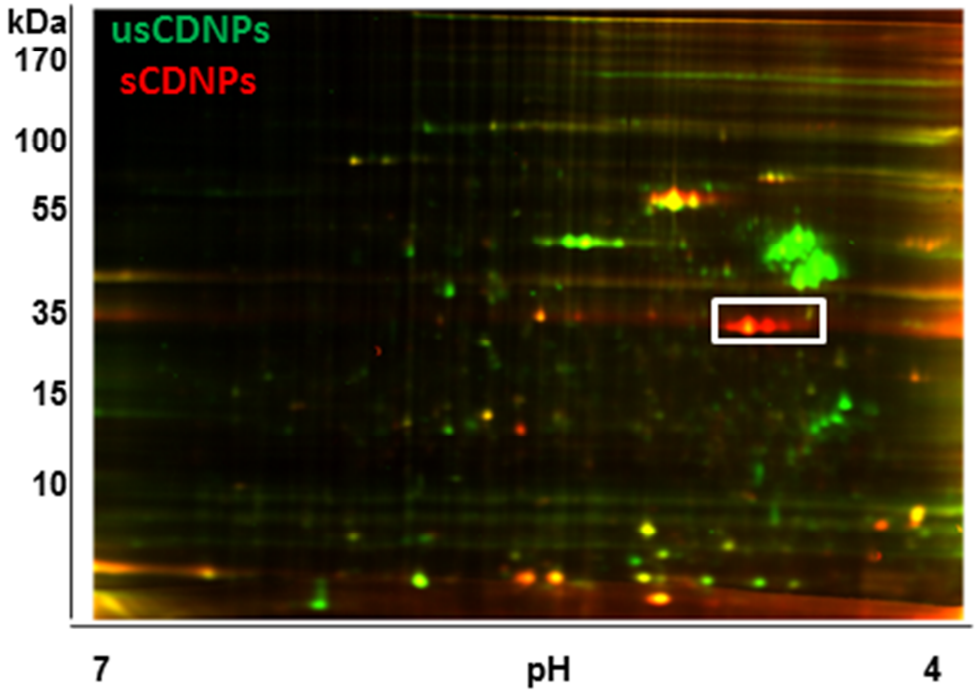


Fig. 4-2-7: sCDNPs have a different protein composition as compared to usCDNPs. CDNP preparations derived from stressed and unstressed cells were compared by 2D DIGE. sCDNPs were labeled with Cy5 and usCDNPs were labeled witch Cy3. Representative overlay for 4 independent experiments. Annexin A5 is marked (see chapter 4.2.3).

Principal component analysis of the proteins derived from s- and usCDNPs demonstrated that proteins from sCDNPs and usCDNPs indeed clustered together, suggesting that both CDNPs can be distinguished by their protein expression (Fig. 4-2-8).

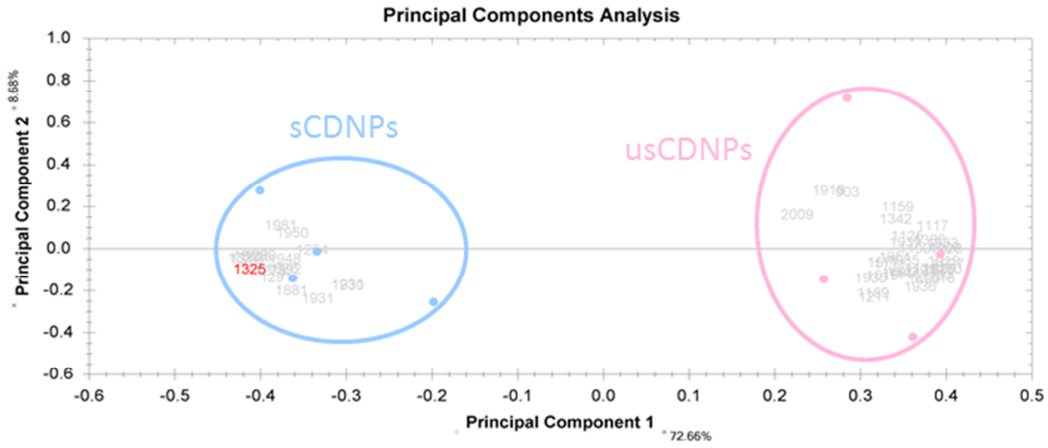


Fig. 4-2-8: s- and usCDNPs can be distinguished based on their protein composition. Principal component analysis of 52 proteins enriched in sCDNPs vs. usCDNPs. The clustering reveals that proteins from s- and usCDNPs, respectively, cluster together. X and Y-axis depict first and second principal components, respectively. CDNP samples were run in quarduplicates and each colored point represents the accumulation of all proteins present in one sample.

To identify the proteins enriched upon stress, the highest expressed proteins of CDNPs derived from stressed vs. unstressed cells were picked from the gel and analyzed by MALDI-TOF. Tab. 4 lists the most upregulated proteins in sCDNPs compared to usCDNPs. Interestingly, two isoforms of annexin A5 ranked first with a 12-14-fold increase in CDNPs derived from stressed vs. unstressed cells.

Tab. 4: Proteins enriched in sCDNPs vs. usCDNPs. Proteins which were upregulated in CDNPs from stressed vs. unstressed cells were identified by MALDI-TOF. Depicted are proteins from sCDNPs with the highest increase as compared to usCDNPs. p-values were determined using ANOVA with Bonferroni post-hoc test.

Protein	x-fold vs. unstressed	P value
ANXA5_Mouse	14,963709	2,91E-05
ANXA5_Mouse	12,3026627	6,82E-05
CCD62_Mouse DTNA_Mouse	6,68388548	0,00156
ANXA3_Mouse	2,87186936	0,01076
NCOR1_Mouse	2,79767932	0,00501
ANXA7_Mouse	2,57036121	0,00156
ANXA4_Mouse	2,50838784	0,00226
ANXA1_Mouse	2,37903542	0,00017
H4_Mouse	2,0217036	0,01118

ANXA3: annexin A3, ANXA4: annexin A4, ANXA5: annexin A5, ANXA7: annexin A7, CCD62: Coiled-Coil Domain Containing 62, DTNA: Dystrobrevin Alpha, H4: Histon 4, NCOR1: Nuclear Receptor Corepressor 1.

Western Blots of s- and usCDNP preparations using an annexin A5-specific antibody confirmed the presence of annexin A5 in sCDNPs, but not in usCDNPs (Fig. 4-2-9). Thus, annexin A5 is a characteristic marker for sCDNPs and might be mediating its anti-inflammatory effects.

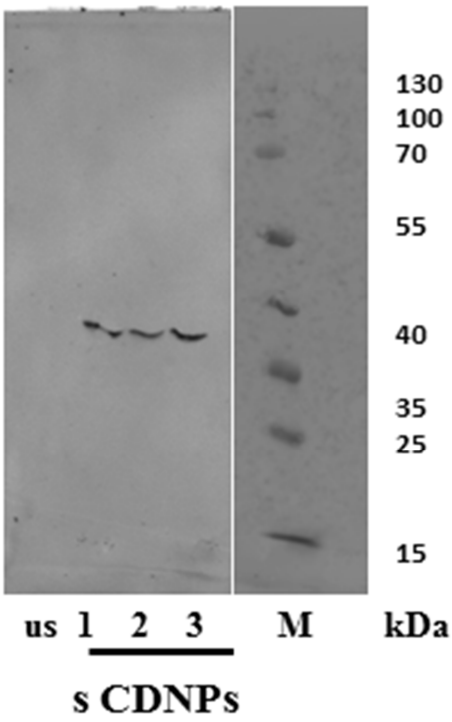


Fig. 4-2-9: Only sCDNPs are enriched in annexin A5. Annexin A5 content from usCDNPs (left line) and from 3 different sCDNP preparations (lines 1-3) was determined by Western Blot using annexin A5-specific antibodies.

4.3 CDNPs are beneficial in sepsis and slightly modulate *L. major* infection

Previous findings suggest that CDNPs have protective effects in viral infections in mice and humans [69,72]. To test, whether this effect is restricted to viral infections, CDNP treatment was applied in a *L. major* model of intracellular infection and in the setting of extracellular polybacterial sepsis. In order to mimic therapeutic CDNP usage [67,159], low doses of CDNPs (5µg) were used for these experiments.

4.3.1 CDNPs induce an anti-inflammatory milieu at the infection site, drive DC activation and increase Treg frequencies in the draining lymph node of *L. major*-infected mice

Similar to viral infections, *L. major* represents an intracellular pathogen. Moreover, TLR2, whose cytokine expression has been shown to be modulated by sCDNPs (chapter 4.2.2.1) specifically senses LPG from *Leishmania* [160]. Thus it appears likely that CDNPs would have an effect in this setting. Four weeks post infection, when the peak of foot-pad swelling was reached [115], mice were sacrificed and draining lymph nodes and food pad skins were harvested. The clearance of *L. major* infection crucially relies on the formation of IFNγ-producing Th1 cells which activate macrophages to kill the parasite [82]. Thus, the analysis conducted here, focused on the adaptive immune response. usCDNPs were used as an additional control group in these experiments in order to confirm their lack of immunomodulatory effects *in vivo*.

4.3.1.1 CDNPs increase MHCII surface expression on DCs in the draining lymph node of *L. major*-infected mice

The protective Th1 response in *L. major*-infected mice is initiated by antigen-presenting cells, whose incubation with CDNPs slightly increased MHCII surface expression *in vitro* (chapter 4.2.2.2.2). To test whether CDNPs also modulate antigen presentation in the context of *L. major*-infection, MHCII expression on DCs in the draining lymph nodes of infected mice was analyzed. The two prototypic lymphatic DC subsets were identified based on the expression of B220 and CD11c: $B220^{-}CD11c^{+}$ cells were considered cDCs and $B220^{+}CD11c^{+}$ were considered pDCs (Fig. 4-3-1).

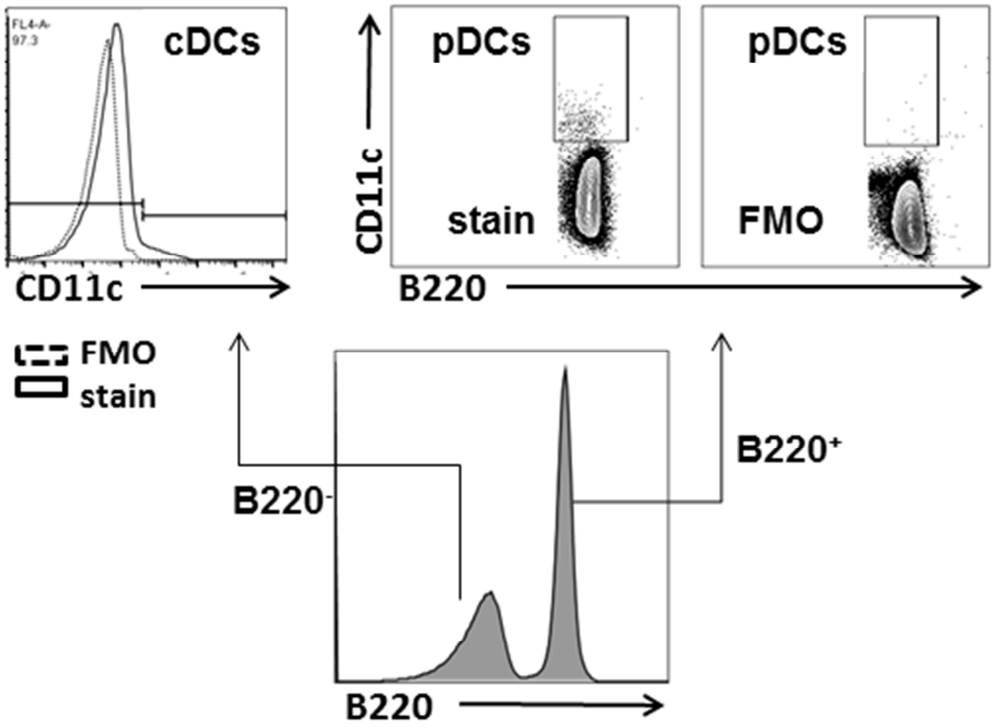


Fig. 4-3-1: Gating strategy for c- and pDCs. C56BL/6 mice were infected with 1x10^6 viable *L. major* promastigotes into the hind foot pad. 5µg s- or usCDNPs were injected s.c. into the hint legs, every other day. Draining lymph nodes were harvested 4 weeks post infection. Single cell suspensions were stained with fluorescence-labeled mAbs to B220, CD11c and MHCII and analyzed by flow cytometry. cDCs were identified as B220$^-$CD11c$^+$ and pDCs as B220$^+$CD11c$^-$.

The absolute numbers of c- and pDCs remained unaltered by CDNP treatment (data not shown). However, sCDNP application increased the surface expression levels of MHCII on cDCs by 70% and on pDCs by 50%, while usCDNPs had no effect on MHCII surface expression by DCs (Fig. 4-3-2). These results indicate that sCDNPs induce DC maturation and antigen presentation *in vivo*.

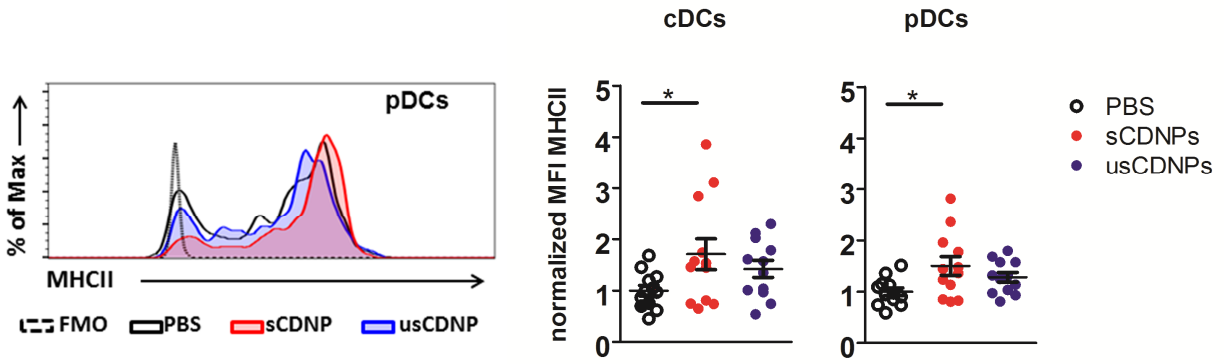


Fig. 4-3-2: CDNPs activate DCs in the draining lymph node of *L. major*-infected mice. C56BL/6 mice were infected with $1x10^6$ viable *L. major* promastigotes into the hind foot pad. 5µg s- or usCDNPs were injected s.c. into the hint legs, every other day. Draining lymph nodes were harvested 4 weeks post infection. Single cell suspensions were stained with fluorescence-labeled mAbs to B220, CD11c and MHCII and analyzed by flow cytometry. Representative histogram of MHCII surface expression on pDCs is depicted. MHCII expression was quantified and normalized to the expression levels of PBS-treated mice. Pooled results from 2-3 independent experiments with n=3-6 mice per group. Data are expressed as means ± SEM. Significance was determined using repeated measurements ANOVA. *p<0.05.

4.3.1.2 CDNPs shift the ratio of naïve vs. effector memory CD4+ T cells in the draining lymph node of *L. major*-infected mice to the effector side

Increased antigen presentation is accompanied by augmented T cell activation. Thus, to test whether CDNP treatment impacts T cell activation, the activation status of $CD4^+$ T and $CD8^+$ T cells in the draining lymph node of *L. major*-infected mice was analyzed. The gating strategy used discriminated naïve, central memory and effector/ effector memory T cells by their expression of CD44 and CD62L (Fig. 4-3-3). CDNP treatment did not affect the activation status of $CD8^+$ T cells (data not shown). Likewise, CDNPs did not significantly alter the frequencies of naïve, central memory or effector/effector memory $CD4^+$ T cells (Fig. 4-3-3). But notably, the ratio of naïve vs. effector (memory) $CD4^+$ T cells was reduced by 20% when mice were treated with sCDNPs (p=0.06; Fig. 4-3-3). usCDNPs in contrast, reduced this ratio by 12% only (p=0.30). Thus, only sCDNP-treatment shifted the naïve vs. effector $CD4^+$ T cell ratio towards the effector (memory) side.

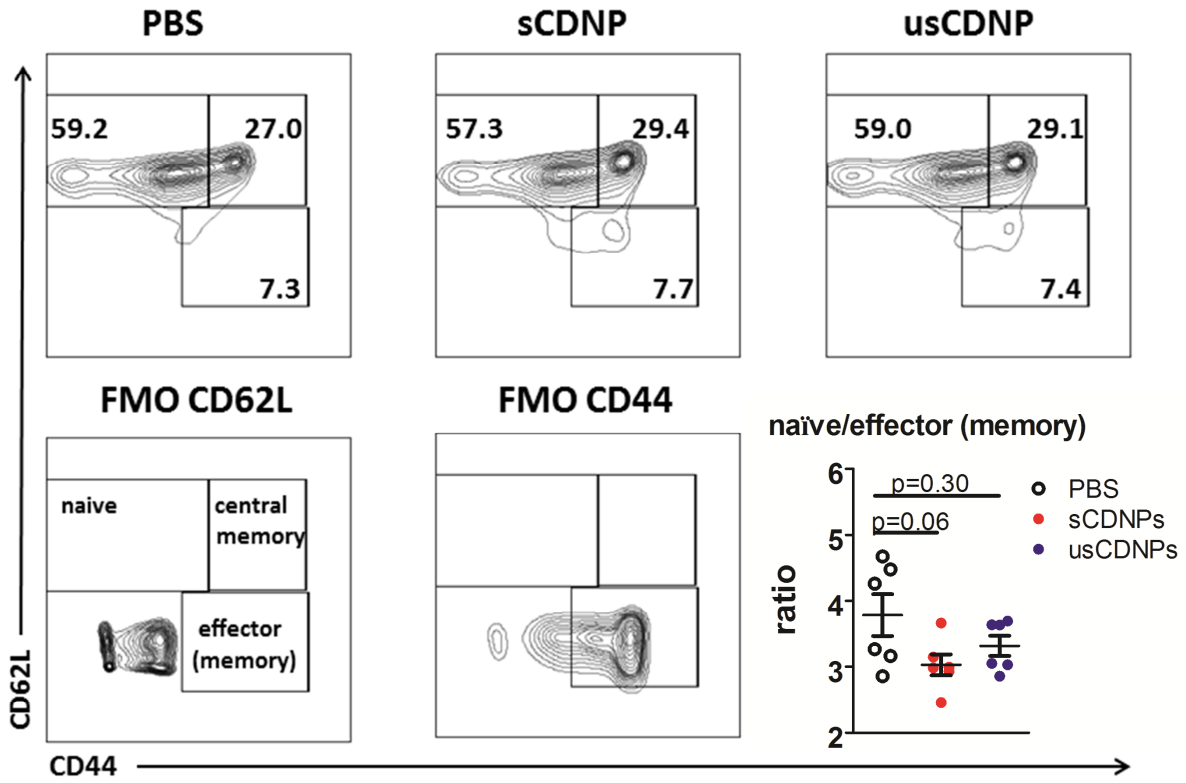


Fig. 4-3-3: CDNPs shift the ratio of naïve vs. effector (memory) CD4$^+$ T cells in the draining lymph node of *L. major*-infected mice to the effector side. C56BL/6 mice were infected with 1x10^6 viable *L. major* promastigotes into the hind foot pad. 5µg s- or usCDNPs were injected s.c. into the hint legs, every other day. Draining lymph nodes were harvested 4 weeks post infection. Single cell suspensions were stained with fluorescence-labeled mAbs to CD4, CD62L and CD44 and analyzed by flow cytometry. Live, single cells were gated on CD4$^+$ cells. CD62L$^+$CD44$^-$ cells were considered naïve, CD62L$^+$CD44$^+$ central memory and CD62L$^-$CD44$^+$ effector/effector memory T cells [162]. The upper panel depicts representative plots for PBS-, sCDNP- and usCDNP-treated mice, while the first two figures of the lower panel depict FMO controls lacking CD62L or CD44, respectively. Numbers indicate the percentage of cells in each gated box. The last figure in the lower panel on the far right shows the ratio of naïve versus effector memory CD4$^+$ T cells. n=6 mice per group. Data are expressed as means ± SEM. p-values were determined using repeated measurements ANOVA with Bonferroni post-hoc test.

4.3.1.3 CDNPs shift the milieu in the draining lymph node and at the site of infection towards Th2

The surface of *Leishmania* parasites is covered by the abundant cell surface glycolipid LPG which is sensed by TLR2 expressed on APCs such as DCs [161]. Triggering of TLR2 by LPG leads to the secretion of Th1-promoting cytokines [163–165]. Thus, interference with *Leishmania*-induced TLR2 signaling, as expected for CDNPs, should alter the cytokine milieu and consequently the T cell polarization pattern of *L. major*-infected mice.

To elucidate whether CDNPs alter the Th1/Th2 polarization in the draining lymph nodes, where antigen presentation and T cell polarization takes place, intracellular IFNγ levels (indicative for Th1 cells) and intracellular IL-4 levels (characterizing Th2 cells) were analyzed (see suppl. Fig. S2 for gating strategy and representative plots). While intracellular IL-4 levels on $CD4^+$ T cells were unaltered by s- or usCDNP treatment (Fig. 4-3-4 A). Intracellular IFNγ levels in contrast, were decreased by 22% (p=0.1) when infected mice were treated with sCDNPs, but not usCDNPs (Fig. 4-3-4 B).

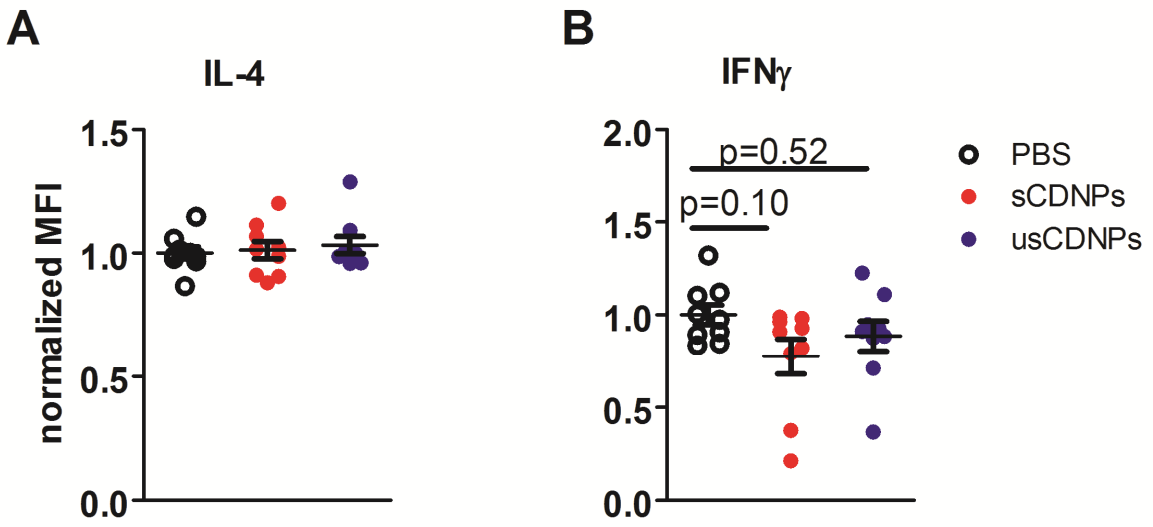


Fig. 4-3-4: CDNPs decrease intracellular IFNγ levels on $CD4^+$ cells of the draining lymph node of *L. major*-infected mice. C56BL/6 mice were infected with $1x10^6$ viable *L. major* promastigotes into the hind foot pad. 5µg s- or usCDNPs were injected s.c. into the hint legs, every other day. The draining lymph node was harvested 4 weeks post infection. $1x10^6$ cells were restimulated with 5 ng/ml PMA and 1µg/ml ionomycin for 1 hour at 37° C. 5 µg/ml Brefoldin A was added and cells were incubated for additional 4 hours. Cells were harvested and first stained with fluorescence-labeled mAbs against surface CD4, then permeabilized and stained for intracellular IL-4 (A) and IFNγ (B). Analysis was carried out via flow cytometry. IL-4 and IFNγ expression was quantified and adjusted to expression levels of PBS-treated mice. Single, viable cells were gated on $CD4^+$ cells. Pooled results from 1-2 independent experiments with n=2-6 mice per group. Data are expressed as means ± SEM.

Polarized T cells migrate to the site of infection to execute their effector functions [166]. Thus, the polarization of T cells in the food pad skin was assessed based on the mRNA expression of IL-4 and IFN-γ. sCDNP treatment of *L. major*-infected mice increased anti-inflammatory IL-4 mRNA levels by 100% (Fig. 4-3-5 A), while pro-inflammatory IFNγ mRNA expression remained constant (Fig. 4-3-5 B). usCDNPs did not alter IL-4 or IFNγ expression. Together, these results indicate that s-, but not usCDNPs skew T cell polarization towards Th2.

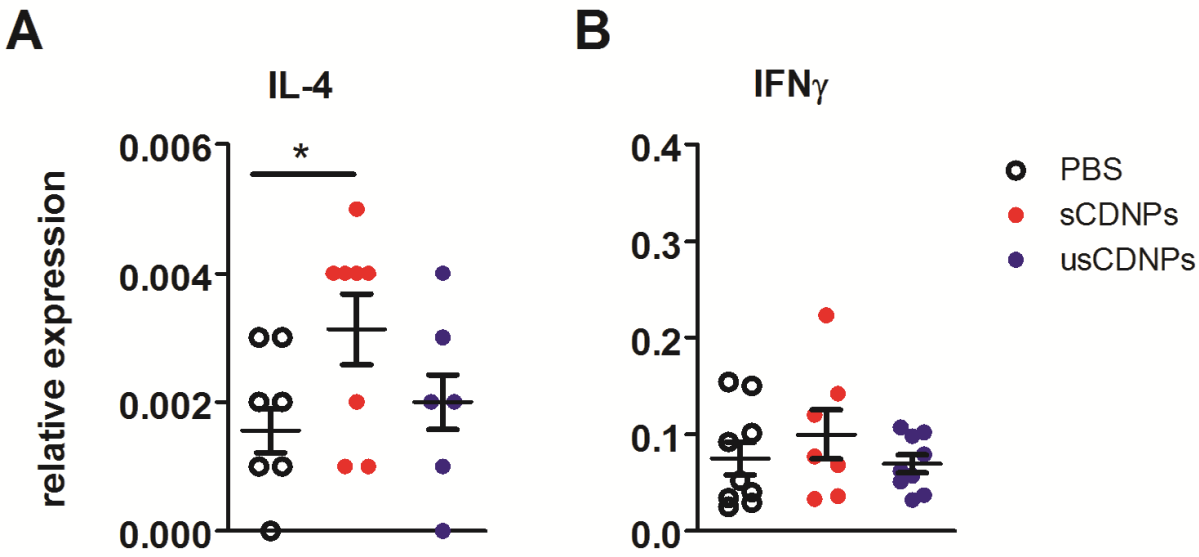


Fig. 4-3-5: CDNPs increase IL-4 mRNA levels at the infection site of *L. major*-infected mice. C56BL/6 mice were infected with $1x10^6$ viable *L. major* promastigotes into the hind foot pad. 5µg s- or usCDNPs were injected s.c. into the hint legs, every other day. Foot pad skins were harvested 4 weeks post infection and immediately frozen at -80°C. 10 cryosections of each skin were lysed for RNA extraction and transcription into cDNA. Cytokine expression was analyzed by quantitative RT-PCR. Expression levels were normalized to the housekeeping gene MLN51. Pooled results from 2-3 independent experiments with n=1-6 mice per group. Data are expressed as means ± SEM. Significance was determined using repeated measurements ANOVA with Bonferroni post-hoc test. *p<0.05.

4.3.1.4 CDNPs increase the frequency of Foxp3$^+$ T cells in the draining lymph node and elevate IL-10 levels at the infection site

Next to Th1 and Th2 cell, regulatory T cells which secrete IL-10 play an important part in the clinical outcome of *L. major* infection. In fact, IL-10 deficient mice as well as mice with IL-

10 deficient T cells were shown to develop increased lesion sizes due to ineffective infection control [167]. Owing to the suppressive role of IL-10 on T cells, decreased IL-10 levels are associated with resistance, while IL-10 overexpression results in susceptibility [167,168]. To test, whether CDNPs would alter the polarization to Tregs, intracellular IL-10 in $CD4^+$ T cells within the draining lymph node of infected mice were analyzed. However, IL-10 levels remained unaffected by CDNP treatment (suppl. Fig. S1). Notwithstanding, sCDNP-treated mice exhibited 20% more $Foxp3^+CD4^+$ T cells than control mice (Fig. 4-3-6). Since the frequency of conventional Tregs ($Foxp3^+$ $CD25^+$ $CD4^+$) was not altered by sCDNP treatment (suppl. Fig. S1), these results indicate that sCDNPs upregulate non-conventional regulatory T cells. Of note, increased $Foxp3^+$ $CD4^+$ T cell frequencies were not observed in usCDNP treated mice (Fig. 4-3-6).

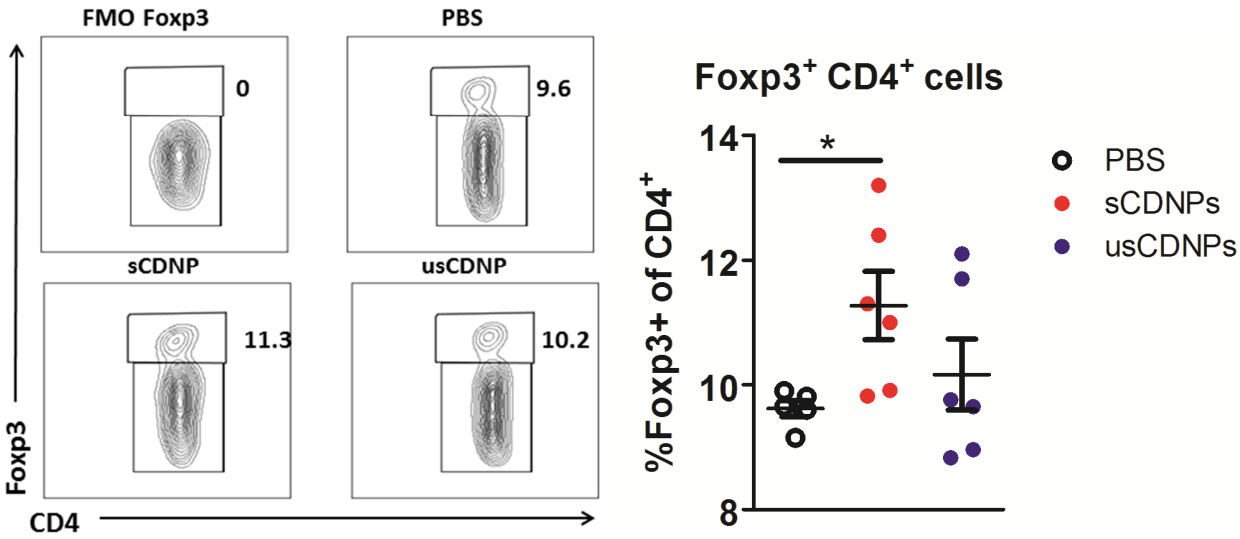


Fig. 4-3-6: CDNPs increase the frequency of regulatory $Foxp3^+CD4^+$ T cells in the draining lymph node of *L. major*-infected mice. C56BL/6 mice were infected with $1x10^6$ viable *L. major* promastigotes into the hind foot pad. 5µg s- or usCDNPs were injected s.c. into the hint legs, every other day. The draining lymph node was harvested 4 weeks post infection. $1x10^6$ cells were stained with fluorescence-labeled mAbs against surface CD4, then permeabilized and stained for intranuclear Foxp3. Depicted are representative FACS plots and quantifications of $Foxp3^+$ cells within $CD4^+$ T cells. Results from 1 experiment with n=6 mice per group. Data are expressed as means ± SEM. Significance was determined using repeated measurements ANOVA with Bonferroni post-hoc test. *$p<0.05$.

At the site of infection, gene expression levels of the regulatory and anti-inflammatory IL-10 were also increased by 50% ($p \geq 0.05$) in response to sCDNP treatment (Fig. 4-3-7), further indicating towards increased polarization to Tregs. In contrast, usCDNP treatment had no effect on the cytokine milieu in the foot pad skin (Fig. 4-3-7).

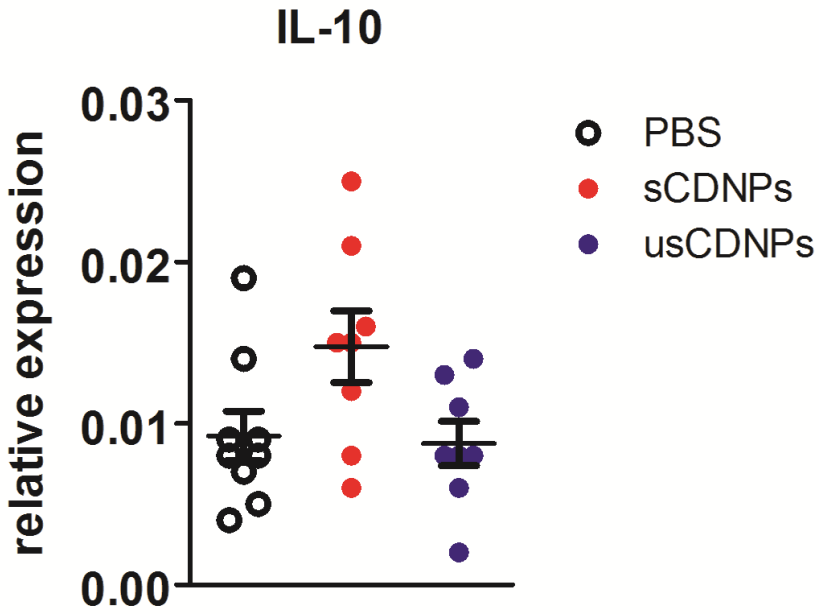


Fig. 4-3-7: CDNPs increase IL-10 mRNA at the infection site of *L. major*-infected mice. C56BL/6 mice were infected with $1x10^6$ viable *L. major* promastigotes into the hind foot pad. 5µg s- or usCDNPs were injected s.c. into the hint legs, every other day. Foot pad skins were harvested 4 weeks post infection and immediately frozen at -80°C. 10 cryosections of each skin were lysed for RNA extraction and transcription into cDNA. Cytokine expression was analyzed by quantitative RT-PCR. Expression levels were normalized to the housekeeping gene MLN51. Pooled results from 3 independent experiments with n=1-6 mice per group. Data are expressed as means ± SEM.

4.3.1.5 CDNP treatment has no effect on the clinical outcome of *L. major* infection

Th1 induction in *L. major*-infected C57BL/6 mice is of critical importance for the resolution of inflammation. Th1 reacting mice demonstrate a transient swelling at the infection site, but eventually control infection by activating macrophages to kill the intracellular parasite. Th2 responses in contrast are incapable to control infection, leading to persistent swelling and constantly high parasite loads at the infection site [169]. To investigate, whether the shifted immune response induced by sCDNP treatment has functional consequences on disease outcome, foot pad swelling was followed during the course of infection. Furthermore,

bacterial loads in the foot pad skin were assessed based on the expression of *Leishmania* POLA expression and Kinetoplast DNA expression.

However, despite clear differences regarding T cell polarization and cytokine milieu, sCDNP application had no effect on foot pad swelling and bacterial loads of *L. major*-infected mice (Fig. 4-3-8 A and B). usCDNPs had likewise no impact on the disease outcome.

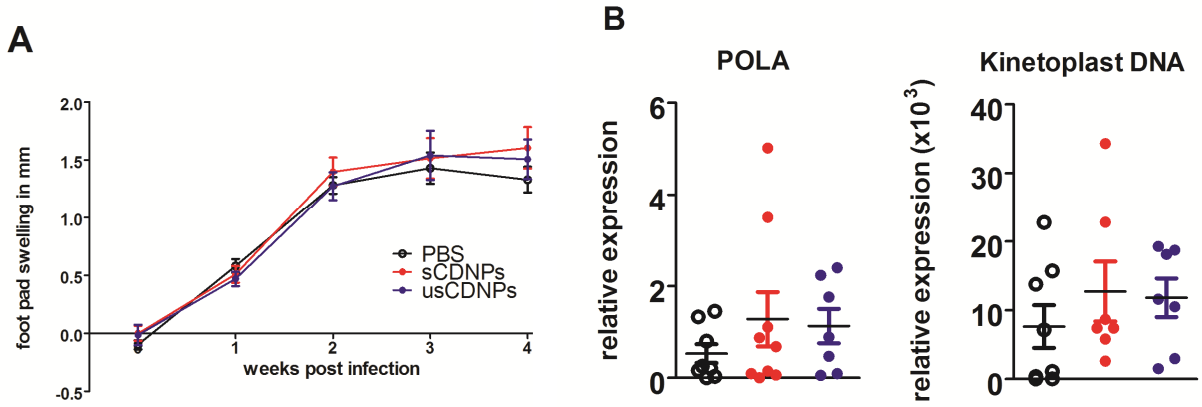


Fig. 4-3-8: CDNPs do not alter the clinical disease outcome of *L. major*-infected mice. C56BL/6 mice were infected with $1x10^6$ viable *L. major* promastigotes into the hind foot pad. 5µg s- or usCDNPs were injected s.c. into the hint legs, every other day. A) Foot pad swelling following the course of infection. B) Foot pad skins were harvested 4 weeks post infection and immediately frozen at -80°C. 10 cryosections of each skin were lysed for DNA extraction. POLA and kinetoplast expression were determined by quantitative RT-PCR. Expression levels were normalized to the murine single-copy gene BDNF. Pooled results from 2-3 independent experiments with n=1-3 mice per group. Data are expressed as means ± SEM.

4.3.2 CDNPs have protective effects in CLP-induced sepsis

CDNPs were shown to increase the survival rate in a virus-induced intracellular infection [69]. Similarly, CDNPs had clear immunomodulatory effects in the setting of intracellular *L. major* infection; although the results presented above indicate that they do not affect the clinical disease outcome. Obviously, the extent of the immunomodulatory effect of CDNPs depends on the type of infection. Nothing is known about the effect of CDNPs in the context of extracellular infections, so far. Thus, to test, whether CDNPs might affect such infections as well, a CLP model of polymicrobial sepsis was used.

Sepsis proceeds as an initial pro-inflammatory state, which is survived by most patients and the subsequent, often lethal immunosuppressed state [87,89] which is characterized by high IL-10 secretion, reduced surface expression of activation markers, limited bacterial clearance and diminished antigen presentation. This state is induced by exhausted and thus dysfunctional effector cells which go into apoptosis [87,90,91]. PS-expressing apoptotic cells and the MPs they release, are ingested by macrophages in a tolerogenic manner, further amplifying immunosuppression [92]. Consequently, the impact of CDNPs in the context of sepsis was studied at the level of innate effector cells at the infection site within the immunosuppressed state.

4.3.2.1 CDNPs increase the survival of septic mice

First, the impact of CDNPs on the clinical disease outcome was determined. To this end, sepsis was induced via CLP and mice were treated with CDNPs at the time of CLP induction. Survival of septic mice was followed for the next 96 hours. Importantly, CDNP treatment increased the survival of septic mice by 20% (38 vs. 61% survival in untreated and CDNP-treated mice, respectively), albeit in a non-significant manner (Fig. 4-3-9). Clearly, CDNP treatment confers a survival advantage in mice subjected to CLP.

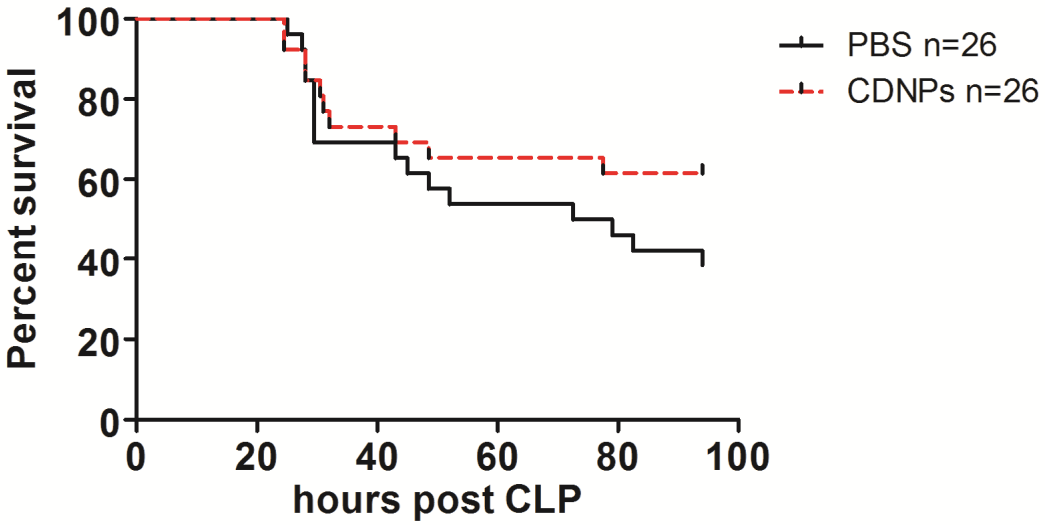


Fig. 4-3-9: CDNPs increase the percentage of surviving mice in response to CLP by trend. Mice were treated with 5µg CDNPs at the time of CLP induction and survival was followed for 96 hours post CLP. The Kaplan-Meier Plot for pooled data from 3 independent experiments with n=6-10 mice is shown.

4.3.2.2 CDNPs are ingested by effector cells at the infection site 4 hours after CLP

To gain insights into the mechanism responsible for increased survival of septic mice after CDNP treatment, CDNP-ingesting cells at the infection site were identified by usage of CFSE-labeled CDNPs. Mice were treated with 5µg CFSE-labeled CDNPs at the time of CLP and peritoneal lavages were harvested 4 hours following treatment. Similar to 4.2.2.1.1, association of CDNPs with peritoneal cells was determined by positive CFSE expression. As expected, ungated peritoneal cells showed significantly increased CFSE fluorescence in CDNP- vs. PBS-treated mice (Fig. 4-3-10, upper panel). In order to discriminate between CDNPs, which are bound to the cell surface and truly ingested CDNPs, surface fluorescence was quenched using trypan blue followed by re-analysis of each sample for intracellular CFSE expression [131]. Intriguingly, almost 98% of CFSE MFI remained after trypan blue quenching (10031±2248 quenched vs. 10162±1646 unquenched, Fig. 4-3-10, lower panel), indicating that almost all CDNPs associated with peritoneal cells were located intracellularly.

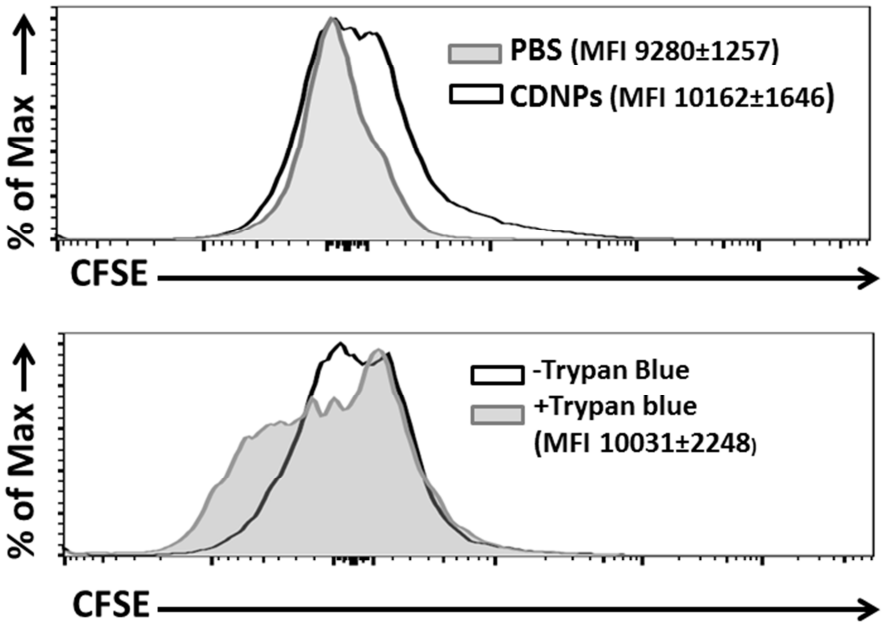


Fig. 4-3-10: Identification of CDNP-ingesting peritoneal cells. Mice were treated with 5µg CFSE-labeled CDNPs at the time of CLP induction and peritoneal lavages were harvested 4h later. Peritoneal cells were stained with fluorescence-labeled mAbs to Ly-6G, Ly-6C and F4/80 and analyzed by flow cytometry. Representative FACS plots gated on all cells are depicted. Association of CDNPs with peritoneal cells was determined by CFSE fluorescence (upper panel). Ingestion of CDNPs was assessed after surface fluorescence quenching with trypan blue (lower panel). Pooled data from 2 independent experiments with n=8-9 mice per group.

Given that the great majority of CDNPs was located inside cells, it was reasonable to assume that all $CFSE^+$ cells indeed ingested CDNPs. Thus, it was possible to identify ingesting cells based on the expression of characteristic surface markers in unquenched samples. The gating strategy focused on the three most abundant cell populations at the infection site 4 hours post CLP: Ly-$6G^+Ly6C^+$ neutrophils, $Ly6G^-Ly6C^+$ inflammatory monocytes (infl. monocytes), and $F4/80^+$ macrophages (Fig. 4-3-11).

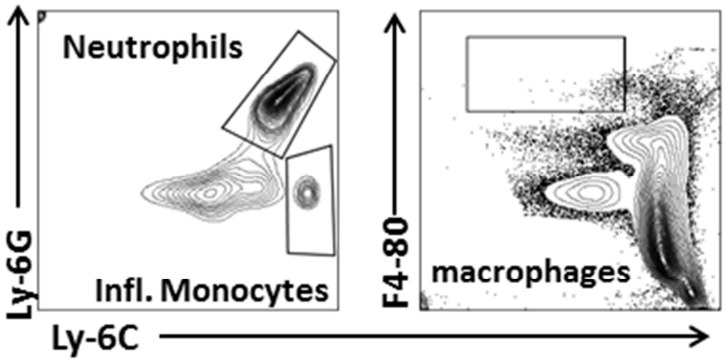


Fig. 4-3-11: Gating strategy for neutrophils, infl. monocytes and macrophages. Peritoneal cells 4 hours after CLP were stained with fluorescence-labeled mAbs to Ly-6G, Ly-6C and F4/80 and analyzed by flow cytometry. Neutrophils (Ly-6G^{+}Ly-6C^{+}), inflammatory Monocytes (Ly-6G^{-}Ly-6C^{+}) and macrophages (F4/80^{hi}) were identified by expression of specific marker combinations. Depicted are a representative FACS plots 4 hours post CLP.

Interestingly, 5-10% of cells within each population exhibited CDNP ingestion (Fig. 4-3-12 A). The MFI of CFSE within each cell population is indicative for the amount of CDNPs which has been ingested. Hence, F4/80+ macrophages ingested the highest amounts of CDNPs as indicated by 20-fold increased CFSE levels vs. PBS-treated mice (Fig. 4-3-12 B). In contrast, neutrophils and inflammatory monocytes ingested very small CDNP levels per cell. Thus, neutrophils, inflammatory monocytes, and F4/80^{+} macrophages at the infection site of septic mice all ingest CDNPs, with F4/80^{+} macrophages accounting for the highest CDNP uptake.

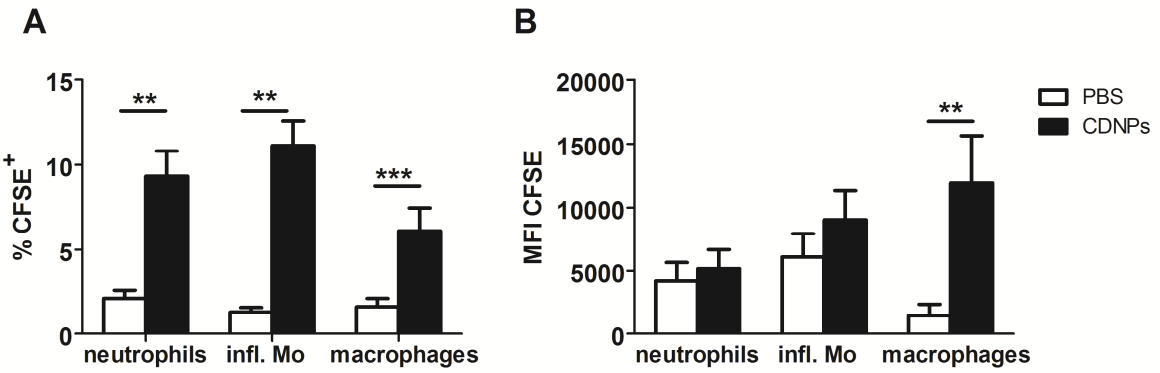


Fig. 4-3-12: CDNPs are ingested by neutrophils, infl. monocytes and macrophages at the infection site of septic mice. Mice were treated with 5µg CFSE-labeled CDNPs at the time of CLP induction and peritoneal lavages were harvested 4h later. Peritoneal cells were stained with fluorescence-labeled mAbs to Ly-6G, Ly-6C and F4/80 and analyzed by flow cytometry. A) Frequencies of CDNP ingesting ($CFSE^+$) cells among unquenched peritoneal cell subsets. B) MFI of CFSE reflecting the amount of ingested CDNPs among unquenched peritoneal cell subsets. Pooled data from 2 independent experiments with n=8-9 mice per group. Data are expressed as means ± SEM. Significance was determined using student t-test. **p<0.01, ***p<0.001.

4.3.2.3 CDNP ingestion induces cell activation at the infection site 4 hours after CLP

To assess whether the uptake of CDNPs by neutrophils, infl. monocytes, and F4/80+ macrophages has functional consequences, surface expressions of the surrogate activation markers CD11b and MHCII in CDNP-treated and control mice were measured 4 hours after CLP. To specifically address the effect of CDNP ingestion, expression of CD11b and MHCII was compared between cells that ingested ($CFSE^+$) and cells that did not ingest CDNPs ($CFSE^-$). Importantly, both CD11b and MHCII expression by cells that ingested CDNPs was significantly increased compared to non-ingesting cells in all three cell types (Fig. 4-3-13). The highest CD11b increase was observed on macrophages (approximately 30%), followed by neutrophils (16%), and inflammatory monocytes (11%). Regarding MHCII, 3.6-fold more neutrophils expressed MHCII after ingesting CDNPs as compared to 2-fold more macrophages and 1.5-fold more inflammatory monocytes. Undoubtedly, CDNP treatment improved the immunosuppressed condition characteristic for the second phase of sepsis.

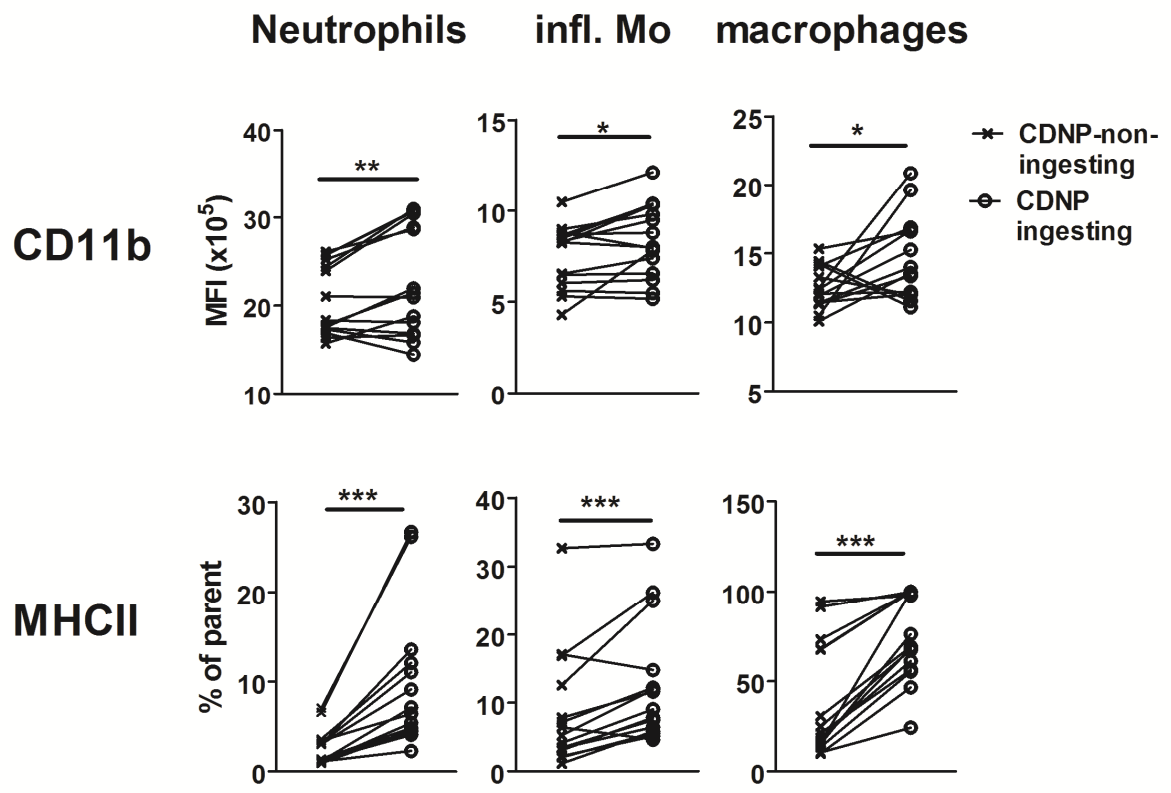


Fig. 4-3-13: CDNPs enhance the activation of effector cells at the site of infection 4 hours post CLP. Mice were treated with 5µg or 10µg CFSE-labeled CDNP at the time of CLP induction and peritoneal lavages were analyzed 4h later. Surface expression of activation markers on CDNP-ingesting ($CFSE^+$) and non-ingesting ($CFSE^-$) peritoneal cell subsets was quantified. Significance was determined using students t-test. *p<0.05,**p<0.01, ***p<0.001.

4.3.2.4 CDNP treatment reduces IL-6 and IL-10 levels at the site of infection 24 hours after CLP

To determine whether increased cell activation induced by CDNP ingestion had functional outcomes, intraperitoneal IL-6 and IL-10 levels were measured as markers for macrophage/monocyte and neutrophil activation. IL-6 and IL-10 secretion by APCs has been shown to negatively correlate with survival in sepsis and thus is often used for the prediction of clinical sepsis outcomes [170,171]. Thus, both cytokine levels were expected to be decreased after CDNP treatment. C57BL/6 mice were injected with PBS or 5µg CDNPs at the time of CLP-induction. 24 hours following CLP, peritoneal cavities were lavaged and peritoneal fluids analyzed for protein levels of IL-6 and IL-10. In fact, CDNPs reduced peritoneal IL-6 levels by 30 to 60% in a dose-dependent manner (Fig. 4-3-14).

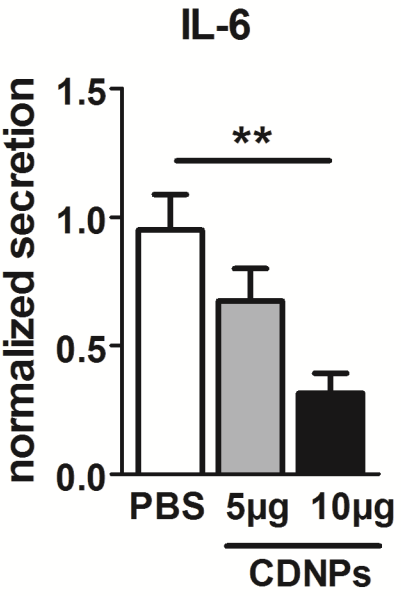


Fig. 4-3-14: CDNPs reduce peritoneal IL-6 levels in septic mice 24 hours post CLP. Mice were treated with 5µg or 10µg CDNPs, respectively, at the time of CLP induction and peritoneal concentrations of IL-6 were determined using CBA. Expression levels were normalized to those of PBS-treated mice. Pooled data from 2 independent experiments with n=5-9 mice per group. Data are expressed as means ± SEM. Significance was determined using ANOVA with Bonferroni post-hoc test. **p<0.01.

Corresponding to decreased peritoneal IL-6 levels, mice treated with CDNPs at the time of CLP demonstrated a dose-dependent decrease in IL-10 levels ranging from 30 to 60% (Fig. 4-3-15), although no significance was reached. These findings are consistent with increased survival rates among CDNP-treated mice.

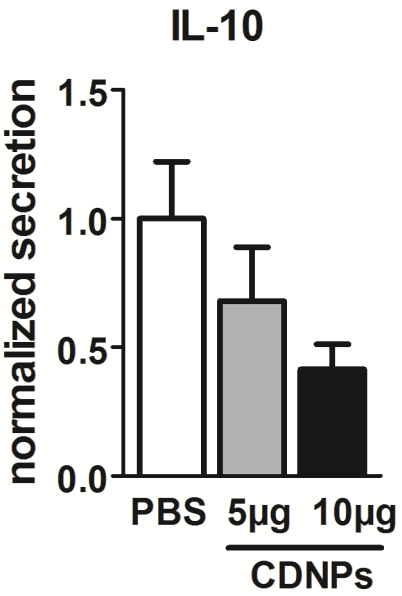


Fig. 4-3-15: CDNPs dose-dependently reduce IL-10 levels at the site of infection 24 hours post CLP. Mice were treated with 5µg or 10 µg CDNPs at the time of CLP induction and peritoneal lavages were analyzed 24h later. Peritoneal concentrations of IL-10 were determined using CBA. Expression levels were normalized to those of PBS-treated mice. Pooled data from 2 independent experiments with n=5-9 mice per group. Data are expressed as means ± SEM.

4.3.2.5 CDNP treatment increases NDMP levels at the site of infection 24 hours after CLP

Neutrophils are the most abundant cell type at the infection site 24 hours post CLP (see Fig. 4-3-11). Activated neutrophils rapidly release ROS to destroy bacteria, while immunosuppressed neutrophils go into immunotolerance-inducing apoptosis and release anti-inflammatory NDMPs. To test, whether increased neutrophil activation after CDNP treatment has functional outcomes, both parameters were measured 24 hours post CLP induction. While ROS production was not affected by CDNP treatment (suppl. Fig. S3), CDNPs surprisingly increased Ly-6G$^+$ NDMPs 5-fold as compared to PBS (Fig. 4-3-16).

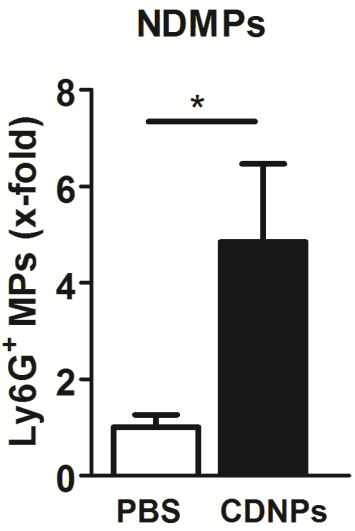


Fig. 4-3-16: CDNPs increase NDMP levels at the site of sepsis 24 hours post CLP. Mice were treated with 5µg CDNPs at the time of CLP induction. Peritoneal lavages were isolated 4 hours post CLP, NDMPs were isolated by differential centrifugation and Ly-6G$^+$ particles were enumerated by NTA. Pooled data from 2 independent experiments with n=3-12. Data are expressed as means ± SEM. Significance was determined using students t-test. *p<0.05.

4.3.2.6 CDNPs reduce peritoneal bacterial loads 24 hours post CLP

Previous reports suggest that IL-6 promotes the polarization to alternatively activated M2 macrophages thereby limiting inflammation and bacterial clearance [172]. Contrary, the failure to clear bacteria correlates with increased IL-6 release [173]. To test, whether this was true in this setting, intraperitoneal fluid was diluted and plated on agar. CFUs resulting from single bacteria were counted 24 hours later. In fact, CDNP-treated mice exhibited 2-log lower CFU counts as their PBS-treated counterparts (Fig. 4-3-17), indicating that CDNP treatment improves bacterial clearance.

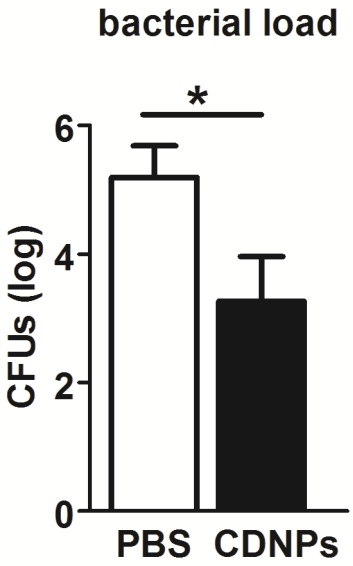


Fig. 4-3-17: CDNPs reduce peritoneal bacterial loads 24 hours post CLP. Mice were treated with 5µg CDNPs at the time of CLP induction and peritoneal bacterial loads were determined 24h later. Pooled data from 3 independent experiments with n=5-8 mice per group. Data are expressed as means ± SEM. Significance was determined using students t-test. *p<0.05.

4.3.2.7 Identification of possible mechanisms mediating the enhanced immune response in CDNP-treated mice

The previous results demonstrate that CDNPs activate macrophages, infl. monocytes and neutrophils at the site of infection leading to i) decreased peritoneal IL-6 and IL-10 levels, ii) increased NDMP concentrations and, iii) improved bacterial clearance. To elucidate the potential mechanisms underlying these effects, a set of *in vitro* experiments was performed specifically addressing these three observations.

4.3.2.7.1 CDNPs directly impact IL-6 expression and secretion *in vitro*

First, the direct influence of CDNPs on IL-6 and IL-10 secretion was addressed. The results presented in chapter 4.1 already demonstrated that CDNPs directly influence the cytokine expression of activated macrophages *in vitro*. Allogeneic CDNPs increased IL-10 mRNA expression of stimulated macrophages (Fig. 4-1-9), while IL-10 protein levels were below detection limits (data not shown). IL-6 mRNA was decreased by tendency (Fig. 4-1-8); however the power of the statistical test was low since four different groups were compared in this experiment. IL-6 protein levels were not measured in the above experiments. Thus, to find out whether CDNPs directly impede IL-6 production, peritoneal macrophages were obtained from naïve mice and incubated with 5µg CDNPs for 24 hours. To mimic the context

of sepsis, cells were stimulated with LPS [174]. Cells and supernatants were then harvested and analyzed for IL-6 mRNA and protein expression, respectively. Strikingly, CDNP-treated macrophages expressed less IL-6 mRNA, reaching levels comparable to those of unstimulated cells (Fig. 4-3-18). Similarly, IL-6 protein levels were markedly reduced by ~40% in CDNP- vs. PBS-treated macrophages, indicating that CDNPs modulate macrophagial IL-6 gene and protein expression.

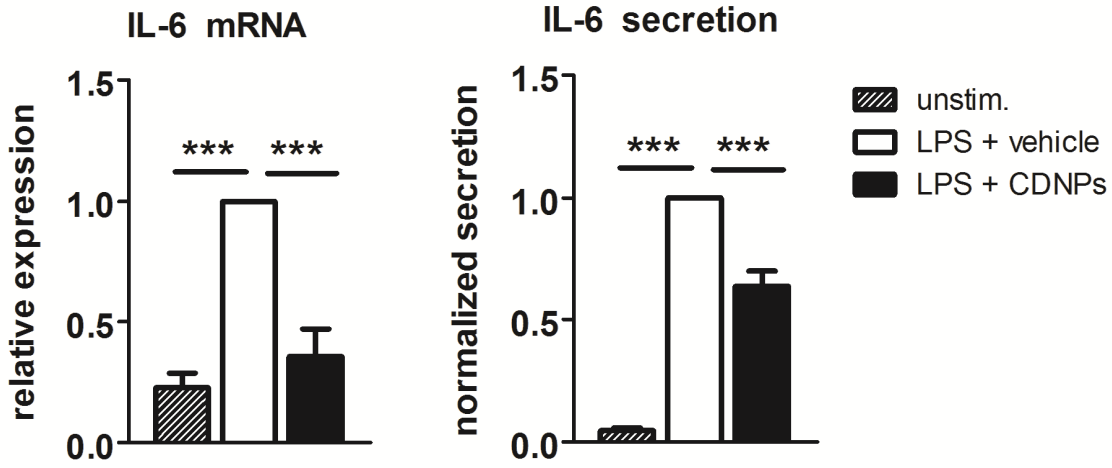


Fig. 4-3-18: CDNPs reduce mRNA and protein IL-6 levels *in vitro*. Peritoneal lavages from naïve C56BL/6 mice were harvested and $1x10^5$ cells were pre-incubated 2 hours in media containing 1% serum to let macrophages adhere. Supernatants were then replaced with media containing 5% serum and the resulting culture enriched in macrophages was incubated with 50µg /ml CDNPs and 1 ng/ml LPS. 24 hours later cells were harvested and lysed for the detection of IL-6 mRNA levels by quantitative RT-PCR. mRNA expression levels were adjusted to the housekeeping gene MLN51 and then normalized to the cytokine expression of stimulated cells. IL-6 protein levels in the supernatant were determined by ELISA and normalized to secretion of stimulated cells. n=4-6 cell preparations from individual mice. Data are expressed as means ± SEM. Significance was determined using ANOVA for repeated measurements with Bonferroni post-hoc test. ***$p<0.001$.

4.3.2.7.2 CDNPs impede the production and function of immuno-suppressing NDMPs *in vitro*

To find out whether the increased CDNP concentration observed in chapter 4.3.2.5 was a direct effect of CDNPs, BM-derived neutrophils were incubated with CDNPs over night and Ly-6G$^+$ NDMPs were enumerated by NTA. Unexpectedly, incubation of CDNPs with neutrophils did not increase, but diminished NMDP production by 30% as compared to controls (Fig. 4-3-19).

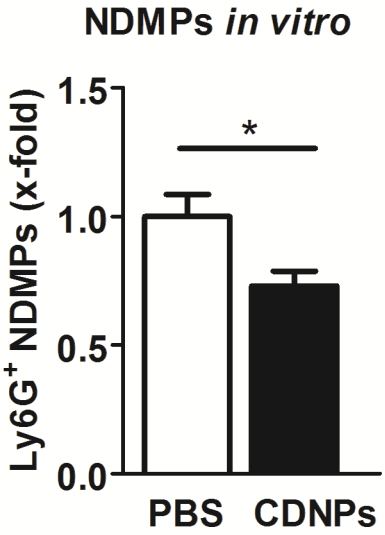


Fig. 4-3-19: CDNPs impede NDMP production *in vitro*. Neutrophils were isolated from BM and incubated with CDNPs for 24h. NDMPs were isolated by differential centrifugation and Ly-6G$^+$ particles were quantified using NTA. NDMP levels were normalized to those of PBS-treated cells. Pooled data from 4 independent experiments with n=3-4. Data are expressed as means ± SEM. Significance was determined using students t-test. *$p<0.05$.

This surprising finding led to the speculation that CDNPs might reduce NDMP production *in vivo*, but inhibit NDMP uptake and therefore factually increase NDMP concentrations at the infection site. The rational for inhibited NDMP uptake through CDNPs is given by a possible interaction of annexin A5 within CDNPs and PS expressed on the NDMPs surface [175]. PS is mediating tolerogenic ingestion by macrophages, one of the major deteriorating effects of NDMPs [94]. When CDNPs indeed bind and mask PS on the NDMP surface, this should result in a decreased NDMP uptake by macrophages and thus higher NDMP concentrations in the peritoneum.

First experiments addressed whether CDNPs bind NDMPs. To this end, CFSE-labeled CDNPs

were incubated with Ly-6G^{+} NDMPs in the presence of Ca^{2+} at 37°C for a time period of 30 min. In fact, CDNPs bound NDMPs in a dose-dependent manner, as demonstrated by increased frequencies of Ly-6G^{+}CFSE^{+} particles (Fig. 4-3-20), with almost 60% of all NDMPs bound at the highest CDNP concentration tested.

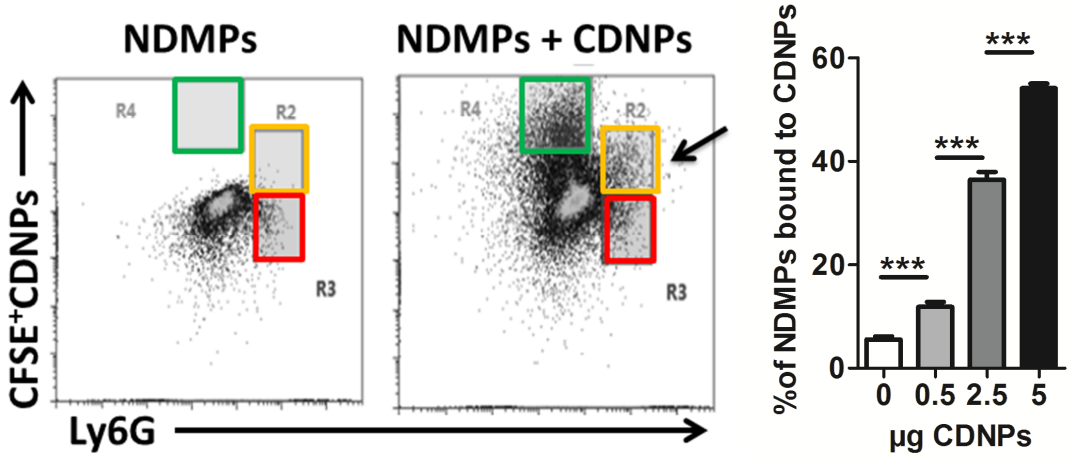


Fig. 4-3-20: CDNPs bind to NDMPs *in vitro*. NDMPs were isolated from peritoneal lavages of TGA-elicited mice and incubated with CFSE-labeled CDNPs (green) for 30min at 37°C. NDMPs were labeled with anti-Ly6G antibodies (red) and CDNP-NDMP binding was identified as CSFE^{+}Ly-6G^{+} particles (yellow, gate indicated by an arrow) by flow cytometry. Representative plots and quantification of pooled data from 2 independent experiments with n=3-4 mice are shown. Data are expressed as means ± SEM. Significance was determined using repeated measurements ANOVA with Bonferroni post-hoc test. ***p<0.001.

The next experiment was designed to assess whether CDNP-NDMP binding would prevent NDMP ingestion. Therefore, CDNPs were pre-incubated with CFSE-labeled NDMPs and NDMP ingestion by peritoneal macrophages was assessed via flow cytometry. Indeed, pre-incubation with CDNPs reduced NDMP ingestion by 10%, suggesting that CDNPs impede NDMP uptake and function (Fig. 4-3-21). Optimization of incubation time and Ca^{2+}-concentration (needed for annexin A5-PS interaction), will likely result in further decrease of NDMP uptake and prevent the immune-silencing effect of CDNPs while increasing local NDMP concentrations.

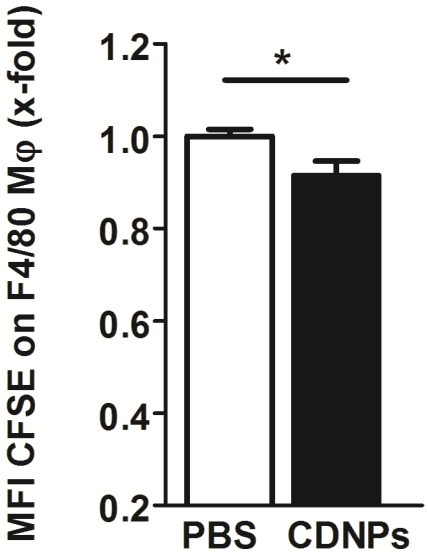


Fig. 4-3-21: Pre-incubation of CDNPs with NDMPs impedes NDMP ingestion by peritoneal macrophages *in vitro*. NDMPs were isolated from peritoneal lavages of TGA-elicited mice and stained with CFSE. CFSE-labeled NDMPs were pre-incubated with CDNPs for 30 min at 37°C and then incubated with peritoneal macrophages for 2 additional hours. NDMP-ingesting macrophages were identified by CFSE positivity after surface fluorescence quenching with trypan blue. Ingestion levels were normalized to those of PBS-treated cells. Pooled data from 3 independent experiments with n=3-4. Data are expressed as means ± SEM. Significance was determined using students t-test. *$p<0.05$.

4.3.2.7.3 CDNPs directly reduce bacterial growth *in vitro*

The reduced bacterial loads after CDNP-treatment observed in chapter 4.3.2.6 prompt to speculate whether CDNPs might directly inhibit bacterial growth. To answer this question, *P. aeruginosa* cultures were pre-incubated with CDNPs, plated on agar plates and incubated overnight. Surprisingly, *P. aeruginosa* cultures treated with only 1/5th of the CDNP dose used *in vivo* exhibited significantly reduced CFU counts (Fig. 4-3-22), indicating that CDNPs directly impair bacterial growth and/or survival.

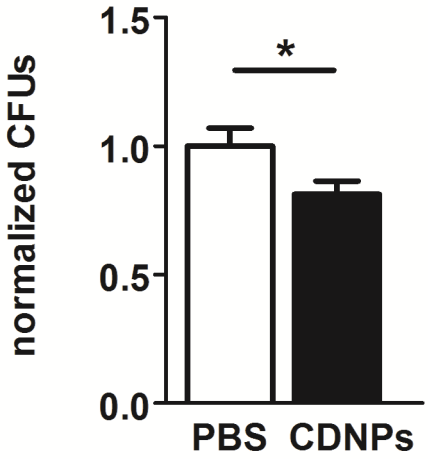


Fig. 4-3-22: CDNPs directly reduce bacterial growth *in vitro*. 1.25µg CDNPs were incubated with *P. aeruginosa* for 24h. CFUs were normalized to those of PBS-treated cultures. Pooled data from 4 independent experiments with n=3-4. Significance was determined using students t-test. *p<0.05.

4.4 Endogenous CDNPs accumulate at the infection site in sepsis

CDNPs were described as new particulate mediators of intercellular communication and could be part of a stress response system [66]. As such, they were speculated to be released under conditions of cellular stress to provide pro-survival and resistance signals to neighboring cells [68]. However, due to the difficulties associated with the isolation and identification of membrane-less nanoparticles [176], all CDNPs described in the literature to date are derived from *in vitro* cell cultures or detected in tissue sections *ex vivo*. Thus, the existence of endogenously produced CDNPs still remains controversial. Therefore, the following chapter focuses on the detection of endogenously produced CDNPs. As infections are associated with severe cellular stress including hypoxia, metabolic and oxidative stress, it seems likely that CDNPs would be present at the site of infection. To test this hypothesis, the polymicrobial sepsis model in response to CLP was chosen since the infection site is easily accessible in this setting.

4.4.1 Endogenous CDNPs accumulate at the infection site in sepsis

To test whether CDNPs are endogenously produced, cell stress in the peritoneum of C57BL/6 mice was induced by CLP. Septic mice were sacrificed 3, 4 or 24 hours post CLP to collect peritoneal lavages. Cell-free fractions of the lavages were further subjected to CDNP isolation using differential centrifugation by an adapted CDNP isolation protocol (Fig. 4-4-1). High centrifugation speeds and Triton-X treatment guaranteed the exclusion of apoptotic bodies, MPs, and exosomes, respectively.

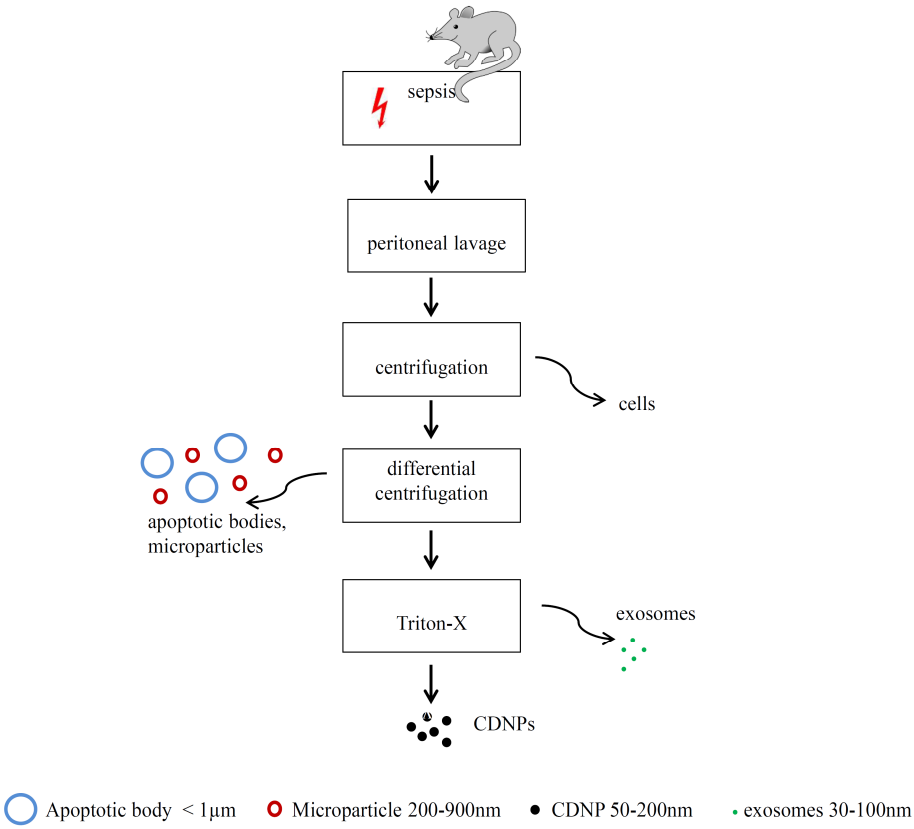


Fig. 4-4-1: Isolation of endogenously produced CDNPs from septic mice. Sepsis was induced in naïve C57BL/6 mice by CLP. Mice were sacrificed and peritoneal lavages were conducted 3, 4 or 24 hours post CLP. Cells were pelleted at 400g and cell-free supernatants were subjected to an adopted CDNP isolation protocol. Apoptotic bodies and MPs were pelleted at 25,000g, followed by centrifugation at 100,000g to pellet CDNPs and exosomes. Finally, lipid membranes of exosomes were disrupted by Triton-X treatment.

Similar to the approach in chapter 4.1.2.1 and 4.2.1., CDNPs were identified due to their particularity, size, and protein composition using NTA, SEM and SDS-PAGE. Under the SEM, both CLP- and cell culture-derived CDNPs (Fig. 4-4-2 A lower pannel, for cell culture-derived CDNPs compare Fig. 4-2-1) appeared as similar spherical structures of approximately 100nm diameter which exist as single particles or aggregates (Fig. 4-4-2 A). A size distribution between 100 and 500nm with a mean CDNP size of approximately 200nm (183nm for cell culture-derived and 211nm for CLP-derived CDNPs) was confirmed using NTA (Fig. 4-4-2 B). The protein composition, as assessed by SDS-PAGE, differed between cell culture-derived and CLP-derived CDNPs (Fig. 4-4-2 C, for cell culture-derived CDNPs compare Fig. 4-2-1). However, considering the completely different context and the

accumulation of immune cells and their mediators at the infection site, this result was not unexpected. Thus, further studies are needed to analyze the context-dependent composition of CDNPs. Interestingly, peritoneal lavages from naïve mice analyzed by SEM also contained CDNPs, albeit in very low amounts as compared to CLP-derived CDNPs (Fig. 4-2-2 A, upper panel), suggesting that CDNPs are constitutively produced at low levels, but are highly enriched upon sepsis induction.

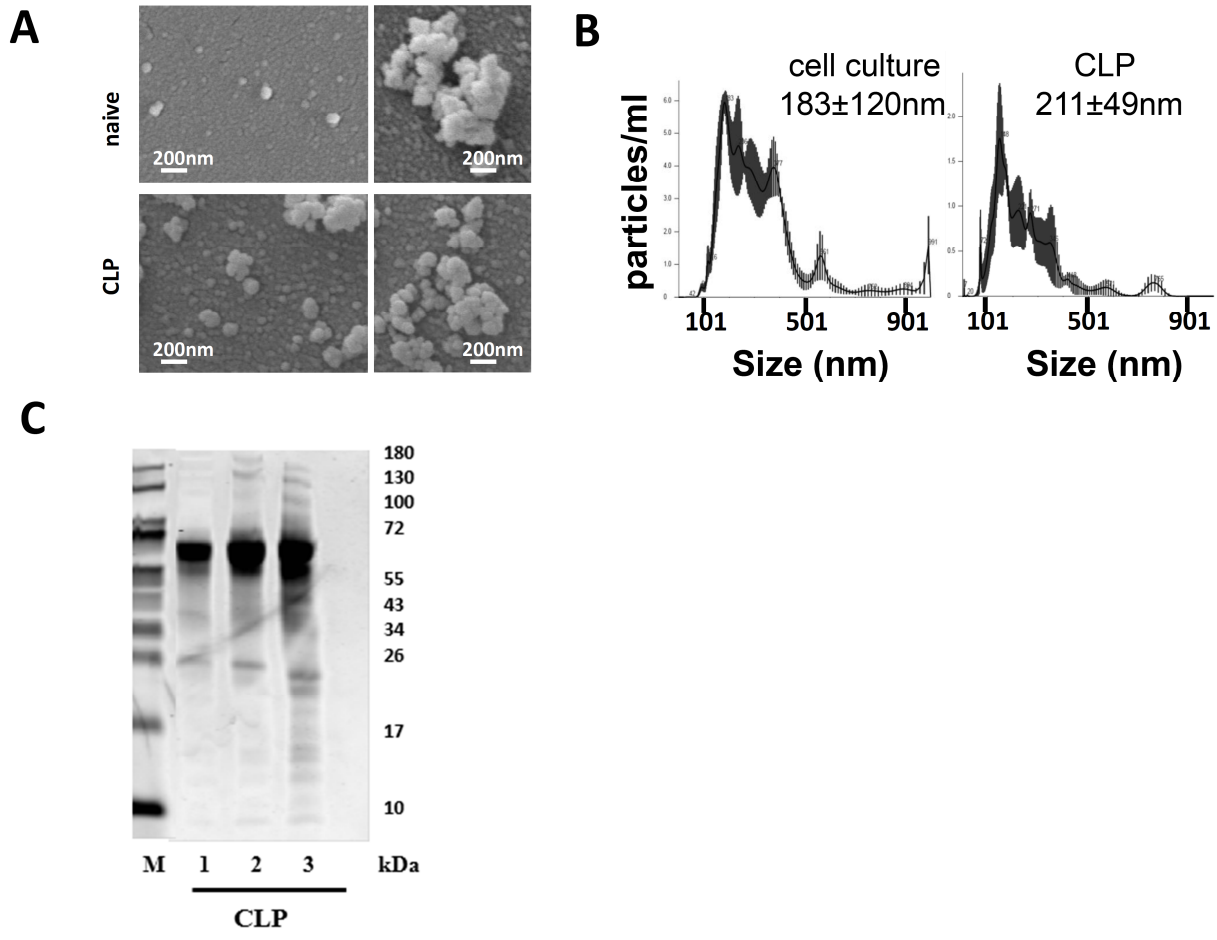


Fig.4-4-2: CDNPs accumulate at the infection site of sepsis. Characterization of CDNPs isolated from the cell-free fraction of peritoneal lavages of septic mice 3 or 4 hours post CLP compared to CDNPs isolated from naïve mice or cell culture-derived CDNPs. A) Representative scanning electron micrographs of CDNPs derived from naïve mice and mice 3h post CLP. Left panels show single CDNPs, right panels depict CDNP aggregates. Note that CDNPs were hardly present in isolates from naïve mice and the depicted amount of CDNP is not representative for the whole sample. B) Particularity and size distribution of CDNPs as assessed by NTA. Representative plots for CDNP preparations from 4 individual mice 4h post CLP are shown in comparison to cell culture-derived CDNPs. C) SDS gel electrophoresis of CDNPs from 3 different mice 3 hours post CLP.

4.4.2 Endogenous CDNPs contain annexin A5

Given that the protein composition of cell culture- and CLP-derived CDNPs differed due to the different context they were isolated from, the presence of annexin A5, which was identified as a specific marker for sCDNPs (Fig. 4-2-8 and 4-2-9), was detected via Western Blot. Indeed, annexin A5 was also present in CLP-derived CDNPs (Fig. 4-4-3). Of note, the samples in Fig. 4-4-3 were denaturated at a lower temperature using a milder reducing agent than the samples in Fig. 4-3-3. Hence, not all disulfide-bonds were reduced under these conditions preventing the complete disassociation of annexins, which are known to form aggregates. Thus, annexin A5 was still partly present in dimeric form.

Interestingly, the annexin A5 content in CDNP preparations from individual mice was highly variable.

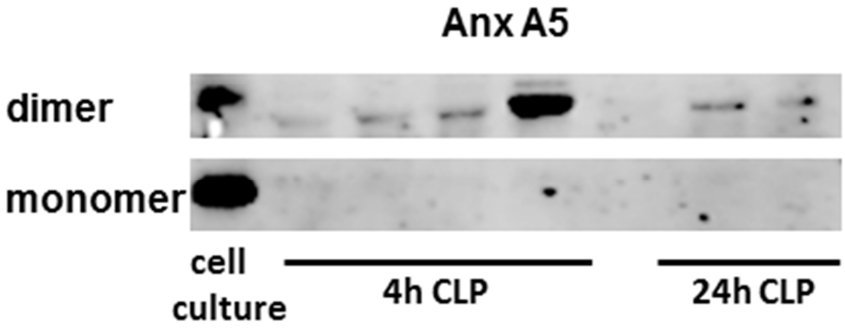


Fig.4-4-3: CLP-derived CDNPs contain annexin A5. CDNPs isolated from the cell-free fraction of peritoneal lavages of septic mice 4 or 24 hours post CLP compared to cell culture-derived CDNPs. Annexin A5 content of CDNP isolates from 6 individual mice was determined by Western Blot using annexin A5-specific antibodies

5. Discussion

In order to enable a broad therapeutic use of CDNPs, the most fundamental questions still need to be answered. The present study contributes to this pre-requirement, by demonstrating that

i) Xenogeneic CDNPs do not induce xenogeneic rejection *in vitro*. Instead, they reduce the expression of pro-inflammatory cytokines and increase the expression of anti-inflammatory IL-10 by zymosan-stimulated macrophages.

ii) Allogeneic CDNPs exhibited the same anti-inflammatory effects on murine peritoneal macrophages as xenogeneic CDNPs *in vitro*.

iii) Stress such as nutrient deprivation or infection is the premise for the formation of anti-inflammatory CDNPs. Only sCDNPs reduce zymosan-induced TNFα expression *in vitro*. Moreover, in the context of *L. major*-infections, only sCDNPs activate DCs, increase $Foxp3^+$ $CD4^+$ T cells and drive Th2 cell polarization.

iv) Annexin A5 in particular is considerably enriched in CDNPs derived from stressed cells, presumably mediating its immunomodulatory effects.

v) CDNPs do not alter the clinical outcome of *L. major*-infection.

vi) CDNPs are beneficial in sepsis.

vii) Endogenous CDNPs are enriched at the infection site.

The following chapters will discuss these findings and their overall implications for the potential therapeutic use of CDNPs. For the sake of clarity and consistency, the effects of xenogeneic CDNPs, the effects of stress on CDNP function, the identification of a possible mediator for CDNP function, the effects of CDNPs in *L. major* infection and sepsis, the endogenous production of CDNPs and finally the overall therapeutic potential of CDNPs will be discussed separately.

5.1 Xenogeneic CDNPs do not induce xenogeneic rejection *in vitro*

All CDNPs used so far in animal experiments as well as in humans, were of xenogeneic origin. Xenogeneic antigens might be recognized by PRRs leading to the activation of the complement system and induction of inflammation ultimately resulting in xenogeneic rejection of the antigen [19,25]. Moreover, CDNPs contain traces of RNA and DNA [66], which are known to trigger TLRs and likewise induce inflammation [8]. Thus, the usage of xenogeneic CDNPs raises strong safety concerns regarding a possible induction of excessive,

uncontrolled inflammation. However, when porcine CDNPs were incubated with resting murine macrophages, no effect on the expression of pro-inflammatory cytokines (Fig. 4-1-1) was found. This applied to cytokines induced by both MyD88-dependent and MyD88-independent pathways. These results are in line with the observations in patients who received xenogeneic CDNP treatment without showing any side effects [72]. Moreover, preliminary and unpublished experiments by the author suggest that injection of xenogeneic CDNPs into murine foot pads does not induce inflammation as assessed by foot pad swelling, even if xenogeneic CDNPs were injected together with the potent adjuvant alum.

Regarding the protein components of CDNPs, these results are consistent with the notion that xenogeneic proteins do not elicit immune responses *per se*. Instead, it has long been known, that the injection of highly purified xenogeneic proteins alone induces tolerance [177]. Hence, proteins such as OVA have to be injected in combination with adjuvant to evoke an immune response. Moreover, the immunogenic potential of a given xenogeneic protein is dependent on the degree of sequence similarity to the host [20] and it has been shown that stress response proteins [178] and annexins [179], the main components of CDNPs (Tab. 1 and [66]) are highly conserved between species. Importantly, xenogeneic rejection generally occurs when whole tissues, organs or cells are transplanted [25]. Thus, the lack of a membrane expressing typical PAMPs as well as species specific glycosylation patterns might further prevent the rejection of CDNPs.

The absence of a pro-inflammatory immune response directed against the nucleic acids present in CDNPs is a more surprising finding. Since CDNPs mostly consists of proteins which form large aggregates, nucleic acids might simply be sequestered inside such complexes, preventing them from detection by PRRs. This hypothesis should be addressed in further experiments, e.g. by testing the immunogenic effect of CDNPs after protein degradation.

5.1.1 Xenogeneic and allogeneic CDNPs reduce the expression of pro-inflammatory cytokines after TLR-stimulation

Surprisingly, xenogeneic CDNPs were not only tolerated by resting macrophages, but actually had anti-inflammatory effects on TLR-triggered macrophages. Obviously, CDNPs are not anti-inflammatory *per se* and their effect is dependent on an inflammatory context. This anti-inflammatory effect of xenogeneic CDNPs was highly dependent on the TLR triggered: CDNPs had no effect on TLR3-triggered TNFα or IFNβ expression (Fig. 4-1-2). The same held true for TLR4-triggered macrophages, although only a very small number of replicates

was tested for TLR4-triggering due to difficulties with the production of endotoxin-free, highly concentrated CDNPs in sufficient amounts (Fig. 4-1-2). In contrast, xenogeneic CDNPs reduced TLR7/8-triggered TNFα expression 4 hours post stimulation (Fig. 4-1-3). Of note, the strongest anti-inflammatory effect of xenogeneic CDNPs was found after treatment of TLR2-triggered macrophages: Xenogeneic CDNPs reduced zymosan-induced IFNβ expression, as well as almost reversed zymosan-induced TNFα expression (Fig. 4-1-4). This effect was not due to their xenogenicity, as allogeneic CDNPs had the same diminishing effect on zymosan-induced TNFα and IL-1β expression (Fig. 4-1-7 and 4-1-8). However, zymosan- and LPS-induced IL-6 expression was downregulated by allogeneic CDNPs only (Fig. 4-1-8 and Fig. 4-3-18), indicating that a xenogeneic origin might be associated with weaker anti-inflammatory properties. Of note, reduced mRNA expression of TNFα and IL-6 corresponded with reduced protein secretion (Fig. 4-2-2 and 4-3-18). Importantly, CDNPs also reduced Pam_3CSK_4-induced expression of pro-inflammatory cytokines (Fig. 4-1-10), confirming that CDNPs affect TLR2 signaling instead of simply interfering with the phagocytosis of zymosan [125,153].

Strikingly, xenogeneic as well as allogeneic CDNPs both also considerably increased the expression of anti-inflammatory IL-10 mRNA (Fig. 4-1-9). Both the reduction of pro-inflammatory cytokine expression/secretion and increased expression of anti-inflammatory IL-10 suggest that CDNP polarize macrophages towards the anti-inflammatory M2 phenotype. Based on the research of Mantovani, activated macrophages acquire specialized functional phenotypes depending on the activation stimuli. Classical macrophage activation is induced by IFN-γ combined with LPS or TNFα and induces polarization to M1 macrophages. M1 macrophages promote inflammation by secretion of IL-1, IL-6 and TNFα as well as drive bacterial clearance via NO production. Alternative activation in contrast is triggered by IL-4 and IL-10. It drives the polarization to M2 macrophages characterized by IL-10 secretion and Th2 induction [180,181]. However, a better characterization of the CDNP-induced macrophages phenotype is required to confirm whether they indeed induce M2 macrophages and if so, which of the four M2 subtypes.

These data raise the question how CDNPs might interfere with TLR signaling. The exact mechanisms by which CDNPs reduce the production of pro-inflammatory cytokines were not assessed in this study. But since both MyD88-dependent (TNFα, IL-1β, IL-6) and MyD88-independent (IFNβ) pathways are affected, it is plausible to suggest that CDNPs affect adaptor molecules downstream of TIR-domain containing proteins. In further support of this possibility, Rönnau and al. found that xenogeneic CDNPs diminish IκBα degradation and thus

reduce nuclear translocation of the NF-κB subunits p50 and p65 [66]. Indeed, early expression of IFNβ, TNFα, IL-1β, and IL-6 were all shown to be NFκB-dependent [182–185]. This implies that the altered cytokine expression by CDNP treatment might be due to an impaired NFκB activation and/or translocation.

5.1.2 Possible protective roles for anti-inflammatory CDNPs in viral infections

Xenogeneic CDNPs were shown to be protective in the foot-and-mouth-disease in guinea pigs, however the mechanism was not addressed in this study. The only readout parameters used were complete disease generalization, amount of lesions and time of recovery, all of whom were positively affected by xenogeneic CDNP treatment [69]. Foot-and-mouth-disease is caused by the foot-and-mouth disease virus, a member of the *Picornaviridae* family and manifests as an acute response with fever followed by the formation of vesicular lesions, mainly on the mouth and feet [186]. Of note, previous studies suggest that uncontrolled virus replication together with excessive production of the pro-inflammatory cytokines IL-1β, IL-6, and TNF-α strongly correlate with disease severity [187–189]. Therefore, a down-regulation of these cytokines by CDNPs would likely result in reduced viral loads and diminished tissue-destruction. Moreover, CDNP-driven IL-10 release would also be beneficial since the results of a study by Segundo et al., point towards an IL-10 induction by the virus itself, thereby promoting Th2 responses and the production of virus-specific neutralizing antibodies, which are required to clear the infection [190].

Given that IFNβ generally is crucial for the limitation of viral replication, it appears surprising that xenogeneic CDNPs ameliorate foot-and-mouth disease while decreasing IFNβ expression (Fig.4-1-4). In particular, as IFNβ-treatment was reported to be protective in a foot-and-mouth disease model [191]; making this finding the more paradoxically. However, recent results from Ng et al. challenged the notion of IFNβ as being purely beneficial in lymphocytic choriomeningitis virus (LCMV) and other persistent infections [192]. In the experiments they performed, IFNβ blockade in fact accelerated virus clearance due to a compensatory increase of anti-viral T cell responses. Considering this result, the effect of IFNβ is likely dose- and context-dependent. Accordingly, IFNβ reduction by CDNPs might well be beneficial in the foot-and-mouth disease.

5.2 The anti-inflammatory effects of CDNPs *in vitro* and *in vivo* are dependent on their origin from stressed cells

When comparing the potential to reduce TNFα secretion by zymosan-stimulated macrophages between s- and usCDNPs *in vitro*, only sCDNPs considerably reduced TNFα protein levels (Fig. 4-2-2), indicating that CDNP function is induced by stress.

However, both us- and sCDNPs are ingested by resting and activated macrophages, with unstimulated macrophages significantly preferring usCDNPs (Fig. 4-2-4). After ingestion, both us- and sCDNPs slightly increase macrophage activation and antigen presentation as reflected by increased MHCII expression (Fig. 4-2-5). In LPS-stimulated macrophages, usCDNPs have an even larger effect on MHCII expression than sCDNPs. While such a small increase might not have functional consequences itself, these results might point towards an incipient or subsiding activation. Hence, more time points need to be studied in order to detect the maximal macrophage activation in response to CDNPs. Since CDNPs are self-antigens and thus might be presented in the context of MHCI [193], the expression of this marker should also be addressed in future experiments.

Taken together, these results indicate that ingestion and MHCII upregulation which are both induced by s- and usCDNPs are not sufficient to induce an anti-inflammatory M2 phenotype in APCs which is seen after treatment with sCDNPs only.

5.2.1 The induction of anti-inflammatory T cell phenotypes *in vitro* and *in vivo* requires sCDNPs

Only sCDNPs were able to reduce CD69 surface expression on $CD4^+$ T cells after culture of LPS-stimulated complete spleen cell fractions *in vitro* (Fig. 4-2-6). CD69 is an early activation marker, whose expression starts already 2 hours post activation and subsides 72 hours later. CD69 surface expression has been shown to be induced by triggering the TCR, costimulatory receptors such as CD28 or TLR4 on T cells [194]. Thus, sCDNPs could either directly interfere with TLR4 signaling on T cells or mediate their function by reducing the secretion of pro-inflammatory cytokines by APCs leading to decreased T cell activation. Considering the induction of an anti-inflammatory macrophage phenotype by sCDNPs, it appears plausible, that CD69 downregulation on LPS-stimulated T cells in whole spleen cultures is mediated by M2 macrophages induced by sCDNPs. However, more experiments addressing the exact mechanism of this effect are needed. Overall, analogous to macrophages, the anti-inflammatory effect of CDNPs on T cells was detected with CDNPs derived from stressed cells, only.

In contrast, *in vivo* more T cells were activated by sCDNPs which was reflected in a decrease of the ratio of naïve vs. effector (memory) $CD4^+$ T cells (Fig. 4-3-3). However, a mild decrease of intracellular IFNγ levels within $CD4^+$ T cells (Fig. 4-3-4) and increased abundance of $Foxp3^+CD4^+$ T cells (Fig. 4-3-6) in the draining lymph node indicates that increased effector cell ratio correlates with a shift of the direction of T cell polarization towards more anti-inflammatory and regulatory subtypes by sCDNPs. Additionally, increased IL-4- (Fig. 4-3-5) and a strong tendency towards increased IL-10 (Fig. 4-3-7) mRNA expression at the site of infection, likewise demonstrate the induction of an anti-inflammatory milieu by sCDNPs. In contrast, usCDNPS had either no or a very mild, non-significant and in all cases considerably less pronounced effect than sCDNPs *in vivo*.

5.2.2 CDNPs display the anti-inflammatory properties of RAMPs

Considering that the anti-inflammatory and regulatory effects of CDNPs are selectively induced by CDNPs derived from stressed cells while usCDNPs have no immunomodulatory effects, these results clearly demonstrate that stress is the decisive factor for the formation of functional CDNPs.

Moreover, these results provide a basis for the classification of CDNPs within the PAMP-DAMP-RAMP spectrum. Since CDNPs are endogenous molecules, their classification as PAMPs can easily be rejected. Endogenous, stress- or injury-derived molecular patterns are either assigned as DAMPs when they induce host tissue inflammation or RAMPs triggering regulation and resolution of inflammation [53]. The data presented above strongly suggest that CDNPs act as RAMPs which suppress and/or resolve inflammation. Whether all kinds of stress such as hypoxia, inflammation and nutrient deprivation as studied in these experiments induce the same anti-inflammatory effects or whether different stressors induce different CDNP compositions and functions, or even dictate whether CDNPs act as RAMPs or DAMPs, needs to be established in further experiments.

5.2.3 Stressed-induced enrichement of annexin A5 might be the mediator of the anti-inflammatory effect of CDNPs

Since anti-inflammatory effects *in vitro* and *in vivo* were observed only when CDNPs derived from stressed cells were used, size, particularity and composition of s- and usCDNPs were compared in order to elucidate the underlying cause. While the physical appearance and size were comparable between both CDNP groups (Fig. 4-2-1 A and B), the protein composition differed extensively as already seen on the different protein patterns on SDS gel (Fig. 4-2-1

C). The differences were more pronounced when both protein patterns were compared after separation in two dimensions. Only few proteins were co-expressed by s- and usCDNPs (depicted as yellow spots in the overlay, Fig. 4-2-7). Moreover, PCA revealed that the proteins from each CDNP preparation clustered in a distinct group (Fig. 4-2-8), indicating that the circumstances during CDNP formation dictate their composition. This finding is not surprising in the light of the well-described UPR reaction. Under conditions of severe stress, the subsiding protein synthesis is stopped and all proteins not essential for survival and stress resistance are degraded. In contrast, the expression and translation of stress-specific proteins is upregulated. Well-known examples of such proteins are HSPs which function as chaperones to allow proper re-folding of damaged proteins [64]. Interestingly, none of the classical stress-induced proteins were enriched in CDNPs (Tab. 4), although HSPs were shown to be part of the complexes [66,67]. Instead, eight proteins which have not been associated with stress responses before, plus annexin A1 [195] which was shown to be stress-related and conducting a chaperon-like function were overrepresented in sCDNP. However, most of the classical stress proteins were identified by comparing the total protein expression patterns of stressed and unstressed cells, while the proteins identified here might be selectively enriched in sCDNPs and hence might have been missed in an whole protein analysis.

In large part, the proteins enriched in sCDNPs were annexins, in particular, annexin A5 and its isoform which exhibited dramatically 14 to 12 fold upregulation upon stress (Tab. 4). Detection of annexin A5 content of s- vs. usCDNPs by Western Blot confirmed that annexin A5 was present in sCDNPs only (Fig. 4-2-9). Thus, it appears likely that annexin A5 might be one of the most important CDNP components.

Annexins comprise a family of evolutionary conserved proteins which bind negatively charged phospholipids in a Ca^{2+}-dependent manner. 12 annexin families have been identified in vertebrates so far: A1 to A11 and A13. All family members moreover exist as different functional splice variants (isoforms) [196]. Annexins have been implicated in several intra- and extracellular processes including the inhibition of blood coagulation, control of membrane trafficking and ion channel formation. However, their physiological function remains a matter of debate [197,198].

Annexin A5 is a protein of 35.7 kDa that preferentially binds to PS [198,199]. This annexin is known to form di- and trimers and can even polymerize to two-dimensional lattices upon binding to PS, which shields the cell surface from further interactions. This mechanism could account for the impaired uptake of PS-expressing NDMPs observed after incubation with

CDNPs (Fig. 4-3-21). Indeed, annexin A5 binding to apoptotic cells prevented their phagocytosis [200]. Similarly, annexin A5 lattices were suggested to be a physical constraint preventing the release of MPs from the cell surface of PS-expressing cells as demonstrated by Gidon-Jeangirard [201]. Again, these results are in high accordance with the diminished NDMP production after incubation with CDNPs *in vitro* (Fig. 4-3-19). Moreover, this function of annexin A5 seems also to be involved in membrane repair upon cell rapture [198], which would explain why annexin A5 is enriched upon stress.

Importantly, annexin A5 has also been shown to possess anti-inflammatory properties, emphasizing its possible contribution to the function of CDNPs. First, a recent study from Linke et. al. confirmed the downregulation of pro-inflammatory cytokines by annexin A5 on LPS stimulated DCs *in vitro* [202]. These results are in line with the *in vitro* reduction of TNFα by CDNPs (Fig. 4-2-2). Notably, this paper suggests that the anti-inflammatory effect is mediated by the core domain which is shared by most members of the annexin family, which might explain the enrichment of several annexin isotypes in sCDNPs (Tab. 4). Secondly, the same paper found a negative effect of annexin A5 on the formation of antigen-specific IFNγ-producing cytotoxic $CD8^+$ T cells *in vivo* [202]. Although, $CD4^+$ T cells were not analyzed in that study, these results clearly correspond with the reduced T cell activation after CDNP treatment *in vitro* (Fig. 4-2-6) as well as the induction of anti-inflammatory T cell phenotypes *in vivo* (Fig. 4-3-4 and 4-3-6). Thirdly, annexin A5 has been reported to inhibit PKC [203]. Immunological functions of PKCs include TCR activation, signaling and T cell proliferation. Of note, the PKC isotype θ has been reported to interact with promoters of CD69-, INF-γ-, and TNF-α genes to induce their expression on T cells [204]. Thus, inhibition of PKC function would lead to an anti-inflammatory phenotype on T cells. Finally, annexin A5 also inhibits secretory phospholipase A_2 (PLA_2) [205] involved in acute inflammation [206]. Moreover, annexin A5 was also shown to improve survival in an endotoxemia model of sepsis [207], coinciding with the results obtained for CDNPs. However, all these functions were confirmed for pure annexin A5. Whether this also applies to annexins present in protein-nucleic-acid complexes has to be established. Clearly, further studies are required to define the role of annexin A5 for the function of CDNPs.

5.3 CDNPs have different effects in distinct infection models

5.3.1 CDNPs shift the T cell polarization towards anti-inflammatory and regulatory T cell subsets but have no impact on the clinical outcome of *L. major* infection

CDNPs have protective effects in the virus-induced foot-and-mouth disease [69]. To test whether this effect was limited to viral- or also applied to other intracellular infections, CDNPs were applied in the context of *L. major*-infection. The clearance of *L. major* infection crucially relies on the formation of IFNγ-producing Th1 cells activating macrophages to kill the parasite [82]. Thus, the analysis conducted here, focused on the adaptive immune response.

5.3.1.1 CDNPs induce DC maturation

DCs are professional APCs which take up antigen, process it and present it on its surface in the context of MHCII molecules. Additionally, triggering of PRRs by pathogens induces the expression of costimulatory molecules such as CD80 and CD86 and the secretion of cytokines. This process is called DC maturation and takes place while DCs which ingested antigens at the infection site migrate to lymphoid organs to present them to T cells. Naïve T cells with a specific TCR for the antigen-MHCII complex get activated in secondary lymphoid organs and undergo clonal proliferation. In contrast, DCs which ingest endogenous antigens remain immature and express only low MHCII levels on their surface [208]. T cells interacting with immature DCs are either deleted by induction of apoptosis, silenced by the induction of anergy or instructed to become Tregs [209]. Surprisingly, CDNP treatment of *L. major*-infected mice increased the MHCII surface expression on DCs, indicating DC maturation and antigen-presentation (Fig. 4-3-2). This finding underscores that CDNPs are not continuously presented self-antigens, but are only released under conditions of stress leading to their induction of DC maturation. Consequently, this finding is in line with a classification of CDNPs as RAMPs.

Mature DCs secrete cytokines directing the polarization of T cells toward specific effector cell subsets. While IL-12 drives Th1 polarization, IL-10 induces Tregs and IL-4 promotes Th2 cells. The nature of the cytokines induced is dependent on the antigen dose, the stage of maturation of the DC and the DC subtype [210]. Based on the expression of characteristic surface antigens and their specialized function, DCs can be divided into two major subsets: $CD11c^{+/low}$ $B220^{+}$ pDCs which possess the unique ability to secrete both IL-12 and IFN-α and

thus specifically induce Th1 and counter-balancing Treg responses, while conventional $CD11c^+$ $B220^-$ cDCs comprise many different sub-subsets which can induce both Th1 and Th2 responses [211–213]. In the context of *L. major* infection, IL-12 production and Th1 polarization have been linked to monocyte-derived cDCs [214], while pDCs have been shown to be increased in Th2 dominant, susceptible BALB/c mice suggesting that pDCs might rather support anti-inflammatory T cells in this setting [212]. CDNPs increased MHCII surface expression on both c- and pDCs, thus no conclusion on a possible shift in the direction of T cell polarization can be drawn from these data (Fig. 4-3-2). Hence, the cytokine profiles of both DC subsets should be analyzed in further experiments. Although, cytokine secretion of DCs was not analyzed in this study, the experiments presented in Fig. 4-1-8 to 4-1-10 and 4-2-2 indicate that CDNPs might support the secretion of Th2 driving anti-inflammatory cytokines while suppressing Th1-inducing pro-inflammatory ones.

5.3.1.2 CDNPS decrease the ratio of naïve vs. effector (memory) $CD4^+$ T cells

Increased DC activation was found to correlate with a decreased ratio of naïve vs. effector (memory) T cells, indicating increased activation of T cells (Fig. 4-3-3). Activated effector T cells upregulate the expression of the activation marker CD44 on their surface [215], while downregulating CD62L, which is responsible for the entry into lymph nodes [216]. Thus, effector cells lacking CD62L migrate to the site of infection, where they secrete effector cytokines such as INFγ or IL-4. A T cell response typically peaks 7–15 days after the first antigen encounter, followed by the death of 90–95% of antigen-specific effector T cells. The remaining T cells form a pool of central or effector memory T cells [217]. Central memory T cells upregulate CD62L anew, thus the resulting $CD62L^+CD44^+$ cells are homing to secondary lymphoid organs, where they stimulate DCs and provide help to B cells to induce a new round of effector cells, while having no direct effector functions themselves. In contrast, effector memory T cells remain $CD62L^-CD44^+$ and therefore are tissue-homing, representing the first responders at the infection site, where they produce effector cytokines such as IFNγ or IL-4 [217,218]. CDNPs selectively increase the ratio of naïve vs. effector/effector memory T cells (Fig. 4-3-3). Since both effector and effector memory T cells show the same expression pattern of CD62L and CD44, it is impossible to conclude which of those cell subsets are actually increased with the gating strategy used here. However, both effector and effector memory T cells migrate to the infection site, where the nature of the cytokines they secrete dictates the disease outcome [166].

5.3.1.3 CDNPs shift the micromilieu at the infection site to the anti-inflammatory side

It is well known that *Leishmania* LPG which is sensed by TLR2 on DCs [161] induces the secretion of Th1-promoting cytokines [163–165]. Consequently, interference with this pathway by CDNPs as shown *in vitro* (Fig. 4-1- to 10) should alter the cytokine milieu and thus T polarization pattern of infected mice. When investigating the polarization pattern in the draining lymph node, where polarization takes place, a tendency towards slightly diminished intracellular IFNγ levels on $CD4^+$ T cells was detected in CDNP-treated mice, indicating reduced Th1 polarization (Fig. 4-3-4). Since this effect was limited to IFNγ MFI within the whole $CD4^+$ T cell population, while the frequency of $IFN\gamma^+CD4^+$ T cells remained constant, CDNPs may induce qualitatively weaker polarization instead of a quantitative change in Th1 vs. Th2 amounts. Altered levels of intracellular IL-4 characteristic for Th2 cells, were, however, not detected in the draining lymph node after CDNP treatment (Fig. 4-3-4). Yet, IL-4 expression is difficult to induce after restimulation *in vitro* and usually activated T cells express IL-4 in frequencies below 2%, making it very difficult to measure small differences in expression levels via FACS [219,220]. The usage of IL-4 reporter mice or the enumeration of $IL\text{-}4^+CD4^+$ T cells by ELISPOT would be advantageous to assess the expression of IL-4 more adequately. Moreover, four weeks post infection, polarization might be already tailing off, since most effector cells are already at the infection site. Thus, following the polarization pattern over the course of infection would provide a clearer picture of the influence of CDNPs on T cell polarization.

Likewise, no change in intracellular IL-10 levels indicative of regulatory T cells was detected in the draining lymph node upon CDNP treatment (suppl. Fig. S1). However, the abundance of $Foxp3^+CD4^+$ T cells was significantly increased (Fig. 4-3-6), clearly suggesting increased polarization towards regulatory T cells. Of note, this applied to the whole fraction of $Foxp3^+CD4^+$ T cells, with CDNPs having no effect on conventional $Foxp3^+CD25^+CD4^+$ Tregs. Although, the majority of Tregs usually express CD25 on their surface [221], CD25 is regarded as an unspecific marker of activation by now which is therefore not necessary for the function of regulatory T cells [221]. Instead, Foxp3 was shown to be the commitment factor, strictly required for the induction of regulatory T cells, while CD25 can be down-regulated and regained without a loss of function [222,223]. As such, Foxp3 suppresses the function of NFκB thereby blocking the expression of effector cytokines [224]. Indeed, $CD25^-Foxp3^+$ $CD4^+$ T cells have been shown to have regulatory functions *in vitro* and *in vivo*, mediated mainly via IL-10 [221,225]. In light of these findings, it appears surprising that increased frequencies of $Foxp3^+CD4^+$ T cells were not accompanied by increased IL-10 levels (suppl.

Fig. S1), however the Tregs induced by CDNPs might mediate their effector function rather at the site of infection, where Tregs accumulate in *Leishmania* infections [83].

In fact, a strong tendency towards increased IL-10 mRNA expression at the infection site was detected after CDNP treatment (Fig. 4-3-7). IL-10 is known to promote intracellular infections in general and *L. major* infection in particular. The mechanisms involve suppression of macrophage phagocytosis, induction of MHCII expression and secretion of pro-inflammatory cytokines, thus preventing parasite killing as well as inhibition of pro-inflammatory Th1 cells. Hence, susceptible IL-10 knockout mice infected with *L. major* were shown to control infection [226].

IL-10 can be produced by a broad range of myeloid as well as lymphoid cells, with macrophages, DCs, B cells and Tregs being the major sources [227]. Moreover, the increased mRNA levels may result from the increased IL-10 production by different immune cells. However, considering the increased $Foxp3^{+}CD4^{+}$ cell frequencies in the draining lymph node (Fig. 4-3-6), it appears likely, that CDNPs induce increased Treg polarization and such Tregs then migrate to the infection site to produce IL-10. Further cytokine analysis on the single-cell levels are needed to confirm this hypothesis, but were not undertaken in this study due to the technical difficulties associated with the isolation of the small amounts of T cells present in the foot pad skin.

In addition, IL-4 mRNA expression at the infection site was considerably increased after CDNP treatment (Fig. 4-3-5). IL-4 promotes the polarization of Th2 cells which are unable to control intracellular infection and additionally inhibit Th1 cells which are crucial for healing [74]. Basophils, eosinophils and mast cells are known producers of IL-4 [228], yet Th2 cells are commonly regarded as the main IL-4 source [228]. Moreover, Th2 cells are known to migrate to the infection site, where they produce IL-4 in *Leishmania* infections [229], indicating that increased IL-4 levels at the infection site after CDNP treatment are due to increased Th2 cell polarization.

Taken together, these results indicate that in the draining lymph node CDNP treatment induces a mild shift in the polarization of T cells towards anti-inflammatory Th2 and regulatory T cell subsets. These T cell subsets then migrate to the infection site, where they produce increased amounts of IL-10 and IL4.

The polarization pattern of effector T cells dictates the clinical outcome of leishmaniasis. Th1 cells producing IFNγ and thereby activating macrophages to kill *Leishmania* [82] are crucial for clearance of the parasite, while Th2 cells hardly secreting IFNγ are unable to control

infection and instead exacerbate inflammation [74]. Thus, it is not surprising that CDNP treatment increasing Th2 cells is reflected by mildly increased bacterial loads at the infection site (Fig. 4-3-8 B), although this effect was not clinically relevant in terms of foot pad swelling which mirrors the extent of inflammation (Fig. 4-3-8 A). Probably, CDNP-induced Tregs amplifying the secretion of the anti-inflammatory cytokine IL-10 suppress macrophages and Th effector cells at the infection site thereby preventing inflammation [83].

In conclusion, CDNPs clearly display immunomodulatory properties in *L. major* infection by increasing DC activation and likely antigen-presentation, thereby decreasing the ratio of naïve vs. effector (memory) T cells, leading to the induction of an anti-inflammatory milieu at the infection site. However, since such a milieu is detrimental in *Leishmania* infection and no significant effect on the clinical outcome of *L. major* infection was found after CDNP treatment, CDNP treatment appears unfavorable in this infection model.

5.3.2 CDNPs are beneficial in sepsis

In contrast to intracellular *Leishmania* infection, CDNPs proved to have a beneficial effect in polymicrobial sepsis which was reflected by decreased bacterial loads (Fig. 4-3-17) and a strong tendency towards increased survival (Fig. 4-3-9).

Importantly, sepsis differs from *Leishmania* infection by the fact that sepsis proceeds in two phases: an initial pro-inflammatory state followed by severe immunosuppression. During the first phase, monocytes, macrophages, and neutrophils are recruited to the infection site and excessively secrete pro-inflammatory mediators such as IL-1β, TNFα and IL-6 [86], resulting in vascular leakage and organ damage. However, most patients survive this early inflammation and die due to the following immunosuppression. This state is characterized by reduced surface expression of activation markers, limited phagocytosis and bacterial clearance, downregulated antigen presentation and excessive apoptosis rendering the immune system unable to eradicate the primary infection as well as highly susceptible to secondary infections [87–89]. Thus, ameliorating therapies in sepsis need to overcome immunosuppression.

5.3.3 CDNPs enhance the activation of effector cells at the infection site of sepsis

CDNP treatment of septic mice at the time of CLP, demonstrated that CDNPs are ingested by neutrophils, inflammatory monocytes, and macrophages at the site of infection 4 hours after

CLP (Fig. 4-3-12). In accordance with the *in vitro* results, peritoneal macrophages took up the largest quantity of CDNPs (see Fig. 4-3-12 B and 4-2-4). However, even the small CDNP amounts ingested per cell by inflammatory monocytes and neutrophils were sufficient to promote the same activated phenotype as seen on CDNP-ingesting macrophages: increased MHCII surface expression (Fig. 4-3-13). Increased MHCII expression indicates increased antigen presentation, which in turn enhances the activation of adaptive effector cells. In fact, decreased HLA-DR expression is characteristic for septic patients and low expression levels are associated with higher mortality [230]. Additionally, CD11b surface expression was also upregulated after CDNP ingestion on all three cell types (Fig. 4-3-13). CD11b is a subunit of the leukocyte adhesion receptor Mac-1 (complement receptor 3), which is expressed by phagocytes rapidly after cell activation [231]. Since CD11b is involved in leukocyte recruitment and receptor-mediated phagocytosis [232], both pre-requirements for effector cell activation and bacterial clearance, increased CD11b expression is likely beneficial in sepsis. In contrast, Mac-1 deficiency is associated with impaired bacterial clearance and reduced survival [232]. Overall, these results suggest, that ingestion of CDNPs activate macrophages, infl. monocytes and neutrophils at the site of infection. All of these cells contribute to the reduction of sepsis-induced immunosuppression. Macrophages and infl. monocytes in particular, phagocytose bacteria, secrete pro-inflammatory cytokines such as TNFα and IL-1β and release cytotoxic ROS and nitric oxide [233]. Neutrophils phagocytose and clear bacteria, but also capture extracellular bacteria via neutrophil extracellular traps (NETs). Moreover, activated neutrophils release cytotoxic granules and serine proteases which have antimicrobial properties and inactivate bacterial toxins [234]. Finally, all of these cells are capable of antigen-presentation and T cell activation.

The finding of CDNP-driven cell activation was supported by decreased levels of the anti-inflammatory cytokine IL-10 at the infection site 24 hours post CLP (Fig. 4-3-15). IL-10 has been shown to be one of the key modulators during the anti-inflammatory state of sepsis [235]. Its release suppresses the secretion of pro-inflammatory cytokines, impairs phagocytotic capacities, and respiratory bursts of APCs [235]. Notably, high systemic IL-10 levels have been shown to increase mortality [171], while inhibition of IL-10 expression using the immunomodulator AS101 improved bacterial clearance and increased survival in a mouse model of sepsis [236].

Interestingly, CDNPs might also impair the anti-inflammatory functions of neutrophils. Although, neutrophils are generally considered as major inflammatory cells in acute inflammation crucial for controlling of bacterial infections, neutrophils exert disease-

deteriorating effects in the context of sepsis. Here, they are the main producers of IL-10, excessively go into apoptosis and release anti-inflammatory NDMPs [92,94]. Both apoptotic neutrophils and the NDMPs they release express PS on their cell surface [93–95] which is recognized by macrophages and monocytes which then phagocytose them in a non-inflammatory, silent manner [92]. While the amount of apoptotic neutrophils at the infection site 24 hours post CLP was unaffected by CDNP treatment (data not shown), the finding of increased anti-inflammatory NDMP levels (Fig. 4-3-16) seemed contradictory to the otherwise immune-enhancing effects of CDNPs in sepsis. Yet, a possible explanation for this conflicting result is provided by *in vitro* experiments demonstrating that i) direct incubation of neutrophils with CDNPs in fact reduced NDMP formation (Fig. 4-3-19), and that ii) annexin A5-containing CDNPs are able to bind to PS on the NDMP surface (Fig. 4-3-19) and, iii) thereby impede their uptake by macrophages (Fig. 4-3-20). This is not surprising, considering that PS-annexin A5 binding is a well-established molecular interaction, which is even the basis of frequently used assays to detect apoptotic cells [237]. Consequently, NDMPs, whose PS is masked by CDNP binding would not be phagocytosed and instead would accumulate at the infection site.

5.3.4 CDNPs reduce bacterial loads at the infection site of sepsis

CDNP treatment led to dramatically reduced bacterial loads at the infection site 24 hours post CLP (Fig. 4-3-17). This fact can be attributed to the increased activation of effector cells as discussed above. Surprisingly, however, a direct antimicrobial effect of CDNPs *in vitro* was also observed (Fig. 4-3-22). Although the underlying mechanisms were not addressed further, it is reasonable to speculate that annexin A5, which is selectively increased in sCDNPs vs. usCDNPs might be involved. Rand et al. reported high-affinity binding of annexin A5 to the lipid A domain of LPS from the outer membrane of *P. aeruginosa* [238]. Thus, it seems possible that the annexins present in CDNPs bind LPS on several bacteria at once, thereby clumping them together and inducing a contact-dependent growth-inhibition of the bacteria.

CDNP-driven down-regulation of peritoneal IL-6 levels *in vivo* (Fig. 4-3-14) is in accordance with the reduced bacterial loads. Although, IL-6 is considered a pro-inflammatory cytokine with IL-6 deficient mice being unable to control infection [170,239], it also has been reported that IL-6 can have anti-inflammatory effects via promoting the polarization to alternatively activated M2 macrophages [172] thereby limiting inflammation and bacterial clearance. Along these lines, increased IL-6 release correlates with the failure to clear bacteria [173], while IL-6 was shown to suppress inflammation in a murine model of alveolar endotoxemia

[240]. Importantly, there is abundant evidence on the clinical importance of decreased IL-6 levels as a predictive marker for survival in sepsis [170,241]. Consequently, Barkhausen et. al. observed improved survival in CLP-induced sepsis after selectively blocking IL-6 trans-signaling [242]. Importantly, CDNPs were able to downregulate IL-6 mRNA and protein expression of LPS-stimulated peritoneal macrophages *in vitro* (Fig. 4-3-18), demonstrating that IL-6 reduction is a direct effect of CDNPs.

5.3.5 The impact of CDNPs on survival in sepsis

Given that reduced bacterial clearance due to immunosuppression is one of the major causes of death in septic patients [87,89] and the recovery of effector cells is associated with improved survival [243], it is reasonable to expect that immune enhancing CDNP treatment will result in increased survival rates in sepsis. In support of this hypothesis, decreased bacterial loads, lower IL-6 and IL-10 levels, as well as higher CD11b and MHCII expression seen in CDNP treated mice, were all shown to be predictive for enhanced survival [171,230,241]. Indeed, increased survival rates 96 hours after CLP-induction were observed upon CDNP treatment (Fig. 4-3-19). Yet, this effect was not significant. This might be due to the considerable variance of animal models *per se* and the CLP sepsis model in particular. Despite being the gold standard in the induction of sepsis, CLP is associated with relatively high variance. Mortality of CLP-induced sepsis mainly depends on two factors, the extent of the puncture and the ligation length. Ligation results in necrosis of the cecum, providing a permanent source of inflammation [244]. The extent of the puncture as well as the amount of feces which is squeezed out, defines how many bacteria will be present in the peritoneum. Thus, in contrast to other, less variable disease models, CLP is not induced by application of a defined dose of elicitor, but by ligation and extrusion of stool which is handled by visual judgement resulting in small differences of the procedure for each animal. This might lead to substantial variability in survival. Moreover, each mouse is slightly different regarding its cecum size, the fecal composition as well as the amount of stool present in the cecum at the time of CLP [244]. Hence, an increased amount of animals and probably also an increase in CDNP dose will likely prove the beneficial effect of CDNPs on mouse survival in sepsis.

5.3.6 Hypothetic model of immune-enhancement in sepsis due to the initial anti-inflammatory effect of CDNPs

Collectively, the results discussed above clearly point towards an immune-enhancing role of CDNPs in sepsis partly restoring sepsis-induced immunosuppression. A critical question is

why CDNPs drive a pro-inflammatory response in this setting, while *in vitro* as well as in *L. major*-infection immunosuppression is induced.

Sepsis proceeds in two phases, an initial pro-inflammatory state and the subsequent immunosuppressed phase. This phase is also called compensatory anti-inflammatory response syndrome (CARS) since it represents the direct counter response to the exacerbated inflammation induced in the first phase with the aim of restoring homeostasis [245]. Therefore, the extent of immuno-paralysis directly correlates with the severity of the primary inflammation. For example, extensive TLR4 triggering by LPS results in unresponsiveness to further stimulation [88]. Similarly, constant T cell activation leads to functional unresponsiveness and/or T cell deletion. Uncontrolled activation of immune cells furthermore results in excessive apoptosis due to cell exhaustion [246]. Thus, extreme inflammation entails an overshooting anti-inflammatory response leading to a dysfunction of the immune system.

Since all results presented in this study beyond the sepsis experiments clearly indicate an anti-inflammatory role of CDNPs and since CDNPs were applied at the time of CLP, it is plausible to suggest that CDNPs dampen the very early inflammation induced by CLP. In return, the counterbalancing anti-inflammatory response is diminished as reflected by increased activation of immune cells. Of note, the anti-inflammatory effect of CDNPs *in vitro* and in *L. major*-infection was clearly measurable, however not completely reversing inflammation. Analogous, the anti-inflammatory effect of CDNPs in sepsis is likely strong enough to reduce excessive inflammation but also weak enough to allow infection control. This hypothesis should be addressed in further experiments analyzing the very early, hyperinflammatory phase of sepsis 30 min to 4 hours post CLP.

Taken together, these results emphasize the therapeutic potential of CDNPs in sepsis. This finding is highly significant, considering that despite extensive research in the field of sepsis and long lasting efforts in the identification of septic modulators, all clinical trials conducted so far have failed to translate into successful therapeutic medications [247,248]. The urgent need for development of therapeutic innovations is emphasized by the extremely high mortality rates of 20-30% in sepsis [249].

5.4 CDNPs are endogenously produced *in vivo*

CDNPs were described as new particulate mediators of intercellular communication [66]. However, to date, CDNPs have been shown to be present in stressed cell cultures *in vitro* and in tissue sections under the EM *ex vivo*, only. Although, the latter results hints towards a presence *in vivo*, sample preparation for EM might have introduced artificial formation of CDNPs *ex vivo*. Therefore, it remains unknown whether CDNPs indeed exist *in vivo*. To confirm CDNP production *in vivo*, a murine sepsis model was used, since sepsis induces severe cellular stress at the site of infection. Moreover, the infection site in this model is the peritoneum which is easily accessible. In contrast to most other mouse models like *Leishmania* infection, where CDNPs would be difficult to isolate from solid tissue, CDNPs were expected to accumulate in the peritoneal fluid which can be harvested without difficulties.

The lack of *in vivo* data is mainly due to the difficulty associated with the detection of membrane-less nanoparticles without sample manipulation [176]. Here, the innovative NTA method was used to detect CDNPs. This technique is commercially available since 2006 and allows the sizing and visualization of nanoparticles without further preparation [100]. In fact, NTA confirmed the presence of endogenous CDNPs in peritoneal fluid of mice which underwent CLP. Size and distribution of cell culture-derived and CLP-derived CDNPs showed very similar size distributions, although cell culture-derived CDNPs appeared to contain more larger CDNPs (Fig. 4-4-2 B). Similarly, SEM analysis revealed comparable sizes and shapes of both CDNPs (compare Fig. 4-4-2 A and 4-2-1 A). In contrast, the protein composition between cell culture-derived (Fig. 4-2-1 C) and CLP-derived CDNPs (Fig. 4-4-2 C) differed considerably as assessed by SDS-PAGE. This result was not unexpected, due to the very different context of sepsis as compared to nutrient-deprived cell culture composed of a single cell type. First, multiple cells are present at the infection site of sepsis. These cells release various pro- or anti-inflammatory mediators. Secondly, bacteria-derived LPS or other bacterial factors are released in sepsis. All of those might stick to or even be incorporated into CDNPs. Additionally, albumin is present in the peritoneum which is very sticky and thus might represent the large spots around 66-69 kDa seen on the gel (Fig. 4-4-2 C). Whether the association with additional factors appears *in vivo* and has functional implications or whether it occurs during the purification process, needs to be established in further experiments.

However, the most compelling evidence for the particles isolated post CLP indeed being CDNPs, comes from Western Blot analysis detecting annexin A5. All preparations from septic mice contained annexin A5, although the annexin content was highly variable among

individual mice (Fig. 4-4-3). Thus, it will be interesting to correlate bacterial loads, intraperitoneal cytokine levels and disease severity with the annexin A5 content in future experiments.

The negligible amount of CDNPs found in naïve mice (Fig. 4-4-2 A, upper panel), confirms the accumulation of CDNPs upon induction of stress. However, CDNPs could be isolated from cells which were not cultured under nutrient-deprived conditions as evidenced by SEM and NTA (Fig. 4-2-1 A and B). This finding is not necessarily contradicting the hypothesis of CDNPs as a specific response to cellular stress, since the artificial cultivation of cells as a monolayer without surrounding tissue and extracellular matrix might represent a mild stressing condition itself. Likewise, confluency, i.e. overcrowding, as well as passaging of the cells may cause cellular stress, explaining CDNP formation of such cells. However, this stress is relatively mild as compared to the additional stress induced by nutrient deprivation.

These data point towards CDNPs being part of the intercellular communication network under conditions of cellular stress, within a stress observation and response system [66]. In this respect, the role of CDNPs would be to dampen inflammation, prime cells to efficiently use their resources and thereby preventing cell exhausting, while promoting resistance and survival [58,68].

5.4.1 Possible mechanisms of CDNP release and uptake

The critical question remains, how CDNPs are released and how their “message” is received by other cells. No research has been conducted so far to elucidate the mechanisms of CDNP release, however it is understood that the mechanism significantly differs from those of other mediators of cell communication such as exosomes and MPs. Since the latter ones are surrounded by a lipid membrane they can simply be released by endo- or exocytosis. In contrast, membraneless proteins which are secreted normally possess a 5´-leader sequence in their messenger RNA directing them to the ER, where they are translated in protein and released via Golgi-derived secretion vesicles [250]. Since CDNPs are composed of intracellular proteins, none of their components possesses a signal sequence. Thus, a non-classical secretion pathway similar to the one used by IL-1β could be involved in CDNP release. IL-1β is embedded in secretary endolysosomes which fuse with the plasma membrane thereby releasing their content into the extracellular space [251]. This possibility would be supported by Solisch et al, who observed that intracellularly located CDNPs are sometimes surrounded by a membrane [68]. Another intriguing possibility for CDNP-release would be

the annexin A5-mediated binding to PS within the inner leaflet of the plasma membrane and subsequent PS "flipping" to the cell surface with its annexin cargo attached [252].

Since CDNPs are clearly ingested by recipient cells, the CDNP "message" is apparently transmitted via ingestion and not binding to surface receptors. Similar to the hypothetical annexin-PS-mediated release of CDNPs, it is reasonable to speculate that CDNP uptake could also be mediated by a novel pinocytic pathway involving such interactions. Kenis et. al. demonstrated that annexin A5 molecules bind to healthy, non-apoptotic cells via surface expressed PS. Aggregation of single PS-bound annexin molecules leads to the inward bending of the membrane (invagination) and results in vesicle formation [199]. Importantly, such vesicles do not only contain annexin A5, but also all other proteins in direct vicinity to the membrane patch invaginated [197,199]. Thus, it appears possible, that annexin A5 mediated endocytosis might be shuttling whole CDNPs inside the cell. However, CDNPs could also utilize one of the ingestion pathways demonstrated to be used for the uptake of other nanoparticles: CD64-mediated phagocytosis, dynamin II-dependent endocytosis and macropinocytosis [253,254].

In this regard, further experiments should focus on inhibition of PS expression on the cell surface or saturation of already expressed PS to assess the contribution of the PS-annexin A5 pathway to CDNP release and uptake.

5.5 Implication for the potential use of CDNPs as therapeutics

As discussed above, CDNPs are beneficial in sepsis and were also shown to be protective in virus-induced mouth-and-foot disease [69]. In contrast, they had no to a deteriorate effect in *L. major* infection. Obviously, the effect of CDNPs is highly dependent on the context.

Given, that CDNPs have anti-inflammatory effects *in vitro* and both mouth-and-foot disease as well as sepsis are characterized by an initial phase of excessive inflammation, it appears likely that in a broader context, CDNPs are beneficial whenever overshooting potentially tissue- and organ-damaging hyper-inflammation takes place. Indeed, CDNPs were shown to reduce disease severity in a murine model of an autoimmune blistering disease [99]. In fact, it is widely appreciated that most of the severe complications associated with infectious diseases results from excessive inflammation [227]. Thus, therapeutic interventions aiming at improving the immune response to clear infection often demonstrated the opposite effect leading to tissue and organ damage and ultimately increased mortality - in particular well-documented for sepsis [247,248]. These experiences underscore the need of therapeutic

strategies which indeed contain inflammation. Yet, such treatments must not completely interfere with the inflammatory response, since pathogen clearance is still a major therapeutic aim. CDNPs meet these criteria, as their anti-inflammatory effects do not completely reverse inflammation *in vitro* (chapter 4.2) and despite clearly modulating the micromilieu at the infection site and in the draining lymph node, has no effect on the clinical outcome of *L. major* infection (chapter 4.5).

Exogenous application of CDNPs might be a safe option regarding the results obtained with the treatment on a single scale basis in human patients [72]. Of note, no side effects were witnessed upon these treatments, although xenogeneic CDNPs were used. Another therapeutic strategy would be the modulation of endogenous CDNP levels. However, more studies on the induction and the pathophysiological role of endogenous CDNPs are needed.

All in all, despite the need of more studies addressing the mechanism, dose-response relation and possible cytotoxicity of CDNP application, the results presented here clearly demonstrate the therapeutic capacity of CDNPs to regulate excessive inflammation in infectious diseases.

6. References

1. Akira S, Uematsu S, Takeuchi O. (2006). Pathogen Recognition and Innate Immunity. Cell *124*,783–801.
2. Bowie A, O'Neill LA. (2000). The interleukin-1 receptor/Toll-like receptor superfamily: signal generators for pro-inflammatory interleukins and microbial products. J. Leukoc. Biol. *67*, 508–14.
3. O'Neill LAJ, Golenbock D, Bowie AG. (2013). The history of Toll-like receptors - redefining innate immunity. Nat. Rev. Immunol. 13, 453–60.
4. Dowling JK, Mansell A. (2016). Toll-like receptors: the swiss army knife of immunity and vaccine development. Clin. Transl. Immunol. *5*, e85. doi: 10.1038/cti.2016.22.
5. Srivastava S, Pandey SP, Jha MK, Chandel HS, Saha B. (2013). Leishmania expressed lipophosphoglycan interacts with Toll-like receptor (TLR)-2 to decrease TLR-9 expression and reduce anti-leishmanial responses. Clin. Exp. Immunol. *172*,403–9.
6. Becker I, Salaiza N, Aguirre M, Delgado J, Carrillo-Carrasco N, Kobeh LG, et al. (2003). Leishmania lipophosphoglycan (LPG) activates NK cells through toll-like receptor-2. Mol. Biochem. Parasitol. *130*, 65–74.
7. Takeda K, Akira S. (2005). Toll-like receptors in innate immunity. Int. Immunol. *17*, 1–14.
8. Takeda K, Kaisho T, Akira S. (2013). Toll-like receptors. Annu. Rev. Immunol. *21*, 335–76.
9. Broz P, Monack DM. (2013). Newly described pattern recognition receptors team up against intracellular pathogens. Nat Rev Immunol *13*, 551–65.
10. Holodick NE, Tumang JR, Rothstein TL. (2010). Immunoglobulin secretion by B1 cells: Differential intensity and IRF4-dependence of spontaneous IgM secretion by peritoneal and splenic B1 cells. Eur. J. Immunol. *40*, 3007–16.
11. Panda S, Ding JL. (2014). Natural Antibodies Bridge Innate and Adaptive Immunity. J. Immunol. *194*, 13–20.
12. Grönwall C, Vas J, Silverman GJ. (2012). Protective roles of natural IgM antibodies. Front. Immunol. *3*, 66. doi: 10.3389/fimmu.2012.00066.
13. Meri S. (2016). Self-nonself discrimination by the complement system. FEBS Lett. *590*, 2418–34.
14. Smith KA. (2004). The quantal theory of how the immune system discriminates between "self and non-self." Med. Immunol. *3*, 3. doi: 10.1186/1476-9433-3-3.

15. Kappler JW, Roehm N, Marrack P. (1987). T cell tolerance by clonal elimination in the thymus. Cell *49*, 273–80.
16. Xing Y, Hogquist KA. (2012). T-Cell Tolerance : Central and Peripheral. Cold Spring Harb. Perspect. Biol. *4*, a006957. doi: 10.1101/cshperspect.a006957.
17. Pelanda R, Torres RM. (2012). Central B-Cell Tolerance: Where Selection Begins. Cold Spring Harb. Perspect. Biol. *4*, a007146. doi: 10.1101/cshperspect.a007146.
18. Klein L, Hinterberger M, Wirnsberger G, Kyewski B. (2009). Antigen presentation in the thymus for positive selection and central tolerance induction. Nat. Rev. Immunol. *9*, 833–44.
19. Andrade CF, Waddell TK, Keshavjee S, Liu M. (2005). Innate Immunity and Organ Transplantation: The Potential Role of Toll-like Receptors. Am. J. Transplant. *5*, 969–75.
20. Hammer C, Chaussy C, Brendel W. (1973). Preformed natural antibodies in animals and man. Outlook on xenotransplantation. Eur. Surg. Res. *5*, 162–6.
21. Galili U. (2001). The α-Gal epitope (Galα1-3Galβ1-4GlcNAc-R) in xenotransplantation. Biochimie *83*, 557–63.
22. Sachs DH. (1995). The Immunologic Response to Xenografts. ILAR J. *37*, 16–22.
23. Huang J, Gou D, Zhen C, Jiang D, Mao X, Li W, et al. (2001). Protection of xenogeneic cells from human complement-mediated lysis by the expression of human DAF, CD59 and MCP. FEMS Immunol. Med. Microbiol. *31*, 203–9.
24. Yu J, Dong S, Rushmere NK, Morgan BP, Abagyan R, Tomlinson S. (1997). Mapping the Regions of the Complement Inhibitor CD59 Responsible for Its Species Selective Activity. Biochemistry *36*, 9423–8.
25. Cascalho M, Platt JL. (2001). The immunological barrier to Xenotransplantation. Immunity. *14*, 437–46.
26. Matzinger P. (1994). Tolerance, Danger, and the Extended Family. Annu. Rev. Immunol. *12*, 991–1045.
27. Piccinini AM, Midwood KS. (2010). DAMPening inflammation by modulating TLR signalling. Mediators Inflamm. *2010*, 672395. doi:10.1155/2010/672395.
28. Matzinger P. (2002). The Danger Model: A Renewed Sense of Self. Science 296, 301–5.
29. Green DR, Ferguson T, Zitvogel L, Kroemer G. (2009). Immunogenic and tolerogenic cell death. Nat. Rev. Immunol. *9*, 353–63.
30. Leist M, Jäättelä M. (2001). Four deaths and a funeral: from caspases to alternative mechanisms. Nat. Rev. Mol. Cell Biol. *2*, 589–98.

31. Fiers W, Beyaert R, Declercq W, Vandenabeele P. (1999). More than one way to die: apoptosis, necrosis and reactive oxygen damage. Oncogene. *18*, 7719–30.
32. Fadok VA, Bratton DL, Konowal A, Freed PW, Westcott JY, Henson PM. (1998). Macrophages that have ingested apoptotic cells in vitro inhibit proinflammatory cytokine production through autocrine/paracrine mechanisms involving TGF-beta, PGE2, and PAF. J. Clin. Invest. *101*, 890–8.
33. Sauter B, Albert ML, Francisco L, Larsson M, Somersan S, Bhardwaj N. (2000). Consequences of cell death: exposure to necrotic tumor cells, but not primary tissue cells or apoptotic cells, induces the maturation of immunostimulatory dendritic cells. J. Exp. Med. *191*, 423–34.
34. Gallucci S, Lolkema M, Matzinger P. (1999). Natural adjuvants: endogenous activators of dendritic cells. Nat. Med. *5*, 1249–55.
35. Scheffer SR, Nave H, Korangy F, Schlote K, Pabst R, Jaffee EM, et al. (2003). Apoptotic, but not necrotic, tumor cell vaccines induce a potent immune responsein vivo. Int. J. Cancer *103*, 205–11.
36. Fadok VA, Bratton DL, Guthrie L, Henson PM. (2001). Differential effects of apoptotic versus lysed cells on macrophage production of cytokines: role of proteases. J. Immunol. *166*, 6847–54.
37. Casares N, Pequignot MO, Tesniere A, Ghiringhelli F, Roux S, Chaput N, et al. (2005). Caspase-dependent immunogenicity of doxorubicin-induced tumor cell death. J. Exp. Med. *202*, 1691–701.
38. Shi Y, Zheng W, Rock KL. (2000). Cell injury releases endogenous adjuvants that stimulate cytotoxic T cell responses. Proc. Natl. Acad. Sci. U. S. A. *97*, 14590–5.
39. Obeid M, Tesniere A, Ghiringhelli F, Fimia GM, Apetoh L, Perfettini JL, et al.(2007). Calreticulin exposure dictates the immunogenicity of cancer cell death. Nat. Med. *13*, 54–61.
40. Kono H, Rock KL. (2008). How dying cells alert the immune system to danger. Nat. Rev. Immunol. *8*, 279–89.
41. Schaefer L. (2014). Complexity of danger: The diverse nature of damage-associated molecular patterns. J. Biol. Chem. *289*, 35237–45.
42. Rock KL, Lai J-J, Kono H. (2011). Innate and adaptive immune responses to cell death. Immunol. Rev. *243*, 191–205.

43. Ohashi K, Burkart V, Flohe S, Kolb H. (2000). Cutting Edge: Heat Shock Protein 60 Is a Putative Endogenous Ligand of the Toll-Like Receptor-4 Complex. J. Immunol. *164*, 558–61.

44. Vabulas RM, Ahmad-Nejad P, Ghose S, Kirschning CJ, Issels RD, Wagner H. (2002). HSP70 as Endogenous Stimulus of the Toll/Interleukin-1 Receptor Signal Pathway. J. Biol. Chem. *277*, 15107–12.

45. Wheeler DS, Chase MA, Senft AP, Poynter SE, Wong HR, Page K. (2009). Extracellular Hsp72, an endogenous DAMP, is released by virally infected airway epithelial cells and activates neutrophils via Toll-like receptor (TLR)-4. Respir. Res. *10*, 31. doi: 10.1186/1465-9921-10-31.

46. Foell D, Wittkowski H, Vogl T, Roth J. (2006). S100 proteins expressed in phagocytes: a novel group of damage-associated molecular pattern molecules. J. Leukoc. Biol. *81*, 28–37.

47. Lotze MT, Tracey KJ. (2005). High-mobility group box 1 protein (HMGB1): nuclear weapon in the immune arsenal. Nat. Rev. Immunol. *5*, 331–42.

48. Kono H, Chen C-J, Ontiveros F, Rock KL. (2010). Uric acid promotes an acute inflammatory response to sterile cell death in mice. J. Clin. Invest. *120*, 1939–49.

49. Trautmann A. (2009). Extracellular ATP in the Immune System: More Than Just a "Danger Signal". Sci.Sig. *2*, pe6. doi: 10.1126/scisignal.256pe6.

50. Kariko K, Ni H, Capodici J, Lamphier M, Weissman D. (2004). mRNA Is an Endogenous Ligand for Toll-like Receptor 3. J. Biol. Chem. *279*, 12542–50.

51. Vollmer J, Tluk S, Schmitz C, Hamm S, Jurk M, Forsbach A, et al. (2005). Immune stimulation mediated by autoantigen binding sites within small nuclear RNAs involves Toll-like receptors 7 and 8. J. Exp. Med. *202*, 1575–85.

52. Van Eden W, Spiering R, Broere F, Van Der Zee R. (2012). A case of mistaken identity: HSPs are no DAMPs but DAMPERs. Cell Stress Chaperones *17*, 281–92.

53. Shields AM, Panayi GS, Corrigall VM. (2011). Resolution-associated molecular patterns (RAMP): RAMParts defending immunological homeostasis? Clin. Exp. Immunol. *165*, 292–300.

54. Yang H, Antoine DJ, Andersson U, Tracey KJ. (2013). The many faces of HMGB1: molecular structure-functional activity in inflammation, apoptosis, and chemotaxis. J. Leukoc. Biol. *93*, 865–73.

55. Shi Y, Evans JE, Rock KL. (2003). Molecular identification of a danger signal that alerts the immune system to dying cells. Nature *425*, 516–21.

56. Levy BD, Clish CB, Schmidt B, Gronert K, Serhan CN. (2001). Lipid mediator class switching during acute inflammation: signals in resolution. Nat. Immunol. *2*, 612–9.

57. Serhan CN, Savill J. (2005). Resolution of inflammation: the beginning programs the end. Nat. Immunol. *6*, 1191–7.

58. De Maio A. (2011). Extracellular heat shock proteins, cellular export vesicles, and the Stress Observation System: A form of communication during injury, infection, and cell damage: It is never known how far a controversial finding will go! Cell Stress Chaperones *16*, 235–49.

59. Ling ZL, Combes V, Grau GE, King NJC. (2011). Microparticles as Immune Regulators in Infectious Disease ? An Opinion. Front. Immunol. *2*, 67. doi: 10.3389/fimmu.2011.00067.

60. Joly E, Hudrisier D. (2003). What is trogocytosis and what is its purpose? Nat. Immunol. *4*, 815–815.

61. Davis D, Sowinski S. (2008). Membrane nanotubes: dynamic long-distance connections between animal cells. Nat. Rev. Mol. Cell Biol. *9*, 431–6.

62. De Maio A, Vega VL, Contreras JE. (2002). Gap junctions, homeostasis, and injury. J. Cell. Physiol. *191*, 269–82.

63. De Maio A. (1999). Heat shock proteins: facts, thoughts, and dreams. Shock *11*, 1–12.

64. Wu J, Kaufman RJ. (2006). From acute ER stress to physiological roles of the Unfolded Protein Response. Cell Death Differ. *13*, 374–84.

65. Giffard RG, Han RQ, Emery JF, Duan M, Pittet JF. (2008). Regulation of Apoptotic and Inflammatory Cell Signaling in Cerebral Ischemia. Anesthesiology *109*, 339–48.

66. Rönnau C, Liebermann HEH, Helbig F, Staudt A, Felix SB, Ewert R, et al. (2009). The bio-complex “reaction pattern in vertebrate cells” reduces cytokine-induced cellular adhesion molecule mRNA expression in human endothelial cells by attenuation of NF-kappaB translocation. BMB Rep. *42*, 106–12.

67. Solisch P, Kalies KU, Bergmann S. (1999). BK-RiV preparations for treatment of proliferative cellular disorders. Patent EP 0889053A2.

68. Solisch P. (1986). [Hitherto unknown pattern of reaction in vertebrate cells - ultrastructural studies of virus-host cell relationship and cell cultures. 1]. Zentralblatt für Allg. Pathol. u. Pathol. Anat. *131*, 49–57.

69. Solisch P, Nöckler A, Schäfer D, Riebe R, Holl U, Schirrmeier H, et al. (1986). [A hitherto unknown reaction pattern in vertebrate cells (RiV). 2. The protective effect of RiV particle preparations against foot-and-mouth disease in guinea pigs]. Zentralblatt für Allg. Pathol. u. Pathol. Anat. *131*, 563–8.

70. Stedman TL. (2000). Stedman's Medical Dictionary. *27th ed.* Philadelphia: Lippincott Williams & Wilkins.

71. Brubaker RR. (1985). Mechanisms of Bacterial Virulence. Annu. Rev. Microbiol. *39*, 21–50.

72. Solisch P, Bergmann S. (1994). A drug for the therapy of AIDS. Patent EP 07029551.

73. Roberts MTM. (2005). Current understandings on the immunology of leishmaniasis and recent developments in prevention and treatment. Br. Med. Bull. *75-76*, 115–30.

74. Sacks D, Noben-Trauth N. (2002). The immunology of susceptibility and resistance to Leishmania major in mice. Nat. Rev. Immunol. *2*, 845–58.

75. Mougneau E, Bihl F, Glaichenhaus N. (2011). Cell biology and immunology of Leishmania. Immunol. Rev. *240*, 286–96.

76. Salerno C, Carlucci AM, Gorzalczany S, Bregni C. (2014). In vitro Inhibition of Leishmania braziliensis Promastigotes Growth by a Fluconazole Microemulsion. Mol. Pharm. Org. Process Res. *2*, 115.

77. Scharton-Kersten T, Scott P. (1995). The role of the innate immune response in Th1 cell development following Leishmania major infection. J. Leukoc. Biol. *57*, 515–22.

78. Abou Fakher FH, Rachinel N, Klimczak M, Louis J. (2009). TLR9-Dependent Activation of Dendritic Cells by DNA from Leishmania major favors Th1 Cell Development and Resolution of Lesions *182*, 1386-96.

79. Rhee EG, Mendez S, Shah JA, Wu C, Kirman JR, Turon TN, et al. (2002). Vaccination with heat-killed leishmania antigen or recombinant leishmanial protein and CpG oligodeoxynucleotides induces long-term memory CD4+ and CD8+ T cell responses and protection against leishmania major infection. J. Exp. Med. *195*, 1565–73.

80. Osanya A, Song E-H, Metz K, Shimak RM, Boggiatto PM, Huffman E, et al. (2011). Pathogen-Derived Oligosaccharides Improve Innate Immune Response to Intracellular Parasite Infection. Am. J. Pathol. *179*, 1329–37.

81. de Veer MJ, Curtis JM, Baldwin TM, DiDonato JA, Sexton A, McConville MJ, et al. (2003). MyD88 is essential for clearance of Leishmania major: Possible role for lipophosphoglycan and Toll-like receptor 2 signaling. Eur. J. Immunol. *33*, 2822–31.

82. Heinzel FP, Sadick MD, Holaday BJ, Coffman RL, Locksley RM. (1989). Reciprocal Expression of Interferon y or Interleukin 4 during the Resolution or Progression of Murine Leishmaniasis. Evidence for Expansion of Distinct Helper T Cell Subsets J . Exp. MED. *169*, 59–72.

83. Belkaid Y, Piccirillo CA, Mendez S, Shevach EM, Sacks DL. (2002). CD4+CD25+ regulatory T cells control Leishmania major persistence and immunity. Nature *420*, 502–7.

84. Reiner SL, Locksley RM. (1995). The Regulation of Immunity to Leishmania Major. Annu. Rev. Immunol. *13*, 151–77.

85. Singer M, Deutschman CS, Seymour CW, Shankar-Hari M, Annane D, Bauer M, et al. (2016). The Third International Consensus Definitions for Sepsis and Septic Shock (Sepsis-3). JAMA *315*, 801–10.

86. Calandra T, Gerain J, Heumann D, Baumgartner JD, Glauser MP. (1991). High circulating levels of interleukin-6 in patients with septic shock: evolution during sepsis, prognostic value, and interplay with other cytokines. Am. J. Med. *91*, 23–9.

87. Hotchkiss RS, Monneret G, Payen D. (2013). Immunosuppression in sepsis: A novel understanding of the disorder and a new therapeutic approach. Lancet Infect. Dis. *13*, 260–8.

88. Iskander KN, Osuchowski MF, Stearns-Kurosawa DJ, Kurosawa S, Stepien D, Valentine C, et al. (2013). Sepsis: multiple abnormalities, heterogeneous responses, and evolving understanding. Physiol. Rev. *93*, 1247–88.

89. Boomer JS, To K, Chang KC, Takasu O, Osborne DF, Walton AH, et al. (2011). Immunosuppressio in patients who die of sepsis and multiple organ failure. JAMA *306*, 2594–605.

90. Hotchkiss RS, Swanson PE, Freeman BD, Tinsley KW, Cobb JP, Matuschak GM, et al. (1999). Apoptotic cell death in patients with sepsis, shock, and multiple organ dysfunction. Crit. Care Med. *27*, 1230–51.

91. Oberholzer A, Oberholzer C, Moldawer LL. (2001). Sepsis syndromes: understanding the role of innate and acquired immunity. Shock *16*, 83–96.

92. Kasten KR, Muenzer JT, Caldwell CC. (2010). Neutrophils are significant producers of IL-10 during sepsis. Biochem. Biophys. Res. Commun. *393*, 28–31.

93. Gasser O. (2004). Activated polymorphonuclear neutrophils disseminate anti-inflammatory microparticles by ectocytosis. Blood *104*, 2543–8.

94. Prakash PS, Caldwell CC, Lentsch AB, Pritts TA, Robinson BRH. (2012). Human microparticles generated during sepsis in patients with critical illness are neutrophil-derived and modulate the immune response. J. Trauma Acute Care Surg. *73*, 401–6.

95. Owens AP, Mackman N. (2011). Microparticles in Hemostasis and Thrombosis. Circ. Res. *108*, 1284–97.

96. Huang X, Venet F, Wang YL, Lepape A, Yuan Z, Chen Y, et al. (2009). PD1 expression by macrophages plays a pathologic role in altering microbial clearance and the innate inflammatory response to sepsis. Proc. Natl. Acad. Sci. U. S. A. *106*, 6303–8.

97. Reddy RC, Chen GH, Tekchandani PK, Standiford TJ. (2001). Sepsis-Induced Immunosuppression From Bad to Worse. Immunol. Res. *24*, 273–88.

98. Heinbockel L, Marwitz S, Barcena Varela S, Ferrer-Espada R, Reiling N, Goldmann T, et al. (2015). Therapeutical Administration of Peptide Pep19-2.5 and Ibuprofen Reduces Inflammation and Prevents Lethal Sepsis. PLoS One *10*, e0133291. doi:10.1371/journal.pone.0133291.

99. Kunz N, Hauenschild E, Maass S, Kalies KU, Barra M, Hecht L, et al. (2017). Xenogeneic cell-derived nanoparticles support the healing of cutaneous inflammation in mice and wound re-epithelialization in human skin. Manuscript submitted.

100. Filipe V, Hawe A, Jiskoot W. (2010). Critical evaluation of nanoparticle tracking analysis (NTA) by NanoSight for the measurement of nanoparticles and protein aggregates. Pharm. Res. *27*, 796–810.

101. Dunlap M, Adaskaveg JE. (1997). Introduction to the Scanning Electron Microscope Microsc. Microanal. Facility for advanced instrumentalisation, U.C. Davies.

102. Bob H. (2007). Scanning Electron Microscopy Primer. University of Minnesota's Characterization Facility.

103. http://www.microscopemaster.com/scanning-electron-microscope.html. Last visited on 13/09/2016.

104. https://www.purdue.edu/ehps/rem/rs/sem.htm. Last visited on 13/09/2016.

105. Laemmli UK. (1970). Cleavage of structural proteins during the assembly of the head of bacteriophage T4. Nature *227*, 680–5.

106. Rabilloud T, Lelong C. (2011). Two-dimensional gel electrophoresis in proteomics: A tutorial. J. Proteomics *74*, 1829–41.

107. Tannu NS, Hemby SE. (2006). Two-dimensional fluorescence difference gel electrophoresis for comparative proteomics profiling. Nat. Protoc. *1*, 1732–42.

108. Gemoll T, Epping F, Heinrich L, Fritzsche B, Roblick UJ, Szymczak S, et al. (2015). Increased cathepsin D protein expression is a biomarker for osteosarcomas, pulmonary metastases and other bone malignancies. Oncotarget *6*, 16517–26.

109. Gemoll T, Laubert T, Grimme C, Roblick UJ, Habermann JK. (2012). Hochauflösende 2D-Gelelektrophorese von Knochengewebsproben. BIOspektrum 18, 520.

110. Lewis JK, Wei J, Siuzdak G. (2006). Matrix-assisted Laser Desorption / Ionization Mass Spectrometry in Peptide and Protein Analysis. Encyclopedia of Analytical Chemistry, *1st ed*, John Wiley & Sons, Inc.

111. Chaurand P, Manier L. MALDI MS Tutorial. downloaded from: http://www.cigs.unimo.it/cigsdownloads/labs/malditof/didattica/maldi_ms_tutorial.pdf on 10/04/2016.

112. Jolliffe IT, Cadima J. (2016). Principal component analysis: a review and recent developments. Philos. Trans. R. Soc. A 374, 20150202.

113. Ringner M. (2008). What is principal component analysis? Nat. Biotechnol. *26*, 303–4.

114 https://coolstatsblog.com/2015/03/21/principal-component-analysis-for-dummies/. Last visited on 02/11/2016.

115. Kunz N. (2013). Characterisation of the humoral immune response in C57BL/6 mice after Leishmania major infection. Master Thesis at the University of Lübeck.

116. Nicolas L, Prina E, Lang T. (2002). Real-Time PCR for Detection and Quantitation of Leishmania in mouse tissues. J. Clin. Microbiol. *40*, 1666–9.

117. Bretagne S, Durand R, Olivi M, Garin J, Sulahian A, Rivollet D, et al. (2001). Real-Time PCR as a New Tool for Quantifying Leishmania infantum in Liver in Infected Mice. Clin. Diag. Lab. Immunol. *8*, 821-31.

118. Unsinger J, McGlynn M, Kasten KR, Hoekzema AS, Watanabe E, Muenzer JT, et al. (2010). IL-7 promotes T cell viability, trafficking, and functionality and improves survival in sepsis. J. Immunol. *184*, 3768–79.

119. Ray A, Dittel BN. (2010). Isolation of Mouse Peritoneal Cavity Cells. J. Vis. Exp. e1488, doi: 10.3791/1488.

120. Furze RC, Rankin SM. (2008). Neutrophil mobilization and clearance in the bone marrow. Immunology *125*, 281–8.

121. Swamydas M, Luo Y, Dorf ME, Lionakis MS. (2015). Isolation of Mouse Neutrophils. Curr. Protoc. Immunol. *110*, 3.20.1-3.20.15. doi: 10.1002/0471142735.im0320s110.

122. Youssef PP, Mantzioris BX, Roberts-Thomson PJ, Ahern MJ, Smith MD. (1995). Effects of ex vivo manipulation on the expression of cell adhesion molecules on neutrophils. J. Immunol. Methods *186*, 217–24.

123. Midura EF, Prakash PS, Johnson BL, Rice TC, Kunz N, Caldwell CC. (2016). Impact of caspase-8 and PKA in regulating neutrophil-derived microparticle generation. Biochem. Biophys. Res. Commun. *469*, 917–22.

124. Nagendra S, Schlueter AJ. (2004). Absence of cross-reactivity between murine Ly-6C and Ly-6G. Cytometry *58*, 195–200.

125. Ozinsky A, Underhill DM, Fontenot JD, Hajjar AM, Smith KD, Wilson CB, et al. (2000). The repertoire for pattern recognition of pathogens by the innate immune system is defined by cooperation between toll-like receptors. Proc. Natl. Acad. Sci. U. S. A. *97*, 13766–71.

126. Gantner BN, Simmons RM, Canavera SJ, Akira S, Underhill DM. (2003). Collaborative Induction of Inflammatory Responses by Dectin-1 and Toll-like Receptor 2. J. Exp. Med. *197*, 1107–17.

127. Aliprantis AO, Yang RB, Mark MR, Suggett S, Devaux B, Radolf JD, et al. (1999). Cell activation and apoptosis by bacterial lipoproteins through toll-like receptor-2. Science *285*, 736–9.

128. Alexopoulou L, Holt AC, Medzhitov R, Flavell RA. (2008). Recognition of double-stranded RNA and activation of NF-kappaB by Toll-like receptor 3. Nature 413, 732–8.

129. Lu YC, Yeh WC, Ohashi PS. (2008). LPS/TLR4 signal transduction pathway. Cytokine *42*, 145–51.

130. Hemmi H, Kaisho T, Takeuchi O, Sato S, Sanjo H, Hoshino K, et al. (2002). Small anti-viral compounds activate immune cells via the TLR7 MyD88–dependent signaling pathway. Nat. Immunol. *3*, 196–200.

131. Patiño T, Soriano J, Barrios L, Ibáñez E, Nogués C. (2015). Surface modification of microparticles causes differential uptake responses in normal and tumoral human breast epithelial cells. Sci. Rep. *5*, 11371. doi: 10.1038/srep11371.

132. Rice TC, Seitz AP, Edwards MJ, Gulbins E, Caldwell CC. (2016). Sphingosine rescues burn-injured mice from pulmonary Pseudomonas aeruginosa infection. J. Leukoc. Biol. *100*, 3–8.

133. Livak KJ, Schmittgen TD. (2001). Analysis of Relative Gene Expression Data Using Real-Time Quantitative PCR and the 2−ΔΔCT Method. Methods *25*, 402–8.

134. Smith PK, Krohn RI, Hermanson GT, Mallia AK, Gartner FH, Provenzano MD, et al.(1985). Measurement of protein using bicinchoninic acid. Anal. Biochem. *150*, 76–85.

135. Brown M, Wittwer C. (2000). Flow Cytometry: Principles and Clinical Applications in Hematology. Clin. Chem. *46*, 1221–9.

136. Tung JW, Heydari K, Tirouvanziam R, Sahaf B, Parks DR, Herzenberg LA, et al. (2007). Modern Flow Cytometry: A Practical Approach. Clin. Lab. Med. *27*, 453–68.

137. Roederer M. (2001). Spectral compensation for flow cytometry: visualization artifacts, limitations, and caveats. Cytometry *45*, 194–205.

138. Freeman CM, Quillin RC, Wilson GC, Nojima H, Johnson BL, Sutton JM, et al.(2014). Characterization of microparticles after hepatic ischemia-reperfusion injury. PLoS One *9*, e97945. doi:10.1371/journal.pone.0097945.

139. Joiner T, Kraus P, Kupiec T. (2002). Comparison of Endotoxin Testing Methods for pharmaceuticals Products. Int. J. Pharm. *6*, 408–9.

140. https://www.thermofisher.com/order/catalog/product/88282. Last visited on 29/10/2016.

141. Magalhães PO, Lopes AM, Mazzola PG, Rangel-Yagui C, Penna TC V, Pessoa A. (2007). Methods of endotoxin removal from biological preparations: a review. J. Pharm. Pharm. Sci. *10*, 388–404.

142. Gorbet MB, Sefton MV. (2005). Endotoxin: The uninvited guest. Biomaterials *26*, 6811–7.

143. http://www.biolegend.com/LEAF. Last visited on 29/10/2016.

144. Tukey JW. (1977). Exploratory Data Analysis. *1st ed*, Addison-Wesley Publishing Company.

145. http://www.statisticalmisses.nl/index.php/frequently-asked-questions/77-what-is-wrong-with-tests-of-normality. Last visited on 01/12/2016.

146. http://graphpad.com/support/faqid/1598/. Last visited on 30/10/2016.

147. Grubbs FE. (1969). Procedures for Detecting Outlying Observations in Samples. Technometrics *11*, 1–21.

148. https://www.graphpad.com/support/faqid/959/. Last visited on 02/11/2016.

149. Noppert SJ, Fitzgerald KA, Hertzog PJ. (2007). The role of type I interferons in TLR responses. Immunol. Cell Biol. *85*, 446–57.

150. Gusnard D, Kirschner RH. (1977). Cell and organelle shrinkage during preparation for scanning electron microscopy: effects of fixation, dehydration and critical point drying. J. Microsc. *110*, 51–7.

151. Ramadori G, Van Damme J, Rieder H, Zum Büschenfelde KHM. (1988). Interleukin 6, the third mediator of acute-phase reaction, modulates hepatic protein synthesis in human and mouse. Comparison with interleukin 1 β and tumor necrosis factor-α. Eur. J. Immunol. *18*, 1259–64.

152. Gruys E, Toussaint MJM, Niewold TA, Koopmans SJ. (2005). Acute phase reaction and acute phase proteins. J. Zhejiang Univ. Sci. *6*, 1045–56.

153. Cambi A, Koopman M, Figdor CG. (2005). How C-type lectins detect pathogens. Cell. Microbiol. *7*, 481–8.

154. Kajava AV, Vasselon T. (2010). A network of hydrogen bonds on the surface of TLR2 controls ligand positioning and cell signaling. J. Biol. Chem. *285*, 6227–34.

155. Personal communication with Varicula Life Science AG.

156. Simms PE, Ellis TM. (1996). Utility of flow cytometric detection of CD69 expression as a rapid method for determining poly- and oligoclonal lymphocyte activation. Clin. Diagn. Lab. Immunol. *3*, 301–4.

157. Radulovic K, Rossini V, Manta C, Holzmann K, Kestler HA, Niess JH. (2013). The Early Activation Marker CD69 Regulates the Expression of Chemokines and CD4 T Cell Accumulation in Intestine. PLoS One *8*, e65413. doi: 10.1631/jzus.2005.B1045.

158. Vazquez BN, Laguna T, Carabana J, Krangel MS, Lauzurica P. (2009). CD69 Gene Is Differentially Regulated in T and B Cells by Evolutionarily Conserved Promoter-Distal Elements. J. Immunol. *183*, 6513–21.

159. Liebermann HEH, Sietmann R, Bange R, Wazel W, Riebe R. (2005). RiV particles are heat stable. Eng. Life Sci. *5*, 240–6.

160. Faria MS, Reis FCG, Lima APCA. (2012). Toll-like receptors in Leishmania infections: Guardians or promoters? J. Parasitol. Res. *2012*, 930257. doi:10.1155/2012/930257.

161. Franco LH, Beverley SM, Zamboni DS. (2012). Innate Immune Activation and Subversion of Mammalian Functions by Leishmania Lipophosphoglycan. J. Parasitol. Res. *2012*, 165126. doi:10.1155/2012/165126.

162. Dillon SR, Sprecher C, Hammond A, Bilsborough J, Rosenfeld-Franklin M, Presnell SR, et al. (2004). Interleukin 31, a cytokine produced by activated T cells, induces dermatitis in mice. Nat. Immunol. *5*, 752–60.

163. Flandin JF, Chano F, Descoteaux A. (2006). RNA interference reveals a role for TLR2 and TLR3 in the recognition of *Leishmania donovani* promastigotes by interferon-gamma-primed macrophages. Eur. J. Immunol.. *36*, 411–420

164. Murray HW, Zhang Y, Zhang Y, Raman VS, Reed SG, Ma X. (2013). Regulatory Actions of Toll-Like Receptor 2 (TLR2) and TLR4 in Leishmania donovani Infection in the Liver. Infect. Immun. *81*, 2318–26.

165. Kavoosi G, Ardestani SK, Kariminia A. (2009). The involvement of TLR2 in cytokine and reactive oxygen species (ROS) production by PBMCs in response to Leishmania major phosphoglycans (PGs). Parasitology *136*, 1193-99.

166. Abbas A, Lichtman A, Pillai S. (2014). Cellular and Molecular Immunology. *8th ed*. Elsevier Ltd.

167. Schwarz T, Remer KA, Nahrendorf W, Masic A, Siewe L, Müller W, et al. (2013). T Cell-Derived IL-10 Determines Leishmaniasis Disease Outcome and Is Suppressed by a Dendritic Cell Based Vaccine. PLoS Pathog. *9*, e1003476. doi:10.1371/journal.ppat.1003476.

168. Groux H, Cottrez F, Rouleau M, Mauze S, Antonenko S, Hurst S, et al. (1999) A transgenic model to analyze the immunoregulatory role of IL-10 secreted by antigen-presenting cells. J. Immunol. *162*, 1723–9.

169. Barthelmann J, Nietsch J, Blessenohl M, Laskay T, van Zandbergen G, Westermann J, et al. (2012). The protective Th1 response in mice is induced in the T-cell zone only three weeks after infection with Leishmania major and not during early T-cell activation. Med. Microbiol. Immunol. *201*, 25–35.

170. Remick DG, Bolgos GR, Siddiqui J, Shin J, Nemzek JA. (2002). Six at six: interleukin-6 measured 6 h after the initiation of sepsis predicts mortality over 3 days. Shock *17*, 463–7.

171. Heper Y, Akalin EH, Mistik R, Akgöz S, Töre O, Göral G, et al. (2006). Evaluation of serum C-reactive protein, procalcitonin, tumor necrosis factor alpha, and interleukin-10 levels as diagnostic and prognostic parameters in patients with community-acquired sepsis, severe sepsis, and septic shock. Eur. J. Clin. Microbiol. Infect. Dis. *25*, 481–91.

172. Fernando MR, Reyes JL, Iannuzzi J, Leung G, McKay DM. (2014). The pro-inflammatory cytokine, interleukin-6, enhances the polarization of alternatively activated macrophages. PLoS One *9*, e94188. doi:10.1371/journal.pone.0094188.

173. Deng M, Scott MJ, Loughran P, Gibson G, Sodhi C, Watkins S, et al. (2013). Lipopolysaccharide Clearance, Bacterial Clearance, and Systemic Inflammatory Responses Are Regulated by Cell Type-Specific Functions of TLR4 during Sepsis. J. Immunol. *190*, 5152–60.

174. Anel R, Kumar A. (2005). Human endotoxemia and human sepsis: limits to the model. Crit. Care *9*, 151-2.

175. Johnson BL, Goetzman HS, Prakash PS, Caldwell CC. (2013). Mechanisms underlying mouse TNF-α stimulated neutrophil derived microparticle generation. Biochem. Biophys. Res. Commun. *437*, 591–6.

176. Varenne F, Makky A, Gaucher-Delmas M, Violleau F, Vauthier C. (2016). Multimodal Dispersion of Nanoparticles: A Comprehensive Evaluation of Size Distribution with 9 Size Measurement Methods. Pharm. Res. *33*, 1220–34.

177. Marrack P, McKee AS, Munks MW. (2009). Towards an understanding of the adjuvant action of aluminium. Nat. Rev. Immunol. *9*, 287–93.

178. Li Z, Srivastava P. (2004). Heat-Shock Proteins. Curr. Protoc. Immunol. *58*, 1T:A.1T.1–A.1T.6.

179. Gerke V, Moss SE. (2002). Annexins: From Structure to Function. Physiol. Rev. *82*, 331–71.

180. Martinez FO, Gordon S. (2014). The M1 and M2 paradigm of macrophage activation: time for reassessment. F1000Prime Rep. *6*, 13. doi: 10.12703/P6-13.

181. Mantovani A, Sica A, Sozzani S, Allavena P, Vecchi A, Locati M. (2004). The chemokine system in diverse forms of macrophage activation and polarization. Trends Immunol. *25*, 677–86.

182. Wang J, Basagoudanavar SH, Wang X, Hopewell E, Albrecht R, Garcia-Sastre A, et al. (2010). NF-κB RelA Subunit Is Crucial for Early IFN- Expression and Resistance to RNA Virus Replication. J. Immunol. *185*, 1720–9.

183. Parameswaran N, Patial S. (2010). Tumor necrosis factor-α signaling in macrophages. Crit. Rev. Eukaryot. Gene Expr. *20*, 87–103.

184. Libermann TA, Baltimore D. (1999). Activation of interleukin-6 gene expression through the NF-kappa B transcription factor. Mol. Cell. Biol. *10*, 2327–34.

185. Cogswell JP, Godlevski MM, Wisely GB, Clay WC, Leesnitzer LM, Ways JP, et al. (1994). NF-kappa B regulates IL-1 beta transcription through a consensus NF-kappa B binding site and a nonconsensus CRE-like site. J. Immunol. *153*, 712–23.

186. Grubman MJ, Baxt B. (2004). Foot-and-Mouth Disease. Clin. Microbiol. Rev. *17*, 465–93.

187. Khong WX, Foo DGW, Trasti SL, Tan EL, Alonso S. (2011). Sustained high levels of interleukin-6 contribute to the pathogenesis of enterovirus 71 in a neonate mouse model. J. Virol. *85*, 3067–76.

188.Lin TY, Chang LY, Huang YC, Hsu KH, Chiu CH, Yang KD. (2002). Different proinflammatory reactions in fatal and non-fatal enterovirus 71 infections: implications for early recognition and therapy. Acta Paediatr. *91*, 632–5.

189. Lin T, Hsia S, Huang Y, Wu C, Chang L. (2003). Proinflammatory Cytokine Reactions in Enterovirus 71 Infections of the Central Nervous System. Clin. Infect. Dis. *36*, 269–74.

190. Díaz-San Segundo F, Rodríguez-Calvo T, de Avila A, Sevilla N. (2009). Immunosuppression during acute infection with foot-and-mouth disease virus in swine is mediated by IL-10. PLoS One *4*, e5659. doi:10.1371/journal.pone.0005659.

191. Diaz-San Segundo F, Moraes MP, de los Santos T, Dias CCA, Grubman MJ. (2010). Interferon-Induced Protection against Foot-and-Mouth Disease Virus Infection Correlates with Enhanced Tissue-Specific Innate Immune Cell Infiltration and Interferon-Stimulated Gene Expression. J. Virol. *84*, 2063–77.

192. Ng CT, Sullivan BM, Teijaro JR, Lee AM, Welch M, Rice S, et al. (2015). Blockade of Interferon Beta, but Not Interferon Alpha, Signaling Controls Persistent Viral Infection. Cell Host Microbe *17*, 653–61.

193. Monaco JJ. (1992). A molecular model of MHC class-I-restricted antigen processing. Immunol. Today *13*, 173–9.

194. Risso A, Smilovich D, Capra MC, Baldissarro I, Yan G, Bargellesi A, et al. (1991). CD69 in resting and activated T lymphocytes. Its association with a GTP binding protein and biochemical requirements for its expression. J. Immunol. *146*, 4105–14.

195. Rhee HJ, Kim GY, Huh JW, Kim SW, Na DS. (2004). Annexin I is a stress protein induced by heat, oxidative stress and a sulfhydryl-reactive agent. Eur. J. Biochem. *267*, 3220–5.

196. Rescher U, Gerke V. (2004). Annexins - unique membrane binding proteins with diverse functions. J. Cell. Sci. *117*, 2631–9.

197. Ravassa S, Bennaghmouch A, Kenis H, Lindhout T, Hackeng T, Narula J, et al. (2005). Annexin A5 down-regulates surface expression of tissue factor: A novel mechanism of regulating the membrane receptor repertoir. J. Biol. Chem. *280*, 6028–35.

198. Lizarbe MA, Barrasa JI, Olmo N, Gavilanes F, Turnay J. (2013). Annexin-phospholipid interactions. Functional implications. Int. J. Mol. Sci. *14*, 2652-83.

199. Kenis H, Van Genderen H, Bennaghmouch A, Riniaj HA, Frederik P, Narula J, et al. (2004). Cell surface-expressed phosphatidylserine and annexin A5 open a novel portal of cell entry. J. Biol. Chem. *279*, 52623–9.

200. Kenis H, van Genderen H, Deckers NM, Lux PAG, Hofstra L, Narula J, et al. (2006). Annexin A5 inhibits engulfment through internalization of PS-expressing cell membrane patches. Exp. Cell Res. *312*, 719–26.

201. Gidon-Jeangirard C, Hugel B, Holl V, Toti F, Laplanche JL, Meyer D, et al. (1999). Annexin V delays apoptosis while exerting an external constraint preventing the release of CD4+ and PrPc+ membrane particles in a human T lymphocyte model. J. Immunol. *162*, 5712–8.

202. Linke B, Abeler-Dorner L, Jahndel V, Kurz A, Mahr A, Pfrang S, et al. (2015). The Tolerogenic Function of Annexins on Apoptotic Cells Is Mediated by the Annexin Core Domain. J. Immunol. *194*, 5233–42.

203. Schlaepfer DD, Jones J, Haigler HT. (1992). Inhibition of protein kinase C by annexin V. Biochemistry *31*, 1886–91.

204. Sutcliffe EL, Bunting KL, He YQ, Li J, Phetsouphanh C, Seddiki N, et al. (2011). Chromatin-Associated Protein Kinase C-θ Regulates an Inducible Gene Expression Program and MicroRNAs in Human T Lymphocytes. Mol. Cell *41*, 704–19.

205. Buckland AG, Wilton DC. (1998). Inhibition of secreted phospholipases A2 by annexin V. Competition for anionic phospholipid interfaces allows an assessment of the relative interfacial affinities of secreted phospholipases A2. Biochim. Biophys. Acta *1391*, 367–76.

206. Meyer MC, Rastogi P, Beckett CS, McHowat J. (2005). Phospholipase A2 inhibitors as potential anti-inflammatory agents. Curr. Pharm. Des. *11*, 1301–12.

207. Arnold P, Lu X, Amirahmadi F, Brandl K, Arnold JMO, Feng Q, et al. (2014). Recombinant human annexin A5: a novel drug candidate for treatment of sepsis? Crit. Care Med. *42*, 219–20.

208 .Inaba K, Turley S, Iyoda T, Yamaide F, Shimoyama S, e Sousa CR, et al. (2000). The Formation of Immunogenic Major Histocompatibility Complex Class II–Peptide Ligands in Lysosomal Compartments of Dendritic Cells Is Regulated by Inflammatory Stimuli. J. Exp. Med. *191*, 927–36.

209. Mahnke K, Schmitt E, Bonifaz L, Enk AH, Jonuleit H. (2002). Immature, but not inactive: the tolerogenic function of immature dendritic cells. Immunol. Cell Biol. *80*, 477–83.

210. Asselin-Paturel C, Brizard G, Chemin K, Boonstra A, O'Garra A, Vicari A, et al. (2005). Type I interferon dependence of plasmacytoid dendritic cell activation and migration. J. Exp. Med. *201*, 1157–67.

211. Kapsenberg ML. (2003). Dendritic-cell control of pathogen-driven T-cell polarization. Nat. Rev. Immunol. *3*, 984–93.

212. Baldwin T, Henri S, Curtis J, O'Keeffe M, Vremec D, Shortman K, et al. (2004). Dendritic Cell Populations in Leishmania major-Infected Skin and Draining Lymph Nodes. Infect. Immun. *72*, 1991–2001.

213. Wakkach A, Fournier N, Brun V, Breittmayer J-P, Cottrez F, Groux H. (2003). Characterization of Dendritic Cells that Induce Tolerance and T Regulatory 1 Cell Differentiation In Vivo. Immunity *18*, 605–17.

214. León B, López-Bravo M, Ardavín C. (2007). Monocyte-Derived Dendritic Cells Formed at the Infection Site Control the Induction of Protective T Helper 1 Responses against Leishmania. Immunity *26*, 519–31.

215. Hegde VL, Singh NP, Nagarkatti PS, Nagarkatti M. (2008). CD44 mobilization in allogeneic dendritic cell-T cell immunological synapse plays a key role in T cell activation. J. Leukoc. Biol. *84*, 134-42.

216. Rosen SD. (2004). Ligands for L-Selectin: Homing, Inflammation, and Beyond. Annu. Rev. Immunol. *22*, 129–56.

217. Pennock ND, White JT, Cross EW, Cheney EE, Tamburini BA, Kedl RM. (2013). T cell responses: naïve to memory and everything in between. Adv. Physiol. Educ. *37*, 273–83.

218. Sallusto F, Lenig D, Förster R, Lipp M, Lanzavecchia A. (1999). Two subsets of memory T lymphocytes with distinct homing potentials and effector functions. Nature. *401*, 708–12.

219. Sullivan KE, Cutilli J, Piliero LM, Ghavimi-Alagha D, Starr SE, Campbell DE, et al. (2000). Measurement of Cytokine Secretion, Intracellular Protein Expression, and mRNA in Resting and Stimulated Peripheral Blood Mononuclear Cells. Clin. Vaccine Immunol. *7*, 920–4.

220. http://www.bdbiosciences.com/documents/Detecting_Cytokines_Lymphocytes.pdf. Last visited on 01/12/2016.

221. Coleman MM, Finlay CM, Moran B, Keane J, Dunne PJ, Mills KHG. (2012). The immunoregulatory role of CD4+FoxP3+CD25- regulatory T cells in lungs of mice infected with Bordetella pertussis. FEMS Immunol. Med. Microbiol. *64*, 413–24.

222. Zelenay S, Lopes-Carvalho T, Caramalho I, Moraes-Fontes MF, Rebelo M, Demengeot J. (2005). Foxp3+CD25-CD4 T cells constitute a reservoir of committed regulatory cells that regain CD25 expression upon homeostatic expansion. Proc. Natl. Acad. Sci. U. S. A. *102*, 4091–6.

223. Fontenot JD, Rasmussen JP, Williams LM, Dooley JL, Farr AG, Rudensky AY. (2005). Regulatory T Cell Lineage Specification by the Forkhead Transcription Factor Foxp3. Immunity *22*, 329–41.

224. Kim CH. (2009). FOXP3 and its role in the immune system. Adv. Exp. Med. Biol. *665*, 17–29.

225. Ono M, Shimizu J, Miyachi Y, Sakaguchi S. (2006). Control of Autoimmune Myocarditis and Multiorgan Inflammation by Glucocorticoid-Induced TNF Receptor Family-Related Proteinhigh, Foxp3-Expressing CD25+ and CD25- Regulatory T Cells. J. Immunol. *176*, 4748–56.

226. Kane MM, Mosser DM. (2001). The role of IL-10 in promoting disease progression in leishmaniasis. J. Immunol. *166*, 1141–7.

227. Couper K, Blount D, Riley E. (2008). IL-10: the master regulator of immunity to infection. J. Immunol. *180*, 5771–7.

228. Gessner A, Mohrs K, Mohrs M. (2005). Mast cells, basophils, and eosinophils acquire constitutive IL-4 and IL-13 transcripts during lineage differentiation that are sufficient for rapid cytokine production. J. Immunol. *174*, 1063–72.

229. Katzman SD, Fowell DJ. (2008). Pathogen-imposed skewing of mouse chemokine and cytokine expression at the infected tissue site. J. Clin. Invest. *118*, 101-11.

230. Monneret G, Lepape A, Voirin N, Bohé J, Venet F, Debard AL, et al. (2006). Persisting low monocyte human leukocyte antigen-DR expression predicts mortality in septic shock. Intensive Care Med. *32*, 1175–83.

231. Simms HH, D'Amico R. (1995). Lipopolysaccharide Induces Intracytoplasmic Migration of the Polymorphonuclear Leukocyte CD11B/CD18 Receptor. Shock *3*, 196-203.

232. Liu JR, Han X, Soriano SG, Yuki K. (2014). The role of macrophage 1 antigen in polymicrobial sepsis. Shock *42*, 532–9.

233. Yang J, Zhang L, Yu C, Yang X-F, Wang H. (2014). Monocyte and macrophage differentiation: circulation inflammatory monocyte as biomarker for inflammatory diseases. Biomark. Res. *2*, 1. doi: 10.1186/2050-7771-2-1.

234. Borregaard N. (2010). Neutrophils, from Marrow to Microbes. Immunity *33*, 657–70.

235. Ocuin LM, Bamboat ZM, Balachandran VP, Cavnar MJ, Obaid H, Plitas G, et al. (2011). Neutrophil IL-10 suppresses peritoneal inflammatory monocytes during polymicrobial sepsis. J. Leukoc. Biol *89*, 423–32.

236. Kalechman Y, Gafter U, Gal R, Rushkin G, Yan D, Albeck M, et al. (2002). Anti-IL-10 therapeutic strategy using the immunomodulator AS101 in protecting mice from sepsis-induced death: dependence on timing of immunomodulating intervention. J. Immunol. *169*, 384–92.

237. van Engeland M, Nieland LJ, Ramaekers FC, Schutte B, Reutelingsperger CP. (1998). Annexin V-affinity assay: a review on an apoptosis detection system based on phosphatidylserine exposure. Cytometry *31*, 1–9.

238. Rand JH, Wu X-X, Lin EY, Griffel A, Gialanella P, McKitrick JC. (2012). Annexin A5 Binds to Lipopolysaccharide and Reduces Its Endotoxin Activity. MBio *3*, e00292–11 – e00292–11. doi: 10.1128/mBio.00292-11.

239. Dalrymple SA, Slattery R, Aud DM, Krishna M, Lucian LA, Murray R. (1996). Interleukin-6 Is Required for a Protective Immune Response to Systemic Escherichia coli Infection. Infect. Immun. *64*, 3231–5.

240. Xing Z, Gauldie J, Cox G, Baumann H, Jordana M, Lei XF, et al. (1998). IL-6 is an antiinflammatory cytokine required for controlling local or systemic acute inflammatory responses. J. Clin. Invest. *101*, 311–20.

241. Damas P, Ledoux D, Nys M, Vrindts Y, De Groote D, Franchimont P, et al. (1992). Cytokine serum level during severe sepsis in human IL-6 as a marker of severity. Ann Surg. *215*, 356–62.

242. Barkhausen T, Tschernig T, Rosenstiel P, van Griensven M, Vonberg R-P, Dorsch M, et al. (2011). Selective blockade of interleukin-6 trans-signaling improves survival in a murine polymicrobial sepsis model. Crit. Care Med. *39*, 1407–13.

243. Unsinger J, Burnham CAD, McDonough J, Morre M, Prakash PS, Caldwell CC, et al.(2012). Interleukin-7 ameliorates immune dysfunction and improves survival in a 2-hit model of fungal sepsis. J. Infect. Dis. *206*, 606-16.

244. Schabbauer G. (2012). Polymicrobial sepsis models: CLP versus CASP. Drug Discov. Today *9*, e17–21.

245. Ward NS, Casserly B, Ayala A. (2008). The Compensatory Anti-inflammatory Response Syndrome (CARS) in Critically Ill Patients. Clin. Chest Med. *29*, 617–25.

246. Boomer JS, Green JM, Hotchkiss RS. (2014). The changing immune system in sepsis. Virulence *5*, 45–56.

247. Marshall JC. (2016). Why have clinical trials in sepsis failed? Trends Mol. Med. *20*, 195–203.

248. Opal SM, Phillip Dellinger R, Vincent J-L, Masur H, Angus DC. (2014). The next generation of sepsis trials: What's next after the demise of recombinant human activated Protein C? Crit. Care Med. *42*, 1714–21.

249. Fleischmann C, Scherag A, Adhikari NKJ, Hartog CS, Tsaganos T, Schlattmann P, et al. (2015). Assessment of Global Incidence and Mortality of Hospital-treated Sepsis. Current Estimates and Limitations. Am. J. Respir. Crit. Care Med. *193*, 259–72.

250. Martoglio B, Dobberstein B. (1998). Signal sequences: more than just greasy peptides. Trends Cell Biol. *8*, 410–5.

251. Andrei C, Dazzi C, Lotti L, Torrisi MR, Chimini G, Rubartelli A. (1999). The Secretory Route of the Leaderless Protein Interleukin 1β Involves Exocytosis of Endolysosome-related Vesicles. Mol. Biol. Cell *10*, 1463–75.

252. Mambula SS, Stevenson MA, Ogawa K, Calderwood SK. (2007). Mechanisms for Hsp70 secretion: Crossing membranes without a leader. Methods *43*, 168–75.

253. Lunov O, Syrovets T, Loos C, Beil J, Delacher M, Tron K, et al. (2011). Differential Uptake of Functionalized Polystyrene Nanoparticles by Human Macrophages and a Monocytic Cell Line. ACS Nano *5*, 1657–69.

254. Witasp E, Kupferschmidt N, Bengtsson L, Hultenby K, Smedman C, Paulie S, et al. (2009). Efficient internalization of mesoporous silica particles of different sizes by primary human macrophages without impairment of macrophage clearance of apoptotic or antibody-opsonized target cells. Toxicol. Appl. Pharmacol. *239*, 306–19.

7. Appendix

7.1 Supplemental data

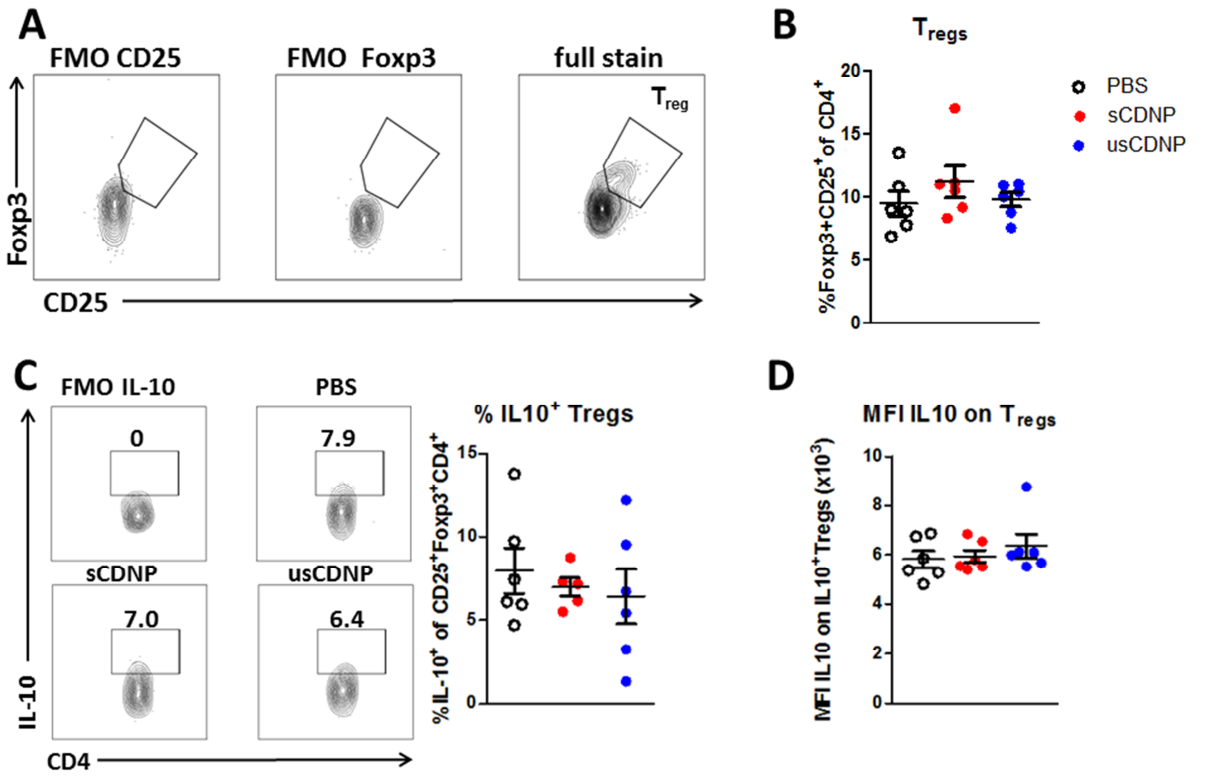


Fig. S1: CDNPs have no effect on Treg frequencies and intracellular IL-10 levels of Foxp3$^+$CD25$^+$Tregs in the draining lymph node of *L. major*-infected mice. C56BL/6 mice were infected with 1x10^6 viable *L. major* promastigotes into the hind foot pad. 5µg s- or usCDNPs were injected s.c. into the hint legs, every other day. Draining lymph nodes were harvested 4 weeks post infection and cells were isolated. 1x 10^6 cells were restimulated with 5ng/ml PMA and 1µg/ml Ionomycin for 1 hour at 37° C. 5µg/ml Brefoldin A was added and cells were incubated for additional 4 hours. Cells were harvested and first stained with fluorescence-labeled mAbs to CD4 and CD25, then permeabilized and stained for nuclear Foxp3 and intracellular IL-10. Analysis was carried out via flow cytometry. A) nventional Tregs. Cells were gated on CD4$^+$ cells. B) Quantification of Foxp3$^+$CD25$^+$CD4$^+$ T cells (conventional Tregs) . C) Representative plots and quantification of the frequencies of IL-10$^+$ Tregs and B) IL-10 MFI on Tregs. Cells were gated on CD4$^+$CD25$^+$Foxp3$^+$. Pooled results from 2 independent experiments with n=3 mice per group. Data are expressed as means ± SEM.

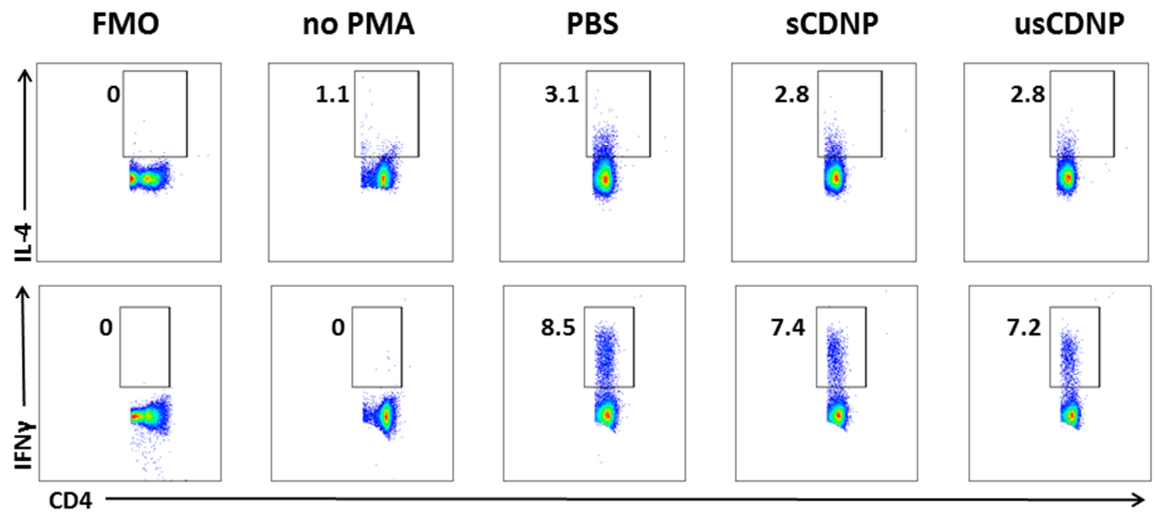


Fig. S2: Gating strategy and representative plots for intracellular IFNγ- and IL-4 levels on CD4$^+$ T cells: C56BL/6 mice were infected with 1x10^6 viable *L. major* promastigotes into the hind foot pad. 5µg s- or usCDNPs were injected s.c. into the hint legs, every other day. The popliteal, draining lymph node was harvested 4 weeks post infection. 1x10^6 cells were restimulated with 5 ng/ml PMA and 1µg/ml Ionomycin for 1 hour at 37° C. 5 µg/ml Brefoldin A was added and cells were incubated for additional 4 hours. Cells were harvested and first stained with fluorescence-labeled mAbs against surface CD4, then permeabilized and stained for intracellular IL-4 and IFNγ. Analysis was carried out via flow cytometry. Single cells were gated on CD4$^+$ cells. Representative plots from 1-2 independent experiments with n=2-6 mice per group. Data are expressed as means ± SEM.

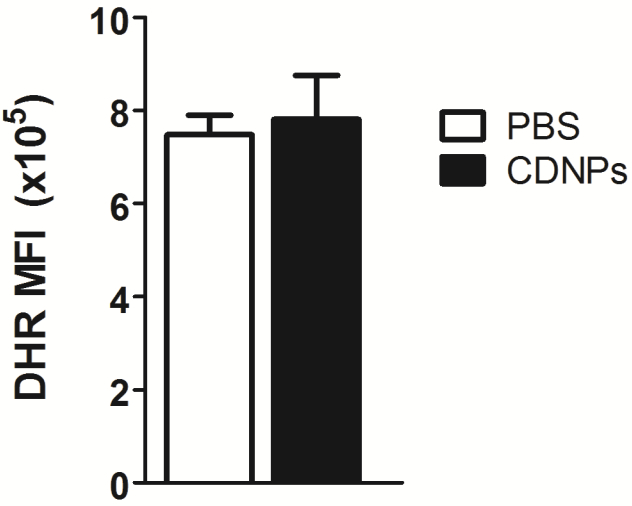


Fig.S3: CDNPs do not affect ROS production by neutrophils. Neutrophils were isolated from BM and incubated with CDNPs for 24h. Neutrophils were then harvested and incubated with 2.5µl 400x Ddihydrorhodamine 123 (DHR) for 15 min at 37°C. DHR is ingested by neutrophils and intracellularly oxidized by ROS to the highly fluorescent rhodamine 123. Quantification of rhodamine 123 (DHR) expression on Ly-6G^{high} neutrophils as assessed by flow cytometry. Pooled data from 3 independent experiments with n=4-6. Data are expressed as means ± SEM.

7.2 Abbrevations

%	percent
2D	two-dimensional
°C	degrees of Celsius
Ab	antibody
A. dest.	*Aqua destillatum*
ANOVA	analysis of variance
AP-1	activator protein 1
APC	antigen presenting cell or allophycocyanine
ATP	adenosine triphosphate
BCA	bicinchoninic acid
BDNF	brain-derived neurotrophic factor
BiP	Binding immunoglobulin protein
BK-RiV	**„***Biokomplex Reaktionsmuster in Vertebratenzellen***“** (biocomplex reaction pattern in vertebrate cells), the official trade name of CDNPs
BM	bone marrow
BSA	bovine serum albumin
CARS	compensatory anti-inflammatory response syndrome
CBA	cytometric bead array
CCD	camera-coupled device
CD	cluster of differentiation
cDC	conventional dendritic cell
cDNA	complementary deoxyribonucleic acid
CDNP	cell-derived nanoparticle
CFSE	carboxyfluorescein succinimidyl ester
CFU	colony forming unit
CLP	cecal ligation and puncture
CLR	c-type lectin receptors
CpG	cytosine–phosphate–guanosine
conc.	concentration
CREB	cyclic adenosine monophosphate-responsive element-binding protein
C_T	cycle of threshold
Cy	cyanine

DAMP	danger-associated molecular pattern
DC	dendritic cell
DEPC	diethylpyrocarbonate
DIGE	difference gel electrophoresis
DMSO	dimethyl sulfoxide
DNA	*desoxyribunucleic acid*
DNase	desoxyribonuklease
dNTP	deoxynucleoside triphosphate
ds	double strand
DTT	dithiothreitol
ECF	enhanced chemiluminicsence (a chemiluminescent HRP Substrates)
ELISA	enzyme-linked immunosorbant assay
EM	electron microscope/electron microscopy
ER	endoplasmatic reticulum
EU	endotoxin unit
FACS	fluorescence-activated cell sorting
Fc	cryctallized fragment
FCS	fetal calf serum
Fig.	figure
FITC	fluorescein isothiocyanate
FMO	fluorescence minus one control
Foxp3	Forkhead box P3
FSC	forward scatter
g	gravitational acceleration
gal	galactose
GMP	good manufacturing practice
h	hour
HBSS	hank’s balanced salt solution
HIV	human immunodeficiency virus
HMGB 1	high mobility group box protein 1
HRP	horseradish peroxidase
HS	high salt
HSP	heat shock protein
IEF	isoelectric focusing

IFN	interferone
Ig	immunglobuline
IgA	immunglobuline A
IgG	immunglobuline G
IgM	immunglobuline M
IκB	inhibitor of kappa B
IKK	inhibitor of NF-κB kinase
IL	interleukine
i.m.	intramuscular injection
infl.	inflammatory
iNOS	inducible nitric oxide synthase
IPG	immobilized pH gradient
IRAK	interleukin-1 receptor-associated kinase
IRF	interferon-regulatory factor
kDA	kilo dalton
l	litre
LAL	limulus amebocyte lysate
LB	lysogeny broth
L. major	*Leishmania major*
LPG	lipophosphoglycan
LPS	lipopolysaccharide
LS	low salt
µl	microlitre
M	molar or magnification or marker
mA	milliampere
mAb	monoclonal antibody
Mal	MyD88-adaptor like protein
MALDI	Matrix-assisted laser desorption/ionization
max.	maximal/maximum
MEM	minimum essential medium
MES	2-(N-morpholino)ethanesulfonic acid
MFI	median fluorescence intensity
MHCII	major histocompatibility complex
min	minute

MKK	mitogen-activated protein kinase kinase
ml	mililitre
MLN51	metastatic lymp hnode 51
mo	monocyte
MP	microparticle
Mϕ	macrophage
mRNA	messenger ribonucleic acid
MWCO	molecular weight cut-off
MyD88	myeloid differentiation factor 88
n	sample size
NaCl	sodium chloride
n.d.	not detected
NDMP	neutrophil-derived nanoparticle
NET	neutrophil extracellular trap
NFκB	nuclear factor kappa light chain enhancer of activated B cells
nm	nanometer
NOD	nucleotide-binding oligomerization domain
n.s.	not significant
NTA	nanoparticle tracking analysis
OD	optical density
OVA	ovalbumin
p	probability
P. aeruginosa	*Pseudomonas aeruginosa*
PAMP	pathogen-associated molecular pattern
PBS	phosphate-buffered saline
PC	principal component
PCA	principal component analysis
PCR	polymerase chain reaction
pDC	plasmacytoid dendritic cell
PE	phycoerythrin
PerCP	peridinin chlorophyll protein complex
PFA	parafolmaldehyde
pK	negative logarithm of the dissociation constant
PKC	protein kinase C

PLA_2	phospholipase A_2
PMA	phorbol 12-myristate 13-acetate
PMT	photomultiplier tubes
PNAC	protein-nucleic acid complex, former synonym for CDNPs
POLA	*Leishmania* DNA polymerase alpha catalytic polypeptide
Poly(I:C)	polyinosinic:polycytidylic acid
PRR	pattern recognition receptor
PS	phosphatidylserine
PVFD	polyvinylidene fluoride
qPCR	quantitative PCR
RAGE	receptor for advanced glycation endproducts
RAMP	resolution-associated molecular pattern
RIG-I	retinoic-acid-inducible protein I
RNA	ribonucleic acid
RNase	ribonuclease
ROS	reactive oxygen species
rpm	revolutions per minute
RT	reverse transkriptase or room temperature
RPMI	Roswell Park Memorial Institute medium
sec	second
s.c.	subcutaneous
sCDNP	CDNPs wich are derived from stressed cells
SDS	sodium dodecyl sulfate
SDS-PAGE	SDS-polyacrylamide gel electrophoresis
SEM	scanning electron microscopy or standard error of the mean
SFP	specific pathogen-free
SOS	stress observation system
SPF	specific pathogen-free
ss	single strand
SSC	side scatter
SYBR Green	the asymmetrical cyanine dye $C_{32}H_{37}N_4S^+$
Tab.	table
Taq	*Thermus/Thermophilus aquaticus*
TCR	T cell receptor

TGA	thioglycolate
TGF	transforming growth factor
Th1-/Th2-cell	T helper cell type 1/type 2
TIR	Toll-IL1 receptor
TIRAP	TIR domain-containing adaptor protein
TLR	Toll like receptor
TMB	3,3',5,5'-tetramethylbenzidine
TNF	tumor necrosis factor
TOF	time of flight
TRAF	TNF receptor-associated factor
TRAM	TRIF-related adapter molecule
Treg	regulatory T cell
TRIF	TIR-domain-containing adapter-inducing interferon-β
TWEEN	polyoxyethylene sorbitan mono-laurate
UPR	unfold protein response
usCDNP	CDNPs which are derived from unstressed cells
V	volt
v/v	volume per volume
w/v	weight per volume
zy	zymosan

7.3 List of Figures

Fig. 2-1: MyD88-dependent and MyD88-independent signaling pathways of TLRs 6
Fig. 2-2: Integrative concept of PAMPs, DAMPs and RAMPs 12
Fig. 2-3: T cell polarization and its consequences in *Leishmania* infection 16
Fig. 2-4: The two phases of sepsis 18
Fig. 3-1: CDNP preparations derived from stressed and unstressed cells contain very low endotoxin levels 55
Fig. 4-1-1: Incubation with xenogeneic CDNPs has no effect on unstimulated peritoneal macrophages 57
Fig. 4-1-2: Xenogeneic CDNPs do not alter cytokine expression of LPS- or Poly(I:C)-triggered macrophages 58
Fig. 4-1-3: Xenogeneic CDNPs decrease TLR7/8-triggered TNFα expression 4 hours after incubation 60
Fig. 4-1-4: Xenogeneic CDNPs decrease TLR2-triggered IFNβ and TNFα expression 4 and 24 hours after incubation, respectively 61
Fig. 4-1-5: Production of murine CDNPs 63
Fig. 4-1-6: Murine CDNPs display similar particularity, size and composition as xenogeneic CDNPs 64
Fig. 4-1-7: Similar to xenogeneic CDNPs, allogeneic CDNPs decrease the TNFα expression of zymosan-stimulated macrophages 24 hours after incubation 66
Fig. 4-1-8: Xenogeneic and allogeneic CDNPs both reduce IL-1β expression of zymosan-stimulated macrophages, while IL-6 expression is reduced by allogeneic CDNPs only 67
Fig. 4-1-9: Xenogeneic and allogeneic CDNPs increase zymosan-induced IL-10 expression 68
Fig. 4-1-10: Allogeneic CDNPs also alter the cytokine expression of peritoneal macrophages after stimulation with Pam_3CSK_4 70
Fig. 4-2-1: Unstressed cells also produce CDNPs 72
Fig. 4-2-2: Only sCDNPs reduce zymosan-induced TNFα secretion 73
Fig. 4-2-3: Gating strategies for the identification of peritoneal macrophages and CDNP ingestion 74
Fig. 4-2-4: Peritoneal macrophages ingest both s- and usCDNPs 75
Fig. 4-2-5: Both a- and usCDNPs slightly increase MHCII surface expression on macrophages 76
Fig. 4-2-6: Only sCDNPs reduce LPS-induced $CD4^+$ T cell activation 77
Fig. 4-2-7: sCDNPs have a different protein composition as compared to usCDNPs 78
Fig. 4-2-8: s- and usCDNPs can be distinguished based on their protein composition 79
Fig. 4-2-9: Only sCDNPs are enriched in annexin A5 81
Fig. 4-3-1: Gating strategy for c- and pDCs 83
Fig. 4-3-2: CDNPs activate DCs in the draining lymph node of *L. major*-infected mice 84
Fig. 4-3-3: CDNPs shift the ratio of naive vs. effector (memory) $CD4^+$ T cells in the draining lymph node of *L. major*-infected mice to the effector side 85
Fig. 4-3-4: CDNPs decrease intracellular IFNγ levels in $CD4^+$ cells of the draining lymph node of *L. major*-infected mice 86
Fig. 4-3-5: CDNPs increase IL-4 mRNA levels at the infection site of *L. major*-infected mice 87
Fig. 4-3-6: CDNPs increase the frequency of regulatory $Foxp3^+CD4^+$ T cells in the draining lymph node of *L. major*-infected mice 88

Fig. 4-3-7:	CDNPs increase IL-10 mRNA at the infection site of *L. major*-infected mice	89
Fig. 4-3-8:	CDNPs do not change the clinical disease outcome of *L. major*-infected mice	90
Fig. 4-3-9:	CDNPs increase the percentage of surviving mice in response to CLP by trend	92
Fig. 4-3-10:	Identification of CDNP-ingesting peritoneal cells	93
Fig. 4-3-11:	Gating strategy for neutrophils, infl. monocytes and macrophages	94
Fig. 4-3-12:	CDNPs are ingested by neutrophils, infl. monocytes and macrophages at the infection site of septic mice	96
Fig. 4-3-13:	CDNPs enhance the activation of effector cells at the site of infection 4 hours post CLP	96
Fig. 4-3-14:	CDNPs reduce peritoneal IL-6 levels in septic mice 24 hours post CLP	97
Fig. 4-3-15:	CDNPs dose-dependently reduce IL-10 levels at the site of infection 24 hours post CLP	98
Fig. 4-3-16:	CDNPs increase NDMP levels at the site of sepsis 24 hours post CLP	99
Fig. 4-3-17:	CDNPs reduce peritoneal bacterial loads 24 hours post CLP	100
Fig. 4-3-18:	CDNPs reduce mRNA and protein IL-6 levels *in vitro*	101
Fig. 4-3-19:	CDNPs impede NDMP production *in vitro*	102
Fig. 4-3-20:	CDNPs bind to NDMPs *in vitro*	103
Fig. 4-3-21:	Pre-incubation of CDNPs with NDMP impede NDMP ingestion by peritoneal macrophages *in vitro*	104
Fig. 4-3-22:	CDNPs directly reduce bacterial growth *in vitro*	105
Fig. 4-4-1:	Isolation of endogenously produced CDNPs from septic mice	107
Fig. 4-4-2:	CDNPs accumulate at the infection site of sepsis	108
Fig. 4-4-3:	CLP-derived CDNPs contain annexin A5	109
Fig. S1:	CDNPs have no effect on Treg frequencies and intracellular IL-10 levels of $Foxp3^{+}CD25^{+}$Tregs in the draining lymph node of *L. major*-infected mice	152
Fig. S2:	Gating strategy and representative plots for intracellular IFNγ- and IL-4 levels on CD4+ T cells	153
Fig. S3:	CDNPs do not affect ROS production by neutrophils	154

7.4 List of Tables

Tab. 1:	Typical composition of CDNPs	14
Tab. 2:	TLR ligands used to stimulate peritoneal macrophages	44
Tab. 3:	Specifications used for quantitative RT-PCR	47
Tab. 4:	Proteins enriched in sCDNPs vs. usCDNPs	80

7.5 Curriculum Vitae Natalia Kunz

Date of Birth: 03 March 1984
City of Birth: Barnaul, Russia

Education

4/2013-9/2016	Member and student spokesperson of the International Research Training Group IRTG 1911: Immunoregulation in Allergy and Infection, Lübeck, Germany
1/2013-9/2016	Institute of Anatomy, University of Lübeck, Lübeck, Germany Doctoral candidate under the supervision of Kathrin Kalies. PhD thesis: Dissecting the immunomodulatory roles of cell-derived nanoparticles (CDNPs) in infectious diseases.
10/2010-01/2013	University of Lübeck, Lübeck, Germany M.Sc. in Molecular Life Science, Master thesis: Characterization of the humoral immune response in C57BL/6 mice after *Leishmania major* infection.
10/2007-10/2010	University of Lübeck, Lübeck, Germany B. Sc. in Molecular Life Science, Bachelor thesis: Gene expression analysis of Fcγ receptor I, IIB, III and IV in the compartments of spleens and lymph nodes of Epidermolysis bullosa aquisita diseased mice.

Research stays

9/2015 –2 /2016	Department of Surgery, University of Cincinnati College of Medicine, Cincinnati, USA. Under the supervision of Charles C. Caldwell. Investigation of the immunomodulatory effects of CDNPs in sepsis.
7/2012 –8 /2012	Division of Cellular and Molecular Immunology, Cincinnati Children's Hospital Medical Center, Cincinnati, USA. Investigation of protein-nucleic acid uptake by splenic DC subsets.
12/2011 –3 /2012	Departments of Biochemistry/Physiology and Pharmacology, University of Bristol, Bristol, UK. Under the supervision of Chrissy Hammond. Characterization of the EGFL6 Knock Down Phenotype in Zebrafish.

7.6 Contributions to conferences

- Oral Presentation at the retreat of the IRTG1911 2013, Neumünster, Germany: Immunomodulatory role of protein-nucleic acid complexes (PNACs) in Leishmania infections – Impact on TLR signaling by macrophages. **Kunz N**, Kalies K.

- Poster at the retreat of the IRTG1911 2014, Cincinnati, USA: Immunomodulatory roles of protein-nucleic acid complexes (PNACs) in *Leishmania* infections. **Kunz N**, Westermann J, Kalies K.

- Poster at the 37. Symposium of the North German Immunologists, Borstel, Germany: Immuno-modulatory roles of protein-nucleic acid complexes (PNACs) in Leishmania infections. **Kunz N**, Westermann J, Kalies K.

- Poster at the International Cluster Symposium Inflammation at Interfaces 2015, Kiel, Germany: Exploring the immunonodulatory effects of intracellular proteins. **Kunz N**, Wilhelm N, Allan S, Kalies KU, Caldwell CC, Westermann J, Kalies K.

- Poster at the DGfI Spring School on Immunology, Ettal, Germany: Exploring the immunomodulatory effects of intracellular proteins. **Kunz N**, Wilhelm N, Allan S, Kalies KU, Caldwell CC, Westermann J, Kalies K.

- Poster at the Annual Immunology Retreat 2015 of the Immunology Graduate Program at Cincinnati Children's Hospital Medical Center, Cincinnati, USA: Protein-Nucleic Acid-Complexes produced by stressed cells induce anti-inflammatory and regulatory T cell subsets in Leishmania infections. **Kunz N**, Gemoll T, Allan S, Kalies KU, Caldwell CC, Westermann J, Kalies K.

- Poster at the 1st international Symposium Allergy Meets Infection, Luebeck, Germany: Protein-Nucleic Acid-Complexes produced by stressed cells induce anti-inflammatory and regulatory T cell subsets in Leishmania infections. **Kunz N**, Gemoll T, Allan S, Kalies KU, Caldwell CC, Westermann J, Kalies K.

- Poster at the 1st international Symposium Allergy Meets Infection, Luebeck, Germany: Neutrophil derived microparticles (NDMPs) increase mortality in sepsis by enhancing the counter-inflammatory response in a murine model. Johnson, BJ III, Midura EF, Prakash PS, Kuethe JW, Rise TC, **Kunz N**, Caldwell CC.

- Poster at the 39th Annual Conference on Shock, Austin, Texas, USA: Protein-Nucleic Acid Complexes are endogenous modulators of Sepsis. **Kunz N**, Xia BT, Kalies KU, Allan S, Whitacre B, Seitz A, Westermann J, Kalies K, Caldwell CC.

- Oral presentation at the 46th Annual Meeting of the German Society for Immunology, Hamburg, Germany: Reactivity to xenogeneic cell-derived nanoparticles induce Th2 immunity and support healing of cutaneous lesions. **Kunz N**, Hauenschild E, Maass S, Kalies KU, Barra M, Hecht L, Helbig F, Soellner S, Caldwell CC, Ludwig RL, Westermann J, Kalies K.

7.7 Publications

- Stamm C, Barthelmann J, **Kunz N**, Toellner KM, Westermann J, Kalies K. Dose-dependent induction of murine Th1/Th2 responses to sheep red blood cells occurs in two steps: antigen presentation during second encounter is decisive. PLoS One. 2013 Jun 28;8(6):e67746.

- Midura EF, Prakash PS, Johnson BL 3rd, Rice TC, **Kunz N**, Caldwell CC. Impact of caspase-8 and PKA in regulating neutrophil-derived microparticle generation. Biochem Biophys Res Commun. 2016 Jan 22;469(4):917-22.

- Milicevic N, Schmidt F, **Kunz N**, Kalies K, Milicevic Z, Schlosser A, Holmskov U, Sorensen GL, Westermann J. The role of microfibrillar-associated protein 4 (MFAP4) in the formation and function of splenic compartments during embryonic and adult life. Cell Tissue Res. 2016 Jul;365(1):135-45.

- **Kunz N**, Xia BT, Kalies KU, Klinger M, Gemoll T, Habermann J, Whitacre B, Seitz A, Kalies K, Caldwell CC. Cell-derived nanoparticles are endogenous modulators of Sepsis. Shock. 2017 Feb 22. doi: 10.1097/SHK.0000000000000855.

- **Kunz N*,** Hauenschild E*, Maass S, Kalies KU, Barra M, Hecht L, Helbig F, Soellner S, Caldwell CC, Ludwig RL, Westermann J, Kalies K. Nanoparticles prepared from porcine cells support the healing of cutaneous inflammation in mice and wound re-epithelialization in human skin.
  In revision at Experimental Dermatology (EXD-17-0146); *denotes equal contribution

7.8 Declaration/Erklärung

Erklärung

Hiermit versichere ich, die vorliegende Dissertation selbstständig verfasst und nur unter Verwendung der angegebenen Quellen und Hilfsmittel angefertigt zu haben. Ich versichere, dass ich nicht vorher oder gleichzeitig anderenorts einen Zulassungsantrag gestellt und mich bisher keinem anderen Promotionsverfahren unterzogen habe.

Declaration

No part of the work referred to in this dissertation has been submitted in support of an application for any degree or qualification of The University of Lübeck or any other University or Institute of learning.

Natalia Kunz